

# ResearchOnline@JCU

This file is part of the following reference:

**Saptarshi, Shruti R. (2015) *Nanoparticle-protein corona formation and immunotoxicity of zinc oxide nanoparticles.* PhD thesis, James Cook University.**

Access to this file is available from:

<http://researchonline.jcu.edu.au/43787/>

*The author has certified to JCU that they have made a reasonable effort to gain permission and acknowledge the owner of any third party copyright material included in this document. If you believe that this is not the case, please contact*

*[ResearchOnline@jcu.edu.au](mailto:ResearchOnline@jcu.edu.au) and quote  
<http://researchonline.jcu.edu.au/43787/>*

# **Nanoparticle-Protein Corona Formation and Immunotoxicity of Zinc Oxide Nanoparticles**

A thesis submitted in fulfilment of the requirements for the degree of

Doctor of Philosophy

By

**Shruti R. Saptarshi**

*MSc. Biotechnology*

*BSc. (Microbiology)*

**College of Public Health, Medical and Veterinary Sciences  
James Cook University  
January, 2015**

## STATEMENT ON THE CONTRIBUTION OF OTHERS

<b>Nature of Assistance</b>	<b>Contribution</b>	<b>Name and Affiliation</b>
<b>Intellectual support</b>	Project plan and development	<ul style="list-style-type: none"> <li>• A/Prof. Andreas Lopata, James Cook University</li> <li>• Dr. Bryce Feltis, RMIT University</li> <li>• A/Prof. Paul Wright, RMIT University</li> <li>• Prof. James Burnell, James Cook University</li> </ul>
	Editorial support	<ul style="list-style-type: none"> <li>• A/Prof. Andreas Lopata, James Cook University</li> <li>• Dr. Bryce Feltis, RMIT University</li> <li>• A/Prof. Paul Wright, RMIT University</li> <li>• Prof. Albert Duschl, University of Salzburg</li> </ul>
	Grant proposal writing (Graduate research scheme)	<ul style="list-style-type: none"> <li>• A/Prof. Andreas Lopata, James Cook University</li> </ul>
<b>Financial support</b>	Research	<ul style="list-style-type: none"> <li>• NHMRC project grant#616621</li> <li>• ARC Future Fellowship for A/Prof. Andreas Lopata</li> <li>• Graduate Research Scheme, Faculty of Medicine, Health and Molecular Sciences, James Cook University</li> </ul>
	Conference travel	<ul style="list-style-type: none"> <li>• Queensland Tropical Health Alliance</li> <li>• European Academy of Allergy and Clinical Immunology</li> <li>• North Queensland Festival of Life sciences, Faculty of Medicine, Health and Molecular Sciences, James Cook University</li> <li>• Robert Logan Bursary, James Cook University</li> </ul>
	Stipend	<ul style="list-style-type: none"> <li>• Australian Postgraduate Award, Australian Federal Government</li> <li>• School of Pharmacy and Molecular Sciences, James Cook University (Top-up)</li> </ul>
	Write-up support	<ul style="list-style-type: none"> <li>• Doctoral Completion Fund, Faculty of Medicine, Health and Molecular Sciences, James Cook University</li> </ul>
<b>Data collection</b>	ZnO NPs	<ul style="list-style-type: none"> <li>• Prof. Terry Turney, Monash University and Micronisers Pty. Ltd</li> </ul>
	Inductively Coupled Plasma Atomic Emission Spectroscopy	<ul style="list-style-type: none"> <li>• Advanced Analytical Centre, James Cook University</li> </ul>
	Mass spectrometric analysis	<ul style="list-style-type: none"> <li>• Dr. David Wilson, James Cook University</li> </ul>
<b>Technical support</b>	Particulate characterisation	<ul style="list-style-type: none"> <li>• Dr. Victoria Coleman, National Measurement Institute</li> </ul>
	Cell culture	<ul style="list-style-type: none"> <li>• Dr. ShanShan Sun, James Cook University</li> </ul>
	Confocal microscopy Animal handling	<ul style="list-style-type: none"> <li>• Dr. Fiona Baird, James Cook University</li> <li>• Mr. Scott Blyth, James Cook University</li> </ul>

## **Animal Ethics**

This research presented and reported in this thesis was conducted in compliance with the National Health and Medical Research Council (NHMRC) Australian Code of Practice for the Care and Use of Animals for Scientific Purposes, 7th Edition, 2004 and the Qld Animal Care and Protection Act, 2001. The proposed research study received animal ethics approval from the JCU Animal Ethics Committee

**Approval Number A1795**

### Contribution of Authors to co-authored publications

Details of publications on which chapter is based	
<p><b>Saptarshi S</b>, Duschl A and Lopata AL. Interaction of nanoparticles with proteins: relation to bio-reactivity of the nanoparticle. <i>Journal of Nanobiotechnology</i> 2013, 11:26</p>	
Name of Candidate and other co-authors	Nature and extent of the intellectual input of each author, including the candidate
<p><b><u>Candidate:</u></b> Shruti Saptarshi (S.S.)</p> <p><b><u>Co-authors:</u></b> Albert Duschl (A.D.) Andreas L. Lopata (A.L.)</p>	<p>S.S. has conducted the literature review and written the first draft of the manuscript. A.D. and A.L. and provided advice on the theme of the manuscript and also helped to edit, revise and provided final approval of the manuscript. All authors read and approved the final manuscript.</p>

Details of publications on which chapter is based	
<p><b>Saptarshi S</b>, Feltis B, Wright P, and Lopata AL. Investigating the immunomodulatory nature of zinc oxide nanoparticles at sub-cytotoxic levels <i>in vitro</i> and after intranasal instillation <i>in vivo</i>. <i>Journal of Nanobiotechnology</i> 2015, 13:6</p>	
Name of Candidate and other co-authors	Nature and extent of the intellectual input of each author, including the candidate
<p><b><u>Candidate:</u></b> Shruti Saptarshi (S.S.)</p> <p><b><u>Co-authors:</u></b> Bryce Feltis (B.F.) Paul Wright (P.W.) Andreas L. Lopata (A.L.)</p>	<p>S.S. participated in planning the experimental strategy, conducted the experiments and wrote the first draft of the manuscript. B. F., P.W and helped in critical assessment of the data and drafting of the manuscript. A.L. provided advice on the theme of the manuscript, supervised the study, participated in data analysis and provided final approval of the manuscript. All authors have approved the final manuscript.</p>

---

<b>Saptarshi S</b> , Duschl A and Lopata AL. Biological reactivity of zinc oxide nanoparticles in mammalian test systems: an overview. <i>Nanomedicine</i> (Editorially accepted)	
<b>Name of Candidate and other co-authors</b>	<b>Nature and extent of the intellectual input of each author, including the candidate</b>
<p><b><u>Candidate:</u></b> Shruti Saptarshi (S.S.)</p> <p><b><u>Co-authors:</u></b> Albert Duschl (A.D.) Andreas L. Lopata (A.L.)</p>	<p>S.S. has conducted the literature review and written the first draft of the manuscript. A.D. and A.L. and provided advice on the theme of the manuscript and also helped to edit, revise and provided final approval of the manuscript. All authors read and approved the final manuscript.</p>

## Acknowledgements

My journey as a PhD student has been an exciting and enlightening experience of my life and throughout there have been so many wonderful people who have helped me accomplish my goal. Not only has this experience made me a better academic but also a better human being. Through the medium of this thesis, I would like to extend my sincere gratitude and appreciation to all these amazing people

First and foremost, I would like to thank my mentor **A/Prof. Andreas L Lopata**. I cannot thank him enough for his patience, encouragement, inspiration and support with this project. I consider myself extremely lucky to have met Andreas. He has been instrumental in shaping my research outlook, inculcating in me, critical thinking and ability to apply scientific knowledge. His knowledge, interdisciplinary approach to problem solving, perfectionism has left a long lasting impression on me.

I would also like to thank my co-supervisors **Dr. Bryce Feltis** and **A/Prof. Paul Wright** at RMIT University for their continued assistance and great guidance. Also thanks to **Prof. Albert Duschl** from University of Salzburg and his team including **Ms Isabella Radauer-Preiml** and **Dr. Matthew Boyles** for sharing their lab and knowledge on novel scientific technologies.

My sincere thanks to **Dr. Yi Hu** (Advanced Analytical Centre) and **Dr. David Wilson** (Cairns campus Mass spectrometry facility), of James Cook University for their help with sample analysis for my thesis. Thanks the **Dr. ShanShan Sun** for teaching me the basics of animal cell culture, **Dr. Fiona Baird** for teaching me how to use the confocal laser scanning microscope and **Ms. Dinh Thi Xuyen** for teaching me flow cytometry. Thank you **Mr. Scott Blyth** from the Veterinary sciences at James Cook University for teaching basics of animal handling and helping me organise my mouse experiments. Your help was central to this project.

I would like to acknowledge all the funding bodies – NHMRC project grant #616621, ARC Future Fellowship for A/Prof. Andreas Lopata, Australian Post Graduate award and JCU School of Pharmacy and Molecular Sciences top-up

scholarship for my stipend. North Queensland Festival of Life sciences, Faculty of Medicine, Health and Molecular Sciences, James Cook University for providing me the opportunity to attend two international conferences, Robert Logan Bursary and the Doctoral completion fund for providing me the much needed financial support.

I would like to thank my colleagues Sandip, ShanShan, Rony, Michael, Juan for all the fun times and brainstorming sessions on different topics during the course of my PhD journey. Special thanks to **Dr. Kasturi Reddy Lopata** for patiently going through every word and sentence of my thesis and helping me polish it. Also I appreciate all those wonderful conversations, coffee shop visits with her.

I am grateful to **Ms. Maree Hines, Ms Mel Hines, Ms. Ohlu Wickramaratna, Mr. David Jusseaume, Mr Startis Manolis and Mr. Darren Mylrea** who helped me with complicated endeavours besides research including administrative paperwork, ordering and IT support. All their help, time and patience are much appreciated.

Through the medium of this thesis I would like to convey my heartfelt thanks to **Dr. Sandip Kamath** my loving best-friend, partner, guide and husband. Thank you for being so understanding and patient with me, keeping me sane and positive especially during difficult times. You have always encouraged me to do my best have always seen confidence in me that sometimes even I am unaware of. I owe all my accomplishments to you....your endless love, positive attitude and support has made this possible. I love you.

Finally thanks to my most beloved **Aai, Papa and Aaji** for their unconditional love, support, prayers and sacrifices for making all the possible opportunities available to me. All that I have accomplished today is because you all believed in me. I hope I have made you proud. Also thanks to my **extended family, my in-laws** for their love support and blessings.

**-Shruti Saptarshi-Kamath**

**Dedication**

*To Almighty God*

*My dearest parents Bhagyashree Saptarshi, Ravindra*

*Saptarshi, my grandmother Vibha Kalele and*

*My most beloved, my life-partner Dr. Sandip Kamath*

## Abstract

Engineered zinc oxide nanoparticles (ZnO-NPs) offer versatility and properties that have a vast array of applications, and are widely used in cosmetics and sunscreens, because of their excellent UV filtering properties and aesthetic appeal. Interestingly, despite high production volumes and a broad application base, there is always a possibility of unintentional side-effects of NPs due to their increased reactivity at the biological level. Bio-reactivity of nanoparticles can be influenced by their physical characteristics such as size, surface coating and propensity to interact with proteins. The main objective of this PhD thesis was to investigate and characterise the phenomenon of protein corona formation on ZnO NP surface in a protein rich environment such as cell culture medium, evaluate the nanotoxicological potential of these NPs using *in vitro* as well as *in vivo* test systems and furthermore relate this information to their physico-chemical properties

NP-protein interactions as reviewed in chapter II can be affected by the primary size and agglomeration state of the NPs. Therefore accurate characterisation of the NP physico-chemical properties is vital. ZnO NP solutions of three different sizes, 30 nm, 80 nm and 200 nm in pristine and surfactant dispersed forms were characterised for their size, agglomeration and solubility in chapter III. Analytical disc centrifugation technique was chosen to determine the agglomeration state of the ZnO NPs in a protein enriched cell culture medium. The pristine ZnO NPs formed micron-sized agglomerates whereas; surfactant-treated material remained relatively mono-dispersed. Extracellular dissolution of ZnO NPs has been shown to affect their cellular interaction. Using ICP-AES technique I confirmed that the ZnO NPs used in this study have a low dissolution rate in cell culture medium.

Chapter IV of this thesis explored the identification and characterisation of the proteins adsorbed on the surface of ZnO NPs upon interaction with protein fortified cell culture medium which forms the foundation of good nanotoxicological studies. NPs due to their unique sizes interact with protein molecules, forming the NP-protein corona (NP-PC) that may influence their bio-reactivity. The adsorption of proteins on ZnO NP surface was instantaneous and did not change with time. Subsequent mass spectrometric analysis of the isolated ZnO NP-PC revealed enrichment of proteins

with definite physiological roles, on the two 30 nm ZnO NP surfaces analysed. Interestingly, pristine and surfactant-dispersed ZnO-NP formed specific protein coronas by selectively binding low molecular weight proteins, derived from larger proteins such as haemoglobin, histones, fibrinogen etc. Interestingly, ZnO-NP induced protein conformational change depended on the type of protein interacting with the NP surface. ZnO NPs were also able to retain their BSA pre-coating after transfer into a new solution of cell lysate proteins, which demonstrated for the first time that, the protein corona formation of ZnO NPs is a constantly evolving process. Flow cytometry based side and forward scatter (measures of cytoplasmic granularity and size of cells respectively) analysis of human lung epithelial cells (A549) was largely affected when they were exposed to the 30 nm ZnO NP solutions dispersed in the absence of proteins vs 10% fetal bovine serum proteins. Furthermore, ZnO NP induced cytotoxicity at 100 µg/mL concentration was also significantly affected in the presence of increasing amounts of FBS proteins (10 or 40%). This clearly demonstrated that the adsorbed protein layer onto the NP surface influenced ZnO NP uptake and cytotoxicity.

Zinc oxide nanoparticles have been classified in to the category of highly reactive metal oxide NPs as outlined in chapter V. Exposure to ZnO NPs can occur not only via skin contact, but also via inhalation especially in the manufacturing sector and is an important occupational safety concern. Chapter VI of this thesis evaluates the capacity ZnO NPs in eliciting cytotoxicity and immunomodulation in human lung epithelial (A549) cells. The A549 cells represent the type II alveolar cells which form the first line of defence against inhaled particulate matter and were therefore chosen as suitable targets for this study. Direct exposure to ZnO NPs resulted in a size and dose-dependent cytotoxic response, indicated by decreased cell viability and increased lactate dehydrogenase release. DAPI staining of nuclear material in exposed cells revealed that cytotoxicity was mediated by apoptosis. The main objective of this section was to further investigate the immunomodulatory potential of ZnO NPS at the sub-cytotoxic level. The sub-cytotoxic ZnO NP concentration (20 µg/mL) induced significant up-regulation of the key pro-inflammatory cytokine IL-8 and redox stress marker heme oxygenase-1 at the mRNA level along with increased release of IL-8 protein in a time-dependent manner. The low doses of ZnO NPs also demonstrated that the increased expression of IL-8 involved transcriptional activation

of NF $\kappa$ B, followed by further stabilisation of IL-8 mRNA by p38 mitogen activated protein kinase pathway. Pre-treatment of A549 cells with the sulfhydryl antioxidant N-acetyl cysteine resulted in significant reduction in the up-regulation of inflammatory markers, thus confirming the role of reactive oxygen species in the observed reactivity. This data highlights the inflammatory potential of ZnO NP at sub-cytotoxic doses, possibly due to a redox imbalance generated in exposed cells. This chapter increases our understanding of the kinetics and mechanisms underlying the observed immune modulatory and cytotoxic effects of ZnO NPs.

The last module of this thesis, chapter VII analysed the reactivity of ZnO NPs-*in vivo* system. 30nm ZnO NPs not only demonstrated differential protein binding but also higher cytotoxicity and pro-inflammatory potential *in vitro* and were consequently selected for the murine model investigation. Intranasal instillation of ZnO NPs and their ability to cause systemic inflammatory response in an acute high-dosage exposure animal model has not been investigated before. In this study, administration of a single dose (5 mg/kg BW) of either 30nm ZnO NP solutions resulted in substantial inflammatory infiltration into the alveoli and peri-bronchial regions of exposed mice. 24hr after the NP challenge. Significant up-regulation of eotaxin mRNA was also observed in the lung tissue obtained from mice treated with pristine 30nm. Cytokine profiling of pooled mouse serum from each NP treated or control mice groups revealed the presence of pro-inflammatory chemokines such as MCP-1, RANTES, IP-10 which known to recruit leukocytes to inflammatory sites. The preliminary results of the *in vivo* study highlight the inflammatory potential of inhaled ZnO NPs.

In conclusion, this thesis describes the dynamic interaction of serum proteins with sunscreen ZnO NPs and their strong immunomodulatory potential at a sub-cytotoxic dose. Moreover exposure to a single but relatively high dose of ZnO NPs via intranasal instillation causes acute pulmonary inflammatory reactions *in vivo*. The outcome of this thesis assists towards development of bio-compatible ZnO NPs for future use.

---

## Table of Contents

<b>Statement of Contribution .....</b>	<b>i</b>
<b>Author Contributions .....</b>	<b>iii</b>
<b>Acknowledgements .....</b>	<b>v</b>
<b>Abstract .....</b>	<b>viii</b>
<b>Table of contents .....</b>	<b>xi</b>
<b>List of tables .....</b>	<b>xvii</b>
<b>List of figures .....</b>	<b>xviii</b>
<b>List of abbreviations .....</b>	<b>xxii</b>
<b>Chapter I: Introduction and thesis outline .....</b>	<b>1</b>
1.1 Introduction.....	1
1.2 Zinc oxide nanoparticles.....	2
1.3 Research motivation.....	2
1.4 Thesis synopsis.....	6
1.4.1 Chapter II.....	6
1.4.2 Chapter III.....	6
1.4.3 Chapter IV.....	7
1.4.4 Chapter V.....	7
1.4.5 Chapter VI.....	7
1.4.6 Chapter VII.....	8
1.4.7 Chapter VIII.....	8
1.5 References .....	8

---

<b>Chapter II: Literature review of nanoparticle-protein interactions and relation to bio-reactivity of the nanoparticle.....</b>	<b>9</b>
2.1 Introduction.....	9
2.2 Nanoparticle protein corona .....	9
2.3 Nanoparticles induced changes in the structure of adsorbed proteins .....	13
2.4 Nanoparticle-protein corona: implication on cellular interactions....	18
2.5 Physico-chemical characteristics of the nanoparticle surface influence protein adsorption and therefore cellular interactions.....	22
2.6 Analytical approaches to study nanoparticle-protein interactions ...	25
2.7 Conclusion.....	29
2.8 References .....	30
<b>Chapter III: Physico-chemical characterisation of zinc oxide nanoparticles .....</b>	<b>40</b>
3.1 Introduction.....	40
3.2 Materials and methods .....	40
3.2.1 Nanoparticles.....	40
3.2.2 Dispersion protocol .....	41
3.2.3 Transmission electron microscopy (Cryo-TEM).....	42
3.2.4 Differential centrifugation sedimentation .....	42
3.2.5 Quantification of ZnO-NP dissolution in cell culture medium .....	43
2.3 Results .....	45
3.3.1 Determination of ZnO NP morphology and size (Cryo-TEM) .....	45
3.3.2 Determination of agglomerate size of ZnO NPs in cell culture medium (Disc centrifugation) .....	46

---

---

3.3.3 Quantification ZnO-NP dissolution in cell culture medium	49
3.4 Discussion .....	50
3.6 Conclusion.....	51
3.7 References .....	52
<b>Chapter IV: Physico-chemical characterisation of zinc oxide nanoparticles</b> .....	<b>54</b>
4.1 Introduction.....	54
4.2 Materials and methods .....	56
4.2.1 Nanoparticle characterisation.....	56
4.2.2 Isolation and detection of the ZnO NP-FBS protein corona using SDS PAGE.....	56
4.2.3 Protein identification by mass spectrometry .....	56
4.2.3.1 In-gel digestion.....	56
4.2.3.2 HPLC and MS/MS analysis.....	57
4.2.3.3 Mascot searches.....	58
4.2.4 Investigating the evolution of NP-PC on ZnO NP surface.....	58
4.2.5 Quantification of bound protein on ZnO NP surface .....	58
4.2.6 Circular Dichroism spectroscopy .....	59
4.2.7 ZnO NP protein corona and bio-reactivity .....	60
4.2.7.1 Cell culture .....	60
4.2.7.2 Protein dependent association of ZnO NPs with A549 cells .....	60
4.2.7.3 ZnO NP interactions and effect on cytotoxicity....	61
4.3 Results .....	63
4.3.1 ZnO NP protein profiling using SDS PAGE.....	63

---

---

4.3.2 Protein identification by mass spectrometry .....	65
4.3.3 Investigating the evolution of the NP-PC on ZnO NP surface .....	67
4.3.4 Quantification of protein bound on ZnO NP surface .....	69
4.3.5 Circular dichroism spectroscopy .....	72
4.3.6 Protein-dependent association of ZnO NPs with A549 cells .....	76
4.3.7 ZnO NP interactions and effect on cytotoxicity .....	78
4.4 Discussion .....	81
4.5 Conclusion .....	88
4.6 References .....	89
<b>Chapter V: Literature review of the reactive nature of zinc oxide nanoparticles with <i>in vitro</i> and <i>in vivo</i> mammalian test systems .....</b>	<b>95</b>
5.1 Introduction .....	95
5.2 ZnO NP mediated cytotoxicity: Cell type .....	95
5.3 ZnO NP mediated cytotoxicity: Effect of NP size and shape. ....	96
5.4 ZnO NP mediated cytotoxicity: <i>In vitro</i> test systems .....	97
5.5 ZnO NP mediated cytotoxicity: ZnO NP dissolution .....	98
5.6 ZnO NP mediated cytotoxicity: Reactive oxygen species .....	99
5.7 ZnO NP mediated immunomodulatory responses .....	101
5.8 ZnO NP mediated apoptosis and genotoxicity .....	105
5.9 ZnO NP mediated cytotoxicity and inflammatory responses in animal models .....	111
5.10 Conclusions .....	117
5.11 References .....	118

---

---

**Chapter VI: Time dependent pro-inflammatory response of zinc oxide nanoparticles on human lung epithelial cells at sub-cytotoxicity levels .131**

6.1 Introduction.....	131
6.2 Materials and Methods.....	133
6.2.1 Nanoparticles.....	133
6.2.2 <i>In vitro</i> nanoparticle exposure.....	133
6.2.3 Cytotoxicity assays.....	134
6.2.4 Visualisation of intracellular zinc levels of A549 cells exposed to ZnO NPs.....	135
6.2.5 DAPI staining and confocal microscopy.....	135
6.2.6 RNA isolation and quantitative-PCR (q-PCR).....	136
6.2.7 IL-8 ELISA.....	136
6.2.8 Effect of sulfhydryl antioxidant.....	136
6.2.9 Cell signalling: Immunoblotting for NFκB, p-38 MAPK pathway activation.....	137
6.2.10 Statistics.....	137
6.3 Results.....	138
6.3.1 Cytotoxicity profile.....	138
6.3.2 Visualisation of intracellular zinc levels of A549 cells exposed to ZnO NPs.....	141
6.3.3 DAPI staining and confocal microscopy.....	142
6.3.4 Up-regulation of pro-inflammatory IL-8 and stress-responsive HO-1 genes.....	143
6.3.5 IL-8 release upon ZnO NP exposure.....	145
6.3.6 Effect of sulfhydryl antioxidant.....	146
6.3.7 Confirming role of intact ZnO NPs in eliciting pro-inflammation.....	149
6.3.8 Cell signalling.....	151
6.4 Discussion.....	153
6.5 Conclusion.....	158
6.6 References.....	159

---

<b>Chapter VII: Investigating pro-inflammatory effects of acute ZnO NP exposure in a murine model via the intranasal route .....</b>	<b>164</b>
7.1 Introduction.....	164
7.2 Materials and Methods.....	166
7.2.1 Nanoparticles.....	166
7.2.2 Animals.....	166
7.2.3 Experimental strategy.....	166
7.2.4 Serum Collection.....	167
7.2.5 Lung histology.....	167
7.2.6 Lung tissue RNA isolation and quantitative-PCR (q-PCR) .....	167
7.2.7 Proteome profile assay.....	168
7.2.8 Statistical analysis.....	168
7.3 Results.....	169
7.3.1 Lung histology.....	169
7.3.2 Lung tissue RNA isolation and quantitative-PCR (q-PCR) .....	170
7.3.4 Proteome profile assay.....	171
7.4 Discussion.....	173
7.5 Conclusion.....	175
7.6 References.....	176
<b>Chapter VIII: General discussion, conclusion and future directions .....</b>	<b>179</b>
8.1 Discussion.....	179
8.2 Conclusion.....	183
8.3 Future directions.....	184
8.4 References .....	185
<b>Appendix A: Buffers and Solutions.....</b>	<b>188</b>
<b>Appendix B: Author's achievements.....</b>	<b>190</b>

---

---

## List of Tables

<b>Table 2.1</b> Comprehensive overview if serum/plasma proteins adsorbed on the surface of different types of nanomaterials with varies size and surface chemistries.....	<b>12</b>
<b>Table 2.2</b> Table to summarize literature on proteins subjected to conformational changes upon interaction with nanoparticle surfaces.....	<b>17</b>
<b>Table 2.3</b> Summary of analytical techniques to conduct physico-chemical characterisation, monitor nanoparticle surface driven protein conformational changes and uptake of nanoparticles by cellular structures .....	<b>28</b>
<b>Table 3.1</b> Particle primary size and surface area characterisation.....	<b>48</b>
<b>Table 3.2</b> Dissolution rates of ZnO NPs, used in the present study quantified using ICP-AES .....	<b>49</b>
<b>Table 4.1</b> List of identified fetal bovine serum proteins constituting the nanoparticle-protein corona on ZnO NP surface using mass spectrometry.....	<b>66</b>
<b>Table 4.2</b> Protein binding capacity of ZnO NPs when incubated in different protein solutions and estimation of the surface coverage of ZnO NP in terms of number of individual protein molecules assuming spherical NP morphology.....	<b>71</b>
<b>Table 5.1</b> Overview of recent <i>in vitro</i> studies (2012-2014) discussing the interaction of ZnO NPs with different mammalian cell types.....	<b>109</b>
<b>Table 5.2</b> Overview of recent <i>in vivo</i> studies (2012-2014) discussing effect of exposure to ZnO NPs via various routes in animals.....	<b>115</b>

---

## List of Figures

<b>Figure 1.1</b> A schematic depicting the size of nanomaterials relative to bio-molecules and bacteria .....	<b>1</b>
<b>Figure 1.2</b> Applications of ZnO NPs range from sunscreen formulations to cosmetics, UV absorbing paints as well as textiles .....	<b>2</b>
<b>Figure 1.3</b> A schematic of the possible fate of nanoparticles when exposed to a biological system.....	<b>3</b>
<b>Figure 1.4</b> Summary of the experimental approach and methodology used in this thesis.....	<b>5</b>
<b>Figure 2.1</b> A schematic representation of NP surface induced unfolding of the interacting protein molecule and consequences.....	<b>15</b>
<b>Figure 2.2</b> Interaction of nanoparticles with the cellular interface .....	<b>19</b>
<b>Figure 2.3</b> Schematic representation of the commonly used strategy to isolate and identify surface adsorbed proteins, when nanoparticles interact with complex protein mixtures .....	<b>25</b>
<b>Figure 3.1</b> Zinc oxide nanoparticles used in the present study.....	<b>41</b>
<b>Figure 3.2</b> Schematic of the ZnO NP dispersal protocol used throughout this thesis.....	<b>42</b>
<b>Figure 3.3</b> A schematic describing the approach and sample preparation for quantification of dissolved ZnO NP in cell culture medium.....	<b>43</b>
<b>Figure 3.4</b> Transmission electron microscopy images of ZnO NPs dispersed in distilled water.....	<b>45</b>
<b>Figure 3.5</b> Cryo-TEM images of ZnO NPs incubated in cell culture media with 10% serum for 24 hr.....	<b>46</b>

---

<b>Figure 3.6</b> Disc centrifugation plots showing the agglomeration capacity of different ZnO NPs when incubated in protein supplemented cell culture medium for 4 or 24 hr.....	<b>47</b>
<b>Figure 4.1</b> SDS-PAGE of ZnO NP bound fetal bovine serum proteins demonstrating effect of incubation time on protein adsorption .....	<b>64</b>
<b>Figure 4.2</b> SDS-PAGE of proteins adsorbed by pristine or surfactant dispersed 30 nm ZnO NPs used for subsequent identification by mass spectrometry. ....	<b>65</b>
<b>Figure 4.3</b> (A) SDS-PAGE demonstrating difference in protein banding of 30 or s30 ZnO NPs when dispersed in increasing concentrations (0.1-10%) of FBS proteins. (B) Immunoblotting analysis used to confirming the identity of the most prominent protein band on the ZnO NP surface to be that of bovine serum albumin.....	<b>67</b>
<b>Figure 4.4</b> Evolution of the ZnO NP-PC.....	<b>68</b>
<b>Figure 4.5</b> Protein binding capacity of ZnO NP and particulates .....	<b>70</b>
<b>Figure 4.6</b> Comparison of CD spectra of native BSA (blue curve) with BSA adsorbed on varying concentrations of 30 or s30 ZnO NPs .....	<b>73</b>
<b>Figure 4.7</b> CD spectra of common blood proteins after interaction with pristine or surfactant-dispersed ZnO NPs.....	<b>75</b>
<b>Figure 4.8</b> Flow cytometry analysis of ZnO NP uptake or association with A549 cells.....	<b>77</b>
<b>Figure 4.9</b> Changes in cell morphology of lung epithelial A549 cells after treatment with pristine 30 nm ZnO NPs .....	<b>78</b>
<b>Figure 4.10</b> Evaluating the effect ZnO NP-PC formed in the presence of varied amounts of FBS proteins, on the overall cytotoxic capacity of these NPs when exposed to A549 cells.....	<b>79</b>
<b>Figure 5.1</b> A schematic representation of interaction of ZnO NPs with a model cellular interface and resulting pro-inflammatory consequences.....	<b>104</b>

---

- 
- Figure 5.2** Schematic representation of interaction of ZnO NPs with a model cell surface focussing on the cytotoxicity ..... **108**
- Figure 6.1** Cytotoxicity profiles of pristine and surfactant-dispersed ZnO NPs after 24hr exposure of human lung epithelial A549 cells, using the (A) MTS assay and (B) lactate dehydrogenase release assays ..... **139**
- Figure 6.2** Visualizing labile zinc using zinquin a zinc specific dye in A549 cells exposed to sub-cytotoxic concentration of ZnO NPs or ZnCl<sub>2</sub> ..... **141**
- Figure 6.3** Confocal images of A549 cells treated with 100 µg/mL (cytotoxic dose) ZnO NPs for 24hr, followed by staining with DAPI nuclear stain to visualise changes in nuclear morphology characteristic of apoptotic cell death ..... **142**
- Figure 6.4** ZnO NP induced up-regulation of (A) heme oxygenase-1 and (B) interleukin-8 genes in treated A549 cells over a 24hr exposure period..... **144**
- Figure 6.5** Release of pro-inflammatory cytokine IL-8 by ZnO NP-exposed A549 cells over a 24hr exposure period..... **145**
- Figure 6.6** Viability of A549 cells exposed to increasing concentrations of antioxidant NAC for 24hr..... **146**
- Figure 6.7** Mitigation of the up-regulation of (A) HO-1 mRNA expression and (B) IL-8 mRNA expression (C) IL-8 cytokine release in antioxidant treated A549 cells after exposure to ZnO NPs (20 µg/mL) for 6hr..... **147**
- Figure 6.8** Confirming role of intact ZnO NPs in eliciting pro-inflammation .. **150**
- Figure 6.9** Immunoblotting showing (A) phosphorylation of p38 protein, belonging to the redox-sensitive p38 Mitogen activated protein kinase (MAPK) pathway and (B) p65 protein, involved in NFκB activation, after exposing A549 cells to 20 µg/mL dose of ZnO NPs..... **152**
- Figure 6.10** Schematic showing the onset of antioxidant and pro-inflammatory responses of A549 cells when exposed to (A) sub-cytotoxic doses of ZnO NPs or cytotoxic response when exposed to (B) cytotoxic doses of ZnO NPs ..... **157**
-

---

<b>Figure 7.1</b> Schematic of the experimental strategy used for the <i>in vivo</i> experiment .....	<b>167</b>
<b>Figure 7.2</b> H&E staining of lung sections of mice treated with (A) vehicle control, (B) LPS, (C) pristine 30nm ZnO NPs and (D) surfactant-dispersed 30nm ZnO NPs via intratracheal instillation .....	<b>169</b>
<b>Figure 7.3</b> q PCR analyses of mRNA levels for inflammatory markers (A) eotaxin, (B) MCP-1 and (C) TNF $\alpha$ in the lung tissues of treated mice.....	<b>170</b>
<b>Figure 7.4</b> Proteome profile array of pro-inflammatory cytokines quantified in pooled sera from each experimental group .....	<b>172</b>

---

## List of Abbreviations

ALI	Air liquid interface
ANOVA	Analysis of variance
BSA	Bovine serum albumin
BSAI	Biological surface adsorption index
CD	Circular dichroism spectrometry
CO <sub>2</sub>	Carbon dioxide
Cryo-TEM	cryogenic transmission electron microscopy
DCS	Differential centrifugation sedimentation
DPBS	Dulbecco's phosphate buffered saline
EC20	effective concentration causing 20% response
EC50	effective concentration causing 50% response
ELISA	Enzyme-linked immunosorbant assay
FBS	Fetal Bovine serum
FePt-NP	Iron-Platinum Nanoparticles
FS	Fluorescence spectroscopy
FS	Forward Scatter
FTIR	Fourier transformed infrared spectrometry
H&E	Haematoxylin and eosin
HBSS	Hank's Balanced Salt Solution
HDL	High density lipoprotein
HO-1	Heme oxygenase-1
HPLC	High pressure liquid chromatography
HSA	Human serum albumin
ICP-AES	Inductively Coupled Plasma Atomic Emission Spectroscopy
Ig	Immunoglobulin
IL	Interleukin
IT	Intratracheal instillation
LDH	Lactate dehydrogenase
m/z	Mass to charge ratio
MCP-1	Monocyte chemoattractant protein 1
MS	Mass spectrometry
MTS	[3-(4,5-dimethylthiazol-2-yl)-5-(3-carboxymethoxyphenyl)-2-(4-sulfophenyl)-2H-tetrazolium, inner salt
MW	Molecular weight
MWCNT	multi walled carbon nanotubes

NAC	n-acetylcysteine
nm	nanometer
NMR	Nuclear magnetic resonance
NP	Nanoparticles
NP-PC	Nanoparticle-protein corona
PBS	Phosphate buffered saline
PEG	Polyethylene glycol
PMN	Polymorphic neutrophils
PMSF	Phenylmethylsulfonyl fluoride
ppm	Parts per million
RNA	Ribonucleic acid
ROS	Reactive oxygen species
RPMI	Roswell Park Memorial Institute
RS	Raman spectroscopy
SDS-PAGE	Sodium dodecyl sulphate polyacrylamide gel electrophoresis
SiO <sub>2</sub>	Silicon dioxide
SPION	Superparamagnetic iron oxide nanoparticles
SS	Side Scatter
SWCNT	Single walled carbon nanotubes
sZno	Surfactant dispersed zinc oxide
TEM	Transmission electron microscope
TiO <sub>2</sub>	Titanium dioxide
TLR	Toll like receptors
TNF $\alpha$	Tumor necrosis factor alpha
UV	Ultraviolet
Zn	Zinc
ZnO	Zinc oxide



---

## **Chapter I**

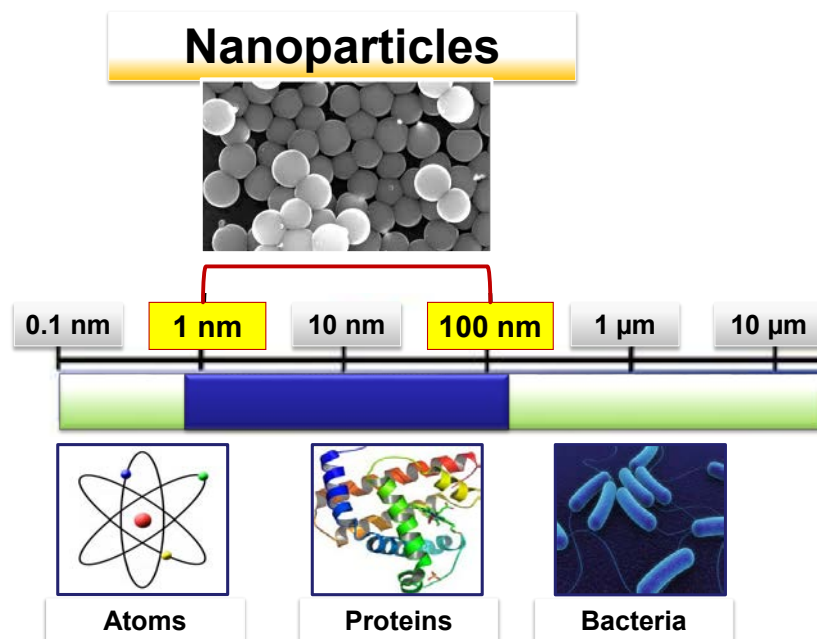
### **Introduction and thesis outline**

---



## 1.1 Introduction

Nanotechnology is the science of miniaturization of matter to the nano scale. It involves controlled synthesis of materials where at least one of their dimensions is  $<100$  nm (Figure 1.1). Interestingly, at the nano scale materials develop unique properties compared to their larger counterparts. This is caused by the enormous increase in their surface area to mass ratio. A rapid advance in the methods of generating newer types of nanomaterials has enabled numerous applications for these novel materials. Applications of nanomaterials in electronics, structural materials, as functional surfaces, packaging, pharmaceuticals and in the medical field are common, and this sector has been estimated to become worth \$1 trillion by the end of 2015 [1].



**Figure 1.1** Schematic depicting the size of nanomaterials relative to biomolecules and bacteria.

## 1.2 Zinc oxide nanoparticles

Zinc oxide has been described as a multifunctional material due to its high chemical, mechanical and thermal stability along with other properties such as broad range radiation absorption and high photo stability. Zinc oxide nanoparticles (ZnO NPs) can be engineered to form nanorods, needles, spheres etc. Among various other metal oxide NPs, ZnO NPs are manufactured in high volumes. In the pharmaceutical and cosmetics industries, ZnO NPs are commonly used in sunscreen formulations due to their ability to absorb UVA and UVB radiations and enhanced aesthetic appeal due to their transparent nature. Recently, ZnO nanowires have also found application in the textile industry as antibacterial and UV absorbing coatings [2]. Also, ZnO NPs are now increasingly used in the nano medicine and biotechnology sectors as potential drug delivery agents, and as anti- cancer therapeutics [3, 4].

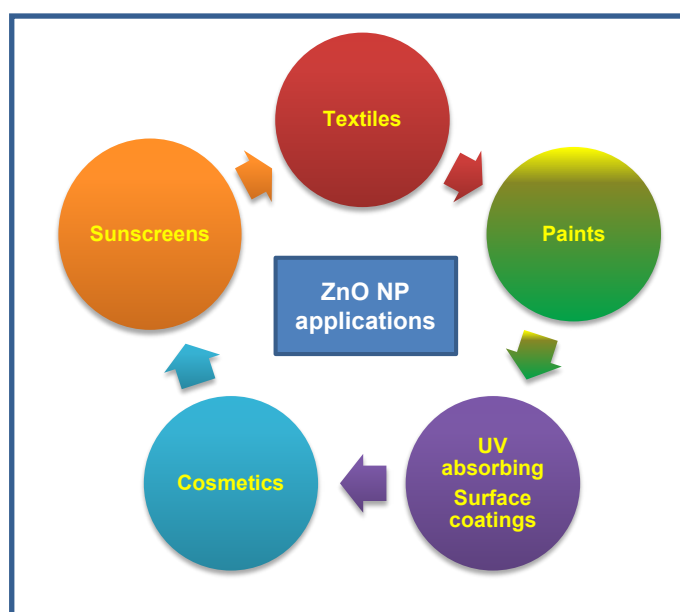
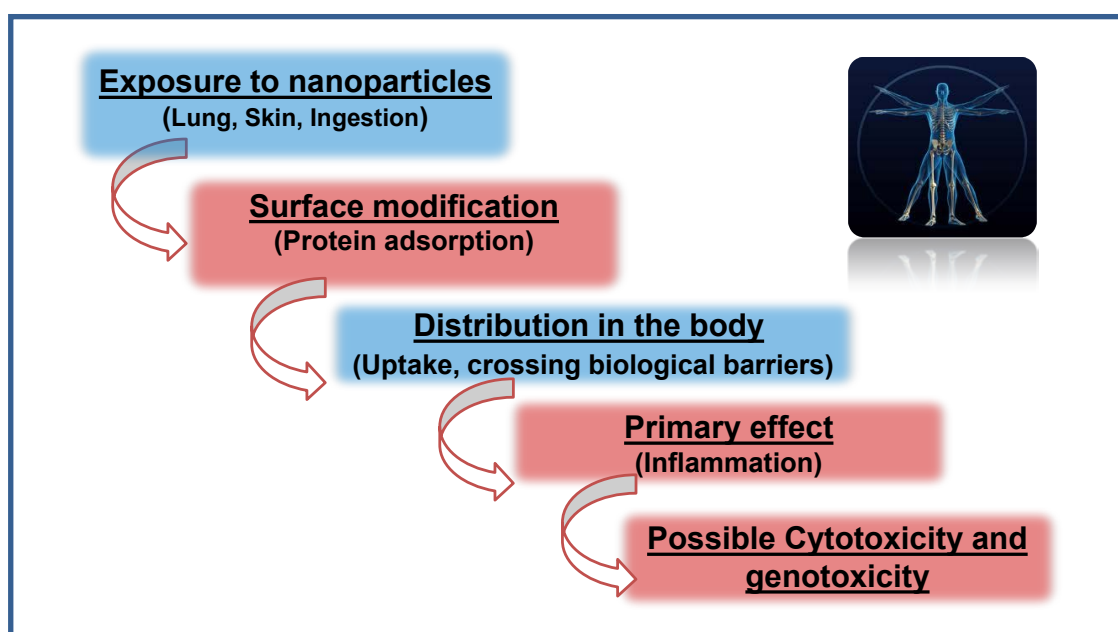


Figure1.2 Applications of ZnO NPs range from sunscreen formulations to cosmetics, UV absorbing paints as well as textiles.

## 1.3 Research Motivation

Despite being a frontier technology, there have been some important safety concerns regarding the use of nanoparticles particularly for ZnO NPs, which are manufactured in high tonnage. Exposure to NPs can occur via several different routes such as ingestion, skin penetration and inhalation. Of all these entry

routes, inhalation of NPs is a major concern particularly considering the work place scenario where NPs are manufactured or added to other products. As compared to larger particulates nanoparticles can access deeper regions of the body and gain direct entry into the vital organs resulting in adverse health effects. Therefore it is imperative to clearly understand their reactivity with complex biological systems. The following schematic (Figure 1.3) explains the possible fate of a NP when it encounters a complex biological system such as the human body.



**Figure 1.3** A schematic of the possible fate of nanoparticles when exposed to a biological system (adapted from [5])

Interestingly, due to their unique size, NPs can easily interact with biomolecules such as proteins, which can lead to modification of the NP surface. Depending on the identity and possible changes in the structure of these adsorbed proteins, the fate of the NP *in vivo* can be affected. Likewise, physico-chemical properties of the NP, such as aggregation state, size, dispersal state etc. can also define their behaviour in biological solutions. Furthermore the overall biological reactivity of the NP can be compounded if the nanomaterial is inherently reactive in nature. This is true for ZnO NPs, which are known to be reactive because of their propensity to dissolve and generate reactive  $Zn^{2+}$  ions. Based on this background information, the principle hypothesis of this thesis is that, **“the agglomeration state and size of ZnO NPs may dictate their overall bio-reactivity including, protein interaction and immunotoxic**

**potential.**” The main aims of this PhD thesis were to achieve biological characterisation of ZnO NPs, which are commercially important in Australia. This was targeted using two separate approaches, 1) The proteomics based approach to identify and characterise the interaction of ZnO NPs with proteins in a typical cell culture medium and 2) The nanotoxicology approach aimed at investigating the immunomodulatory and the cytotoxic potential of these NPs using an *in vitro* cell culture system of human lung epithelial cells (A549) along with an *in vivo* system of mice challenged with an acute yet high dosage of ZnO NPs via a novel route of exposure, intranasal instillation (Figure 1.4).

The chapters of this thesis have the following specific aims and are outlined as follows:

- ❖ Literature review of the NP-protein interactions (**Chapter II**)
- ❖ Physical characterisation of ZnO-NP (size, agglomeration state, solubility) (**Chapter III**)
- ❖ Probing the interactions of ZnO-NP with serum proteins in the cell culture medium environment (**Chapter IV**)
- ❖ Literature review of the biological reactivity of ZnO NPs with mammalian cells (**Chapter V**)
- ❖ Evaluation of the cytotoxic and pro-inflammatory potential of ZnO-NP on human lung epithelial cells (**Chapter VI**)
- ❖ Investigating the pro-inflammatory effects of short term ZnO-NP exposure via intra nasal route using a mouse model (**Chapter VII**)

The data generated from this thesis will add to our current understanding of the bio-reactive nature of these sunscreen metal oxide NPs that will not only help in the safety evaluation of these nanomaterials, but also help in developing a newer generation of bio-compatible NP formulations for future use.

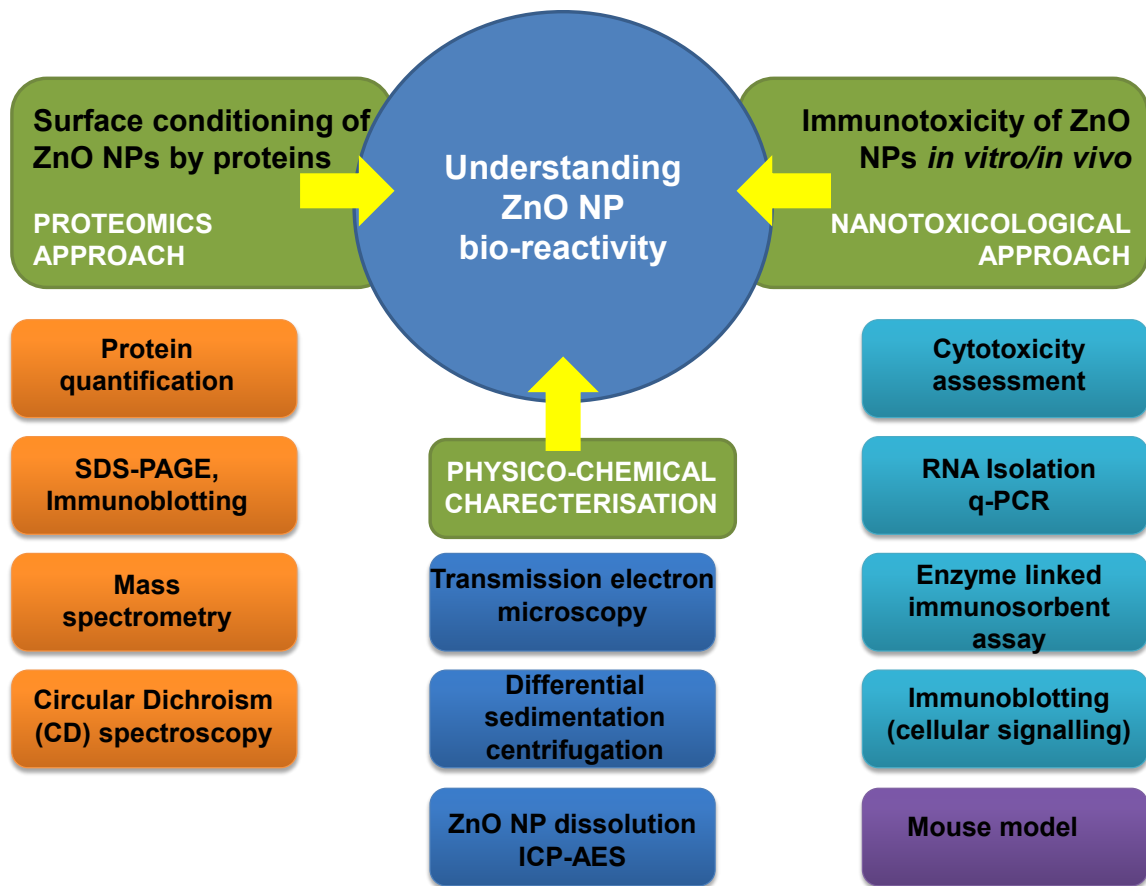


Figure 1.4 Summary of the experimental approach and methodology used in this thesis.

## 1.4 Thesis synopsis

The work undertaken in this thesis describes the bio-reactivity of ZnO NPs, with an emphasis on their physico-chemical characteristics and is based on 1) The characterisation of protein bound ZnO NP surface in a typical cell culture medium; 2) Understanding the cytotoxicity and immunomodulatory potential of these NPs *in vitro* and *in vivo*. The chapter breakdown of this thesis is as follows:

### 1.4.1 Chapter II

Interaction of nanoparticles with proteins is the basis of nanoparticle bio-reactivity. This interaction gives rise to the formation of a dynamic nanoparticle-protein corona (NP-PC). The protein corona may influence cellular uptake, inflammation, accumulation, degradation and clearance of the nanoparticles. The main aim of this review chapter is to introduce the concept of the NP-PC, factors that influence nanoparticle-protein interactions and their implications on cellular uptake.

### 1.4.2 Chapter III

Biological reactivity of engineered nanomaterials is an important repercussion of their most unique physical characteristic, the “nano” size. Apart from this other properties including, material composition, aggregation potential, electronic structure, surface coatings (active or passive), and solubility, are also important physicochemical attributes that need careful understanding. This chapter aims to thoroughly characterise the various physico-chemical attributes of ZnO NPs used in this project. The shape and size of the ZnO NPs have been characterised using transmission electron microscopy and analytical disc centrifugation techniques. The solubility of ZnO NPs has been analysed using inductively Coupled Plasma Atomic Emission Spectroscopy (ICP AES). This chapter is central to the experimental designs of the following working chapters of this thesis.

### 1.4.3 Chapter IV

The nanotoxicological potential of NPs is often assessed using *in vitro* systems. Chapter II introduces the concept of the NP-PC and the possible consequences on the NP reactivity. The protein component (10%) of a typical *in vitro* cell culture system is fetal bovine serum. The main objective of this chapter was to identify and characterise the ZnO NP-fetal bovine serum-corona. Moreover, potential modifications to the structures of the most abundant serum proteins were also investigated. The data generated from this working chapter of the thesis are central for correlating the nanotoxic endpoints of ZnO NP-cell interactions to their surface conditioning by proteins present in the *in vitro* system.

### 1.4.4 Chapter V

Zinc oxide nanoparticles have several physico-chemical advantages over their bulk counterparts and so are used extensively. This has raised concerns regarding the potential toxicity of these nanomaterials. What attributes of ZnO NPs contribute to this cytotoxicity and immune reactivity however seem to vary across literature quite considerably. The main aim of this review chapter is to give a systematic overview of the known postulates explaining cytotoxic, inflammatory and genotoxic effects of ZnO NPs when exposed to different types of cells *in vitro* and in animal models *in vivo*.

### 1.4.5 Chapter VI

A systematic understanding of the interaction of ZnO NPs with complex biological systems, and their ability to induce immune modulation or cytotoxicity, is limited and needs further investigation. Exposure to ZnO NPs via inhalation is an important concern. This chapter evaluates the capacity of industrially manufactured ZnO NPs to elicit an up-regulation of the key pro-inflammatory and stress markers in human lung epithelial (A549) cells at sub-cytotoxic doses. Furthermore, the possible mechanism involved in this response is also suggested.

### 1.4.6 Chapter VII

In the previous working chapters of this thesis the 30 nm ZnO NPs were thoroughly characterised in terms of their capacity to interact with proteins and also their potential to induce cytotoxicity and inflammatory responses in the lung epithelial cells, *in vitro*. These ZnO NPs were employed for the first time in a mouse model to investigate possible immunotoxic effects via intranasal instillation. This chapter deals with understanding the immunotoxic potential of ZnO NPs in an *in vivo* scenario.

### 1.4.7 Chapter VIII

This chapter discusses and provides a summary of the research conducted in this PhD thesis and provides information on possible future research in this area.

## 1.5 References

1. Nel A, Xia T, Madler L, Li N: **Toxic potential of materials at the nanolevel**. *Science* 2006, **311**:622 - 627.
2. Kolodziejczak-Radzimska A, Jesionowski T: **Zinc Oxide-From Synthesis to Application: A Review**. *Materials* 2014, **7**:2833-2881.
3. Hsiao IL, Huang Y-J: **Effects of serum on cytotoxicity of nano- and micro-sized ZnO particles**. *Journal of Nanoparticle Research* 2013, **15**:1-16.
4. Roy R, Singh SK, Das M, Tripathi A, Dwivedi PD: **Toll-like receptor 6 mediated inflammatory and functional responses of zinc oxide nanoparticles primed macrophages**. *Immunology* 2014, **142**:453-464.
5. Landsiedel R, Ma-Hock L, Kroll A, Hahn D, Schnekenburger J, Wiench K, Wohlleben W: **Testing Metal-Oxide Nanomaterials for Human Safety**. *Adv Mater* 2010, **22**:2601-2627.



---

## Chapter II

### Literature review of nanoparticle-protein interactions and relation to bio-reactivity of the nanoparticle

**Published in:**

**Saptarshi SR**, Duschl A, Lopata AL. Interaction of nanoparticles with proteins: relation to bio-reactivity of the nanoparticle J Nanobiotechnol 2013, 11:26. (*Highly accessed with 70 citations*)

---



## 2.1 Introduction

Nanoparticles (NPs) have unique properties that may be useful in a diverse range of applications, and consequently they have attracted significant interest. Particularly in the bio medical field, the use of nano vaccines and nano drugs are being extensively researched. Nevertheless, our knowledge about the bio-compatibility and risks of exposure to nanomaterials is limited. Exposure to nanomaterials for humans may be accidental, for example occupational exposure, or intentional, for example in the use of nano-enabled consumer products. There are an increasing number of studies that demonstrate adverse effects of nanomaterials in *in vitro* cellular systems, but it is unclear whether the available data can be reliably extrapolated to predict the adverse effects of nanotechnology for humans. Hence, there is an urgent need to understand the molecular mechanisms of nanoparticles-to-biological system interaction.

In a biological medium, NPs may interact with bio-molecules such as proteins, nucleic acids, lipids and even biological metabolites due to their nano-size and large surface-to-mass ratio. Of particular importance is the adsorption of proteins on the nanoparticle surface. The formation of nanoparticle-protein complexes is commonly referred to as the nanoparticle-protein corona (NP-PC). A number of consequences of the protein adsorption on the NP surface can be speculated. Overall, the NP-PC can influence the biological reactivity of the NP [1, 2]

This review gives a summary of the current research on the physico-chemical characteristics influencing the formation of the NP-PC, its impact on the structure of adsorbed proteins and the overall implication these interactions have on cellular functions.

## 2.2 Nanoparticle protein corona

Proteins are polypeptides with a defined conformation and carry a net surface charge depending on the pH of the surrounding medium. Adsorption of proteins at the nano-bio interface is aided by several forces such as hydrogen bonds, solvation forces, Van der Waals interactions, etc. The overall NP-PC formation is a multifactorial process and not only depends on the characteristics of the

NP, but also on the interacting proteins and the medium. Specific association and dissociation rates for each protein decide the longevity of their interaction with the NP surface. Irreversible (or at least long-term) binding of proteins on the NP leads to formation of a “hard corona” whereas quick reversible binding of proteins that have faster exchange rates defines a “soft corona” [1, 3-6].

Serum/plasma cellular proteins represent complex biological systems, and it has to be considered that NPs can form bio/nano complexes when exposed to several, very different systems *in vivo*. An inhaled NP may pass through the mucosal layer, lung epithelial cells and finally enter into the blood. Similarly, at the cellular level after being phagocytised by a monocyte, the NP may be taken into the endosomes that ultimately fuse with lysosomes. Each of these proteomes represents unique environments and has specific properties with respect to their protein composition, enzymatic activities, pH, ion composition etc. These environments may cause the NP to undergo a complex sequence of modifications that are far from being fully understood. Even within one environment the NP- protein interactions are constantly changing. For example, when exposed to blood plasma the nano-bio interface has been reported to change with time due to constant adsorption and desorption of proteins [2]. NPs that have entered the body thus have to be considered as evolving systems that are shaped by sequential exposure to different protein rich environments. Kinetics of protein adsorption on the NP surface can be influenced by several factors. Amount of proteins available to interact with the NP surface is one such factor that can greatly influence the NP-PC composition [7]. When plasma proteins were applied at concentrations between 3% and 80% of plasma, Monopoli and co-workers observed that the proteins bound to NPs varied with plasma concentration, while relative amounts of some abundant proteins adsorbed on surfaces of silica or polystyrene NPs increased with increasing plasma concentrations [8]. When travelling through different protein rich environments in an *in vivo* system the NP surface may get pre-coated with specific proteins. This can also determine which new protein will bind to the already formed NP-protein complex. Pre-coating of pulmonary surfactant proteins was shown to influence the subsequent adsorption of plasma proteins on the surface of the

multi walled carbon nanotubes (MWCNT) [9]. Also, silica or polystyrene NPs were shown to retain a “fingerprint” of plasma proteins even after subsequent incubations with other biological fluids [10].

In human plasma, a typical NP-PC consists of proteins like serum albumin, immunoglobulins, fibrinogen, apolipoproteins etc. (Table 2.1). A recent study by Hellstrand and co-workers showed the presence of high density lipoproteins in the protein corona on polystyrene NPs [11]. The adsorption pattern of blood proteins to foreign inorganic surfaces is dynamic where more abundant proteins such as albumin and fibrinogen may initially occupy the surface and get subsequently replaced by other proteins having higher binding affinity for the surface. Such a sequential binding pattern of plasma proteins is based on the Vroman [12] theory and has also been suggested for nano-surfaces. The order of plasma protein binding to single walled carbon nanotubes (SWCNT) was fibrinogen followed by immunoglobulin, transferrin and albumin [13]. Displacement of albumin by other cell lysate proteins was demonstrated for nanomaterials investigated by Sund and co-workers [14]. By contrast, plasma protein binding to ultra-small super paramagnetic iron oxide (SPION) nanoparticle surface did not follow the Vroman theory when exposed to plasma proteins [15]. Therefore, displacement of proteins with time is not a universal rule that can be taken for granted for all types of NPs.

**Table 2.1: A comprehensive overview of the serum/plasma proteins adsorbed on different types of nanomaterials with varied sizes and surfaces**

Nanomaterial used	Size (nm)	Surface chemistry	Dispersal medium	Proteins identified	Ref
Polystyrene NPs	50, 100	NH <sub>2</sub> , COOH	Human Plasma	Coagulation factors, Immunoglobulins, Lipoproteins, Complement proteins, Acute phase proteins	[15]
Polystyrene NPs	100	COOH	Human serum (depleted)	Complement proteins, Plasminogen, Anti-CD4, c4a, Immunoglobulin, Albumin, Complement, Plasminogen	[16]
Latex NPs	80-109	NH <sub>2</sub> ,NHR, NR <sub>2</sub> ,NR <sub>3</sub> <sup>+</sup> COO <sup>-</sup> , SO <sup>-</sup> <sub>3</sub> , SO <sup>-</sup> <sub>4</sub>	Human Serum	Albumin, Apolipoproteins, Immunoglobulins, Hemoglobin, Haptoglobins	[17]
Copolymer NPs	70, 200	-	Human Plasma	Albumin, Apolipoproteins, Fibrinogen, Immunoglobulins, C4BPachain	[2]
MWCNTs	20-30	NH <sub>2</sub> , COOH	Human Plasma	2 Macroglobulin precursor, Complement factors, plasminogen, Coagulation factors	[8]
SPIONs	-	-	Human Plasma	Albumin, α1Antitrypsin, Fibrinogen chains, Immunoglobulin chains, Transferrin, Transthyretin	[14]
Gold	5, 10, 20	(PAA) polymer coated	Human Plasma	Albumin, Fibrinogen chains, Apolipoprotein A1	[18]
Gold	15, 40, 80	-	Bovine Serum	Transport proteins, Coagulation factors, Tissue development proteins	[19]
TiO <sub>2</sub> NPs ZnO NPs Quartz sand Carbon nanotubes SiO <sub>2</sub> NPs	-	Silone, alumina, silica coated	Human Plasma	Fibrinogen chains, Immunoglobulin light chains, Fibrin, albumin, ApoA1, Complement component proteins, Fibronectin,	[13]
SiO <sub>2</sub> NPs	8, 20, 25	-	Human Plasma	Immunoglobulins, Lipoproteins, Complement proteins, Coagulation proteins, Acute phase proteins, Cellular proteins, Serum proteins	[20]
TiO <sub>2</sub> NPs ZnO NPs SiO <sub>2</sub> NPs	-	-	Human Plasma	Albumin, Immunoglobulins, Fibrinogen, Transferrin, Apolipoprotein A1, Complement proteins	[21]
Magnetic NPs	50, 200	Dextran COOH, NH <sub>2</sub> ,PEG COOH, PEG-NH <sub>2</sub>	Bovine Serum	Albumin, Apolipoprotein A-1 Complement factors, Vitronectin, Haemoglobin	[22]

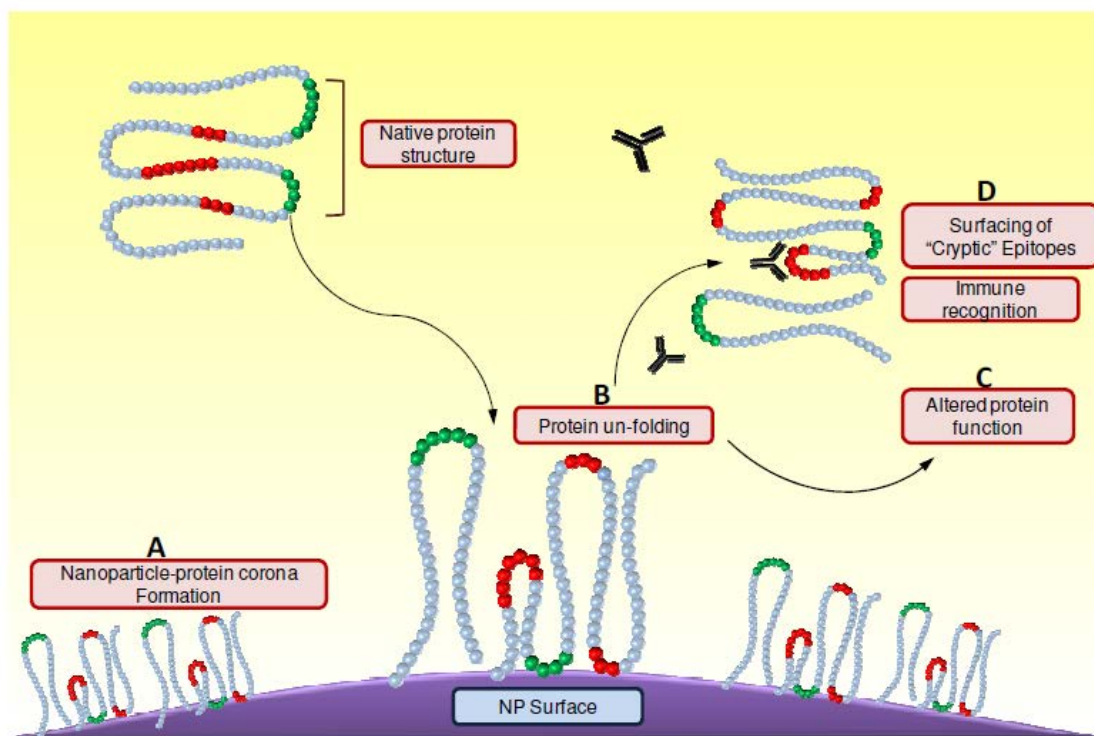
Adsorption of a protein on the NP surface also depends on the affinity of the protein towards the NP surface and its ability to completely occupy the surface. The way in which protein molecules arrange themselves on the NP surface may affect the biological reactivity of the latter at the cellular level [13]. Plasma proteins such as human serum albumin (HSA) and transferrin were shown to adsorb in a monolayer fashion on iron-platinum (FePt) NP surface [16]. Rezwan et al. observed that bovine serum albumin (BSA) adsorbs on the aluminium oxide surface as a monolayer by using 30-36% of its total negative charge and that additional BSA molecules from the medium bind onto this monolayer as dimers [17]. Detailed studies along these lines can be useful in designing protein-conjugated NP surfaces for future applications.

### **2.3 Nanoparticles induce changes in the structure of adsorbed proteins**

The NP surface can modify the structure and therefore the function of the adsorbed protein thus affecting the overall bio-reactivity of the NP. This section further explores the fate of the proteins bound on the NP surface. Curved NP surfaces compared to planar surfaces provide extra flexibility and enhanced surface area to the adsorbed protein molecules [18]. Curved NP surfaces can also affect the secondary structures of proteins, and in some cases cause irreversible changes [19]. It is interesting to note that the chemical properties of individual proteins and their structural flexibility also play an important role in regulating such surface-driven modifications to their secondary structures [20]. Gold NPs were shown to influence conformational changes in the structure of bovine serum albumin (BSA) in a dose-dependent manner [21], whereas no major conformational change was recorded for BSA when adsorbed to carbon C60 fullerene NPs [22]. TiO<sub>2</sub> NPs were shown to cause conformational change and reduce polymerization of tubulin, which is an essential cytoskeletal protein [23]. Spectroscopic investigation of ZnO-NP interaction with BSA also showed no structural perturbation to its overall structure, however, minor conformational changes were reported [24]. An irreversible conformational change in the secondary structure of the protein transferrin was observed upon interaction with SPIONs [25]. NP-induced protein conformational changes may affect the downstream protein-protein interactions, cellular signalling and also DNA

transcription, which is particularly important for enzymes. Loss of enzyme activity can result due to the conformational changes in the active site, brought about by the NP surface. SWCNTs were able to differentially induce loss of structure and catalytic activity for two enzymes investigated [3]. Turci et al. showed that RNase and lysozyme retained their native structures on silica NPs while albumin and lactoperoxidase underwent an irreversible conformational change [26]. Likewise, such conformational changes can also increase the accessibility of the enzyme active site for its substrate. Silica NPs were able to induce a molten globule-like conformational change in human carbonic anhydrase while removal of the NP resulted in the formation of three intermediate native-like conformations each one of which retained catalytic activity. Covalently bound enzymes horse radish peroxidase, subtilisin Carlsberg, and chicken egg white lysozyme on SWCNTs were also shown to retain their activity and their native structure even under denaturing conditions [27].

Conformational epitopes result from the specific folding (tertiary structure) of the protein polypeptide chain and the linear epitopes are based on the primary structure of the protein. For certain proteins these linear epitopes may be responsible for the elicitation of an immune response *in vivo*. The NP surface may induce abnormal unfolding of the bound proteins to form novel conformational epitopes or may also induce unfolding of the native protein structure to expose hidden epitopes (Figure 2.1). Such occult epitopes may affect the functionality of the bound protein example elicitation of an unwanted immune response. Deng et al. showed that negatively charged poly (acrylic acid)-conjugated gold NPs bound fibrinogen from blood plasma and induced its unfolding, which in turn activated the receptor Mac-1 on THP-1 cells, causing release of inflammatory cytokines via the NF- $\kappa$ B pathway [28]. Changes in protein structure may lead to loss of tolerance against self, which may in a worst case provoke autoimmune responses and remains an important concern [29].



**Figure 2.1: A schematic representation of the NP surface induced unfolding of the interacting protein molecule and consequences. (A) Protein molecules adsorb on to the NP surface, to form a complex termed as the (B) NP-PC. NP surface may induce conformational change to the native structure of the adsorbed protein molecule, causing it to unfold. Such protein conformational changes may either, (C) alter the function of the native protein molecule or even lead to (D) the exposure of “cryptic” epitopes, resulting in immunological recognition of the complex.**

NPs can also induce conformational changes in proteins that can lead to fibril formation [30, 31]. Linse et al. showed that a range of NPs (copolymer, ceria, carbon nanotubes, quantum dots) were capable of inducing fibrillation of  $\beta_2$ -microglobulin due to increased protein localization on the NP surface, which led to oligomer formation [32]. Fibrillation of proteins is associated with diseases such as Parkinson's and Alzheimer's. The fact that NPs can act as platforms to initiate such protein structural changes demands further investigation of this phenomenon.

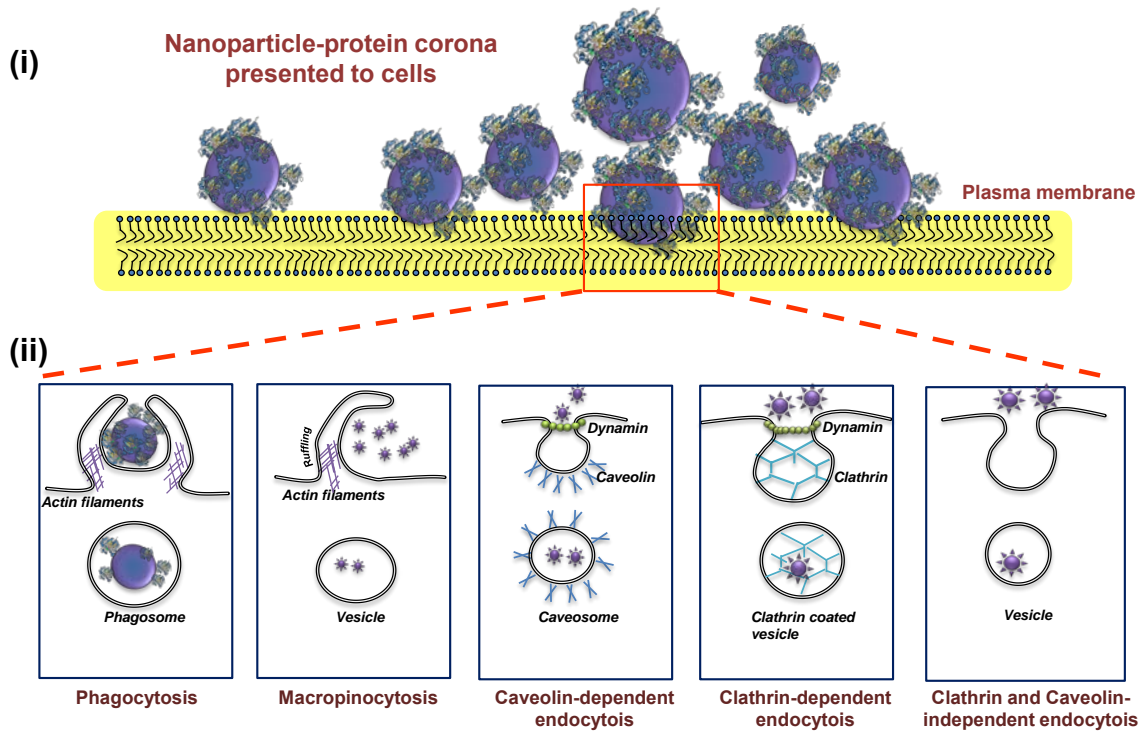
The NP surface can also introduce thermodynamic instability to the adsorbed protein molecule making it susceptible to chemical denaturation. ZnO NPs induced unfolding of the periplasmic domain of the ToxR protein of *Vibrio cholera* making the protein susceptible to denaturation by chaotropic agents [33]. Interestingly, ZnO NPs were able to stabilize the  $\alpha$ -helical content of lysozyme against denaturing agents [34]. The fate of proteins after binding on the NP surface is thus partially governed by their own chemical properties. A comprehensive list of structural modifications induced by interacting NPs with single proteins has been provided in Table 2.2.

**Table 2.2: Table summarizing the literature on proteins subjected to conformational changes upon interaction with different NP surfaces.**

NP type and size	Protein investigated	Protein mol. wt. and size nm (if provided)	Change in protein structure	Analytical technique	Observations	Ref
ZnO NPs (25 nm)	Vibrio cholera Tox r	32.5 kDa	Yes	CD	NP-protein complex susceptible to denaturation	[40]
ZnO NPs (N/A)	BSA	66 kDa	Yes	CD	Minor conformational changes, secondary structure retained	[31]
ZnO NPs (N/A)	BSA	66 kDa	Yes	FTIR	Minor conformational changes in secondary structure	[42]
TiO <sub>2</sub> NPs (20 nm)	Tubulin	55kda	Yes	FS	Protein polymerization affected	[30]
SiO <sub>2</sub> NPs (~40 nm)	BSA	66 kDa	Yes	RS	BSA and lactoperoxidase bound irreversibly	[33]
	Hen egg lysozyme	14.3 kDa	No			
	RNase A	13.7 kDa	No			
SiO <sub>2</sub> NPs (6,9,15 nm)	Lactoperoxidase	77.5 kDa	Yes	NMR	Protein activity was retained	[4]
	Human Carbonic anhydrase	29 kDa	Yes			
	BSA	66 kDa $8 \times 8 \times 3$	Yes			
Alumina and hydroxyapatite particles (100-300 nm)	Hen egg lysozyme	14.3 kDa $4.6 \times 3 \times 3$	Yes	FTIR	Loss in $\alpha$ -helical structure	[43]
	Bovine serum fibrinogen	350 kDa $6 \times 6.5 \times 45$	Yes			
	BSA	66 kDa	Yes			
Gold (45 nm)	BSA	66 kDa	Yes	CD	Conformational change was dose dependent	[28]
Gold (5-100 nm)	Albumin	67 kDa	Yes	CD and FS	Minor conformational changes observed	[27]
	Fibrinogen	340 kDa	Yes			
	$\gamma$ -globulin	120 kDa	Yes			
	Histone H3	15 kDa	Yes			
	Insulin	5.8 kDa	Yes			
Gold (7-22 nm)	Human Fibrinogen	340 kDa $45 \times 5$	Yes	CD	Unfolding induced immune response in THP-1 cells	[35]
SPIONs (5-10 nm)	Transferrin	80 kDa	Yes	CD	Irreversible interaction	[32]
	Horse radish peroxidase	44 kDa	No			
SWCNTs (N/A)	Subtilisin Carlsberg	39 kDa	No	CD	NP-protein complexes retained enzymatic activity	[34]
	Chicken egg white lysozyme	14.3 kDa	No			

## 2.4 Nanoparticle-protein corona: the implication on cellular interactions

Given the small size of NPs, it is quite likely that they can encounter different types of cells and also translocate across membrane barriers in an organism. NPs less than 100 nm in diameter can enter cells, less than 40 nm can enter the cell nucleus and below 35 nm can cross the blood–brain barrier [35, 36]. Uptake of NP can occur via phagocytosis, macropinocytosis or endocytosis (Figure 2.2 ii). NP surface properties and charge may influence the internalisation pathway involved. However it has been suggested that there may be an optimal size range for NPs, independent of the particle composition for endocytosis to occur [37]. Once taken up, NPs can accumulate in the lysosomes [38, 39], intracellular vacuoles as reported in the case of SWCNT uptake by HeLa cells [40], or cytoplasm of cells as observed for copolymer NP [41]. Cytotoxicity and immune-modulation are the two most important repercussions of NP uptake by cells. This is of particular importance when considering NPs that have a propensity to dissolve after reaching the acidic lysosomal compartments of the cell, thus contributing to cellular toxicity. To understand the fate of NPs in the biological context it is imperative to systematically analyse the intricate factors involved in their uptake. Protein adsorption, physical characteristics of the NPs and the properties of interacting cells may influence NP uptake. Kinetics of uptake of the same nanomaterial has been shown to differ with different cell types [42, 43]. Adsorption of proteins on the NP surface can take place almost instantly. Therefore, it can be assumed that interaction of the NP with cellular structures is indirect and occurs mostly via the NP-PC and not the bare NP surface (Figure 2.2 i).



**Figure 2.2: Interaction of nanoparticles with the cellular interface. NPs interact with cells via the protein corona. The optimal NP size for active uptake has been suggested to be in the range of 30-50 nm although there is a strong possibility that the NP charge, surface functionalization and experimental conditions may influence the uptake mechanism (A) Uptake of large sized NP-protein complexes, agglomerates of NP may be ingested by specialized cells such as macrophages and neutrophils via phagocytosis which involves folding of the plasma membrane over the NP complex to form the phagosome. (B) Non-specific uptake of extracellular fluid containing aggregates of NP may also be taken up by cells via micropinocytosis, which involves ruffling of the plasma membrane to form vesicles, which ultimately fuse to form lysosomes. Endocytosis of NP complexes may also be directed by the specific receptors involving the formation of (C) caveolae that are plasma membrane indentations consisting of cholesterol binding proteins called caveolins or (D) clathrin-coated vesicles. (E) Apart from these other endocytic mechanisms, independent of clathrin or caveolae may also facilitate the uptake of NPs.**

The NP-PC can thus influence the uptake of the NP by the cell. This uptake can be either inhibited due to the loss of protein structure of an adsorbed protein, or facilitated due to unfolding of the adsorbed protein to access receptors on the cell surface. This is particularly important when looking at differential binding of physiologically active proteins on the NP. Several *in vitro* studies have explored cellular uptake of NP in the presence of serum proteins [44]. Dutta et al. carried out an elaborate study to show that albumin adsorbed on the surface on SWCNTs was responsible for inducing an anti-inflammatory pathway in RAW macrophages, thus highlighting that the identity of the adsorbed protein may dictate the bio-reactivity of the NP surface [45]. Similarly, adsorption of the lung protein SP-A on magnetite NPs was also shown to enhance their uptake by macrophages when compared to the ones pre-coated with BSA [46]. Caveolae mediated endocytosis of fluorescent polystyrene NPs (20-100 nm) was shown to be dependent on the presence of albumin on the NP surface. Additionally the caveolae that are cell membrane invaginations typically 60-80 nm in diameter were also shown to contain up to three 20 nm and 240 nm polystyrene NPs, which suggested that these structures can be flexible in accommodating larger sized NP-protein complexes [47].

Apolipoproteins are a class of proteins that are often found in the NP-PC in blood for a number of NP surfaces (Table 2.1). These have been of interest because of their ability to aid in uptake of NPs by binding to specific receptors on cells. Apolipoproteins B and E were shown to assist in the transport of drug bound-polysorbate 80 coated NPs across the blood-brain barrier. Receptor mediated endocytosis was speculated to be the means of uptake in this case [48, 49]. The impermeable nature of the blood-brain barrier makes it difficult to deliver essential drugs and other compounds to the brain. While the ability of NPs to translocate across this barrier provides a promising future in this direction, it also raises important safety concerns regarding toxicity of nanomaterials.

Certain serum proteins such as immunoglobulins and complement pathway proteins possess opsonising characteristics. The presence or enrichment of such opsonising proteins on the NP surface in blood can lead to immune recognition of the NP-protein complex, otherwise not intended. In one study,

uptake of NH<sub>2</sub>-polystyrene NPs by macrophages in a protein free medium was shown to change from clathrin-mediated endocytosis to phagocytosis when incubated in serum enriched media [50]. Thus the opsonisation of the NP surface by serum proteins may remarkably influence its uptake. Adsorption of complement protein C3 and opsonising protein IgG, on 50 nm lecithin-coated polystyrene NPs was also shown to increase with time and this directly influenced their uptake by murine Kupffer cells [51].

The large surface area adsorption of proteins on the NP surface often leads to an increase in the hydrodynamic size of the latter. Such large NP-protein complexes can be taken up by phagocytic cell types and also non-phagocytic cells. Lesniak and co-workers. showed that the uptake of polystyrene NP by non-phagocytic lung epithelial cells was significantly higher when incubated in non-heated serum compared to NPs incubated in heat inactivated serum [52]. While this study does not state the exact mechanism of uptake, the authors report that the amount of protein and also the presence of heat labile complement proteins in the non-heat inactivated serum may be responsible for the observed enhanced uptake.

Another possible explanation for the enhanced uptake is that the cellular interaction of the NP is non-specific; depending exclusively on the amount of protein, rather than the presence of certain proteins on the NP surface as discussed above. This was shown by Ehrenberg et al. in their study where, NPs incubated with complete serum or serum, depleted of several abundant proteins did not affect the association of NPs with endothelial cells *in vitro* [53]. While it is interesting to know that the protein binding on the NP surface facilitates its uptake and other interactions, there have been some contradictory reports in the literature. Uptake of FePt NPs by HeLa cells was suppressed in the presence of the NP-PC [16]. Also, silica NPs dispersed in serum free medium were taken up more efficiently by lung epithelial cells as compared to ones in presence of 10% serum. By and large, the amount and identity of the protein adsorbed on the NP surface seems to determine the uptake of the NP.

Apart from protein adsorption other minor differences in physicochemical characteristics such as zeta potential, and size of the NP surface have also

been shown to influence their mode of uptake by cells [42, 54-57]. Interestingly, the sedimentation capacity was proposed to be the driving factor for the uptake of gold NP by human breast cells. This was clearly demonstrated by exposing human breast cancer cells to gold NPs in an upright or inverted configuration [58]. Also, Kim and co-workers reported that the phase of cell cycle was an important factor that influenced the uptake of 40 nm yellow-green PS-COOH by A549 cells. They also demonstrated that the NP taken up by the parent cells were divided between the daughter cells upon cell division suggesting implications on clearance or accumulation of NPs *in vivo* [59].

A review of the literature pertaining to cellular uptake of NPs reveals a number of inconsistencies regarding factors influencing this interaction. It has to be taken into account that most of these studies are conducted under *in vitro* conditions, often with immortal cell lines which may show different characteristics as compared to their *ex vivo* counterparts. Moreover, *in vivo* NPs interact not only with the protein micro-environments but also with other cellular moieties simultaneously, making it a challenging task to correctly extrapolate behaviour of NPs *in vivo*. Perturbation of the native structure of the bound protein depends on the surface of the interacting NP and together these two factors direct the bio-reactivity of the NP.

## **2.5 Physico-chemical characteristics of the nanoparticle surface influence protein adsorption and therefore cellular interactions.**

NP composition [60, 61], hydrophobicity [26], presence of specific functional groups, pH and temperature [62] have been shown to affect protein adsorption on the surface of NPs. Sedimentation of NPs especially in an *in vitro* exposure system has also been reported to influence cellular interactions [58].

Colloidal solutions of NPs often have a tendency to form agglomerates. NP size, concentration, and surface charge can influence agglomerate formation. Coarse NP agglomerates can exert noticeably different biological properties compared to NPs that are efficiently dispersed [63-65]. Agglomeration can also change the available surface area for protein binding. Uneven surface of the agglomerated NP can induce protein conformational changes. NPs dispersed in

protein free media often tend to agglomerate. Studies have reported the use of ultrasonic energy, surfactants [66], polymer coating [67] protein containing dispersion media like serum, alveolar lung fluid, etc. to control agglomeration [45, 68-71]. Dispersal of high concentrations of NPs in solutions containing certain proteins such as fibrinogen can in contrast lead to aggregation, due to the formation of inter-particle bridges by the protein [72, 73].

Yet another physical characteristic of the NP known to influence protein binding is size. Twelve nm sized negatively charged poly acrylic acid Au NPs were reported to bind fibrinogen with higher affinity compared to 7 nm NPs [73]. In another study, 15 nm silica NPs induced a six-fold higher change in the secondary structure of human carbonic anhydrase I protein compared to 6 nm silica NPs [4]. Stability of ribonuclease A was dramatically reduced with binding to silica NPs of increasing sizes [74]. Silica NPs (100 nm) were capable of inducing greater loss of structure and function for the protein lysozyme as compared to 4 nm sized particles [75]. On the other hand, Dutta et al. reported that plasma protein adsorption profiles remained uniform for differentially sized silica NPs [45]. This emphasizes again, that it is very difficult to formulate rules about protein interactions that apply to different types of NPs.

The shape of the NP can be important as well. This was confirmed for titanium dioxide (TiO<sub>2</sub>) nanorods and nanotubes that differentially adsorbed plasma proteins [76]. Likewise, modification of NP surface charge can also influence protein adsorption. Studies have demonstrated that NP surfaces with no charge bind less protein than their negatively charged (COOH functionalized) or positively charged (NH<sub>2</sub> functionalized) counterparts [77, 78]. Polyethyleneimine-functionalization of ZnO NPs favoured their interaction with albumin as compared to pristine ones [37]. A recent study showed that structural modification of a self-protein such as fibrinogen can be affected by the surface properties of gold NPs. Negatively charged gold NPs, unlike positively or neutral charged ones, were shown to bind fibrinogen in an orientation that led to cytokine release in human monocytic THP-1 cells *in vitro* [78]. It should be noted that the pI of the protein may dictate its binding efficiency to the different types of NPs. The influence of the NP surface on immune stimulation by a self-protein is an important concern. However,

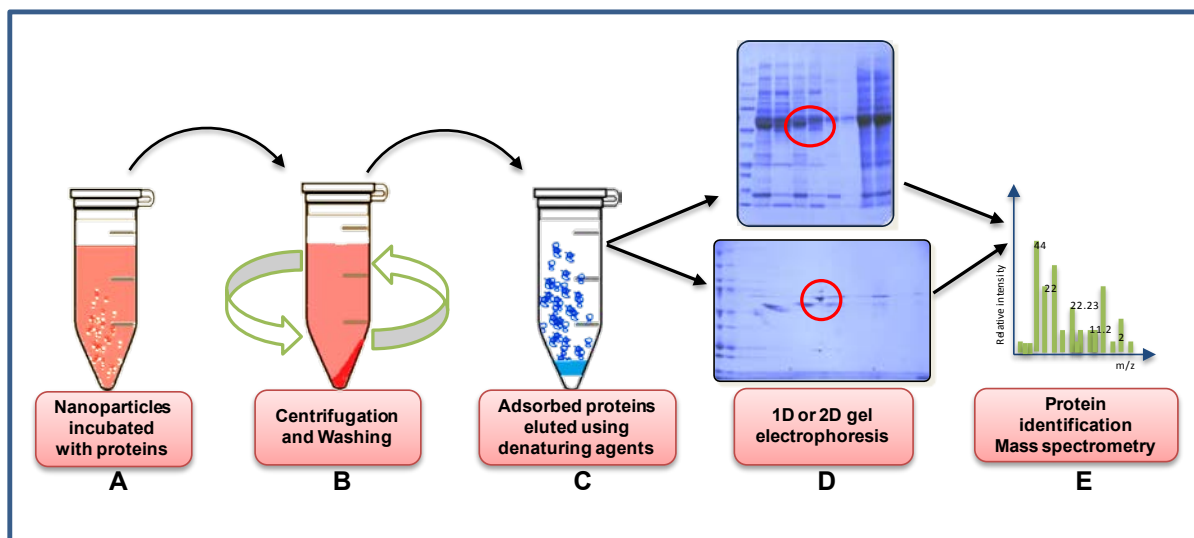
application of this information in extrapolating adverse effects of such interactions under *in vivo* conditions remains to be determined.

Chemical fabrication of the NP surface to avoid adsorption of proteins can be carried out using polyethylene glycol (PEG), also referred to as “PEGylation”. This imparts a “stealth character” to an NP surface, shielding it from being recognized by immune cells [79]. NPs can be made to remain in circulation for longer periods of time by controlling the density of PEG on their surface [79, 80]. Siliconate treatment of the NP surface too has been reported to prevent protein adsorption[76].

An important issue that requires further attention is the indirect influence of the NP-physico-chemical characteristics on cytotoxicity, cell signalling etc. Cytotoxicity and cytokine release by lung epithelial cells when exposed to ZnO or TiO<sub>2</sub> nano-powders was influenced by their shape and crystalline forms, respectively [81]. Differential inflammatory potential and cellular association were recorded for spherically shaped or sheets of nano ZnO [82]. Silver nanorods were shown to be toxic to the human lung epithelial cells, while nanospheres with the same mass concentration were not [83]. Thus, the influence of the proteins adsorbed on the NP surface cannot be disregarded completely when assessing immunotoxic outcomes of NPs.

## 2.6 Analytical approaches to study nanoparticle-protein interactions

Isolation and identification of proteins constituting the NP-PC are imperative to understand bio-reactivity of NPs. Mass spectrometry (MS) based proteomics is the most widely used strategy to study the NP-PC [84, 85] (Figure 2.3).



**Figure 2.3:** A schematic representation of the commonly used strategy to isolate and identify surface adsorbed proteins, when nanoparticles interact with complex protein mixtures. (A) Incubation of NPs with protein solutions results in the adsorption of proteins onto the NP surface. Protein concentration may affect the amount and identity of the proteins adsorbed on the presented NP surface. (B) Centrifugation for removal of the unbound proteins followed by repeated washing of the NP-protein pellet is important for isolation of the “hard protein corona”. (C) Isolation of the NP-PC can be achieved by the elution of the adsorbed proteins using denaturing agents such as Laemmli buffer, which contains sodium dodecyl sulphate and 2-mercaptoethanol that facilitate the overall desorption of the proteins. (D) The desorbed proteins can thus be separated using one or two dimensional gel electrophoresis. (E) Separated protein bands of interest can further be subjected to tryptic digestion and can be subsequently identified using mass spectrometric methods.

Despite the qualitative nature of the outcomes of this technique, it can be applied over a range of NPs, which makes it a preferred choice. A useful development to MS based proteomics is the use of stable isotope labelling by amino acids in cell culture (SILAC). This technique has been used to not only identify but also quantify amounts of proteins bound on NP surfaces [86]. Interactions of NP surfaces with single purified proteins can be investigated by fluorescence spectroscopy and circular dichroism (CD) spectroscopy. Fluorescence spectroscopy makes use of the intrinsic fluorescence of the protein whereas CD spectroscopy uses changes in chiral properties of the protein to predict changes in its secondary structure. High resolution information on protein structure can also be provided by nuclear magnetic resonance (NMR) spectroscopy. Specific interactions of ubiquitin molecules with gold NP surface was studied using NMR, which made it possible to identify the exact ubiquitin domain that bound to the NP surface [87]. Fluorescent correlation spectroscopy has also been used to monitor protein adsorption on NP surfaces and has been shown to be sensitive at nanomolar quantities of nanoparticles.

The use of other techniques such as isothermal titration calorimetry, surface plasmon resonance has also been reported to characterise protein binding to various surfaces (Table 2.3). A recent study showed that 70 nm copolymer NPs bind around 650 human serum albumin molecules and 200 nm particles can accommodate up to 4600 molecules, using isothermal calorimetry [1]. Quartz crystal microbalance, a technique that detects change in mass at the oscillating quartz surface due to NP-protein interaction, was employed to probe adsorption of myoglobin, BSA, and cytochrome c proteins on the surface modified gold NP [88]. The choice of analytical techniques for studying NP-PC greatly depends on the physical state of the NP.

Visualization of NPs uptake by cells is often carried out by fluorescent labelling of the NP surface or synthesis of fluorescent NPs which can be detected by flow cytometry or confocal laser scanning microscopy. Fluorescent labelling of NPs can however modify its surface thus interfering with subsequent protein interactions. Confocal Raman microscopy was recently used to study uptake of Al<sub>2</sub>O<sub>3</sub> and CeO<sub>2</sub> NPs by Lopis and co-workers [89]. This technique was

reported to be label-free and specific at the single cell level. Studies have attempted to propose models to generalize different aspects of NP-protein interactions. Dell'Orco and co-workers formulated a mathematical model to predict kinetics of protein binding to NP surfaces that can be extended to any proteome-NP combination [90]. Nangi et al. developed a simulation model to predict energy barriers, translocation rate constants and half-lives of NPs through lipid membranes as a function of their physical properties [91]. Xia et al. introduced the biological surface adsorption index (BSAI) to predict the order in which factors such as hydrophobicity, hydrogen bonding, polarizability of NP surface and ion-pair electrons affect protein adsorption at the nano-bio interface, using 12 physico-chemically defined protein-mimicking probes and MWCNTs [92]. The experimental approach employed by most studies currently involves detailed study of a single protein with the NP surface rather than the complete NP-PC that consists of several different types of proteins. Strategic use and combination of the available analytical techniques is needed to analyse several aspects of NP-protein interactions simultaneously.

**Table 2.3: Summary of analytical techniques to conduct physico-chemical characterisation, monitor nanoparticle surface driven protein conformational changes and uptake of nanoparticles by cellular structures.**

Analysis of	Analytical technique	Brief description	Ref
<b>Nanoparticle physical characterisation</b>			
Size and charge	Dynamic light scattering	Changes in the hydrodynamic diameter of NP upon binding to proteins	[1]
	Analytical Ultracentrifugation	Changes in the hydrodynamic diameter of NP	[6]
Dissolution	Inductively coupled mass spectrometry	For detecting elemental composition of the nanomaterial	[90]
Shape and structure	X ray diffraction	Determination of crystalline structure	[38]
	Electron microscopy	Visualisation of nanoparticle structure	
Surface area	Braunauer Emmet Teller method	Measures specific surface area using adsorption of gas on the surface	[38]
De-agglomeration	Ultrasonication	Uses sound energy to disrupt large aggregates of NP	[36]
<b>Nanoparticle protein interaction</b>			
Protein binding affinity	Isothermal calorimetry	To measure binding constant, thermodynamic parameters of NP-protein interactions	[2]
	Fluorescence spectroscopy	Measures change in fluorescence spectra due to NP-protein interaction	[65]
	UV-vis spectroscopy	Measures change in absorption spectra due to NP-protein interaction	[57]
	Quartz crystal balance	Detects change in mass at the oscillating quartz surface due to NP-protein interaction	[91]
	Surface Plasmon resonance	Detects change in oscillation of electrons on a metal surface due to NP-protein interaction	[92]
Protein binding affinity	Atomic force microscopy	Gives surface profile of the nanomaterial	[93]
	Fluorescence correlation spectroscopy	Binding characteristics depending on fluctuation in fluorescence	[94]
<b>Nanoparticle surface induced protein structure changes</b>			
Protein structural changes after binding	Circular Dichroism spectroscopy	Measures changes in secondary structure of proteins depending on chiral properties of proteins	[61]
	Fourier transformed infrared spectroscopy	Measures adsorption of amide bonds in the proteins to derive structural change	[43]
	Raman spectroscopy	Studies molecular vibrations to predict structure	[52]
	Nuclear Magnetic Resonance	Relies on magnetic properties of atomic nuclei to predict structure	[4]
<b>Nanoparticle- Cellular interactions</b>			
NP uptake	Confocal microscopy	Visualization of fluorescent nanoparticles <i>in vitro</i>	[59]
	Confocal micro Raman spectroscopy		[95]

## 2.7 Conclusion

Characterization and analysis of proteins bound to the NP surface is the first step towards understanding the true nature of the NP-mediated biological effects. Research thus far highlights the size, shape, and surface characteristics of NPs that affect protein adsorption and also have the capability to modify the protein structure. This can significantly affect the reactivity of the NP with cells and determine the route and efficiency of NP uptake. The adsorbed proteins may also promote translocation of the NP across cellular barriers, and clearance or accumulation in vital organs. Interestingly, most studies conducted in this direction focus on *in vitro* test systems, therefore, extrapolation of this information in predicting behaviour of NPs *in vivo* remains a challenging task and needs further investigation. Systematic analysis of binding characteristics of novel NPs with proteins having different structures, shapes and functional properties can enhance our existing knowledge about NP-protein interactions. A comprehensive understanding of NP-protein interactions might lead to strategic manipulation of NP surfaces to adsorb specific functional proteins or small drug molecules intended for delivery *in vivo*. Furthermore this knowledge might also prove to be useful in predicting nanotoxicity related safety concerns. In summary, NP-PC dictates the overall biological reactivity of the otherwise inorganic NP surface. Understanding the dynamics of this complex interaction can thus provide useful insights into cytotoxic, inflammatory potential and other key properties of these novel materials that can be explored for developing safer and value added nanomaterials for future applications.

## 2.7 References

1. Cedervall T, Lynch I, Foy M, Berggård T, Donnelly S, Cagney G, Linse S, Dawson K: **Detailed identification of plasma proteins adsorbed on copolymer nanoparticles.** *Angewandte Chemie-International Edition* 2007, **46**:5754 - 5756.
2. Casals E, Pfaller T, Duschl A, Oostingh GJ, Püntes V: **Time Evolution of the Nanoparticle Protein Corona.** *ACS Nano* 2010, **4**:3623-3632.
3. Karajanagi SS, Vertegel AA, Kane RS, Dordick JS: **Structure and Function of Enzymes Adsorbed onto Single-Walled Carbon Nanotubes.** *Langmuir* 2004, **20**:11594-11599.
4. Lundqvist M, Sethson I, Jonsson B-H: **Protein Adsorption onto Silica Nanoparticles: Conformational Changes Depend on the Particles' Curvature and the Protein Stability.** *Langmuir* 2004, **20**:10639-10647.
5. Lundqvist M, Sethson I, Jonsson B-H: **Transient Interaction with Nanoparticles "Freezes" a Protein in an Ensemble of Metastable Near-Native Conformations.** *Biochemistry (Mosc)* 2005, **44**:10093-10099.
6. Landsiedel R, et al.: **Testing Metal-Oxide Nanomaterials for Human Safety.** *Advanced Materials* 2010:n/a.
7. Kim JA, Salvati A, Aberg C, Dawson KA: **Suppression of nanoparticle cytotoxicity approaching in vivo serum concentrations: limitations of in vitro testing for nanosafety.** *Nanoscale* 2014.
8. Monopoli MP, Walczyk D, Campbell A, Elia G, Lynch I, Baldelli Bombelli F, Dawson KA: **Physical-Chemical Aspects of Protein Corona: Relevance to in Vitro and in Vivo Biological Impacts of Nanoparticles.** *J Am Chem Soc* 2011, **133**:2525-2534.
9. Gasser M, Rothen-Rutishauser B, Krug HF, Gehr P, Nelle M, Yan B, Wick P: **The adsorption of biomolecules to multi-walled carbon nanotubes is influenced by both pulmonary surfactant lipids and surface chemistry.** *J Nanobiotechnology* 2010, **8**:1477-3155.
10. Lundqvist M, Stigler J, Cedervall T, Berggård T, Flanagan MB, Lynch I, Elia G, Dawson K: **The Evolution of the Protein Corona around Nanoparticles: A Test Study.** *ACS Nano* 2011, **5**:7503-7509.

11. Hellstrand E, Lynch I, Andersson A, Drakenberg T, Dahlbäck B, Dawson KA, Linse S, Cedervall T: **Complete high-density lipoproteins in nanoparticle corona.** *FEBS J* 2009, **276**:3372-3381.
12. Vroman L: **Effect of Adsorbed Proteins on the Wettability of Hydrophilic and Hydrophobic Solids.** *Nature* 1962, **196**:476-477.
13. Ge C, Du J, Zhao L, Wang L, Liu Y, Li D, Yang Y, Zhou R, Zhao Y, Chai Z, Chen C: **Binding of blood proteins to carbon nanotubes reduces cytotoxicity.** *Proceedings of the National Academy of Sciences* 2011, **108**:16968-16973.
14. Sund J, Alenius H, Vippola M, Savolainen K, Puustinen A: **Proteomic Characterization of Engineered Nanomaterial-Protein Interactions in Relation to Surface Reactivity.** *ACS Nano* 2011, **5**:4300-4309.
15. Jansch M, Stumpf P, Graf C, Rühl E, Müller RH: **Adsorption kinetics of plasma proteins on ultrasmall superparamagnetic iron oxide (USPIO) nanoparticles.** *Int J Pharm* 2012, **428**:125-133.
16. Jiang X, Weise S, Hafner M, Rucker C, Zhang F, Parak WJ, Nienhaus GU: **Quantitative analysis of the protein corona on FePt nanoparticles formed by transferrin binding.** *J Royal Soc Interface* 2009, **7**:S5-S13.
17. Rezwan K, Meier LP, Rezwan M, Vörös J, Textor M, Gauckler LJ: **Bovine Serum Albumin Adsorption onto Colloidal Al<sub>2</sub>O<sub>3</sub> Particles: A New Model Based on Zeta Potential and UV-Vis Measurements.** *Langmuir* 2004, **20**:10055-10061.
18. Verma A, Stellacci F: **Effect of Surface Properties on Nanoparticle-Cell Interactions.** *Small* 2010, **6**:12-21.
19. Worrall JWE, Verma A, Yan HH, Rotello VM: **"Cleaning" of nanoparticle inhibitors via proteolysis of adsorbed proteins.** *Chem Commun* 2006:2338-2340.
20. Lacerda SHDP, Park JJ, Meuse C, Pristiniski D, Becker ML, Karim A, Douglas JF: **Interaction of Gold Nanoparticles with Common Human Blood Proteins.** *ACS Nano* 2009, **4**:365-379.
21. Wangoo N, Suri CR, Shekhawat G: **Interaction of gold nanoparticles with protein: A spectroscopic study to monitor protein conformational changes.** *Appl Phys Lett* 2008, **92**.

22. Shufang Liu YS, Kai Guo, Zhijuan Yin and Xibao Gao: **Spectroscopic study on the interaction of pristine C60 and serum albumins in solution.** *Nanoscale Research Letters* 2012, **7**.
23. Gheshlaghi ZN, Riazi GH, Ahmadian S, Ghafari M, Mahinpour R: **Toxicity and interaction of titanium dioxide nanoparticles with microtubule protein.** *Acta Biochim Biophys Sin* 2008, **40**:777-782.
24. Bardhan M, Mandal G, Ganguly T: **Steady state, time resolved, and circular dichroism spectroscopic studies to reveal the nature of interactions of zinc oxide nanoparticles with transport protein bovine serum albumin and to monitor the possible protein conformational changes.** *J Appl Phys* 2009, **106**.
25. Mahmoudi M, Shokrgozar MA, Sardari S, Moghadam MK, Vali H, Laurent S, Stroeve P: **Irreversible changes in protein conformation due to interaction with superparamagnetic iron oxide nanoparticles.** *Nanoscale* 2011, **3**:1127-1138.
26. Turci F, Ghibaudi E, Colonna M, Boscolo B, Fenoglio I, Fubini B: **An Integrated Approach to the Study of the Interaction between Proteins and Nanoparticles.** *Langmuir* 2010.
27. Asuri P, Bale SS, Pangule RC, Shah DA, Kane RS, Dordick JS: **Structure, Function, and Stability of Enzymes Covalently Attached to Single-Walled Carbon Nanotubes.** *Langmuir* 2007, **23**:12318-12321.
28. Deng ZJ, Liang M, Monteiro M, Toth I, Minchin RF: **Nanoparticle-induced unfolding of fibrinogen promotes Mac-1 receptor activation and inflammation.** *Nat Nano* 2011, **6**:39-44.
29. Nel A, Madler L, Velegol D, Xia T, Hoek E, Somasundaran P, Klaessig F, Castranova V, Thompson M: **Understanding biophysicochemical interactions at the nano-bio interface.** *Nat Mater* 2009, **8**:543 - 557.
30. Colvin VL, Kulinowski KM: **Nanoparticles as catalysts for protein fibrillation.** *Proceedings of the National Academy of Sciences* 2007, **104**:8679-8680.
31. Wagner SC, Roskamp M, Pallerla M, Araghi RR, Schlecht S, Kokschi B: **Nanoparticle-Induced Folding and Fibril Formation of Coiled-Coil-Based Model Peptides.** *Small* 2010, **6**:1321-1328.

32. Linse S, Cabaleiro-Lago C, Xue W-F, Lynch I, Lindman S, Thulin E, Radford SE, Dawson KA: **Nucleation of protein fibrillation by nanoparticles.** *Proceedings of the National Academy of Sciences* 2007, **104**:8691-8696.
33. Chatterjee T, Chakraborti S, Joshi P, Singh SP, Gupta V, Chakrabarti P: **The effect of zinc oxide nanoparticles on the structure of the periplasmic domain of the *Vibrio cholerae* ToxR protein.** *FEBS J* 2010, **277**:4184-4194.
34. Chakraborti S, Chatterjee T, Joshi P, Poddar A, Bhattacharyya B, Singh SP, Gupta V, Chakrabarti P: **Structure and Activity of Lysozyme on Binding to ZnO Nanoparticles.** *Langmuir* 2009, **26**:3506-3513.
35. Oberdörster G, Sharp Z, Atudorei V, Elder A, Gelein R, Kreyling W, Cox C: **Translocation of Inhaled Ultrafine Particles to the Brain.** *Inhal Toxicol* 2004, **16**:437-445.
36. Dawson KA, Salvati A, Lynch I: **Nanotoxicology: Nanoparticles reconstruct lipids.** *Nat Nano* 2009, **4**:84-85.
37. Shang L, Nienhaus K, Nienhaus G: **Engineered nanoparticles interacting with cells: size matters.** *J Nanobiotechnol* 2014, **12**:5.
38. Cho WS, Duffin R, Howie SEM, Scotton CJ, Wallace WAH, MacNee W, Bradley M, Megson IL, Donaldson K: **Progressive severe lung injury by zinc oxide nanoparticles; the role of Zn<sup>2+</sup> dissolution inside lysosomes.** *Particle and Fibre Toxicology* 2011, **8**.
39. Lesniak A, Fenaroli F, Monopoli MP, Åberg C, Dawson KA, Salvati A: **Effects of the Presence or Absence of a Protein Corona on Silica Nanoparticle Uptake and Impact on Cells.** *ACS Nano* 2012, **6**:5845-5857.
40. Hadi NY, Rockford KD, Carole M, Erin W, Pooja B, Inga HM, Meredith CD, Gregg RD, Paul P: **Single-walled carbon nanotube interactions with HeLa cells.** *J Nanobiotechnol* 2007, **5**:8-8.
41. Davda J, Labhasetwar V: **Characterization of nanoparticle uptake by endothelial cells.** *Int J Pharm* 2002, **233**:51-59.
42. Albanese A, Chan WCW: **Effect of Gold Nanoparticle Aggregation on Cell Uptake and Toxicity.** *ACS Nano* 2011, **5**:5478-5489.

43. dos Santos T, Varela J, Lynch I, Salvati A, Dawson KA: **Quantitative Assessment of the Comparative Nanoparticle-Uptake Efficiency of a Range of Cell Lines.** *Small* 2011, **7**:3341-3349.
44. Shannahan JH, Podila R, Aldossari AA, Emerson H, Powell BA, Ke PC, Rao AM, Brown JM: **Formation of a Protein Corona on Silver Nanoparticles Mediates Cellular Toxicity via Scavenger Receptors.** *Toxicol Sci* 2014.
45. Dutta D, Sundaram S, Teeguarden J, Riley B, Fifield L, Jacobs J, Addleman S, Kaysen G, Moudgil B, Weber T: **Adsorbed proteins influence the biological activity and molecular targeting of nanomaterials.** *Toxicol Sci* 2007, **100**:303 - 315.
46. Ruge CA, Kirch J, Canadas O, Schneider M, Perez-Gil J, Schaefer UF, Casals C, Lehr C-M: **Uptake of nanoparticles by alveolar macrophages is triggered by surfactant protein A.** *Nanomedicine-Nanotechnology Biology and Medicine* 2011, **7**:690-693.
47. Wang Z, Tirupathi C, Minshall RD, Malik AB: **Size and Dynamics of Caveolae Studied Using Nanoparticles in Living Endothelial Cells.** *ACS Nano* 2009, **3**:4110-4116.
48. Jörg Kreuter DS, Valery Petrov, Peter Ramge, Klaus Cychutek, Claudia Koch-Brandt and Renad Alyautdin: **Apolipoprotein-mediated Transport of Nanoparticle-bound Drugs Across the Blood-Brain Barrier.** *J Drug Target* 2002, **10**:317-325.
49. Kreuter J: **Mechanism of polymeric nanoparticle-based drug transport across the blood-brain barrier (BBB).** *J Microencapsul* 2013, **30**:49-54.
50. Lunov O, Syrovets T, Loos C, Beil J, Delacher M, Tron K, Nienhaus GU, Musyanovych A, Mailander V, Landfester K, Simmet T: **Differential Uptake of Functionalized Polystyrene Nanoparticles by Human Macrophages and a Monocytic Cell Line.** *ACS Nano* 2011, **5**:1657-1669.
51. Nagayama S, Ogawara K, Fukuoka Y, Higaki K, Kimura T: **Time-dependent changes in opsonin amount associated on nanoparticles alter their hepatic uptake characteristics.** *Int J Pharm* 2007, **342**:215-221.

52. Lesniak A, Campbell A, Monopoli MP, Lynch I, Salvati A, Dawson KA: **Serum heat inactivation affects protein corona composition and nanoparticle uptake.** *Biomaterials* 2010, **31**:9511-9518.
53. Ehrenberg MS, Friedman AE, Finkelstein JN, Oberdorster G, McGrath JL: **The influence of protein adsorption on nanoparticle association with cultured endothelial cells.** *Biomaterials* 2009, **30**:603-610.
54. Chithrani BD, Ghazani AA, Chan WCW: **Determining the Size and Shape Dependence of Gold Nanoparticle Uptake into Mammalian Cells.** *Nano Lett* 2006, **6**:662-668.
55. Alexis F, Pridgen E, Molnar LK, Farokhzad OC: **Factors Affecting the Clearance and Biodistribution of Polymeric Nanoparticles.** *Mol Pharm* 2008, **5**:505-515.
56. Angeles Villanueva MC, Alejandro G Roca, Macarena Calero, Sabino Veintemillas-Verdaguer, Carlos J Serna, María del Puerto Morales and Rodolfo Miranda: **The influence of surface functionalization on the enhanced internalization of magnetic nanoparticles in cancer cells** *Nanotechnology* 2009, **20**.
57. Walkey CD, Olsen JB, Guo H, Emili A, Chan WCW: **Nanoparticle Size and Surface Chemistry Determine Serum Protein Adsorption and Macrophage Uptake.** *J Am Chem Soc* 2011, **134**:2139-2147.
58. Cho EC, Zhang Q, Xia Y: **The effect of sedimentation and diffusion on cellular uptake of gold nanoparticles.** *Nat Nano* 2011, **6**:385-391.
59. Kim JA, Aberg C, Salvati A, Dawson KA: **Role of cell cycle on the cellular uptake and dilution of nanoparticles in a cell population.** *Nat Nano* 2012, **7**:62-68.
60. Gojova A, Guo B, Kota RS, Rutledge JC, Kennedy IM, Barakat AI: **Induction of inflammation in vascular endothelial cells by metal oxide nanoparticles: Effect of particle composition.** *Environ Health Perspect* 2007, **115**:403-409.
61. Sohaebuddin SK, Thevenot PT, Baker D, Eaton JW, Tang LP: **Nanomaterial cytotoxicity is composition, size, and cell type dependent.** *Particle and Fibre Toxicology* 2010, **7**.
62. Kopac T, Bozgeyik K, Yener J: **Effect of pH and temperature on the adsorption of bovine serum albumin onto titanium dioxide.** *Colloids*

- and Surfaces A: Physicochemical and Engineering Aspects* 2008, **322**:19-28.
63. Skebo JE, Grabinski CM, Schrand AM, Schlager JJ, Hussain SM: **Assessment of metal nanoparticle agglomeration, uptake, and interaction using high-illuminating system.** *Int J Toxicol* 2007, **26**:135-141.
64. Bihari P, Vippola M, Schultes S, Praetner M, Khandoga AG, Reichel CA, Coester C, Tuomi T, Rehberg M, Krombach F: **Optimized dispersion of nanoparticles for biological in vitro and in vivo studies.** *Particle and Fibre Toxicology* 2008, **5**.
65. Herzog E, Byrne HJ, Davoren M, Casey A, Duschl A, Oostingh GJ: **Dispersion medium modulates oxidative stress response of human lung epithelial cells upon exposure to carbon nanomaterial samples.** *Toxicol Appl Pharmacol* 2009, **236**:276-281.
66. Torres VM, Posa M, Srdjenovic B, Simplício AL: **Solubilization of fullerene C60 in micellar solutions of different solubilizers.** *Colloids and Surfaces B: Biointerfaces* 2011, **82**:46-53.
67. Popov VA, Tyunin MA, Zaitseva OB, Karaev RH, Sirotinkin NV, Dumpis MA, Piotrovsky LB: **C60/PVP complex No Toxicity after Introperitoneal Injection to Rats.** *Fullerenes, Nanotubes and Carbon Nanostructures* 2008, **16**:693-697.
68. Sager TM, Porter DW, Robinson VA, Lindsley WG, Schwegler-Berry DE, Castranova V: **Improved method to disperse nanoparticles for in vitro and in vivo investigation of toxicity.** *Nanotoxicology* 2007, **1**:118-129.
69. Schulze C, Kroll A, Lehr C-M, Schäfer UF, Becker K, Schnekenburger J, Schulze Isfort C, Landsiedel R, Wohlleben W: **Not ready to use – overcoming pitfalls when dispersing nanoparticles in physiological media.** *Nanotoxicology* 2008, **2**:51-61.
70. Allouni ZE, Cimpan MR, Høl PJ, Skodvin T, Gjerdet NR: **Agglomeration and sedimentation of TiO<sub>2</sub> nanoparticles in cell culture medium.** *Colloids and Surfaces B: Biointerfaces* 2009, **68**:83-87.
71. Feltis BN, O'Keefe SJ, Harford AJ, Piva TJ, Turney TW, Wright PFA: **Independent cytotoxic and inflammatory responses to zinc oxide**

- nanoparticles in human monocytes and macrophages.** *Nanotoxicology* 2012, **6**:757-765.
72. Kendall M, Ding P, Kendall K: **Particle and nanoparticle interactions with fibrinogen: the importance of aggregation in nanotoxicology.** *Nanotoxicology* 2011, **5**:55-65.
73. Deng ZJ, Liang M, Toth I, Monteiro MJ, Minchin RF: **Molecular Interaction of Poly(acrylic acid) Gold Nanoparticles with Human Fibrinogen.** *ACS Nano* 2012, **6**:8962-8969.
74. Shang W, Nuffer JH, Dordick JS, Siegel RW: **Unfolding of Ribonuclease A on Silica Nanoparticle Surfaces.** *Nano Lett* 2007, **7**:1991-1995.
75. Vertegel AA, Siegel RW, Dordick JS: **Silica Nanoparticle Size Influences the Structure and Enzymatic Activity of Adsorbed Lysozyme.** *Langmuir* 2004, **20**:6800-6807.
76. Deng Z, Mortimer G, Schiller T, Musumeci A, Martin D, Minchin R: **Differential plasma protein binding to metal oxide nanoparticles.** *Nanotechnology* 2009, **20**:455101.
77. Fertsch-Gapp S, Semmler-Behnke M, Wenk A, Kreyling WG: **Binding of polystyrene and carbon black nanoparticles to blood serum proteins.** *Inhal Toxicol* 2011, **23**:468-475.
78. Deng ZJ, Liang M, Toth I, Monteiro M, Minchin RF: **Plasma protein binding of positively and negatively charged polymer-coated gold nanoparticles elicits different biological responses.** *Nanotoxicology* 2012, **0**:1-9.
79. Gref R, Lück M, Quellec P, Marchand M, Dellacherie E, Harnisch S, Blunk T, Müller RH: **'Stealth' corona-core nanoparticles surface modified by polyethylene glycol (PEG): influences of the corona (PEG chain length and surface density) and of the core composition on phagocytic uptake and plasma protein adsorption.** *Colloids and Surfaces B: Biointerfaces* 2000, **18**:301-313.
80. Perry JL, Reuter KG, Kai MP, Herlihy KP, Jones SW, Luft JC, Napier M, Bear JE, DeSimone JM: **PEGylated PRINT Nanoparticles: The Impact of PEG Density on Protein Binding, Macrophage Association,**

- Biodistribution, and Pharmacokinetics.** *Nano Lett* 2012, **12**:5304-5310.
81. Hsiao IL, Huang Y-J: **Effects of various physicochemical characteristics on the toxicities of ZnO and TiO<sub>2</sub> nanoparticles toward human lung epithelial cells.** *Sci Total Environ* 2011, **409**:1219-1228.
82. Heng BC, Zhao XX, Tan EC, Khamis N, Assodani A, Xiong SJ, Ruedl C, Ng KW, Loo JSC: **Evaluation of the cytotoxic and inflammatory potential of differentially shaped zinc oxide nanoparticles.** *Arch Toxicol* 2011, **85**:1517-1528.
83. Stoehr LC, Gonzalez E, Stampfl A, Casals E, Duschl A, Puentes V, Oostingh GJ: **Shape matters: effects of silver nanospheres and wires on human alveolar epithelial cells.** *Particle and Fibre Toxicology* 2011, **8**.
84. Juang Y-M, Lai B-H, Chien H-J, Ho M, Cheng T-J, Lai C-C: **Changes in protein expression in rat bronchoalveolar lavage fluid after exposure to zinc oxide nanoparticles: an iTRAQ proteomic approach.** *Rapid Commun Mass Spectrom* 2014, **28**:974-980.
85. Pozzi D, Caracciolo G, Capriotti AL, Cavaliere C, Piovesana S, Colapicchioni V, Palchetti S, Riccioli A, Lagana A: **A proteomics-based methodology to investigate the protein corona effect for targeted drug delivery.** *Mol Biosyst* 2014, **10**:2815-2819.
86. Cai X, Ramalingam R, Wong HS, Cheng J, Ajuh P, Cheng SH, Lam YW: **Characterization of carbon nanotube protein corona by using quantitative proteomics.** *Nanomedicine: Nanotechnology, Biology and Medicine* 2013, **9**:583-593.
87. Calzolari L, Franchini F, Gilliland D, Rossi Fo: **Protein-Nanoparticle Interaction: Identification of the Ubiquitin-Gold Nanoparticle Interaction Site.** *Nano Lett* 2010, **10**:3101-3105.
88. Kaufman ED, Belyea J, Johnson MC, Nicholson ZM, Ricks JL, Shah PK, Bayless M, Pettersson T, Feldotö Z, Blomberg E, et al: **Probing Protein Adsorption onto Mercaptoundecanoic Acid Stabilized Gold Nanoparticles and Surfaces by Quartz Crystal Microbalance and ζ-Potential Measurements.** *Langmuir* 2007, **23**:6053-6062.

89. Estrela-Lopis I, Romero G, Rojas E, Moya SE, Donath E: **Nanoparticle uptake and their co-localization with cell compartments – a confocal Raman microscopy study at single cell level.** *Journal of Physics: Conference Series* 2011, **304**:012017.
90. Dell'Orco D, Lundqvist M, Oslakovic C, Cedervall T, Linse S: **Modeling the Time Evolution of the Nanoparticle-Protein Corona in a Body Fluid.** *PLoS ONE* 2010, **5**.
91. Nangia S, Sureshkumar R: **Effects of Nanoparticle Charge and Shape Anisotropy on Translocation through Cell Membranes.** *Langmuir* 2012, **28**:17666-17671.
92. Xia X-R, Monteiro-Riviere NA, Riviere JE: **An index for characterization of nanomaterials in biological systems.** *Nat Nano* 2010, **5**:671-675.



---

## Chapter III

# Physico-chemical characterisation of zinc oxide nanoparticles

### Presented at:

**Saptarshi SR**, Wright PA, Lopata AL Understanding immunomodulatory and cytotoxic effects of zinc oxide nanoparticles on human lung epithelial cells. Presented at the NANOTOX 7th International Nanotoxicology Congress Antalya, Turkey 2014

---



### 3.1 Introduction

Physico-chemical properties of nanomaterials can have a profound effect on their overall bio-reactivity [1-3]. The main aim of this study was to correlate how ZnO NP size, dispersal state and dissolution affect their reactivity with bio-molecules and cellular systems. In this quest, several different types of techniques were employed to accurately characterise the ZnO NPs used in this project. Furthermore, a uniform NP dispersal protocol was established for use in later working chapters for efficient correlation of the observed immunotoxic endpoints of ZnO NP-bio-interactions to their physico-chemical properties. This chapter provides an overview of the methods employed and the overall physico-chemical characterisation data for the different ZnO NPs.

Physical characterisation of ZnO-NP used in the present study was carried out using i) Cryo-transmission electron microscopy (Cryo-TEM) and ii) differential centrifugation sedimentation (DCS), also known as disc centrifugation. Solubility of ZnO-NP was assessed using Inductively Coupled Plasma Atomic Emission Spectroscopy (ICP-AES).

### 3.2 Materials and Methods

#### 3.2.1 Nanoparticles

This research project made use of industrially manufactured ZnO NPs and particulates of three different sizes (30, 80 and 200 nm) (Figure 3.1) and were supplied by Micronisers Pty Ltd (Melbourne, Australia). The 30 nm ZnO NPs corresponded to the OECD standard reference material NM-112. Additionally, to address the effect of agglomeration, two different solutions of ZnO NPs were used, namely pristine material and particles dispersed with 5% by weight of sodium polyacrylate (Orotan 731 DP) surfactant dispersant (designated as “ZnO” or “sZnO”, respectively). All particulate stock suspensions were prepared in de-ionised water (MilliQ systems, Millipore).

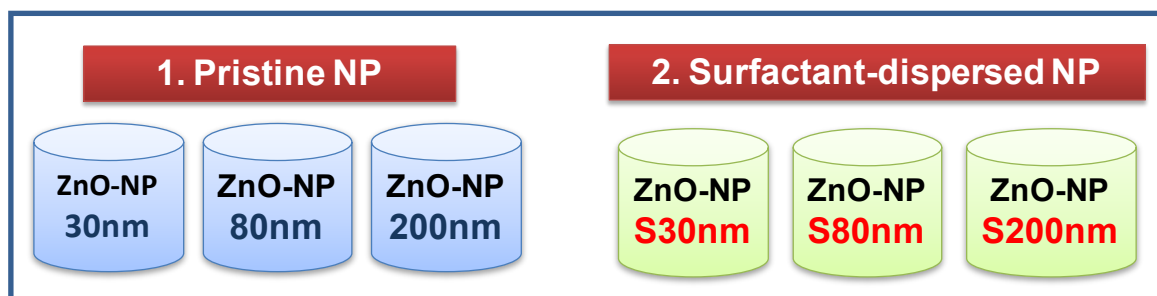
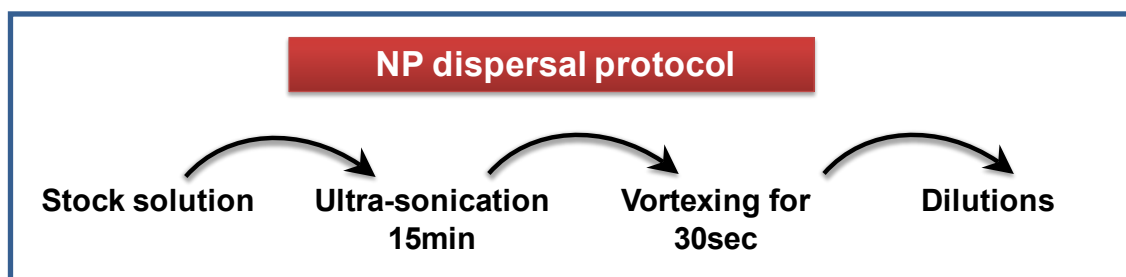


Figure 3.1: Zinc oxide nanoparticles used in the present study.

### 3.2.2 Dispersion protocol

The dispersal state of NPs has been previously reported to affect their biological activity. To address this, a uniform protocol was established and used for all studies conducted in this thesis. Briefly, 40-60 mg of the nanomaterial was weighed into sterile 5 mL flat bottom tubes (VWR, Australia). Sterile de-ionised water (MilliQ, Millipore) was then added to make a stock concentration of 20 mg/mL. The tubes were subjected to ultra-sonication for 15 min using ultra-sonication water bath (Ultrasonics, Australia), following which the tubes were allowed to stand for 24 hr. The stock solutions were only used until the solution levels dropped below 1 mL. All ZnO NP solutions were subjected to vigorous vortexing for 30 sec and sonicated for a further 15 min each time prior to making dilutions. Additionally, tubes were inverted several times and ZnO NPs resuspended 3-5 times in order to prevent rapid sedimentation. Working solution (1 mg/mL) and further dilutions were made by pipetting out the desired volume of the stock solution into a new tube already containing fresh diluent. Thereafter, the tubes were vortexed and used immediately for experiments. Working solutions and dilutions were prepared fresh for each experiment.



**Figure 3.2:** Schematic of the ZnO NP dispersal protocol used throughout this thesis.

### 3.2.3 Transmission electron microscopy (Cryo-TEM)

ZnO-NPs dispersed in distilled water or cell culture medium were visualized using the Gatan 626 cryoholder (Gatan, Pleasanton, CA, USA) and Tecnai 12 Transmission Electron Microscope (FEI, The Netherlands) at an operating voltage of 120 kV. TEM samples were prepared by pipetting 4  $\mu\text{L}$  of each sample on to a 300 mesh copper grid coated with lacy formvar carbon film (ProSciTech, Australia), glow discharged in nitrogen for 15 sec. The samples were allowed to adsorb for 30 sec following which they were placed in liquid nitrogen cooled liquid ethane until required. Images were recorded using the Megaview III CCD camera and analysis camera control software (Olympus, Germany) at magnifications between 70,000X and 110,000X.

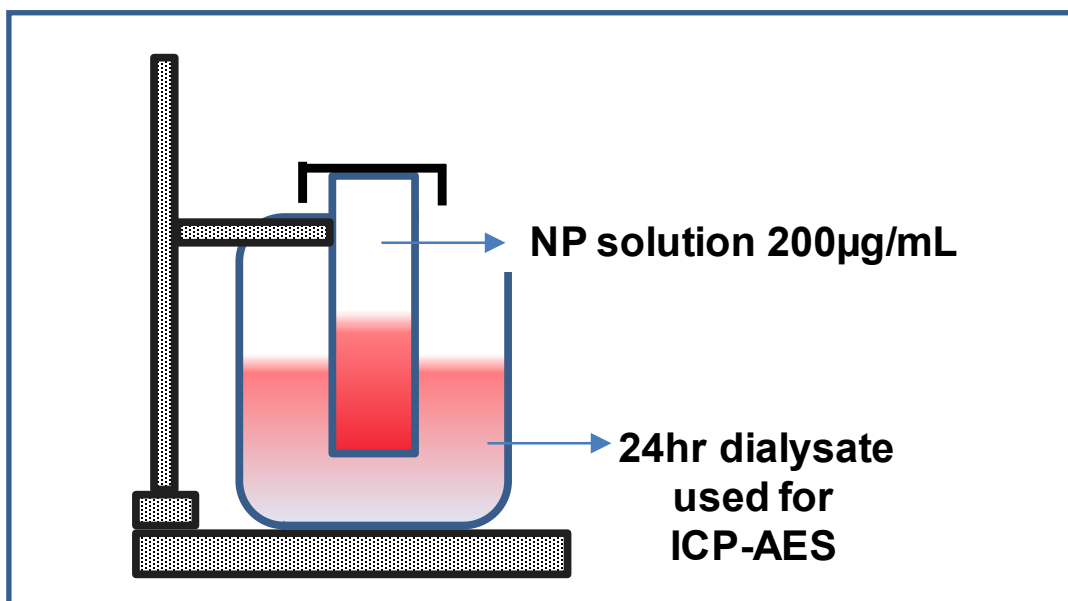
### 3.2.4 Differential centrifugation sedimentation

Quantitative assessment of the agglomeration status of all ZnO-NP in cell culture medium was undertaken using analytical disc centrifugation using the DC1800 disc centrifuge (CPS instruments, USA). ZnO-NP suspensions (2 mg/mL) were incubated in RPMI-1640 (Sigma-Aldrich, USA) cell culture medium supplemented with 10% fetal bovine serum (FBS) (Sigma-Aldrich, USA) for 4 or 24 hr prior to analysis. Fifteen millilitres of a gradient solution containing 24% w/w sucrose dissolved in cell culture media was loaded into the disc and spun at 24,000 RPM for 60 min to equilibrate. An aliquot of 100  $\mu\text{L}$ , at a concentration of 2 mg/mL of relevant ZnO-NP solution was directly injected onto the disk. A standard consisting of polystyrene beads with a diameter of 390 nm was used to calibrate the system before each measurement.

Measurements were recorded in triplicate for each sample. Surface area and particle number were calculated for the ZnO NPs and particulates using the diameters obtained from the CPS experiments as well as ones obtained from manufacturer (original particle sizes) assuming spherical morphology of the NPs.

### 3.2.5 Quantification of ZnO-NP dissolution in cell culture medium

For testing solubility of ZnO-NPs, 5 mL ZnO NP (200  $\mu\text{g}/\text{mL}$ ) solution was added to a 10,000 MW cut off dialysis tubing (Sigma-Aldrich, USA). The dilution medium used for this assay was RPMI-1640 (Sigma-Aldrich, USA) basal medium without proteins. The dialysis tubing was then placed into 30 mL of fresh medium reservoir and incubated at room temperature while gentle tumbling.



**Figure 3.3: A schematic describing the approach and sample preparation for quantification of dissolved ZnO-NP in cell culture medium**

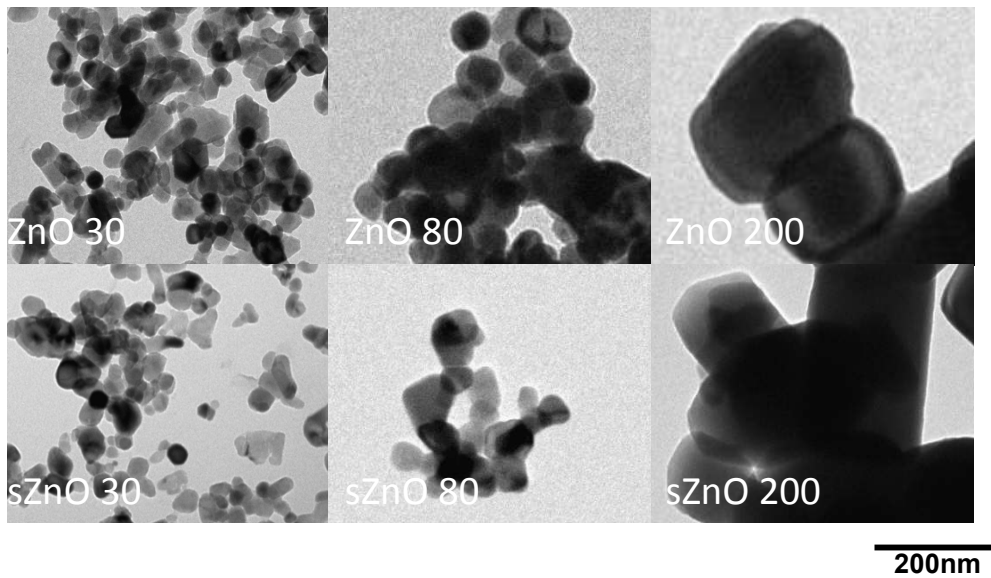
Sample analysis was carried out using a Varian Liberty Series II Inductively Coupled Plasma Atomic Emission Spectrometer (Melbourne, Australia). The Zn emission lines of 213.856 nm and 206.200 nm were monitored. The 213.856 nm emission line was used for quantification. A series of Zn standard solutions

were used to calibrate the instrument, an independent 1 ppm Zn standard solution was measured along with the samples for quality control. Sample recovery achieved was 98%. A medium only control provided the threshold zinc level.

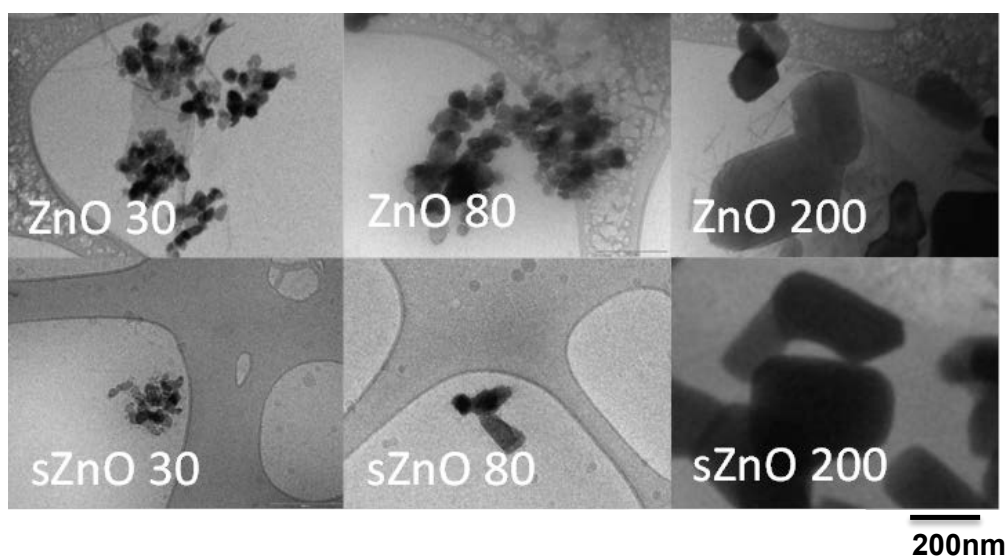
### 3.3 Results

#### 3.3.1 Determination of ZnO NP morphology and size (Cryo-TEM)

ZnO NPs dispersed in water (Figure 3.4) or cell culture medium (Figure 3.5) were characterised using electron microscopy. ZnO NPs displayed hexagonal particle morphology. In the presence of the protein rich cell culture medium (RPMI-1640), agglomeration of all ZnO NPs was observed.



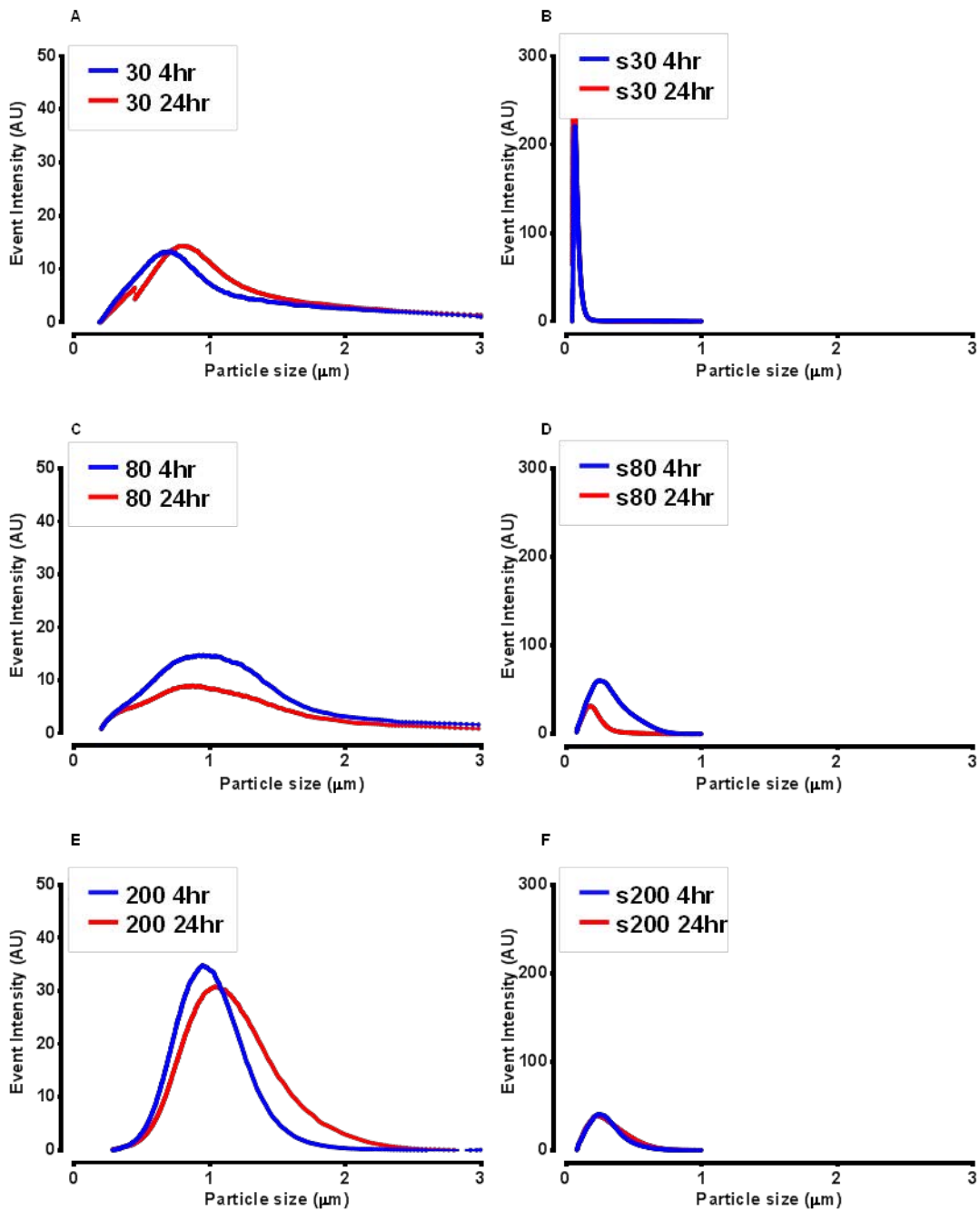
**Figure 3.4:** Transmission electron microscopy images of ZnO NPs used in this study. NPs were dispersed in distilled water prior to imaging (scale bar applies to all images). These images have been previously published in [4, 5]



**Figure 3.5: Cryo-TEM images of ZnO NPs used in this study. NPs were incubated in cell culture media with 10% serum for 24 hr prior to imaging (scale bar applies to all images). These images have been previously published in [4, 5]**

### **3.3.2 Determination of agglomerate size of ZnO NPs in cell culture medium (Disc centrifugation)**

The disc centrifugation technique was employed to measure and compare the agglomeration size of ZnO NPs in RPMI-1640 cell culture medium containing 10% fetal bovine serum after 4 or 24 hr incubation (Figure 3.6). Pristine (30, 80 and 200 nm) ZnO NPs displayed significant agglomeration in cell culture medium already after 4 hr, which did not change even after 24 hr. On the contrary, surfactant-dispersed NPs remained relatively mono-dispersed as compared to their pristine counterparts within the same time parameters. Assuming spherical morphology of the agglomerates specific surface areas were calculated for each ZnO NP, taking into account their primary particle sizes (as received from the manufacturer) and the sizes obtained from the CPS analysis (Table 3.1)



**Figure 3.6:** Disc centrifugation plots (A-F) showing the agglomeration status of different ZnO NPs when incubated in protein supplemented cell culture medium for 4 or 24 hr. Event intensity is shown as arbitrary units (AU). Data represented as mean of two separate experiments.

**Table 3.1 Particle primary size and surface area characterisation of ZnO NPs used in the present study. ZnO NPs were incubated in FBS containing cell culture medium for 4 or 24 hr. This significantly affected the mean diameter of all ZnO NPs. As compared to the pristine ZnO NPs the surfactant dispersed ZnO NPs remained relatively mono-dispersed. Surface area of the ZnO NPs was calculated assuming spherical NP morphology.**

Particle	Incubation time in medium	Mean diameter in cell culture medium measured using disc centrifuge	Surface area	Original particle size	Surface area
	(hr)	(nm)	(m <sup>2</sup> /g)	(nm)	(m <sup>2</sup> /g)
ZnO-NP 30	4	710	1.4	30	34.05
ZnO-NP s30	4	68	15	-	-
ZnO-NP 30	24	800	1.3	-	-
ZnO-NP s30	24	64	16	-	-
ZnO-NP 80	4	1025	1	80	12.8
ZnO-NP s80	4	271	3.8		
ZnO-NP 80	24	870	1.2		
ZnO-NP s80	24	200	5.1		
ZnO-NP 200	4	990	1	200	5.1
ZnO-NP s200	4	265	3.9		
ZnO-NP 200	24	1085	0.9		
ZnO-NP s200	24	253	4		

### 3.3.3 Quantification ZnO-NP dissolution in cell culture medium

Dialysis experiments and subsequent zinc quantification was performed at the highest concentration of (200 mg/mL) for each NP at the end of 24 hr incubation in cell culture media, with and without protein supplementation. Most ZnO NPs used in this study demonstrated less than 1% dissolution.

**Table 3.2: Table of dissolution rates of ZnO NPs, used in the present study. ICP-AES was performed on dialysates of ZnO NPs 200 mg/mL incubated in RPMI-1640 medium without protein for 24hr. \*Data are adapted from [4] and represent values obtained from identical experiments carried out in the presence of 10% fetal bovine serum supplemented RPMI-1640 medium.**

Zinc oxide nanoparticle	Zinc concentration ( $\mu\text{g}\cdot\text{mL}^{-1}$ )	
	RPMI-1640 medium without protein	RPMI-1640 medium supplemented with 10% fetal bovine serum
ZnO-NP 30	1.2	1.85*
ZnO-NP s30	1.8	1.44*
ZnO-NP 80	1.3	NA
ZnO-NP s80	2.2	NA
ZnO-NP 200	1	2.8*
ZnO-NP s200	0.8	2.32*
Basal medium	0.04	NA

NA: Data not available

### 3.4 Discussion

A comprehensive physico-chemical characterisation of NPs under physiological conditions can help in accurate interpretation of their bio-reactivity [6, 7].

Physical parameters such as primary nanoparticle size and agglomeration state arising from particle-particle interaction may affect the NP surface area, protein adsorption capacity and subsequent interaction with cellular structures [3]. Agglomerate formation of ZnO NPs dispersed in protein containing cell culture medium was clearly observed in the Cryo-TEM images (Figure 3.5). Dynamic light scattering (DLS) is a technique routinely used to measure hydrodynamic diameters of colloidal suspensions [8]. DLS was initially used to measure the primary particle size of the ZnO NPs, dispersed in media in the present study. However, the presence of protein molecules confounded the results. Therefore, to measure the agglomerate size, the disc centrifugation technique was used [9]. Pristine ZnO NPs rapidly agglomerated in the presence of proteins whereas the surfactant dispersant assisted in retaining the nano size distribution. This was also reflected in the total surface area of the surfactant dispersed particulates, which was almost ten times larger than their pristine counterparts. Table 3.1 describes the deviation in the mean diameters of the ZnO NPs dispersed in the cell culture medium as compared to their original diameters, received from the manufacturer. The surface area of the NP is inversely proportional to its diameter therefore, the larger the surface area, the higher the possibility of interaction of the NP surface with biomolecules. Protein binding capacity of the six different types of ZnO NPs has been discussed in further details in chapter IV.

All ZnO NPs used in this study displayed low solubility in the cell culture medium. Zinc is an essential trace element and plays an important physiological role in the cellular metabolism [10, 11]. Therefore it was essential to ascertain if the solubility of ZnO NPs affected their cytotoxic and pro-inflammatory (investigated in further details in chapter VI and VII) potentials. Interestingly, the surfactant used to achieve better dispersal of ZnO NPs did not prevent or impact the ZnO NP solubility.

Therefore, it can be assumed that differences observed in the immunotoxic endpoints investigated in this thesis including, protein interactions cytotoxicity and pro-inflammatory potential are indeed due to the interaction of intact ZnO NPs with the cellular systems. The data generated in this chapter can help in better interpretation of the solution phase behaviour of ZnO NPs in the cell culture medium environment.

### 3.5 Conclusion

The physico-chemical properties of the ZnO NPs used in this project are:

- ZnO NPs and particulates rapidly agglomerate in cell culture medium supplemented with proteins. This affects the surface area of the material.
- Surfactant-dispersal helps in retaining nano size distribution of the ZnO NPs
- All ZnO NPs demonstrate low solubility in cell culture medium.

### 3.6 References

1. Stoehr LC, Gonzalez E, Stampfl A, Casals E, Duschl A, Puentes V, Oostingh GJ: **Shape matters: effects of silver nanospheres and wires on human alveolar epithelial cells.** *Particle and Fibre Toxicology* 2011, **8**.
2. Luyts K, Napierska D, Nemery B, Hoet PHM: **How physico-chemical characteristics of nanoparticles cause their toxicity: complex and unresolved interrelations.** *Environmental Science: Processes & Impacts* 2013, **15**:23-38.
3. Saptarshi S, Duschl A, Lopata A: **Interaction of nanoparticles with proteins: relation to bio-reactivity of the nanoparticle.** *J Nanobiotechnol* 2013, **11**:26.
4. Feltis BN, O'Keefe SJ, Harford AJ, Piva TJ, Turney TW, Wright PFA: **Independent cytotoxic and inflammatory responses to zinc oxide nanoparticles in human monocytes and macrophages.** *Nanotoxicology* 2012, **6**:757-765.
5. Shen C, James SA, de Jonge MD, Turney TW, Wright PFA, Feltis BN: **Relating Cytotoxicity, Zinc Ions, and Reactive Oxygen in ZnO Nanoparticle-Exposed Human Immune Cells.** *Toxicol Sci* 2013, **136**:120-130.
6. Nel A, Madler L, Velegol D, Xia T, Hoek E, Somasundaran P, Klaessig F, Castranova V, Thompson M: **Understanding biophysicochemical interactions at the nano-bio interface.** *Nat Mater* 2009, **8**:543 - 557.
7. Nel A, Xia T, Meng H, Wang X, Lin S, Ji Z, Zhang H: **Nanomaterial Toxicity Testing in the 21st Century: Use of a Predictive Toxicological Approach and High-Throughput Screening.** *Acc Chem Res* 2012, **46**:607-621.
8. Lim J, Yeap S, Che H, Low S: **Characterization of magnetic nanoparticle by dynamic light scattering.** *Nanoscale Research Letters* 2013, **8**:381.

9. Neumann A, Hoyer W, Wolff MW, Reichl U, Pfitzner A, Roth B: **New method for density determination of nanoparticles using a CPS disc centrifuge™**. *Colloids and Surfaces B: Biointerfaces* 2013, **104**:27-31.
10. Tubek S: **Zinc Supplementation or Regulation of its Homeostasis: Advantages and Threats**. *Biol Trace Elem Res* 2007, **119**:1-9.
11. Maret W: **Zinc Biochemistry: From a Single Zinc Enzyme to a Key Element of Life**. *Advances in Nutrition: An International Review Journal* 2013, **4**:82-91.



---

## Chapter IV

### Interaction of ZnO-NPs with fetal bovine serum proteins and bio-reactivity

**Publication:**

**Saptarshi SR**, Wilson D, Feltis BN, Wright PF, Lopata AL.  
Interaction of zinc oxide nanoparticles with cell culture medium proteins Nanoscale (*Manuscript in preparation*)

---



## 4.1 Introduction

Nanoparticles possess a large surface area to mass ratio (1-100 nm size range), which facilitates their interaction with bio-molecules and cellular interfaces [1]. This has resulted in potential applications for these materials in the industrial and bio-medical fields. Metal oxide nanomaterials such as zinc oxide nanoparticles (ZnO NPs) are produced in large volumes and are commonly used as active ingredients in sunscreen formulations and other personal care products [2]. Recently, there has been a growing research interest in understanding the impact of nano/bio interactions on human health and the environment [3], as there is now evidence that some nanoparticles can cause cytotoxicity and inflammation [4-7].

The bio-reactive nature of NPs can be attributed to their size, shape and material properties [8-12]. For example, cytotoxicity of ZnO NPs has been linked to their dissolution characteristics [13]. In addition, there is evidence that the surrounding medium in which NPs are dispersed can to some extent affect the overall interaction of the NP surface with cells. Adsorption of proteins on the NP surface can result in the formation of the nanoparticle-protein corona (NP-PC) (Figure 4.1) [14-17]. This protein rich corona can alter the NP surface by giving it a biological character [18-20]. The nano/bio interface is dynamic because of the constant exchange of proteins occurring on the NP surface [15]. Certain proteins tend to be adsorbed on the NP surface with high affinity and do not desorb easily thus forming the long lasting “hard” protein corona [21]. This interaction is also largely influenced by the physicochemical properties of the proteins [22]. Recently, studies have shown that the size, dispersal state and surface properties of NPs may greatly influence their protein adsorption capacity [23-25]. Importantly, once adsorbed on the NP surface the proteins may undergo conformational changes which can in turn affect the reactivity of the protein [26]. The composition of the NP-PC has been previously characterised for silicon dioxide ( $\text{SiO}_2$ ), gold, polystyrene NPs, also carbon nanotubes dispersed in physiological fluids [25, 27-29]. In addition, differential binding of proteins onto ZnO-NP surface after interaction with human plasma has also been reported [30]. Others have described perturbation in the

secondary structures of proteins such as bovine serum albumin (BSA),  $\alpha$  lactalbumin and Vibrio Cholera Tox r proteins after adsorption on the ZnO NP surface [31-33]. Interestingly, these studies have not investigated the ZnO-NP-protein interaction from the nanotoxicological viewpoint.

The nanotoxicological evaluation of nanomaterials is often conducted using *in vitro* cell culture systems. The protein component of a typical *in vitro* tissue culture system comprises of 5-20% fetal bovine serum (FBS), a complex mixture of different types and concentrations of proteins. Detailed understanding of the identities of FBS proteins interacting with the NP surface and subsequent analysis of the consequence of this interaction is required to further elucidate cellular implications of this interaction. Interestingly, not many studies have explored the interaction of ZnO-NP with cell culture medium proteins. Subsequent biological effects of ZnO-NP interaction with cells have shown to be directed by factors such as extracellular dissolution of these NP to generate reactive  $Zn^{2+}$  ions. ZnO NPs used in the present study have been previously shown to have low dissolution rate (Chapter III), which may indicate that intact NPs interact with cells. This makes it important to further explore the interactions of these NPs with the surrounding protein molecules. In addition, the composition of the NP-PC for pristine or surfactant-dispersed ZnO NPs has been analysed for the first time in this study, to identify the effect of NP aggregation on their protein-adsorption potential. The structures of key blood proteins, such as BSA, apolipoprotein A1, transferrin and fibrinogen few of which were also identified on the ZnO NP surface, have been analysed using circular dichroism (CD) spectroscopy.

Cytotoxicity is one of the most important consequences of NP-cellular interaction. While the cytotoxic nature and underlying hypotheses explaining the mechanism of ZnO NP mediated cytotoxicity has been thoroughly investigated, the impact of the ZnO NP-PC on ZnO NP bio-reactivity needs further investigation. In the present chapter, cytotoxicity of 30 or s30 ZnO NPs dispersed in 10 (3.7 mg/mL) or 40% (14.8 mg/mL) FBS containing medium has been compared *in vitro*, using human lung epithelial cells (A549).

The overall aim of this chapter is to identify and characterise the ZnO-NP-fetal bovine serum protein corona, establish if some proteins undergo structural modifications after adsorption onto the ZnO NP surface and finally evaluate the effect of protein concentration on the cytotoxicity of ZnO NPs on A549 cells

## **4.2 Materials and Methods**

### **4.2.1 Nanoparticle characterisation**

Industrially manufactured ZnO NPs and particulates of three different particle sizes (30, 80 and 200 nm), with and without surfactant dispersant, were used in this chapter. Methods for preparation of NP solutions and information on their physico-chemical characterisation are described in the previous chapter III.

### **4.2.2 Isolation and detection of the ZnO NP-FBS protein corona using SDS PAGE**

ZnO NP solutions (2 mg/mL) were incubated with 10% FBS containing RPMI-1640 cell culture medium (Sigma- Aldrich, USA) for 1, 4, and 24 hr to study the effect of incubation time on ZnO NP protein adsorption. All incubations were carried out at 37<sup>0</sup>C for 1 hr on a rocking platform. At the end of the incubation, centrifugation at 16,000 rpm for 15 min was performed to separate unbound proteins from the nanoparticle-protein complexes. The NP-protein complexes were then subjected to repeated washing in 1 mL phosphate buffered saline (PBS) (Life Technologies, Australia). Proteins firmly adsorbed on the NP surface were eluted using 5 X Lammeli buffer (Appendix A) and heat (95<sup>0</sup>C for 3 min). The proteins samples were separated using 4-20% Tris-Glycine gels. (BioRad, USA). All protein corona related experiments were carried out using special low protein binding tubes (Costar®, Sigma-Aldrich).

### **4.2.3 Protein identification by mass spectrometry**

#### **4.2.3.1 In-gel digestion**

Following destaining (Appendix A), gel slices were resuspended in 100 µL of 20 mM dithiothreitol (DTT) in 25 mM NH<sub>4</sub>HCO<sub>3</sub> (pH 8) and reduced at 65<sup>0</sup>C for 1 hr. The liquid was removed using a pipette and the samples alkylated by

addition of 100  $\mu\text{L}$  of 50 mM iodoacetamide (IAA) in 25 mM  $\text{NH}_4\text{HCO}_3$  (pH 8) and incubated at 37°C in darkness for 40 min. The gel slices were washed three times for 15 min each with 200  $\mu\text{L}$  of 25 mM  $\text{NH}_4\text{HCO}_3$  and then dried in a vacuum centrifuge. The dried gel slices were rehydrated with 20  $\mu\text{L}$  of 40 mM  $\text{NH}_4\text{HCO}_3$ /10% acetonitrile (ACN) containing 20  $\mu\text{g}/\text{mL}$  trypsin (Sigma- Aldrich, USA) for 1 hr at room temperature. The samples received a further 50  $\mu\text{L}$  of trypsin digestion solution and were incubated overnight at 37°C. The digestion solution containing the peptides of interest was removed from the gel slices using a pipette, and residual peptides recovered from the gel slices by three 45 min incubations at 37°C with 50  $\mu\text{L}$  of 0.1% trifluoroacetic acid (TFA). The peptide samples were dried in a vacuum centrifuge prior to mass spectral analysis.

#### 4.2.3.2 HPLC and MS/MS analysis

Dried tryptic fragments from in-gel digests were resuspended in 15  $\mu\text{L}$  0.1% formic acid (FA) and 10  $\mu\text{L}$  separated by reversed-phase chromatography (RP-HPLC) using a Dionex Ultimate 3000 HPLC and an Agilent Zorbax 300SB-C18 (3.5  $\mu\text{m}$ , 150 mm  $\times$  75  $\mu\text{m}$ ) column. A linear gradient of 4–60% solvent B (90% ACN/0.1% FA) in solvent A (0.1% FA) over 60 min was employed at a flow rate of 300 nL/min for all experiments. Samples were eluted directly from the RP-HPLC column into the NanoSpray II ionisation source of a QSTAR Elite Hybrid MS/MS System (AB SCIEX) operated in a positive ion electrospray mode. All analyses were performed using Information Dependant Acquisition. Data analysis and peak lists were generated using Analyst 2.0 (AB SCIEX). The acquisition protocol used an Enhanced mass spectrum scan as the survey scan and the three most abundant ions detected over the background threshold were examined using an Enhanced Resolution scan to confirm the charge state of the multiply charged ions. Ions with charge states of +2, +3, or unknown charge were subjected to collision-induced dissociation using a rolling collision energy dependent upon the  $m/z$  and the charge state of the ion. Enhanced Product Ion scans were acquired resulting in full product ion spectra for each of the selected precursors, which were then used in subsequent database searches.

#### 4.2.3.3 Mascot searches

Searches were performed in ProteinPilot™ v4.0.8085 (AB SCIEX) using both the Paragon algorithm and Mascot server version 2.4 (Matrix Science, UK). Paragon searches were performed at a 95% confidence level. Mascot searches were performed at a significance threshold of  $p < 0.05$  and used a peptide mass tolerance 0.1 Da and a fragment mass tolerance of 0.1 Da. Mascot searches allowed for carbamidomethylation and methionine oxidation variable modifications, two missed cleavages, +2 and +3 charge states, and trypsin as the enzyme and standard scoring was used to derive protein scores. All data were searched against the SwissProt database (539, 829 proteins).

#### 4.2.4 Investigating the evolution of NP-PC on ZnO NP surface

Pristine or surfactant dispersed 30 nm ZnO NP solutions (2 mg/mL) were incubated with increasing concentrations of FBS (0.1%, 1% and 10%) containing cell culture medium for 1 hr. After incubation with 10% FBS proteins for 1 hr and subsequent washing steps, pellets of 30 and s30 ZnO NPs were further incubated in 500  $\mu$ l of cell lysate obtained from human lung epithelial cells (A549) using NP40 lysis buffer (Life Technologies, USA) for additional 1 or 24 hr. At the end of the incubation, the hard protein coronas formed on the ZnO NP surface were retrieved as per the methods described in section 4.2.3. Identification of bovine serum albumin (BSA) protein was carried out using immunoblotting. Briefly, SDS-PAGE separated proteins were transferred onto a nitrocellulose membrane using the semi-dry transfer system (BioRad, USA). After blocking with 1% Superblock (Sigma-Aldrich, USA) blocking solution for 1 hr, the membranes were probed with monoclonal anti-BSA antibody (Sigma-Aldrich, USA), followed by washing with PBS three times. BSA was detected using horseradish peroxidase-tagged secondary antibodies (Cell Signalling, USA) and enhanced chemiluminescence substrate (Pierce, USA), followed by exposure to photographic film (GE Healthcare, Australia).

#### 4.2.5 Quantification of bound protein on ZnO NP surface.

ZnO NP solutions (2 mg/mL) were incubated with solutions of BSA, apolipoprotein A1, transferrin and fibrinogen in PBS (0.5 mg/mL) for 1 hr

following which they were subjected to centrifugation (16,000 rpm) for 15 min. The supernatant obtained, was used for protein quantification. The difference in protein amount in the supernatant corresponded to the mass of protein bound on the ZnO NP surface. Total protein quantification was carried out using the 660 assay kit (Thermo Scientific, USA). Readymade BSA standards (Thermo, USA) ranging (0.125-2.00 mg/ml) were used for the standard curve analysis ( $R^2 = 0.96$ ). Briefly, 10  $\mu$ L of the standards or supernatant was transferred into a microwell plate and mixed with 150  $\mu$ L of the 660 assay reagent. Following 5 min incubation at room temperature absorbance of was determined at 660 nm (VersaMax, Molecular Devices, USA). ZnO NP solutions in PBS without the respective protein solutions served as the control to correct for interference in the absorption reading due to individual NPs. The percentage of protein bound to the NPs was determined using the following equation

$$\text{Protein bound\%} = [(\text{Original protein concentration} - \text{blank}) - (\text{Supernatant protein concentration} - \text{protein blank.})] / \text{Original protein conc.} \times 100$$

Furthermore, from known protein molecular weights, particle numbers and protein concentration, number of bound protein molecules on the surface of ZnO NP solutions was calculated. It should be noted that the manufacturer's data regarding the NP sizes was used in the calculations.

#### 4.2.6 Circular Dichroism spectroscopy

The influence of ZnO-NPs on the structure of adsorbed proteins was studied using CD spectroscopy. CD spectra were obtained using the JASCO-715 spectropolarimeter. All measurements were made at room temperature using a 1 mm quartz cuvette over a wavelength range of 190-260 nm. Observations were recorded every 0.2 nm with a bandwidth of 1 nm at 100 nm/min averaging over eight scans.

Protein samples (100  $\mu$ g/mL) were prepared in PBS and incubated with ZnO-NP dilutions for 1 hr at room temperature before each measurement. Final data was expressed as mean residual ellipticity ( $\Theta$ )<sub>MRE</sub> after subtracting the PBS blank spectrum. Mean residual ellipticity calculations were made using the following equation.

$$(\Theta)_{\text{MRE}} = \Delta \Theta * M_w / 10 * l * c$$

Where  $M_w$  is the mean residue weight of the respective protein (molecular weight /number of amino acid residues);  $l$  is the length of cuvette (0.1 cm) and  $c$  is the protein concentration (0.0001 mg/L.)

Furthermore, the percentage alpha helical content of the protein was evaluated using the following equation which takes into account the contribution of the  $\beta$  sheets and random coil conformation at 208 nm (4000) and compared the observed value to the MRE of a pure  $\alpha$  helical protein (33000) [34]

$$\% \alpha \text{ helix} = - (\Theta)_{\text{MRE}} - 4000 / (33000 - 4000)$$

## 4.2.7 ZnO NP protein corona and bio-reactivity

### 4.2.7.1 Cell culture

The *in vitro* test system used in this thesis comprised of the human alveolar lung epithelial A549 cells. These cells were obtained from the American Type Culture Collection (ATCC, USA) and maintained in 25 cm<sup>2</sup> cell culture flasks in an incubator with a humidified atmosphere at 37°C and 5% CO<sub>2</sub>. The cells were cultured in RPMI-1640 medium (Sigma-Aldrich, USA) supplemented with 10% FBS, 1% penicillin–streptomycin and L-glutamine (Life Technologies, Australia), designated as ‘complete medium’. The cells were cultured to a cell density of 1 × 10<sup>6</sup> cells/mL before being sub-cultured into fresh media at a dilution factor of 1 in 10, 2-3 times a week.

### 4.2.7.2 Protein dependent association of ZnO NPs with A549 cells

Flow cytometry based side and forward-scatter analysis was used to evaluate the uptake of ZnO NPs by A549 cells in the presence or absence of proteins, as per the method described by Suzuki et al.[35]. Briefly, A549 cells were allowed to attach overnight in 6-well plates at a density of 10<sup>6</sup> cells per mL following which they were incubated with the ZnO NPs dose (100  $\mu$ g/mL) for 1 hr. At the end of exposure, the NP containing medium was discarded, cells washed with Hank's Balanced Salt Solution (HBSS) (Life Technologies, Australia) three

times. The cells were dislodged using a cell scraper (Nunc, Thermo Fisher, Australia) and re-suspended in 0.4 mL of HBSS. The cells were analysed immediately on BD FACSCalibur™ flow cytometer (BD Biosciences). The mean side-scatter intensity of cells was analysed for each sample by using the BD FACSDiva™ software where series of 10,000 events were recorded for each treatment. Visual analysis revealed no change in the morphology of A549 cells exposed to either ZnO NP solutions. Additionally, cell viability was also assessed using the MTS assay (detailed description stated in the impending section, 4.2.7.3)

#### **4.2.7.3 ZnO NP- protein interactions and effect on cytotoxicity**

To confirm if the protein concentration of the medium in which ZnO NPs are dispersed affect their bio-reactivity, exposure of A549 cells to a relatively high dose of ZnO NPs was carried out for 24 hr following which cell viability was assessed using the MTS (Promega MTS Cell Titer 96® aqueous kit, Promega, USA) assay. Prior to selecting the ZnO NP dose, A549 cells were seeded in 6-well tissue culture plates ( $10^6$  cells) and allowed to attach overnight. Subsequently cells were exposed to 100 µg/mL ZnO NP solution for 24 hr. At the end of exposure, the cells NP containing media was washed and cell morphology was visualised using bright field microscopy.

For the cell viability assay, 10,000 cells in 100 µL were seeded into wells of 96-well tissue culture plates (Sarstedt, Germany). After allowing for overnight attachment, the cells were exposed to 100 µg/mL of the 30 or s30 ZnO NP solutions dispersed in 10 or 40% FBS containing medium for 24 hr. Following the *in vitro* exposure procedure, the viability of A549 cells was assessed using the MTS assay (Promega MTS Cell Titer 96® aqueous kit, Promega, USA), which detects reduction of a tetrazolium salt to a purple formazan product. The NP-containing media in the plates with cells was replaced with fresh medium containing MTS reagent and the plates were further incubated at 37°C for 3 hr. The purple coloured formazan product was read at 490 nm on a micro plate reader (VersaMax, Molecular Devices, USA). ZnO NPs with MTS reagent alone provided the non-specific absorbance readings of cell-free blank controls. Specific absorbance from untreated cells was used as the reference for

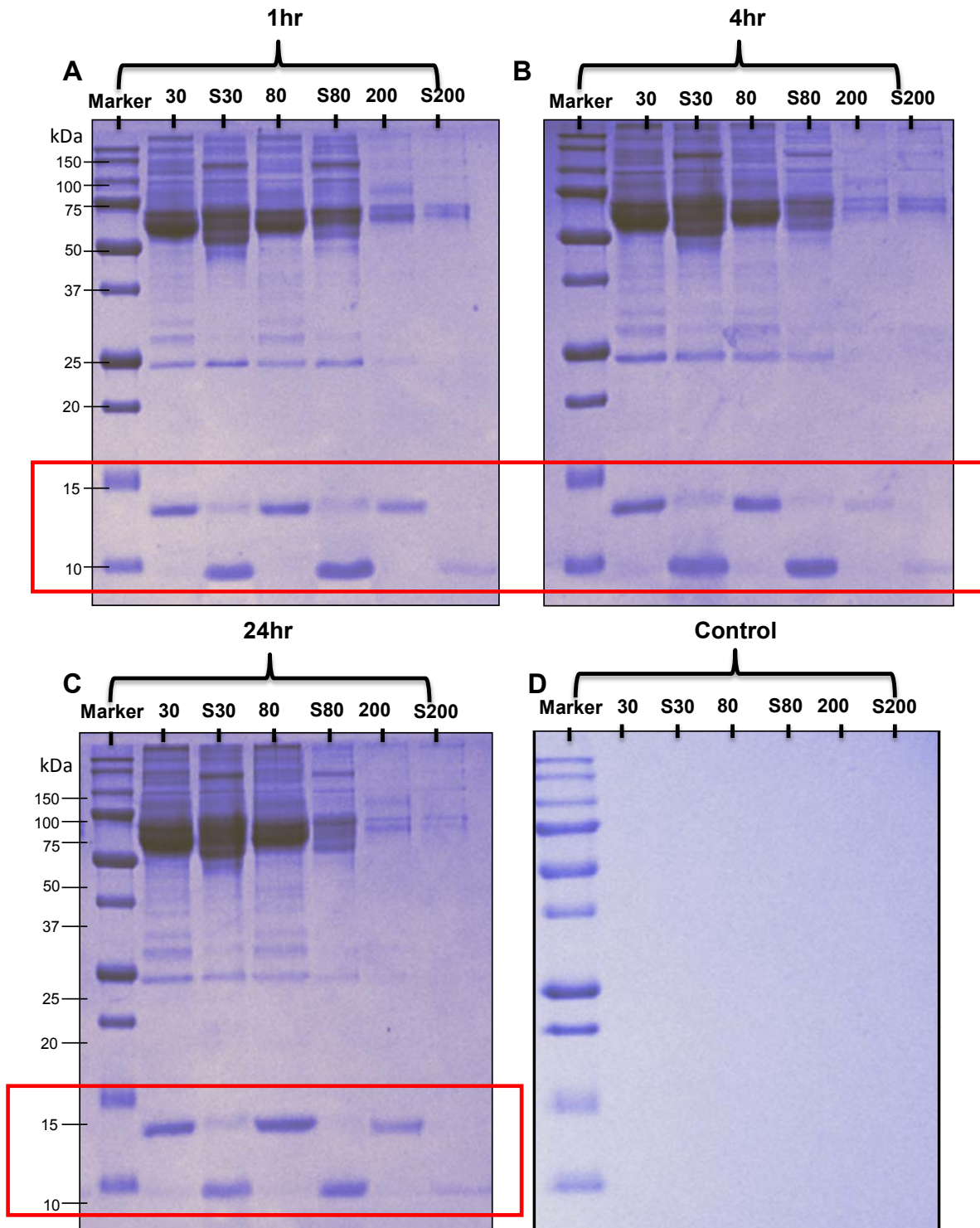
normalising the test-well data to calculate “% of control cell viability”. Dose and time depended cytotoxicity of all ZnO NPs was assessed using this assay to address their cytotoxic potential and has been described in chapter VI in further details.

In addition, DAPI staining was carried out to study the changes in nuclear morphology of A549 cells after treatment with 100 µg/mL of 30 or s30 ZnO NP solutions with 10 or 40 % FBS containing media. A549 cells were allowed to attach overnight in 6-well plates at a density of  $10^6$  cells per mL following which they were incubated with a cytotoxic dose of ZnO NPs of 100 µg/mL for 24 hr. At the end of the incubation period, all cells were collected and washed with HBSS, subjected to fixation and were mounted on Superfrost slides (Proscitech, Australia) using ProLong® Gold Antifade Reagent with DAPI (Molecular Probes, Life Technologies, USA). The slides were subsequently incubated at room temperature for 24 hr in the dark before visualization using a Zeiss LSM710 confocal laser scanning microscope (Carl Zeiss, Germany).

## 4.3 Results

### 4.3.1 ZnO NP protein profiling using SDS PAGE

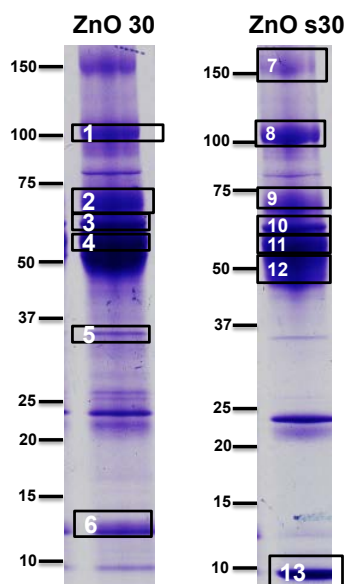
Protein adsorption on the ZnO NP surface reached equilibrium rapidly and did not change over 24 hr. Binding of serum proteins to individual ZnO NP is shown in figure 4.1. Overall, the protein binding patterns for all ZnO-NP types were the same particularly in the case of higher molecular weight proteins (37-250 kDa). Interestingly, in the lower molecular weight range of 10-15 kDa, differential protein binding (highlighted with an empty red box Figure 4.1 A-C) was observed. All pristine NPs bound a 14 kDa protein and the surfactant-dispersed ZnO NPs selectively bound an 11 kDa protein. ZnO NPs bound more proteins as compared to the 200 nm ZnO particulates. Control samples containing proteins alone in absence of NPs demonstrated no detectable protein bands (Figure 4.1 D)



**Figure 4.1 (A-C) SDS-PAGE of ZnO NP bound FBS proteins demonstrating effect of incubation time on protein adsorption. Differential binding of protein in the lower molecular weight range is highlighted using the red box. (D) Negative control**

### 4.3.2 Protein identification by mass spectrometry

Prominent bands of proteins adsorbed on 30 or s30 ZnO-NP surfaces after incubation for 4 hr were excised from the gel, protein identities confirmed using MS/MS analysis and subsequent Mascot search using the SwissProt database (Figure 4.2). Detailed list of identified proteins can be found in table 4.1. The two ZnO NP surfaces adsorbed proteins such as alpha-2-macroglobulin, factor XIIa inhibitor, alpha-1-antitrypsin that are known to be involved in proteolysis. Also BSA, the most abundant blood protein and other albumin-like proteins were found to be present on both the NPs investigated. Complement C3 an important protein from the complement cascade involved in immune function was identified on both NP surfaces. Lastly proteins such as apolipoprotein A-II an important constituent of high density lipoprotein (HDL) also involved in lipid transport were identified on both the surfaces. Interestingly in the lower molecular weight range (10-15kDa) a differential binding of serum proteins was visible for each type of the 30 nm ZnO-NP. For example, while the pristine NP demonstrated a stronger band at 14 kDa comprising of haemoglobin and histone subunits, the s30 NP showed one at 11 kDa binding Alpha-1-antitrypsin, Apo CIII and fibrinogen alpha chain.



**Figure 4.2 SDS-PAGE of protein adsorbed by pristine or surfactant dispersed 30nm ZnO NPs. Numbered boxes represent respective protein bands that were excised from the gel and identified using mass spectrometry.**

**Table 4.1 Identification of FBS proteins constituting the NP-PC on ZnO NP surface using SDS- PAGE and mass spectrometry (MS/MS analysis).**

Band Id.	Proteins identified	Accession No.
<b>ZnO 30</b>		
1	Inter-alpha-trypsin inhibitor heavy chain H4	ITIH4_BOVIN
2	Serum albumin	ALBU_BOVIN
3	Complement C3	CO3_BOVIN
4	Alpha-1-antiproteinase	A1AT_BOVIN
5	Complement C3	CO3_BOVIN
6	Hemoglobin fetal subunit beta	HBBF_BOVIN
	Apolipoprotein A-II	APOA2_BOVIN
<b>ZnO s30</b>		
7	Alpha-2-macroglobulin	A2MG_BOVIN
8	Inter-alpha-trypsin inhibitor heavy chain H4	ITIH4_BOVIN
	Alpha-2-macroglobulin	A2MG_BOVIN
9	• Factor XIIIa inhibitor	F12AI_BOVIN
	• Alpha-fetoprotein	FETA_BOVIN
	• Serum albumin	ALBU_BOVIN
10	• Complement C3	CO3_BOVIN
	• Serum albumin	ALBU_BOVIN
11	Serum albumin	ALBU_BOVIN
12	• Serum albumin	ALBU_BOVIN
	• Alpha-2-HS-glycoprotein	FETUA_BOVIN
	• Alpha-1-antiproteinase	A1AT_BOVIN
13	• Serum albumin	ALBU_BOVIN
	• Alpha-1-antiproteinase	A1AT_BOVIN
	• Apolipoprotein A-II	APOA2_BOVIN
	• Apo CIII	APOC3-BOVIN
	• Fibrinogen alpha chain	FIBA_BOVIN

### 4.3.3 Investigating the evolution of the NP-PC on ZnO NP surface

Incubation of ZnO NPs with increasing concentration of FBS proteins resulted in the development of unique protein coronas on the surface of the two 30 nm ZnO NPs. At the lowest FBS concentration (0.1%) very faint protein bands were observed except a prominent one in the molecular weight range of 50-60 kDa. Subsequent immunoblotting analysis confirmed the identity of this band to be BSA. At the higher protein concentrations (1 or 10%) not only did the intensity of BSA increase, but also novel protein bands were observed comprising the ZnO NP-PC, although the general protein banding patterns remained the same.

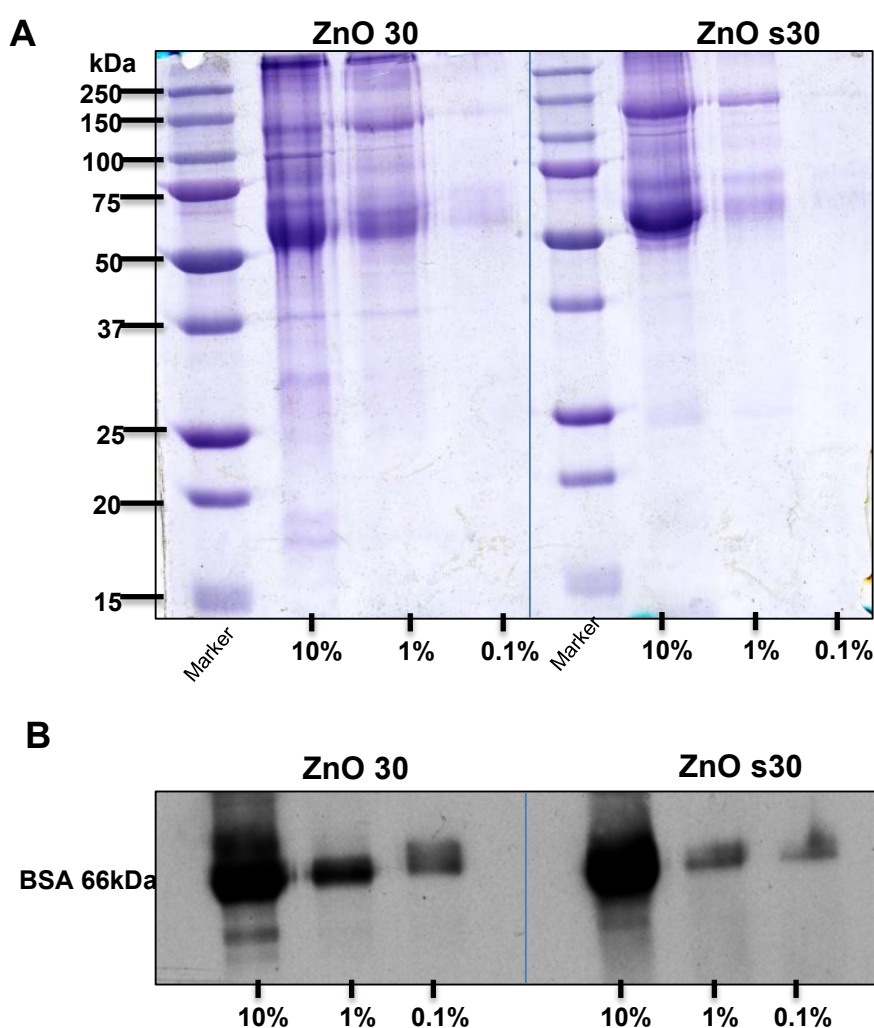
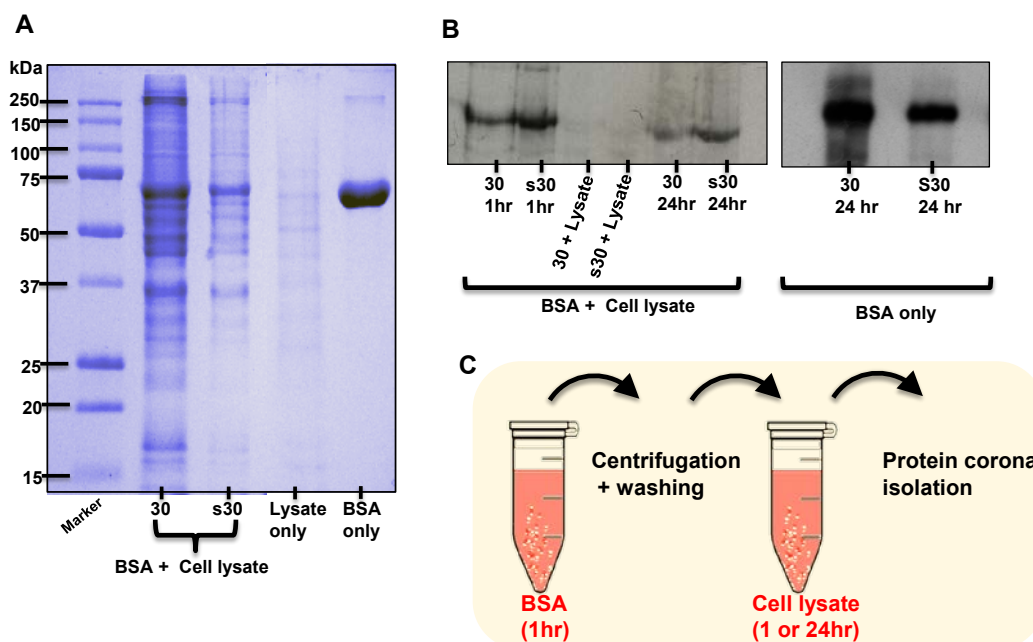


Figure 4.3 (A) SDS-PAGE demonstrating difference in protein banding of 30 or s30 ZnO NPs when dispersed in increasing concentrations (0.1-10%) of FBS proteins. (B) Immunoblotting analysis used to confirm the identity of the most prominent protein band on the ZnO NP surface to be that of bovine serum albumin.

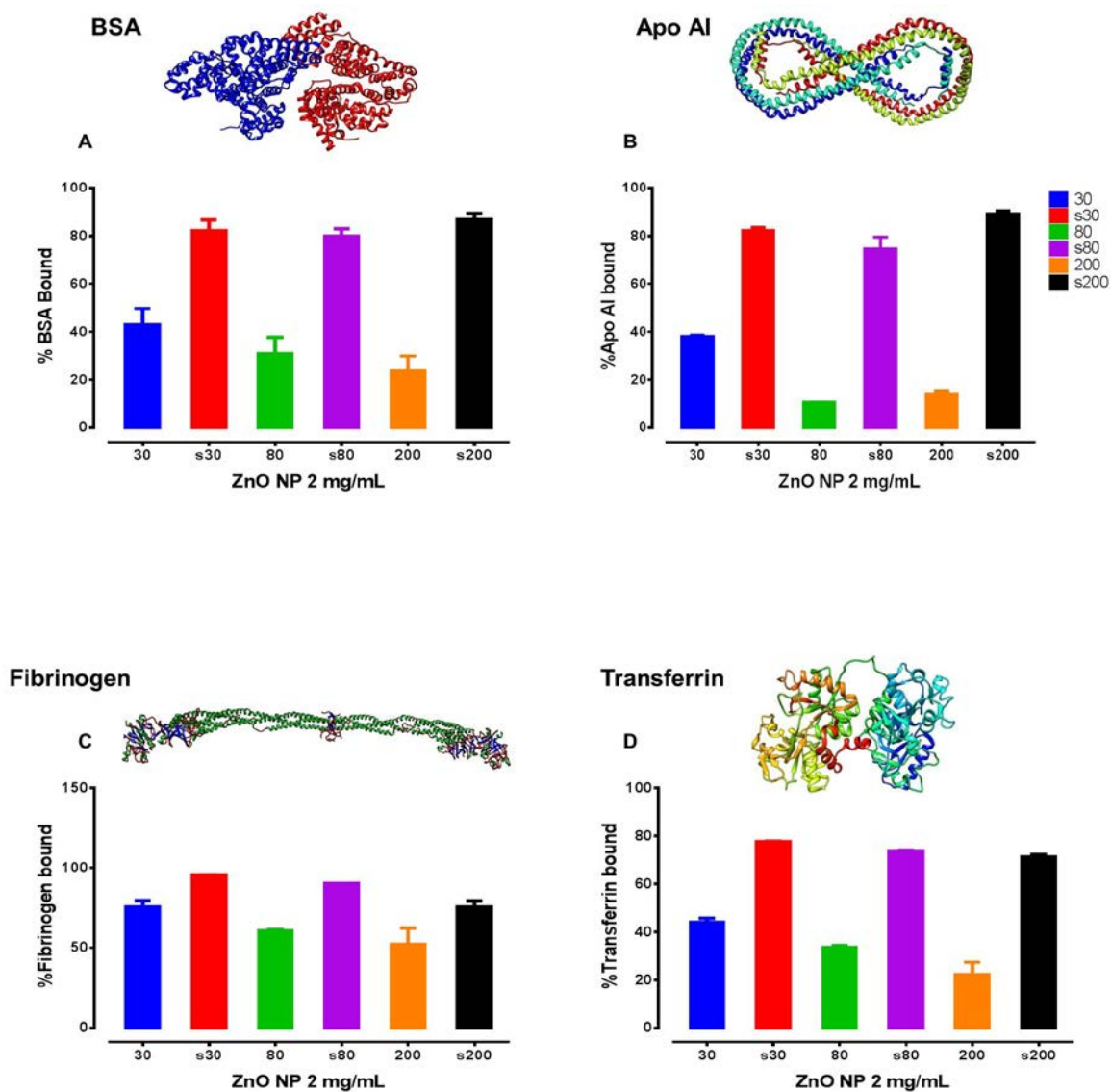
Additionally, ZnO-NP pre-incubated in BSA for 1 hr were further transferred into A549 cell lysate for 1 or 24 hr. SDS-PAGE results clearly demonstrated adsorption of the cell lysate proteins on to the NP surfaces pre-adsorbed with BSA. Subsequent immunoblotting analysis with monoclonal anti-BSA antibody confirmed BSA to be still present on the NP surface after 1 hr incubation in cell lysate proteins. Interestingly, after 24 hr incubation the intensity of the BSA band was found to be lower than that recorded for the 1 hr time point. The intensity and therefore abundance of BSA was found to be greater on the surfactant dispersed NP due to increased surface area available as compared to the pristine NP.



**Figure 4.4 Evolution of ZnO NP-PC.** Pristine or surfactant-dispersed 30 nm ZnO-NPs were pre-incubated with BSA protein solution for 1 hr. After washing the unbound BSA molecules, NPs were further incubated in the cell lysate proteins obtained from A549 cells for further 1 or 24 hr. (A) SDS-PAGE protein profile of the two ZnO NP surfaces demonstrated presence of cell lysate proteins on the surface of BSA pre-coated ZnO NPs. (B) Immunoblot analysis, using monoclonal antibody confirmed presence of the BSA layer on the NP surface despite subsequent incubation with cell lysate proteins. (C) Schematic highlighting the methodology used.

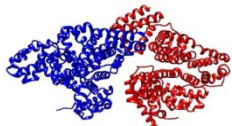
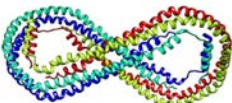

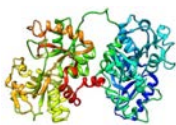
#### **4.3.4 Quantification of protein bound on ZnO NP surface**

The capacity of the ZnO NPs to bind proteins onto their surface was quantified using the protein depletion method (Section 4.2.6) also previously described [29]. At a fixed NP concentration (2 mg/mL) and protein concentration (0.5 mg/mL) the surfactant-dispersed ZnO NPs bound more proteins as compared to their pristine counterparts. For BSA, Apo AI and transferrin, the surfactant-dispersed ZnO NPs bound almost twice the amount of proteins, not observed for fibrinogen. This was also reflected in the number of protein molecules found to be associated for each protein bound on the ZnO NP surface (Table 4.2).



**Figure 4.5 Protein binding capacity of ZnO NP and particulates for (A) BSA (B) Apolipoprotein AI (C) Fibrinogen and (D) Transferrin to ZnO NP surface at a fixed protein concentration (0.5 mg/mL) and ZnO NP concentration (2 mg/mL)  $n = 2$ ; error bars represent standard deviation. Overall surfactant-dispersed ZnO NPs bound more protein compared to pristine counterparts.**

**Table 4.2 Protein binding capacity of ZnO NPs when incubated in different protein solutions and estimation of the surface coverage of ZnO NP in terms of number of individual protein molecules assuming spherical NP morphology**

	Protein characteristics	ZnO NP	Protein bound (%)	Protein molecules per ZnO NP
BSA	<b>Mol. Weight:</b> 66 kDa <b>Size:</b> 8 x 8 x 3 nm* <b>Shape:</b> Globular 	30	43	8
		s30	82	15
		80	31	106
		s80	80	275
		200	23	1265
		s200	87	4668
Apolipoprotein AI	<b>Mol. Weight:</b> 23.8 kDa <b>Size:</b> ~5 nm <b>Shape:</b> Globular 	30	38	16
		s30	83	35
		80	10	84
		s80	78	626
		200	13	1666
		s200	88	11075
Fibrinogen	<b>Mol. Weight:</b> 340 kDa <b>Size:</b> 45 X 5 nm* <b>Shape:</b> Coiled-Coil 	30	76	3
		s30	95	3
		80	60	40
		s80	90	60
		200	52	541
		s200	75	790
Transferrin	<b>Mol. Weight:</b> 80 kDa <b>Size:</b> 9.5 x 6 x 5 nm* <b>Shape:</b> Globular 	30	44	7
		s30	78	12
		80	33	95
		s80	74	209
		200	22	975
		s200	71	3163

\* Protein sizes adopted from [36] for BSA and [26] for fibrinogen and [37] for transferrin

#### 4.3.5 Circular dichroism spectroscopy

CD spectroscopy was employed to ascertain possible changes in the structure of abundant serum proteins after adsorption on ZnO NPs. CD spectra were obtained for proteins in the absence or presence of increasing amounts of 30 or s30 ZnO NPs. BSA is primarily an  $\alpha$  helical protein constituting 68%  $\alpha$  helical structure. In the absence of ZnO NPs the far UV spectrum obtained for BSA showed characteristic negative bands at 208 and 222 nm, respectively, typical for the protein  $\alpha$  helix also previously reported [31]. Interestingly, presence of increasing amounts of pristine 30 nm ZnO NPs caused minor changes in the mean residue ellipticity (MRE) value for the protein, suggestive of conformation change. Evaluation of  $\alpha$  helical content of BSA in presence of highest ZnO NP concentration showed reduction from 68% to 58.3 %. Furthermore, the CD spectrum obtained for the highest ZnO NP concentration also did not vary significantly, indicating the protein could retain most of its secondary structure. On the contrary, addition of 150  $\mu\text{g}/\text{mL}$  s30 ZnO NP to the BSA solution resulted in more positive MRE values and reduction of  $\alpha$  helical content from 68% to 30%.

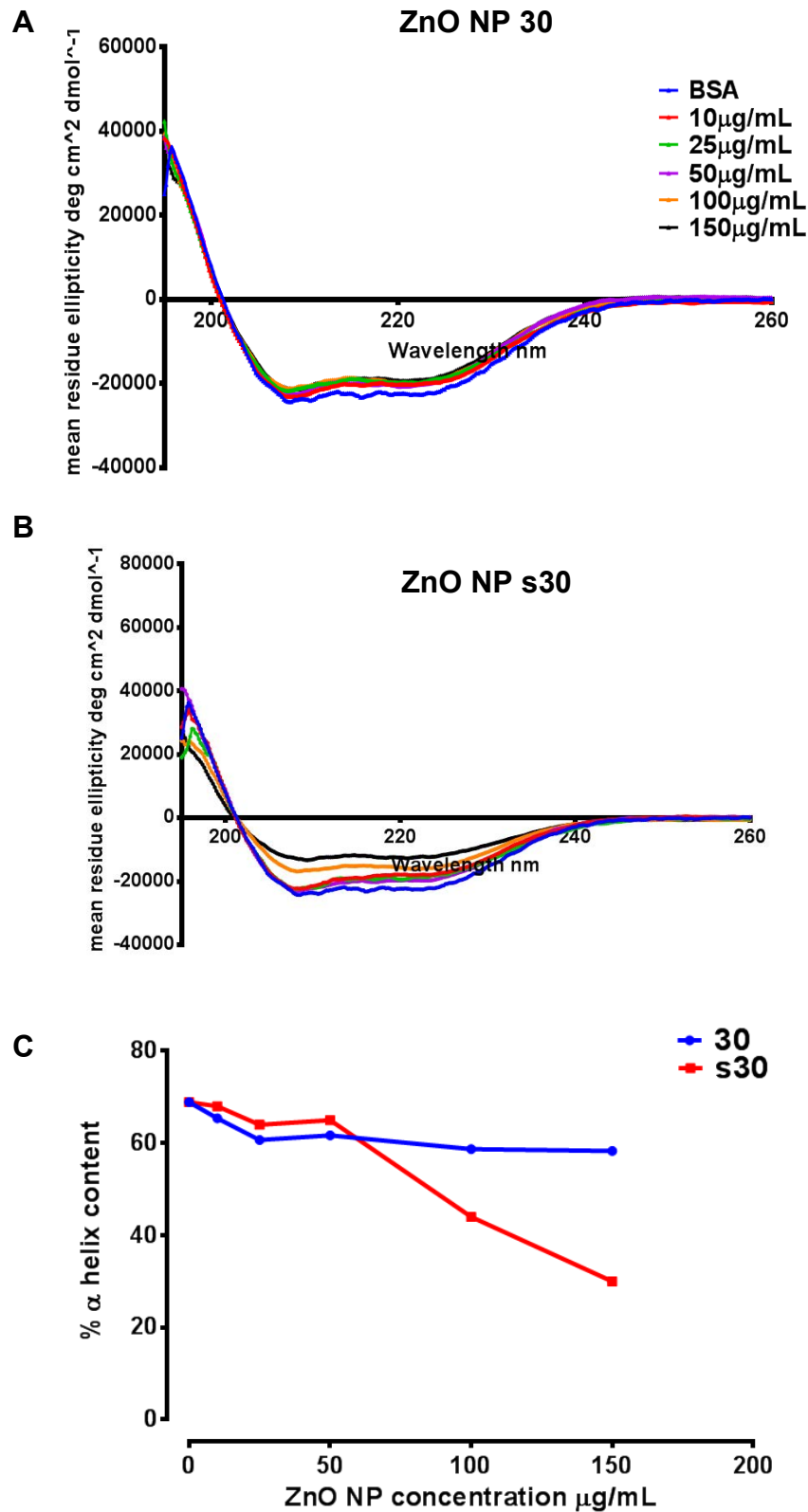


Figure 4.6 Comparison of CD spectra of native BSA (blue curve) with BSA adsorbed on varying concentrations of (A) 30 ZnO NPs or (B) s30 ZnO NPs. (C) compares the variation in alpha helical content of BSA after interaction with ZnO NPs.

Similarly, MRE values of ZnO NP added fibrinogen solution were higher than that of fibrinogen solution alone (Figure 4.7 A & 4.7B). Interestingly, the CD spectra obtained for ZnO NP treated transferrin was similar to that of the original CD spectrum of the protein in absence of NPs (Figure 4.7C & 4.7D). The CD spectra for haemoglobin (Figure 4.7E & 4.7F) and human serum albumin (Figure 4.7G & 4.7H) were also analysed. Neither of these proteins showed significant secondary structure perturbation in the presence of ZnO NPs.

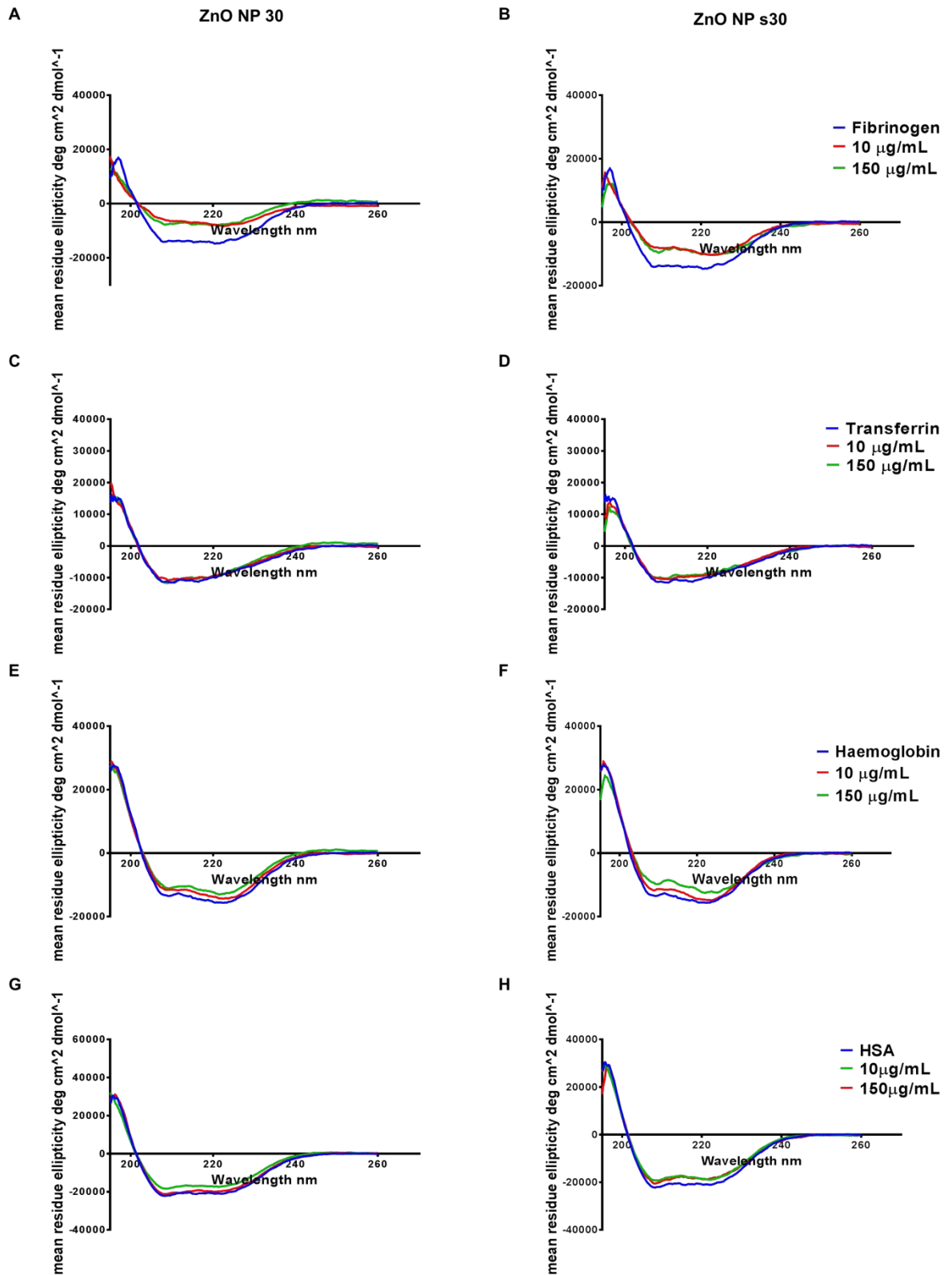
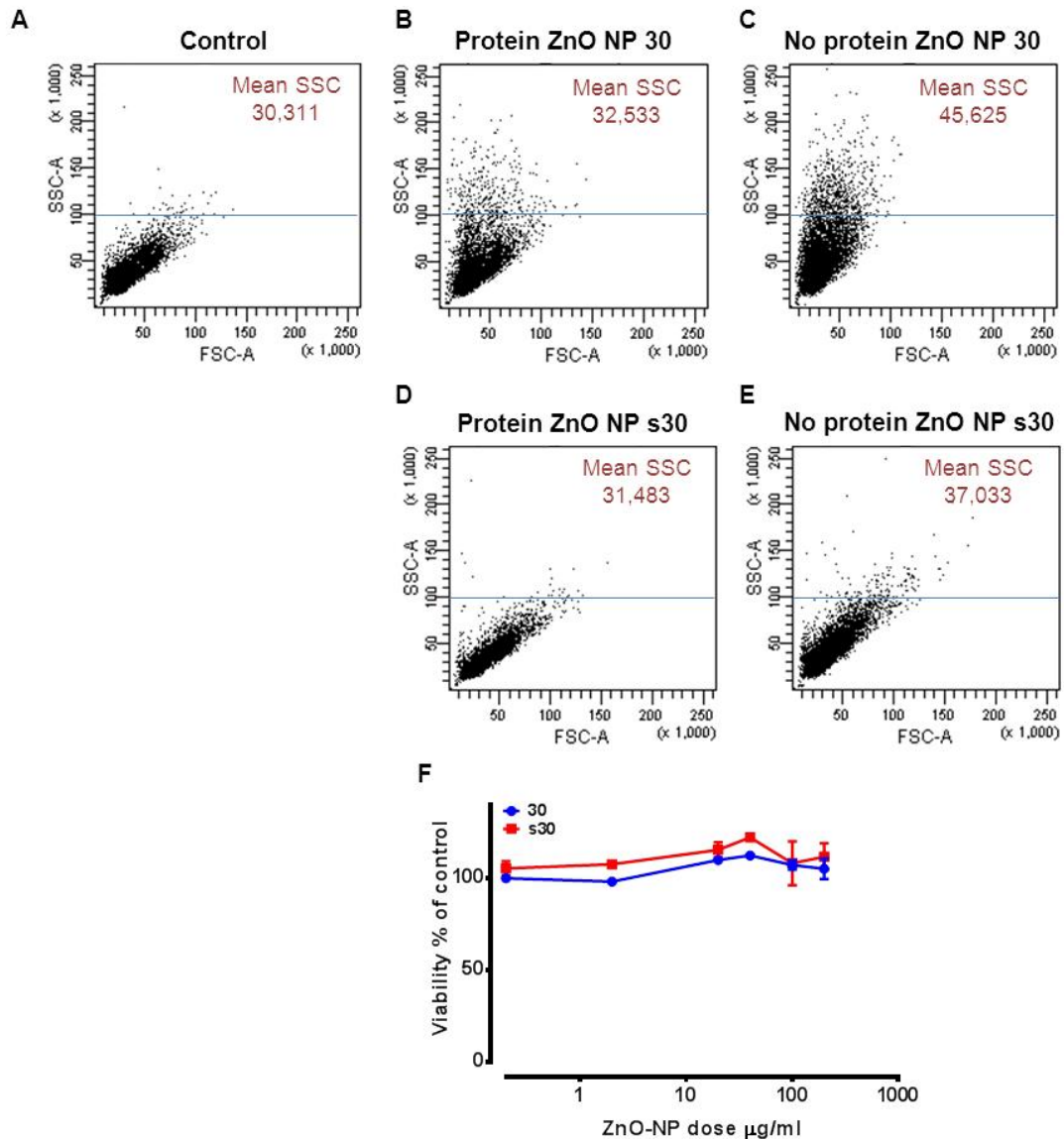


Figure 4.7 CD spectra of common blood proteins after interaction with pristine or surfactant-dispersed ZnO NPs

#### **4.3.6 Protein-dependent association of ZnO NPs with A549 cells**

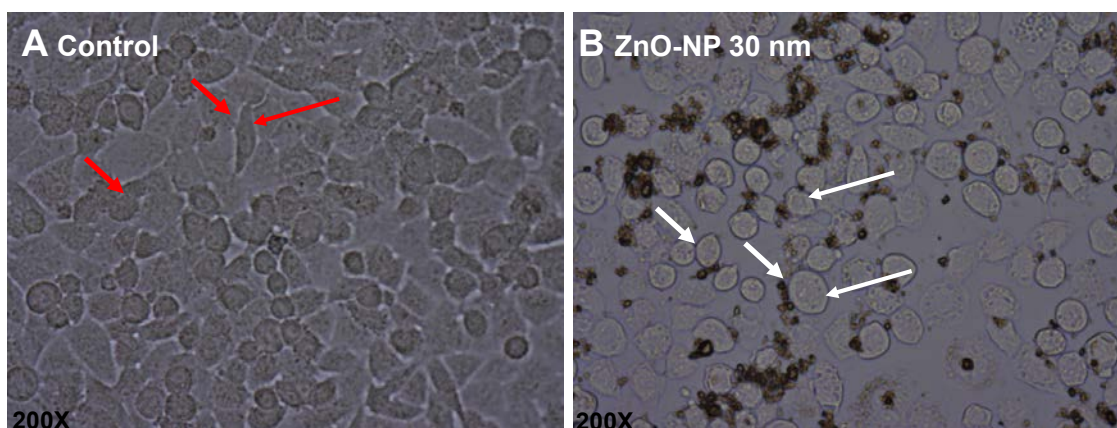
Uptake or association of ZnO NPs with A549 cells after 1hr exposure was studied by analysing the forward and side scatter intensity of the cells using flow cytometry. The forward scatter (FS) and side scatter (SS) intensities represent the size and the cytoplasmic granularity of the cell, respectively. An increase in the side scatter, as compared to untreated cells was observed for A549 cells treated with 30 or s30 ZnO NP solution for 1 hr (Figure 4.8B & 4.8C). Interestingly, under serum-free conditions there was a further increase in the size scatter intensity of ZnO NP treated A549 cells (Figure 4.8D & 4.8E). Figure 4.7F shows assessment of cell viability using MTS assay that confirmed absence of cell death when A549 cells were exposed to 100 µg/mL ZnO NP dose.



**Figure 4.8** Flow cytometry analysis of ZnO NP uptake or association with A549 cells. (A) Untreated population was scanned to establish normal population (B) cells exposed to 30 nm ZnO NPs (100  $\mu\text{g/ml}$ ) in the presence of proteins (C) 30 nm ZnO NPs under serum-free conditions (D) s30 ZnO NPs with protein (E) s30 ZnO NPs without protein for 1hr before analysing their forward and side scatter intensities. Cells exposed to NPs in serum-free conditions showed higher side scatter than untreated cells. Forward and side scatter were determine for the entire cell population.(F) Dose-dependent cell viability assessment of A549 cells exposed to ZnO NPs for 4 hr. The ZnO NP dose used for the flow cytometry analysis did not induce cytotoxicity. Data are expressed as mean  $\pm$  SEM (n = 3 separate experiments for the cell viability assay).

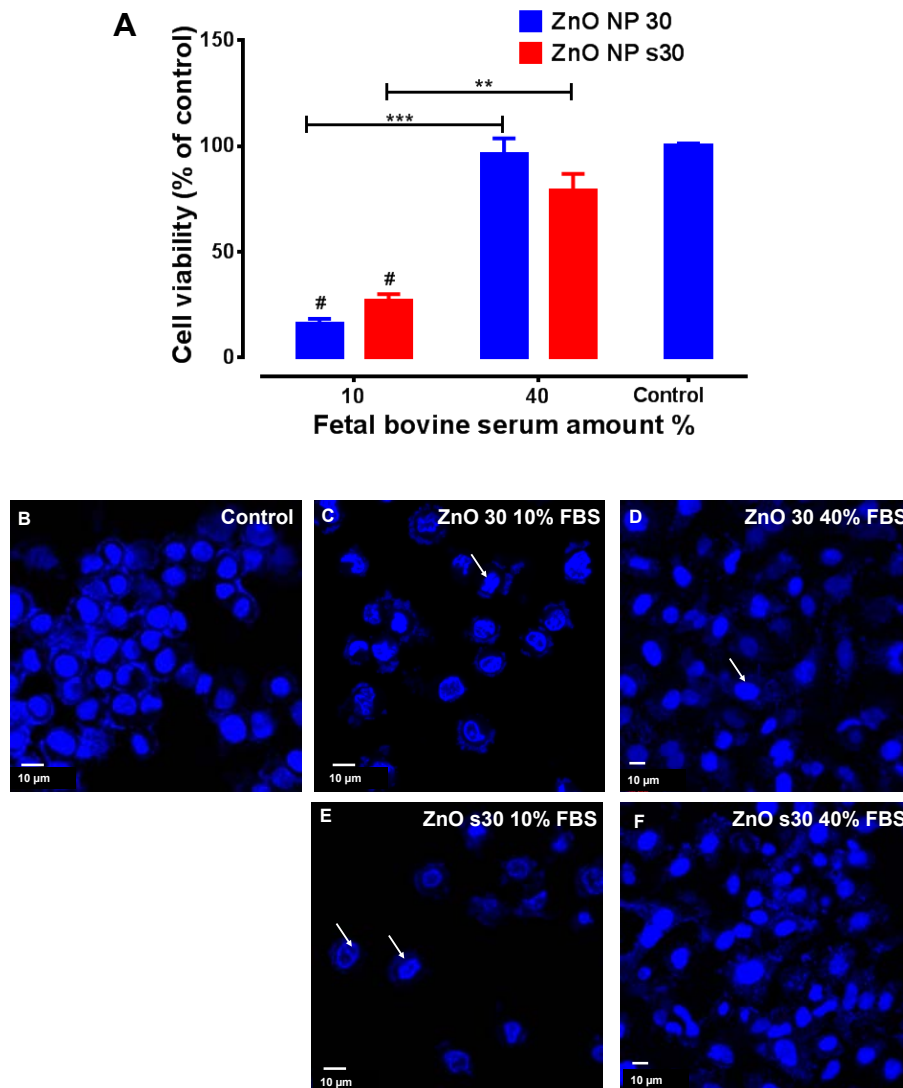
#### 4.3.7 ZnO NP interactions and effect on cytotoxicity

The effect of 100 µg/mL ZnO NP dose on the morphology of A549 cells after 24 hr exposure was studied using bright field microscopy (Figure 4.9). A549 cells in the control group demonstrated normal epithelial cell morphology, consisting of spindle-shaped or triangular cells (see red arrows). However, cells exposed to 100 µg/mL ZnO NPs became detached from the surface of the tissue culture well and demonstrated round-shaped, altered morphology (see white arrows).



**Figure 4.9** Changes in cell morphology of lung epithelial A549 cells after treatment with pristine 30 nm ZnO NPs (A) untreated cells. (B) A549 cells exposed to 100 µg/mL 30 nm ZnO-NP solution for 24 hr. ZnO NP exposure resulted in rounded morphology of A549 cells (white arrows). Untreated control cells revealed normal spindle-shaped and triangular morphology (red arrows).

The viability of A549 cells was assessed after exposure to 100 µg/mL of 30 or s30 ZnO NP solution for 24 hr using the MTS assay. The two ZnO NP solutions used were diluted from the working dilution (1 mg/mL) into media containing 10 or 40% FBS. A549 cells treated with either ZnO NP solutions dispersed in 10% FBS demonstrated significant reduction in cell viability at 24 hr as compared to untreated cells. Interestingly, no difference in cell viability was recorded for cells exposed to the same NP dose in presence of 40% FBS (Figure 4.10 A). Furthermore, ZnO NPs dispersed in 10% FBS also affected the nuclei of A549 cells causing condensation of the nuclear material (white arrows). Nuclei of cells exposed to ZnO NPs in the presence of higher amount of proteins showed normal cell morphology similar to the untreated control.



**Figure 4.10** Evaluating the effect ZnO NP-PC formed in the presence of varied amounts of FBS proteins, on the overall cytotoxic capacity of these NPs when exposed to A549 cells. A549 cells were exposed to the cytotoxic dose (100  $\mu\text{g}/\text{mL}$ ) of 30 or s30 ZnO NPs dispersed in 10 or 40% FBS containing cell culture medium for 24hr. (A) Assessment of cell viability using MTS assay. Cytotoxic potential of ZnO NPs was significantly reduced  $***p < 0.001$  for pristine 30 nm NPs and  $**p < 0.01$  for the s30 ZnO NPs, respectively in presence of higher amount of FBS protein in the *in vitro* test system.  $\#p < 0.0001$  is the significant reduction in cell viability caused by ZnO NPs dispersed in 10% FBS containing medium as compared to the untreated control. Data are expressed as mean  $\pm$ SEM ( $n = 3$  separate experiments for the cell viability assay). Statistical significance compared using student's t test. (B) DAPI stained nuclei of

untreated control or (C-F) ZnO NP exposed cells. A549 cells exposed to ZnO NPs dispersed in 10% FBS containing media showed condensation of the nuclear material, characteristic of cells undergoing apoptosis. On the contrary nuclei A549 cells exposed to ZnO NPs prepared in 40% FBS demonstrated morphology similar to those of untreated control cells.

## 4.4 Discussion

Surface conditioning of NPs with bio-molecules such as proteins affects their overall reactivity with the cellular interface [14, 27]. The main objective of this chapter was to characterise the protein coat on the ZnO NP surface when dispersed in cell culture medium consisting of FBS proteins. Besides proteins, other molecules such as lipids and sugars have also been reported to influence NP reactivity [38], however further investigation on the same is beyond the scope of this thesis. Recent studies have demonstrated that the bio-reactivity of NPs can not only be attributed to their material and surface properties, but also to the environment in which the NPs are dispersed [39, 40]. Serum represents a complex proteome, consisting of several types of proteins that not only vary in amounts but also have unique physico-chemical properties adding to the already complex nature of the adsorbed PC.

The adsorbed protein molecules, can mediate either specific or non-specific interactions of the NP surface with cells resulting in the cellular association or uptake of the NP [40]. Furthermore, the orientation, amount and conformation of the adsorbed protein, may either facilitate, or even inhibit [41] the NP-cellular interaction and therefore it is essential to identify and characterise the proteins bound to the NP surface. In this study, serum-ZnO NP protein coronas were harvested as per the methodology described in figure 2.3 (Chapter II) to retrieve the hard (long-term) protein corona. The ZnO NP-PCs obtained at 1, 2 or 24 hr did not show significant differences in their protein profile (Figure 4.1), indicating that, a complete surface coverage is achieved almost instantly when ZnO NP are dispersed in a biological medium containing serum proteins. This also highlights that the NP-PC is encountered by the cells rather than the bare ZnO NP surface. Apart from the 200 nm ZnO particulates, all the other ZnO NPs protein profiles displayed prominent bands in the molecular weight range of (25-250 kDa), even when the disc centrifuge (CPS) derived surface areas of the 200 nm particulates were similar to those of the 80 nm ZnO NPs (Table 3.1 chapter III). This may be due to the heterogeneity in the particle size of the 200 nm ZnO particulates. Mass spectrometric protein identification of prominent bands carried out for the two types of 30 nm ZnO NPs demonstrated the

association of BSA, the most abundant serum protein with both ZnO NP surfaces. Interestingly, proteins such as complement C3 and apolipoproteins (Table 4.1), which occur in very low concentration in the blood, were found to be selectively bound on the ZnO NP surface. Uptake of BSA by A549 cells is known to occur via receptor mediated endocytosis [42]. Moreover, proteins such as complement C3 and apolipoproteins predominantly interact with cells via their specific receptors. Therefore it can be speculated that the presence of these proteins on the ZnO NP surface can promote their uptake by these cells, leading to the accumulation of the NPs within cellular compartments. Dissolution of ZnO NPs in acidic endosomal compartments can impact the intracellular zinc homeostasis and can even have cytotoxic consequences [43]. Interestingly, no immunoglobulins were detected in the NP-PC of ZnO NPs in the present study.

Overall, the surface areas of the sZnO NPs and particulates was at least ten times greater than those of their pristine equivalents, which resulted in formation of specific PCs. This was evident from the preferential binding of proteins observed in the lower molecular weight range (10-15 kDa) for each type of the 30 nm ZnO-NP. The strong band observed for the pristine 30 nm NPs comprised of subunits of larger proteins such as haemoglobin and histone. In contrast, the 11 kDa protein band observed for the s30 ZnO NPs consisted of proteins including alpha-1-antiproteinase, Apo CIII and fibrinogen alpha chain. This preferential binding of certain proteins on the NP surface may be caused because of the agglomeration state of the NP, which is known to affect the available surface area for protein adsorption on nanomaterials and [22] also due to change in the charge of the ZnO NP surface due the presence of the surfactant molecules. This data is indicative of the impact of physical characteristics of the nanomaterial in forming specific protein coronas, which may contribute towards their distinct bio-reactivity.

The interaction of the NP surface with a complex mixture of proteins has been described to be dynamic in nature [15]. Serum proteins typically populate an introduced surface in accordance with the Vroman theory according to which most abundant blood proteins initially occupy the surface and are subsequently replaced by other proteins having higher affinity [44, 45]. In the present study,

30 or s30 ZnO-NP solutions were exposed to increasing concentrations (10%, 1% and 0.1%) of FBS proteins for 1hr duration. At 10% FBS concentration enhancement in the intensity of typical protein bands was observed, indicating increase in the amounts of same proteins being bound on either ZnO NP surfaces, without change in the identity of the proteins. Therefore, immunoblotting was carried out using an anti-BSA antibody which confirmed the presence of BSA on the ZnO NP surfaces at all three FBS concentrations. Being the most abundant protein, BSA is expected to be the one of the first proteins to adsorb on the NP surface. Interestingly, at the higher FBS concentration displacement of BSA was not observed, highlighting the affinity of BSA for the ZnO NP surface. These results are in good agreement with polystyrene NP-human plasma interaction, but are in contrast to observations for SiO<sub>2</sub> NPs dispersed in human plasma, which demonstrate a change in the identity of the proteins with increasing amounts of proteins in the environment [46]. Protein affinity and diffusion are important parameters along with the NP charge and pI of the interacting proteins that decide the composition of the NP-PC.

To further study the progressive displacement/preferential binding of proteins from the ZnO NP surface, when exposed to two different protein environments, 30 or s30 ZnO NPs pre-incubated in BSA for 1 hr were further incubated in human lung epithelial cell lysate for 1 or 24 hr. SDS-PAGE results clearly demonstrated adsorption of the cell lysate proteins on to the NP surfaces pre-adsorbed with BSA. Interestingly, despite low protein concentration of the A549 cell lysate (Figure 4.4A lane 4) the intensity of cell lysate proteins on the BSA pre-adsorbed ZnO NPs was found to be significantly stronger, indicative of preferential interaction of some of the cell lysate proteins with the ZnO NP surface. A subsequent immunoblotting analysis with monoclonal anti-BSA antibody confirmed BSA to be still present on the NP surface after 1 hr incubation with cell lysate proteins. Interestingly, after the 24 hr incubation the intensity of the BSA band was diminished, which may indicate that over time, BSA molecules dissociate from the NP surface and are then replaced by other proteins which ultimately are responsible for the development of the hard protein corona. Clearly, protein affinity and diffusion parameters and

reversibility of binding on to the NP surface are essential for the dynamic nature of the protein corona formation. The intensity and therefore abundance of BSA was found to be greater on the surfactant-dispersed NP due to increased surface area. While encountering different types of protein rich environments, the NP surface is constantly subjected to adsorption and replacement of unique proteins representing these environments [22]. The current results support this premise of “evolution of the NP-PC” and further suggest that presence of certain types of proteins on the NP surface may be responsible for its accumulation or clearance when interacting with cellular systems.

NP-protein interactions greatly depend on the physico-chemical characteristics of the adsorbed protein molecules. Having established the kinetics of the ZnO NPs interaction with FBS proteins, binding characteristics of selected prominent blood proteins onto the ZnO NP surface, and possible impact on protein secondary structure was analysed. The selection of these candidate proteins (BSA, fibrinogen, transferrin and apolipoprotein AI) was made on the differences in their molecular weights, shape and size. The protein binding capacity of all ZnO NPs and particulates was assessed using the protein depletion method, and was in good agreement with the surface areas of the different ZnO NPs. The surfactant dispersed ZnO NPs bound almost double the amount of protein as compared to the pristine ZnO NPs. BSA, ApoA1 and transferrin demonstrated up to 80% protein binding to the surfactant dispersed material as compared to the pristine material.

Interestingly, not much difference was observed in the protein binding capacities of the surfactant-dispersed and pristine material when disseminated in fibrinogen solution. This can be attributed to the elongated coiled-coil structure of the protein as opposed to the globular shape of the other proteins investigated. Among the different ZnO NP sizes the larger particulates bound higher numbers of protein molecules for of all four protein solutions. Interestingly, the number of protein molecules occupying the surface of a given ZnO NP varied greatly when considering individual protein solutions. For example, the 30 nm ZnO NP surface could accommodate 8 molecules of BSA, 16 molecules of Apo A1 and 7 molecules of transferrin but only 3 molecules of fibrinogen. This clearly demonstrates that the protein–surface binding affinity

and packing density of adsorbed proteins is dependent upon the curvature of NPs [47]. The influence of the physico-chemical characteristics of the protein molecules interacting with the NP surface therefore plays an important role in the development of the NP-PC.

Circular dichroism (CD) spectroscopy was used to monitor the influence of ZnO NPs on the alpha helicity (secondary structure) of prominent blood proteins. In addition, impact on secondary structure of human serum albumin (HSA) was studied, because of the high similarity (76% protein identity) HSA shares with its bovine counterpart. Adsorption of proteins on the NP surface can result in perturbation of their secondary structure because of the curvature of the NP [47]. This can give rise to the so-called “cryptic epitope” or unfolded regions of the adsorbed protein that can elicit immunological reactions *in vivo*. If the protein is an enzyme, then NP mediated denaturation can cause loss of its activity. BSA and HSA did not undergo a dramatic change in their secondary structures in the presence of increasing amounts of ZnO NPs in the present study; although s30 treated BSA demonstrated reduction in the overall alpha helical content of the protein. This may be attributed to the surfactant present in the sample and also to the changes in the topography of the nano-surface because of the different agglomeration states of the two 30 nm ZnO NP solutions. The mono-dispersed s30 ZnO NPs were more curved (relative to the sizes of the adsorbed proteins), as compared to their pristine counterparts. This may have affected the conformation of the adsorbed protein molecules. Similarly transferrin and haemoglobin were able to resist conformational changes after interacting with the ZnO NP solutions.

Interestingly, a deviation of the CD spectrum of ZnO NP treated fibrinogen solution was observed from the one recorded for the NP-free protein and is indicative of possible conformational changes. The molecular structure of fibrinogen is that of an elongated coil while BSA, HSA, transferrin and haemoglobin are globular proteins. Previous studies have reported that, albumins demonstrate greater disorder in their structure upon binding to surfaces with larger diameter and are in contrast to fibrinogen, which can easily denature after binding to smaller particles. This may be because the fibrinogen

molecules adsorb in a side-on orientation around the nanoparticle which facilitates changes in the conformation of the molecule [48].

ZnO NPs are often categorised as highly cytotoxic metal oxide NPs. This is mainly because of their propensity to dissolve either in the extracellular environment or within the cellular compartments after uptake by cells [49, 50]. The ZnO NPs used in the present study demonstrated a very low tendency to dissolve in the cell culture medium (Chapter 3), which suggests that the intact ZnO NP may associate with the cellular surface via the adsorbed protein layer and this can have a potential impact on the immunotoxic potential of these NPs. It has been previously shown that the surface of NPs exposed to cells in serum-free condition can display a protein corona composed of cytosolic and cell membrane proteins which can be a result of direct interaction of the cell membrane with the pristine NP surface [51]. In this study, ZnO NP uptake by A549 cells was studied using flow cytometry based analysis of the forward and side scatter intensity of treated cells. An increase in the side scatter of cells is indicative of an increase in the granularity of the cell cytoplasm, which can occur due to uptake of the NPs. In the present study, cells exposed to 30 or s30 ZnO NP without pre-formed PCs demonstrated a larger side scatter as compared to the ones treated with ZnO NPs dispersed in protein containing medium. In protein-free conditions there is a strong possibility of rapid sedimentation of the suspended NPs on the cellular monolayer causing enhanced uptake. In contrast, presence of proteins helps in maintaining the colloidal stability of the NP suspension leading to diminished uptake of the protein covered NPs. This data has important implications in designing experiments for evaluating the nanotoxic potential of ZnO NPs.

Cytotoxicity is one of the major consequences of NP-cellular interaction [52, 53]. ZnO NPs have been previously shown to cause cell death at high doses and are often categorised as highly reactive metal oxide NPs [54]. The main objective of the final module of this chapter was to verify if the cytotoxic potential of ZnO NPs at a fixed cytotoxic dose is impacted by the amount of serum proteins present in the cell culture medium. The choice of the ZnO NP dose (100 µg/mL) for these experiments was based on previous data demonstrating a detailed cytotoxic evaluation of the same ZnO NPs in an *in*

*in vitro* system consisting of human monocytes [55]. A549 cells were exposed to 30 or s30 ZnO NP solutions 100 µg/mL, dispersed in 10% (3.7 mg/mL) or 40% (14.8 mg/mL) FBS protein containing medium for 24hr duration. In a previous study nano and micro sized ZnO NPs were shown to induce the highest toxicity in A549 cells when dosed in serum-free medium [56]. However, the only anomaly of this experimental approach was that, the absence of important FBS growth factors in the culture media can adversely affect the cell growth, making them susceptible to the toxic effects of ZnO NP exposure. Therefore cytotoxicity measurements were conducted in media supplemented with 10% or 40% FBS proteins. As expected, ZnO NPs in the standard cell culture medium (10% FBS) caused maximum cell death, as shown by a drastic reduction in the viability of ZnO NP treated A549 cells compared to untreated cells ( $p < 0.0001$ ); measured using the MTS cell viability assay. Interestingly, A549 cells exposed to the same dose of either ZnO NP solutions dispersed in 40% FBS protein containing media showed significant increase in the cell viability ( $p < 0.001$ ) for 30 and ( $p < 0.01$ ) for s30 ZnO NP treatments when compared to the ZnO NP doses under the typical cell culture conditions. Cells undergoing death when exposed to ZnO NPs may show characteristic nuclear morphology representative of apoptosis [55]. In the presence of low amounts of protein, ZnO NP treated A549 cells nuclei appeared smaller in size with condensed nuclear matter as compared to the cells treated with ZnO NPs in presence of 40% FBS proteins or the untreated control cells. In the presence of 10% FBS protein the cytotoxic potential of the pristine 30 ZnO NPs was marginally higher than the s30 NPs ( $p < 0.04$ ) however, in the presence of higher amounts of protein both ZnO NP solutions showed similar behaviour. These results are in agreement with a recent study published by Kim and co-workers, which demonstrated that suppression of the cytotoxic potential of amino-modified polystyrene NPs can be related to the protein concentration of the *in vitro* system [57].

The most important implication of this observation is that the protein coat on the NP surface may have a protective role for cells exposed to NPs and is dependent on the total amount of protein. Furthermore, at a fixed concentration, NP nanotoxic potential can be varied by varying the amount of protein. So, care should be taken when comparing the toxic potential of the same NP across

different cell culture systems, which make use of different amounts of sera. Correlation of *in vitro* and *in vivo* nanotoxicological data is often challenging due to the discrepancies in the exposure doses used. Comparison of the toxicological potential of NPs in the presence of protein amounts, classically used in *in vitro* systems with those depicting *in vivo* protein amounts can help to better plan experiments involving animal models. The data presented in this chapter suggests that the alteration of ZnO NP surface with the protein layer may be an important determinant for ZnO cytotoxicity besides currently known paradigms including dissolution and reactive oxygen species generation.

#### 4.5 Conclusion

The data presented in this chapter, correlate for the first time, the ZnO NP-PC formation to its bio-reactivity in an *in vitro* cell culture system. It is apparent that, the protein adsorption process on the ZnO NP surface is instant and is dependent on the size of the nanoparticle. Furthermore, non-agglomerated ZnO NPs may be able to absorb specific proteins on their surface due to enhanced surface area of the NPs. The ZnO NP surface is capable of selective binding of several serum proteins with important physiological roles, although the overall protein binding process is not dynamic in nature. Interestingly, the ZnO NP surface may be able to induce structural changes in certain proteins and this may be largely dependent on the biochemical attributes of the adsorbed protein molecule. Finally, the protein coat on the ZnO NP surface may be responsible for reduced association of the particles with a cellular monolayer when compared to pristine ZnO NPs. The amount of protein present in the environment may have in addition, an indirect influence on the cytotoxic potential of ZnO NPs as it clearly affects the NP uptake as demonstrated in this study. The data presented in this chapter can provide a foundation for designing future experiments for nanotoxicology assessment of ZnO NPs.

## 4.6 References

1. Issa B, Obaidat IM, Albiss BA, Haik Y: **Magnetic Nanoparticles: Surface Effects and Properties Related to Biomedicine Applications.** *Int J Mol Sci* 2013, **14**:21266-21305.
2. Kolodziejczak-Radzimska A, Jesionowski T: **Zinc Oxide-From Synthesis to Application: A Review.** *Materials* 2014, **7**:2833-2881.
3. Osmond MJ, Mccall MJ: **Zinc oxide nanoparticles in modern sunscreens: An analysis of potential exposure and hazard.** *Nanotoxicology* 2010, **4**:15-41.
4. Di Pasqua A, Sharma K, Shi Y, Toms B, Ouellette W, Dabrowiak J, Asefa T: **Cytotoxicity of mesoporous silica nanomaterials.** *J Inorg Biochem* 2008, **102**:1416 - 1423.
5. Bhabra G, Sood A, Fisher B, Cartwright L, Saunders M, Evans WH, Surprenant A, Lopez-Castejon G, Mann S, Davis SA, et al: **Nanoparticles can cause DNA damage across a cellular barrier.** *Nat Nano* 2009, **4**:876-883.
6. Andersson-Willman B, Gehrmann U, Cansu Z, Buerki-Thurnherr T, Krug HF, Gabrielsson S, Scheynius A: **Effects of subtoxic concentrations of TiO<sub>2</sub> and ZnO nanoparticles on human lymphocytes, dendritic cells and exosome production.** *Toxicol Appl Pharmacol* 2012, **264**:94-103.
7. Cho W-S, Duffin R, Poland CA, Duschl A, Oostingh GJ, MacNee W, Bradley M, Megson IL, Donaldson K: **Differential pro-inflammatory effects of metal oxide nanoparticles and their soluble ions in vitro and in vivo; zinc and copper nanoparticles, but not their ions, recruit eosinophils to the lungs.** *Nanotoxicology* 2012, **6**:22-35.
8. Lin W, Xu Y, Huang C-C, Ma Y, Shannon K, Chen D-R, Huang Y-W: **Toxicity of nano- and micro-sized ZnO particles in human lung epithelial cells.** *Journal of Nanoparticle Research* 2009, **11**:25-39.
9. Nair S, Sasidharan A, Divya Rani VV, Menon D, Nair S, Manzoor K, Raina S: **Role of size scale of ZnO nanoparticles and microparticles on toxicity toward bacteria and osteoblast cancer cells.** *J Mater Sci: Mater Med* 2009, **20**:235-241.

10. Napierska D, Thomassen LCJ, Rabolli V, Lison D, Gonzalez L, Kirsch-Volders M, Martens JA, Hoet PH: **Size-Dependent Cytotoxicity of Monodisperse Silica Nanoparticles in Human Endothelial Cells.** *Small* 2009, **5**:846-853.
11. Sohaebuddin SK, Thevenot PT, Baker D, Eaton JW, Tang LP: **Nanomaterial cytotoxicity is composition, size, and cell type dependent.** *Particle and Fibre Toxicology* 2010, **7**.
12. Nangia S, Sureshkumar R: **Effects of Nanoparticle Charge and Shape Anisotropy on Translocation through Cell Membranes.** *Langmuir* 2012, **28**:17666-17671.
13. Cho WS, Duffin R, Howie SEM, Scotton CJ, Wallace WAH, MacNee W, Bradley M, Megson IL, Donaldson K: **Progressive severe lung injury by zinc oxide nanoparticles; the role of Zn<sup>2+</sup> dissolution inside lysosomes.** *Particle and Fibre Toxicology* 2011, **8**.
14. Cedervall T, Lynch I, Lindman S, Berggard T, Thulin E, Nilsson H, Dawson K, Linse S: **Understanding the nanoparticle-protein corona using methods to quantify exchange rates and affinities of proteins for nanoparticles.** *Proc Natl Acad Sci U S A* 2007, **104**:2050 - 2055.
15. Casals E, Pfaller T, Duschl A, Oostingh GJ, Puentes V: **Time Evolution of the Nanoparticle Protein Corona.** *ACS Nano* 2010, **4**:3623-3632.
16. Kah JCY, Chen J, Zubieta A, Hamad-Schifferli K: **Exploiting the Protein Corona around Gold Nanorods for Loading and Triggered Release.** *ACS Nano* 2012, **6**:6730-6740.
17. Cai X, Ramalingam R, Wong HS, Cheng J, Ajuh P, Cheng SH, Lam YW: **Characterization of carbon nanotube protein corona by using quantitative proteomics.** *Nanomedicine: Nanotechnology, Biology and Medicine* 2013, **9**:583-593.
18. Pozzi D, Caracciolo G, Capriotti AL, Cavaliere C, Piovesana S, Colapicchioni V, Palchetti S, Riccioli A, Lagana A: **A proteomics-based methodology to investigate the protein corona effect for targeted drug delivery.** *Mol Biosyst* 2014, **10**:2815-2819.
19. Sakulkhu U, Maurizi L, Mahmoudi M, Motazacker M, Vries M, Gramoun A, Ollivier Beuzelin M-G, Vallee J-P, Rezaee F, Hofmann H: **Ex situ evaluation of the composition of protein corona of intravenously**

- injected superparamagnetic nanoparticles in rats.** *Nanoscale* 2014, **6**:11439-11450.
20. Shannahan JH, Podila R, Aldossari AA, Emerson H, Powell BA, Ke PC, Rao AM, Brown JM: **Formation of a Protein Corona on Silver Nanoparticles Mediates Cellular Toxicity via Scavenger Receptors.** *Toxicol Sci* 2014.
21. Lynch I, Dawson KA: **Protein-nanoparticle interactions.** *Nano Today* 2008, **3**:40.
22. Saptarshi S, Duschl A, Lopata A: **Interaction of nanoparticles with proteins: relation to bio-reactivity of the nanoparticle.** *J Nanobiotechnol* 2013, **11**:26.
23. Walkey CD, Olsen JB, Guo H, Emili A, Chan WCW: **Nanoparticle Size and Surface Chemistry Determine Serum Protein Adsorption and Macrophage Uptake.** *J Am Chem Soc* 2011, **134**:2139-2147.
24. Bell NC, Minelli C, Shard AG: **Quantitation of IgG protein adsorption to gold nanoparticles using particle size measurement.** *Analytical Methods* 2013, **5**:4591-4601.
25. Benetti F, Fedel M, Minati L, Speranza G, Migliaresi C: **Gold nanoparticles: role of size and surface chemistry on blood protein adsorption.** *Journal of Nanoparticle Research* 2013, **15**:1-9.
26. Deng ZJ, Liang M, Monteiro M, Toth I, Minchin RF: **Nanoparticle-induced unfolding of fibrinogen promotes Mac-1 receptor activation and inflammation.** *Nat Nano* 2011, **6**:39-44.
27. Cedervall T, Lynch I, Foy M, Berggad T, Donnelly S, Cagney G, Linse S, Dawson K: **Detailed identification of plasma proteins adsorbed on copolymer nanoparticles.** *Angewandte Chemie-International Edition* 2007, **46**:5754 - 5756.
28. Zhou J, Deng GM, Tara Schiller, Anthony Musumeci, Darren Martin, Rodney F Minchin: **Differential plasma protein binding to metal oxide nanoparticles.** *Nanotechnology* 2009.
29. Fertsch-Gapp S, Semmler-Behnke M, Wenk A, Kreyling WG: **Binding of polystyrene and carbon black nanoparticles to blood serum proteins.** *Inhal Toxicol* 2011, **23**:468-475.

30. Deng Z, Mortimer G, Schiller T, Musumeci A, Martin D, Minchin R: **Differential plasma protein binding to metal oxide nanoparticles.** *Nanotechnology* 2009, **20**:455101.
31. Bardhan M, Mandal G, Ganguly T: **Steady state, time resolved, and circular dichroism spectroscopic studies to reveal the nature of interactions of zinc oxide nanoparticles with transport protein bovine serum albumin and to monitor the possible protein conformational changes.** *J Appl Phys* 2009, **106**.
32. Chatterjee T, Chakraborti S, Joshi P, Singh SP, Gupta V, Chakrabarti P: **The effect of zinc oxide nanoparticles on the structure of the periplasmic domain of the *Vibrio cholerae* ToxR protein.** *FEBS J* 2010, **277**:4184-4194.
33. Chakraborti S, Sarwar S, Chakrabarti P: **The Effect of the Binding of ZnO Nanoparticle on the Structure and Stability of  $\alpha$ -Lactalbumin: A Comparative Study.** *The Journal of Physical Chemistry B* 2013, **117**:13397-13408.
34. Fleischer CC, Payne CK: **Secondary Structure of Corona Proteins Determines the Cell Surface Receptors Used by Nanoparticles.** *The Journal of Physical Chemistry B* 2014.
35. Suzuki H, Toyooka T, Ibuki Y: **Simple and Easy Method to Evaluate Uptake Potential of Nanoparticles in Mammalian Cells Using a Flow Cytometric Light Scatter Analysis.** *Environ Sci Technol* 2007, **41**:3018-3024.
36. Brandes N, Welzel PB, Werner C, Kroh LW: **Adsorption-induced conformational changes of proteins onto ceramic particles: Differential scanning calorimetry and FTIR analysis.** *J Colloid Interface Sci* 2006, **299**:56-69.
37. Kilar F, Simon I: **The effect of iron-binding on the conformation of transferrin - a small-angle X-ray-scattering study.** *Biophys J* 1985, **48**:799-802.
38. Xu M, Li J, Iwai H, Mei Q, Fujita D, Su H, Chen H, Hanagata N: **Formation of Nano-Bio-Complex as Nanomaterials Dispersed in a Biological Solution for Understanding Nanobiological Interactions.** *Sci Rep* 2012, **2**.

39. Dutta D, Sundaram S, Teegarden J, Riley B, Fifield L, Jacobs J, Addleman S, Kaysen G, Moudgil B, Weber T: **Adsorbed proteins influence the biological activity and molecular targeting of nanomaterials.** *Toxicol Sci* 2007, **100**:303 - 315.
40. Ehrenberg MS, Friedman AE, Finkelstein JN, Oberdorster G, McGrath JL: **The influence of protein adsorption on nanoparticle association with cultured endothelial cells.** *Biomaterials* 2009, **30**:603-610.
41. Salvati A, Pitek AS, Monopoli MP, Prapainop K, Bombelli FB, Hristov DR, Kelly PM, Aberg C, Mahon E, Dawson KA: **Transferrin-functionalized nanoparticles lose their targeting capabilities when a biomolecule corona adsorbs on the surface.** *Nat Nano* 2013, **8**:137-143.
42. Yumoto R, Suzuka S, Oda K, Nagai J, Takano M: **Endocytic Uptake of FITC-albumin by Human Alveolar Epithelial Cell Line A549.** *Drug Metab Pharmacokinet* 2012, **27**:336-343.
43. Kao Y-Y, Chen Y-C, Cheng T-J, Chiung Y-M, Liu P-S: **Zinc Oxide Nanoparticles Interfere With Zinc Ion Homeostasis to Cause Cytotoxicity.** *Toxicol Sci* 2012, **125**:462-472.
44. Vroman L: **Effect of Adsorbed Proteins on the Wettability of Hydrophilic and Hydrophobic Solids.** *Nature* 1962, **196**:476-477.
45. Jung S-Y, Lim S-M, Albertorio F, Kim G, Gurau MC, Yang RD, Holden MA, Cremer PS: **The Vroman Effect: A Molecular Level Description of Fibrinogen Displacement.** *J Am Chem Soc* 2003, **125**:12782-12786.
46. Monopoli MP, Walczyk D, Campbell A, Elia G, Lynch I, Baldelli Bombelli F, Dawson KA: **Physical-Chemical Aspects of Protein Corona: Relevance to in Vitro and in Vivo Biological Impacts of Nanoparticles.** *J Am Chem Soc* 2011, **133**:2525-2534.
47. Vertegel AA, Siegel RW, Dordick JS: **Silica Nanoparticle Size Influences the Structure and Enzymatic Activity of Adsorbed Lysozyme.** *Langmuir* 2004, **20**:6800-6807.
48. Roach P, Farrar D, Perry CC: **Surface Tailoring for Controlled Protein Adsorption: Effect of Topography at the Nanometer Scale and Chemistry.** *J Am Chem Soc* 2006, **128**:3939-3945.

49. Turney TW, Duriska MB, Jayaratne V, Elbaz A, O'Keefe SJ, Hastings AS, Piva TJ, Wright PFA, Feltis BN: **Formation of Zinc-Containing Nanoparticles from Zn<sup>2+</sup> Ions in Cell Culture Media: Implications for the Nanotoxicology of ZnO.** *Chem Res Toxicol* 2012, **25**:2057-2066.
50. Shen C, James SA, de Jonge MD, Turney TW, Wright PFA, Feltis BN: **Relating Cytotoxicity, Zinc Ions, and Reactive Oxygen in ZnO Nanoparticle-Exposed Human Immune Cells.** *Toxicol Sci* 2013, **136**:120-130.
51. Lundqvist M, Stigler J, Cedervall T, Berggård T, Flanagan MB, Lynch I, Elia G, Dawson K: **The Evolution of the Protein Corona around Nanoparticles: A Test Study.** *ACS Nano* 2011, **5**:7503-7509.
52. Nel A, Xia T, Madler L, Li N: **Toxic potential of materials at the nanolevel.** *Science* 2006, **311**:622 - 627.
53. Nel A, Madler L, Velegol D, Xia T, Hoek E, Somasundaran P, Klaessig F, Castranova V, Thompson M: **Understanding biophysicochemical interactions at the nano-bio interface.** *Nat Mater* 2009, **8**:543 - 557.
54. Bondarenko O, Juganson K, Ivask A, Kasemets K, Mortimer M, Kahru A: **Toxicity of Ag, CuO and ZnO nanoparticles to selected environmentally relevant test organisms and mammalian cells in vitro: a critical review.** *Arch Toxicol* 2013, **87**:1181-1200.
55. Feltis BN, O'Keefe SJ, Harford AJ, Piva TJ, Turney TW, Wright PFA: **Independent cytotoxic and inflammatory responses to zinc oxide nanoparticles in human monocytes and macrophages.** *Nanotoxicology* 2012, **6**:757-765.
56. Hsiao IL, Huang Y-J: **Effects of serum on cytotoxicity of nano- and micro-sized ZnO particles.** *Journal of Nanoparticle Research* 2013, **15**:1-16.
57. Kim JA, Salvati A, Aberg C, Dawson KA: **Suppression of nanoparticle cytotoxicity approaching in vivo serum concentrations: limitations of in vitro testing for nanosafety.** *Nanoscale* 2014, **6**:14180-14184.



---

## Chapter V

### Literature review of the reactive nature of zinc oxide nanoparticles with *in vitro* and *in vivo* mammalian test systems

**Publication:**

**Saptarshi SR**, Duschl A, Lopata AL. Biological reactivity of zinc oxide nanoparticles in mammalian test systems: an overview Nanomedicine. (Editorially accepted)

---



## 5.1 Introduction

Nanotechnology is a frontier technology because of the vast array of innovative applications it can offer. Miniaturization of materials to the nano level greatly changes their physico-chemical attributes. Zinc oxide nanoparticles (ZnO NPs) are produced in high tonnage each year and are now commonly used in a number of consumer and industrial products including cosmetics, sunscreen formulations, paints, UV protection coatings and food additives [1]. Interestingly, ZnO quantum dots are now being explored for their potential application in bio-imaging and drug delivery [2]. However, reduction of size greatly enhances the bio-reactive nature of the NP, resulting in increased interaction with bio-molecules and cellular structures. This can result in cytotoxicity, inflammation and accumulation of NPs in vital organs, which makes it important to evaluate nanotoxicological profiles of different NPs. This review aims to summarise current research on mammalian toxicity of ZnO NPs and discusses the effect of ZnO NP exposure on cytotoxicity, cellular signalling, inflammation and genotoxicity. Furthermore the *in vivo* effects of ZnO NPs via different routes of exposure in mammals have also been highlighted.

## 5.2 ZnO NP mediated cytotoxicity; influence of cell type

The uptake of NPs by cells can occur via several different mechanisms and this depends mainly on the surface properties of the nanomaterial [1]. For ZnO NPs, uptake may be mediated via endocytosis [3-5]. The translocation pathway for ZnO NPs across the human lung adenocarcinoma (Calu-3) cell monolayer was shown to be trans-cellular and did not compromise the epithelial barrier integrity or tight junctions at cell-cell borders [6]. ZnO NPs are known to exert a high toxicity on a number of cell types as compared to other metal oxide nanoparticles. For example, despite having similar sizes, ZnO NPs exerted greater cytotoxicity in exposed alveolar macrophages compared to TiO<sub>2</sub> NPs [7]. Cytotoxicity and inflammatory potential of ZnO NPs not only depend on the particle characteristics but also on the type of interacting cells [8, 9]. This hampers the analysis of ZnO NP toxicity, in particular since many studies are based on stable cell lines, which show some but not all characteristics of the cell lineage from which they are derived. However, considering the need to

reduce animal use, significant species differences e.g. in terms of lung architecture and resulting particle deposition [10] as well as the large number of samples which often have to be dealt with, stable cell lines are often still relevant *in vitro* models for NP cytotoxicity analysis.

ZnO NPs caused maximum death in monocytes followed by natural killer cells while lymphocytes displayed highest resistance [11]. Clearly, some cancer cell lines seem to be more vulnerable to ZnO NP treatment [12, 13]. ZnO NP induced selective cytotoxicity in cancer cells such as hepatocellular carcinoma cells (Hep G2), lung epithelial cells (A549), human bronchial epithelial cells (BEASB-2) but not in primary rat astrocytes or hepatocytes [14]. Toxicity, however, is not always specific for cancer cells. Under conditions where no toxicity was seen in primary human peripheral blood mononuclear cells (PBMC), a clear dose dependent toxic response was observed in monocyte-derived dendritic cells when exposed to ZnO NPs [15]. In another study, ZnO NPs demonstrated greater toxicity in rapidly proliferating cells, independent of their cell lineage: cancerous or primary [16]. Thus, the use of ZnO NPs as potential therapeutic agents in targeting cancer cells, although looks promising, needs further evaluation.

### 5.3 ZnO NP mediated cytotoxicity; effect of NP size and shape

Physical characteristics (size and shape), and surrounding environment may impact nanotoxicological outcomes [1]. ZnO NP interaction with phosphates present in the cell culture may enhance their cytotoxic potential [17]. ZnO NP toxicity may also be influenced by the protein concentration in cell culture medium [18], most simply explained by the shielding of the NP surface by attached proteins. However, the interaction of ZnO NPs with proteins may impact their conformational structure as shown for bovine serum albumin or Tox r protein of *Vibrio cholera* [19, 20]. NP induced changes in the structure of adsorbed proteins can in turn affect the bio-reactivity of the NP although, information on how protein adsorption on the surface of ZnO NPs affects their nanotoxicological properties is unavailable and needs further investigation. Similarly, surface coating may also considerably affect the cytotoxic potential of the particles [21, 22]. In general, smaller NPs due to their large surface area to

mass ratio are more potent in causing cellular damage than larger particulates. Song *et.al* suggested that there may be a critical NP size that may affect the cytotoxic potential of ZnO NPs although not much information was provided to support this premise [23]. Seventy nanometre ZnO NPs, when compared to 420 nm sized particulates, triggered greater cellular damage in exposed A549 cells [24]. Similarly, ZnO NPs (~100 nm) were shown to strongly affect phagocytic capacity of THP-1 cells compared to 5  $\mu\text{m}$  ZnO particulates [25]. On the contrary, De Berardis and co-workers suggested that surface area, also related to NP size, may not directly affect cytotoxic outcomes of ZnO NPs when exposed to human colon carcinoma (LoVo) cells [26].

Interestingly, ZnO NP shape may also influence their cytotoxic potential [27]. Spherical ZnO NPs (10-30 nm) were shown to cause greater cytotoxicity in Ana-1 cells as compared to ZnO nano-rods [23]. The surface area of the NP may change if the shape changes and this can affect the interaction of the NP surface not only with the surrounding biomolecules but also cellular structures. Interestingly, studies on the effect of nanoparticle shape on the toxic potential of ZnO NPs are minimal and further investigation on this aspect is required. Although ZnO spheres and ZnO sheets demonstrated similar levels of toxicity in murine macrophages (RAW 264.7) or BEAS-2B cells, significant differences were recorded in their cellular association and inflammatory potential at low doses [28]. Interestingly, studies on the effect of nanoparticle shape on the toxic potential of ZnO NPs are minimal and further investigation on this aspect is required. These reports further highlight that ZnO NP mediated cytotoxicity is likely to be due to multifactorial effects.

#### **5.4 ZnO NP mediated cytotoxicity; *in vitro* test systems**

When using submerged cell culture conditions, sedimentation of NPs may occur, leading to enhanced NP-cellular contact [29]. This is particularly important when investigating the pulmonary toxicity of particulates. Aerosol and suspension exposure of co-cultured airway cells to ZnO NPs resulted in clear differences in the dose and time based immunotoxic responses [30]. Recently, toxicity of aerosolised ZnO NPs was studied in cells cultured under air liquid interface (ALI) conditions, which better simulate the complex nature of the *in*

*vivo* lung environment as compared to traditional *in vitro* systems. A novel air-liquid interface cell exposure system (ALICE) was developed as a useful tool for dose-controlled NP exposure of ALI cultured cells [31]. Significant differences in levels (three folds lower) of intracellular zinc ( $Zn^{2+}$ ) amounts were reported in ALI sub-cultured or submerged mouse epithelial cells (C10) exposed to ZnO NPs [32]. Xie and co-workers demonstrated distinct oxidative stress dynamics at the ALI and in submerged A549 cell cultures exposed to aerosolised ZnO NPs [33]. Physico-chemical characteristics, cell type and *in vitro* test system being investigated all impact the bio-interaction of ZnO-NPs.

### 5.5 ZnO NP mediated cytotoxicity; ZnO NP dissolution

Perturbation in the cytosolic levels of zinc levels can occur due to extracellular or intracellular  $Zn^{2+}$  formation as a result of ZnO NP dissolution. X-ray fluorescence and scanning electron microscopy analyses revealed a 200% increase in the  $Zn^{2+}$  levels in ZnO NP treated cells, which was also shown to be greater than in cells treated with corresponding concentrations of  $ZnCl_2$  [34]. Extracellular dissolution of ZnO NPs may lead to the formation of  $Zn^{2+}$  in the cellular micro-environment which may be related to their toxicity. Uptake of  $Zn^{2+}$  ions most likely occurs through zinc transporters of the ZIP family and cells store excess  $Zn^{2+}$  ions inside vesicles known as zincosomes [35]. Excess  $Zn^{2+}$  in the cell culture medium is associated with the release of the cytosolic lactate dehydrogenase enzyme and apoptotic cell death [23, 35]. Apical exposure of ZnO NPs to rat alveolar epithelial cell monolayers lead to an increase in the intracellular  $Zn^{2+}$  levels resulting in ROS generation and ultimately loss of the cell membrane integrity [36]. Similar observations were made in the case of ZnO NP exposed glomerular and tubular human renal cells [37].

Intracellular dissolution of ZnO NPs has been proposed to be an important prerequisite for the induction of cytotoxicity, which also highlights the requirement of NP-cellular contact. Overexpression of metallothionein genes is associated with the chelation of metal ions and therefore detoxification. ZnO NP exposure to monocyte-derived dendritic cells, Human Monocyte-Derived Macrophages and Jurkat cells resulted in an up regulation of the common metallothionein genes, highlighting that ZnO NPs are sources of  $Zn^{2+}$  ions which can impact

cellular metabolism [38]. Similar observations were made when human lung cells (L-132) were exposed to 50 nm ZnO NPs for 24 hr [39]. Shen and co-workers demonstrated that ZnO NPs were capable of inducing cytotoxicity at high concentrations only via direct exposure to monocytes and not via indirect exposure by the means of dialysis [40]. pH mediated dissolution of ZnO nanocrystals in the acidic micro-environment of cancer cells was shown to induce ROS formation, collapse of mitochondrial membrane and cell cycle arrest at S/G2 phase in cancer cells [13]. On the contrary, exposure to ZnO NPs alone and not soluble  $Zn^{2+}$  ions was shown to cause greater toxicity in colon cancer cells [41]. Xu and co-workers reported that the analytical techniques currently used, often overestimate the amount of  $Zn^{2+}$  ions in the cell culture medium and that the total contribution of released  $Zn^{2+}$  ions to cytotoxicity is only 10% in A549 cells [42].

Modification of ZnO NPs with different surface coatings to control their dissolution characteristics may help in the mitigation of their toxic potential [35, 43]. Recently, iron doping was suggested to alleviate  $Zn^{2+}$  release from ZnO NPs in order to control their cytotoxicity [44].  $TiO_2$  shell coating of ZnO NPs was reported to decrease their toxicity by controlling the rate of  $Zn^{2+}$  ion release when interacting with cells [45]. Alternatively, alteration of the surface properties of ZnO NPs, which may in turn affect their uptake rather than changing dissolution characteristics of the material, was recommended by Luo et al. [46]. Novel strategies specifically targeting the dissolution tendency of ZnO NPs may help to enhance safe use of these materials in the bio-medical area.

## 5.6 ZnO NP mediated cytotoxicity; Reactive oxygen species

ROS or free radicals such as hydroxyl radicals, superoxide molecules, hydrogen peroxide, etc., are reactive molecules made up of anion containing oxygen atoms. An imbalance in the cellular redox state can be created by reduced antioxidant production or impairment of the cell to repair the oxidative damage. The consequence of this can be the activation of signalling cascades leading to cytotoxicity. Xia et al. proposed the hierarchical oxidative stress model to further explain NP mediated oxidant injury. This paradigm involves three levels. Tier 1 response is characterised by the induction of antioxidant

systems, followed by the tier 2 response, which involves an up regulation of the signalling cascades like those leading to the activation of NF- $\kappa$ B and of MAP kinases, which ultimately shifts into the tier 3 response that involves apoptotic cell death [47]. ZnO NPs have been postulated to generate ROS in different cell types. However the exact mechanism remains unclear. A strong antioxidant response mounted by BEAS-2B cells due to prior exposure to H<sub>2</sub>O<sub>2</sub> assisted them in tolerating ZnO NP better [48]. ZnO NPs when compared to other known cytotoxic nanomaterials such as carbon black, carbon nanotubes and silica nanoparticles were shown to induce maximum toxicity to primary mouse embryo fibroblasts via production of reactive oxygen species [49]. Pre-treatment of cells with antioxidant compounds such as n-acetylcysteine (NAC) or vitamin C can control elevated levels of ROS. However, it is still unclear whether ZnO NPs mediated ROS formation is the consequence of cytotoxicity or vice versa. It has been suggested that presence of excess Zn<sup>2+</sup> in the cells upon exposure to ZnO NPs may cause a disequilibrium in Zn dependent protein activity, causing inactivation of cellular redox maintaining systems thus leading to cell death [40]. Moreover, ZnO NPs were also reported to cause ROS mediated increase in the intracellular calcium levels in a time and concentration dependent manner in BEAS 2B cells [50]. At the concentration of 10  $\mu$ g/mL and below, dissolved zinc ions were reported to induce metallothionein synthesis that offered resistance to oxidative stress in mouse alveolar macrophages [51]. Overexpression of the antioxidant enzyme microsomal glutathione transferase 1 (MGST1) was shown to mitigate toxicity in human breast cancer (MCF-7) cells exposed to silicon dioxide NPs, however, no such effect was observed in ZnO NP treated cells, which could be the result of a direct inhibition of the enzyme, by dissolved Zn<sup>2+</sup> ions [52]. Thus it appears that the ZnO NP exposure disrupts cellular zinc homeostasis, which generates ROS. Impairment of the cellular redox machinery is responsible for the observed toxic effects including up regulation of pro-inflammatory and oxidative stress related markers, activation of signalling pathways and initiation of apoptotic events.

## 5.7 ZnO NP mediated immunomodulatory responses

NPs can cause toxicity in immune cells and stimulate them to release cytokines that can in turn cause inflammation. It has been suggested that the NP type and composition may play an important role in the initiation of specific signalling pathways [53]. A generalised schematic of the possible inflammatory interactions of ZnO NPs with the cellular interface has been described in figure 5.1. ZnO NPs are now finding potential applications in the bio-medical field where their ability to cause immunomodulation can be useful. Increased expression of pro-inflammatory markers tumour necrosis factor alpha (TNF $\alpha$ ), interferon gamma (IFN- $\gamma$ ) and interleukin (IL-12) was reported when primary immune cells were exposed to ZnO NPs of different sizes [11]. Similarly, a dose dependent increase in the TNF- $\alpha$  production showing a 200-fold increase and an up regulation of activation markers such as CD80 and CD86 was reported when RAW 264.7 macrophages or mouse primary dendritic cells were treated with spherical or sheet-shaped ZnO NPs [28]. However ZnO NP exposed THP-1 cells [54, 55] or skin and colon tumour cells failed to induce a TNF $\alpha$  mediated inflammatory response [41]. Moreover, ZnO NPs did not up regulate the pro-inflammatory markers such as HLA DR or CD14 on the surface of activated THP-1 monocytes [54]. Several mechanistic explanations on how the ZnO NPs are able to stimulate production of cytokines can be found across literature. A recent study reported that, ZnO NPs induced TNF- $\alpha$  expression in keratinocytes is mediated via the ROS-ERK-Egr-1 pathway [4]. Another study not only demonstrated an enhanced expression of ICAM-1, an inflammatory marker in 50 nm ZnO NPs treated human endothelial (HUVEC) cells, but also demonstrated that in the presence of an inflammatory cytokine, like TNF $\alpha$ , ZnO NPs induced inflammation can be further intensified [56].

The pro-inflammatory chemokine IL-8 is yet another important and early activator of leukocytes. It has been implicated e.g. in the progression of metal fume fever, a pulmonary condition associated with the inhalation of zinc oxide fumes [57]. Wu and co-workers demonstrated that ZnO NPs induced IL-8 expression in lung epithelial cells required phosphorylation of the proteins p65 and I $\kappa$ B $\alpha$ , which are both part of the NF- $\kappa$ B signalling pathway. They further

confirmed that TNF- $\alpha$ , that is also known to induce IL-8 expression in lung cells, is not involved in ZnO NPs mediated release and mRNA transcription of the IL-8 gene [58]. Transcriptional regulation involving NF- $\kappa$ B or C/EBP $\beta$  factors along with the post-transcriptional regulation was shown to be involved in the expression of IL-8 in ZnO NPs stimulated human bronchial cells [5]. Interestingly, toll like receptors (TLRs) associated with the innate immune response have also been implicated in the ZnO NP-induced expression of pro-inflammatory cytokines. Chen *et al.* reported that ZnO NPs may be involved in a direct interaction with the TLR4 receptor on the surface of bronchial epithelial cells, leading to an increase in the expression of IL-8. They further confirmed this finding by comparing the inflammatory responses in wild type vs. TLR4 deficient mice. Interestingly, while the ZnO NPs used in this study were free of endotoxin contamination (potent stimulator of TLRs) no further explanation was provided regarding the subsequent cellular signalling and mechanisms [59]. MyD88 adaptor protein and TLR4 directed stimulation of pro-inflammatory cytokines TNF- $\alpha$  and monocyte chemoattractant protein (MCP-1) in MLE12 cells (mouse lung epithelial cells) and RAW 264.7 cells (mouse macrophages) were also demonstrated [60]. Furthermore, Roy and co-workers demonstrated that inflammatory responses including upregulation of IL-1 $\beta$ , IL-6, TNF $\alpha$ , cyclooxygenase-2 and inducible nitric oxide synthase by ZnO NPs-activated macrophages strongly depend MAPK signalling mediated by TLR6 [61].

Interaction of NP with immune cells may result in stimulation or suppression of immune function via various mechanisms. Polymorphonuclear neutrophils (PMNs) are hallmarks of acute inflammation. Goncalves and co-workers reported that exposure of human neutrophils to ZnO NPs (100  $\mu$ g/mL) significantly inhibited neutrophil apoptosis by de-novo protein synthesis mechanism without ROS formation. This is an example of indirect cytotoxicity induction by ZnO NPs considering suppression of PMN apoptosis may lead to their persistence at an inflammatory site propagating excessive tissue injury and further highlights the pro-inflammatory potential of ZnO-NP [62].

Yet another undesirable effect of NP mediated stimulation of cytokine production is the development of hypersensitivity reactions. Interestingly, while the contribution of NPs in the development or suppression of allergy has

been investigated for other NPs, limited information is available for ZnO NPs. Cross-linking of IgE antibodies on the surface of sensitised mast cells or basophils by allergenic proteins can cause degranulation of these cells leading to release of histamines and other active chemicals. This can manifest into symptoms of type I hypersensitivity reactions. A recent study revealed that ultra-fine ZnO particulates have the capacity to inhibit IgE mediated degranulation of rat mast cells (RBL2 H3) when challenged with the allergen ovalbumin [63]. Study of allergy induction and of allergic responses towards already established allergic stimuli may well be influenced by ZnO NP similar to other branches of the immune system, but this topic remains largely unexplored. At low doses ZnO NPs were shown to remain relatively compliant and did not induce overexpression of pro-inflammatory genes also observed in case of RAW 264.7 macrophages treated with 1µg/mL NP dose [64]. However, in human colon-derived and skin-derived cells, exposure to low doses resulted in up-regulation not only of pro-inflammatory markers but also proteins involved in metal metabolism, chaperonin proteins, and protein folding [65]. A recent study has shown that ZnO NPs can also affect the immune system by specifically modifying chemotactic agents, like chemokine receptor expression [66]. Global gene expression analysis following exposure to ZnO NPs has identified for example in human monocyte-derived macrophages, 2703 showing significant changes in expression levels [39]. Such observations show that endpoints for assessing immune modulation may not be simple and their definition for specific cases may require substantial efforts.

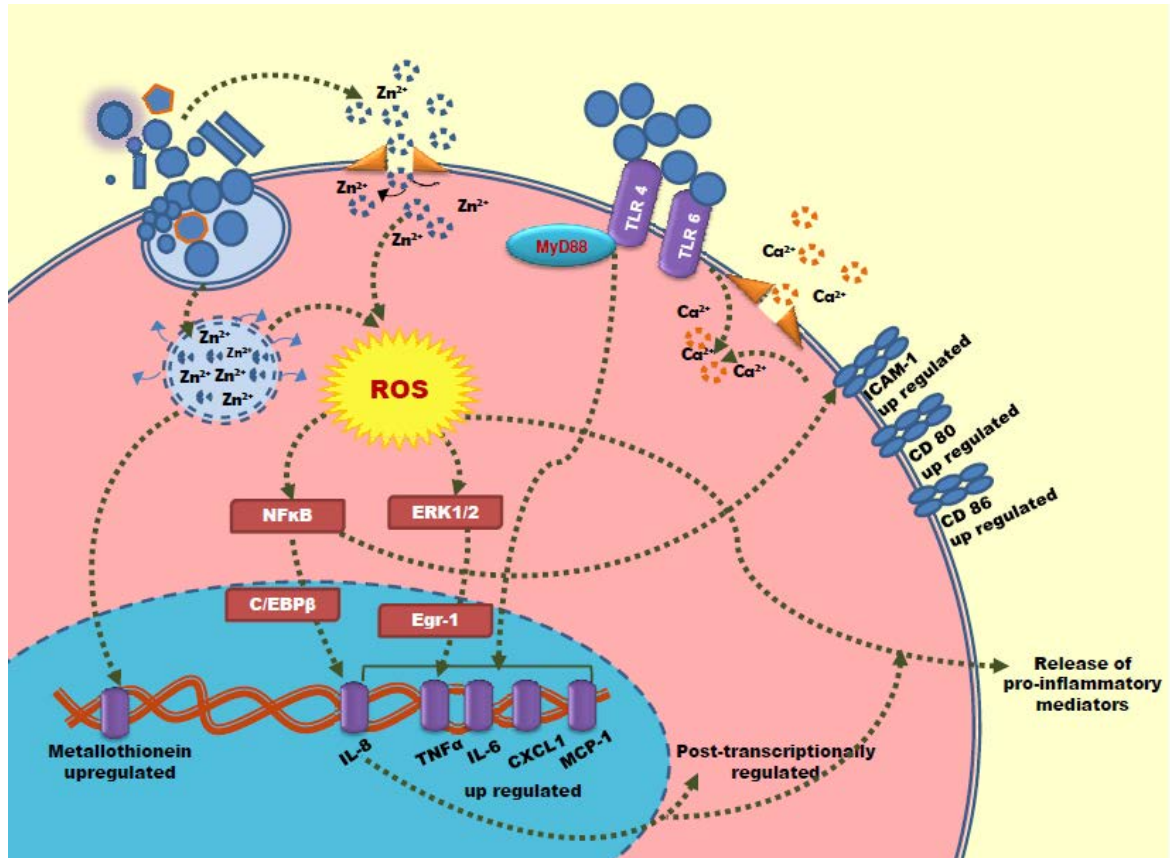


Figure 5.1: A schematic summary of the interaction of ZnO NPs with a model cellular interface and resulting pro-inflammatory consequences. ZnO NPs with different types of physico-chemical properties are taken up by cells. Some ZnO NPs may dissolve in the extracellular environment which can result in transport of the dissolved  $Zn^{2+}$  ions into the cell whereas; some ZnO NPs may dissolve inside the cell in the lysosomal compartments.  $Zn^{2+}$  ion formation ultimately results in reactive oxygen species formation that can trigger signalling cascades in the cell leading to consequences such as increase in calcium influx, gene up-regulation and release of pro-inflammatory markers. Also in certain cell types, up-regulation of surface markers associated with inflammation may occur. Release of chemokines may also be caused by interaction of ZnO NPs with specific receptors on the cell surface

## 5.8 ZnO NP mediated apoptosis and genotoxicity

Mitochondrial health is implicated in apoptotic cell death. Along with being the energy generating machinery of the cell, mitochondria also are sources of important regulators of cellular signalling pathways that direct apoptosis. Depolarisation of the mitochondrial membrane by nanomaterials can cause cell death as reported in case of lung adenocarcinoma (H1355) cells exposed to ZnO NPs [3]. The characteristic features of cells undergoing apoptosis include physical changes in cytoplasm, plasma membrane and nucleus.

ZnO NPs when interacting with *in vitro* cells have been shown to induce several signalling pathways that result in apoptotic cell death. The p53-p38 pathway has been extensively implicated in NP induced apoptotic cell death. Increased activity of pro-apoptotic genes caspase-3, bax and tumor suppressor gene p53 was demonstrated along with fragmentation of DNA for ZnO NPs treated human liver cancer cells (Hep G2), A549 cells and human dermal fibroblasts [14, 67-69]. A recent study on rat retinal ganglion cells (RCG-5) showed that generation of ROS lead to over production of caspase 12 protein which resulted in endoplasmic reticulum stress and finally cell death [70]. Wilhelmi et al. demonstrated that NOX2 the phagocytic NADPH oxidase enzyme complex is the major source of ROS formation and induction of apoptosis/necrosis. Also, other redox responsive pathways such as the Nrf2 cascade, may contribute to the cytotoxicity in ZnO NP exposed macrophages [71]. Similarly a recent study on ZnO NPs exposed cultured primary rat astrocytes confirmed the role of the JNK signalling pathway in apoptosis [72].

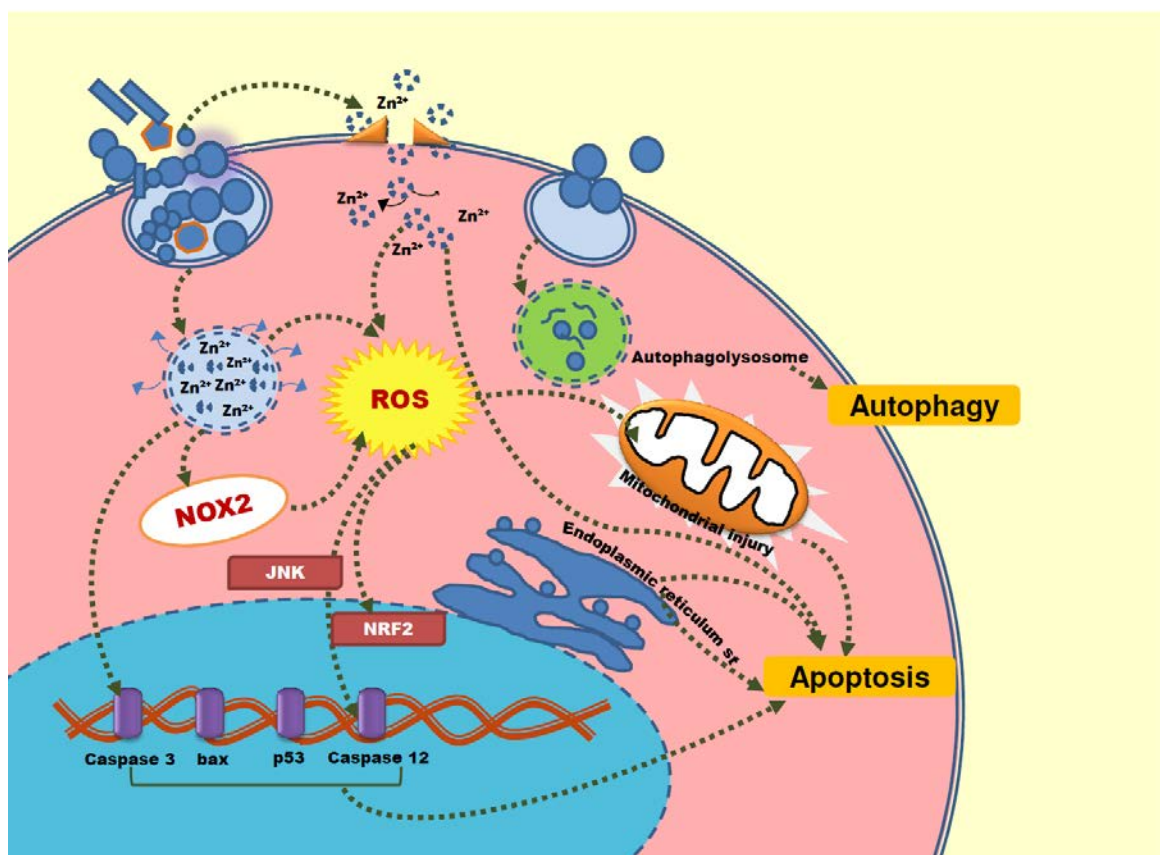
ZnO NPs have also been shown to accumulate inside lysosomal compartments of the different types of cells after uptake. Autophagy (Figure 5.2) is an alternative apoptotic cell death mechanism, wherein cells survive, but sequester aged organelles and proteins in vesicles called autophagosomes that ultimately fuse with lysosomes, leading to the destruction of the encapsulated material [73]. Exposure of mouse skin epidermal cells to ZnO NPs resulted in autophagic vacuole formation and subsequent mitochondrial dysfunction and cell death [74]. Interestingly, for human leukemic T cells, exposure to ZnO NPs

initiated a caspase-independent alternative apoptosis pathway not mediated via ROS [35].

Genotoxicity is the damage to the cellular DNA that may take place either directly due to the interaction of NPs with the nuclear material or indirectly due to the generation of ROS, other reactive ions or mechanical injury. In case of ZnO NPs, mechanisms to process DNA damage may be inactive or even down regulated in exposed cells, which may explain the genotoxic potential of these particulates [22]. ZnO NPs were shown to cause significant damage to the DNA as demonstrated by an increase in olive tail moment (comet assay) in a human epidermal cell line (A431) even at a low concentration of 5  $\mu\text{g/ml}$  [75], also reported in the case of human renal proximal tubule epithelial (HK-2) cells [76]. Similarly, Yang et al. reported high levels of ROS generated by ZnO NPs and noted that, their peculiar shape when compared to other types of nanoparticles could be responsible for the DNA damage in primary mouse embryo fibroblasts, also at low concentrations [49]. ZnO NPs were shown to cause DNA damage in nasal mucosa cells using single-cell micro gel electrophoresis (comet) assay [77]. Concentration dependent oxidative DNA damage resulting in characteristic induction of nuclear condensation, DNA fragmentation, formation of hypodiploid DNA nuclei and apoptotic bodies was also reported in case of ZnO NPs treated macrophages [71]. Intra-nuclear distribution of ZnO NPs was suggested as a possible explanation for the genotoxicity observed in ZnO exposed human head and neck squamous cell carcinoma (HNSCC) cells [78]. Overall, there is still a need to fully understand the mechanism in which ZnO NPs inflict cellular DNA damage. Figure 5.2 gives an overview of the possible ZnO mediated genotoxic and cytotoxic interactions described in the literature.

In contrast to these reports, THP-1 cells exposed to nano or micro ZnO particles did not show any genotoxic damage whatsoever [25]. This may be explained by the size of the ZnO-nano powder used in this study which was  $> 100$  nm. Positively or negatively charged 20 or 70nm ZnO NPs were unsuccessful in inducing clastogenic effects in Chinese hamster lung (CHL) fibroblast cells and also *in vivo* genotoxicity as compared to untreated controls [79]. Similar results were reported in case of mice orally exposed to nano or micro sized ZnO [80].

Due to the prominent use of ZnO NPs as ultraviolet (UV) light filtering agents it is vital to investigate if the genotoxicity induced by ZnO NPs is modified in the presence of UV light. DNA damage was observed in human embryonic kidney (HEK 293) and mouse embryonic fibroblast (NIH/3T3) cells exposed to 100 µg/mL of ZnO NPs, although a significant antagonist interaction effect was observed with UV-B light co-exposure [81]. A number of *in vitro* and *in vivo* studies have investigated if ZnO NPs penetrate the normal skin upon topical application. However, no evidence of penetration of these NPs into the epidermal layers of normal skin has been reported, although a recent study demonstrated that in UV-B-damaged skin, there could be a marginal enhancement in the ZnO NP penetration without transdermal absorption [82-84]. Interestingly, co-exposure to NPs and UV-A generated the same or less ROS than with UV-A exposure in THP-1 cells alone, which points towards minimal participation of the actual ZnO NPs in generating damage [85]. Table 5.1 gives a concise summary of the inflammatory and cytotoxic interactions of ZnO NPs with different mammalian cells.



**Figure 5.2:** A schematic representation of interaction of ZnO NPs with a model cell surface focussing on the cytotoxicity. Reactive oxygen species generated due to imbalance of  $Zn^{2+}$  caused in the intracellular environment due to interaction with ZnO NPs may result in apoptosis. Different types of signalling pathways are switched on which lead to release of important proteins involved in apoptosis. Moreover, ROS may also affect the mitochondrial health that can ultimately result in cytotoxicity. ZnO NP interaction with certain types of cells can also result in autophagy.

**Table 5.1 Overview of recent (2012-2014) in vitro studies discussing the interaction of ZnO NPs with different mammalian cell types**

ZnO NPs	Cell type	Species	Observations	Ref
Citrate 20 nm	HaCaT cells Keratinocytes	H	ZnO-NPs induce inflammatory response via ROS-ERK-Egr-1 pathway	[4]
≤ 35 nm, Particulates, 50–80 nm	Embryonic kidney (HEK293) embryonic fibroblasts (NIH/3T3)	H  M	Antagonistic genotoxic damage mediated by UVB ZnO NP co exposure	[81]
25 nm	Alveolar epithelial C10 ALI subcultured cells	M	low and critical levels of intracellular Zn <sup>2+</sup> concentrated in endosomes and lysosomes vital for toxicity	[32]
20 nm	macrophages RAW 264.7	M	Cytotoxicity induced in p47phox and Nrf2- independent manner	[71]
Pristine, surfactant dispersed 30, 80, 200 nm	THP-1 monocytes	H	Intracellular dissolution of ZnO NPs required for cytotoxicity	[40]
50 nm	Lung epithelial cells (L-132)	H	Toxicity mediated via ROS and apoptosis	[39]
~4 nm	NIH/3T3 fibroblasts	M	Cytotoxicity dependent on presence of phosphates in medium and extent of agglomeration	[17]
Pristine, surfactant dispersed 30, 80, 200 nm	THP-1 monocytes	H	ZnO NP UVA co-exposure generated the same or less ROS than with UVA exposure alone	[85]
Hexagonal 15.5 nm	breast carcinoma cell MCF-7 line	H	Cytotoxicity : ZnO NPs inhibit Microsomal glutathione transferase 1 (MGST1) antioxidant enzyme	[52]
39 nm ZnO@A PTES ZnO@P EG	THP-1 monocytes	H	Surface modification to reduced ZnO NP uptake better option to control cytotoxicity	[46]
coated NM 110 (70 to > 100 ) uncoated NM 111) (58-93)	Renal epithelial cells HK-2	H	Increase in IL-8, IL-6, ROS, DNA damage. No change in TNF $\alpha$ and MCP-1 release	[76]
Uncoated 30 nm	BEAS-2B	H	ZnO-NPs induce IL-8 gene expression through transcriptional activation and mRNA stabilization and depends on endocytosis of	[5]
H <sub>2</sub> O <sub>2</sub> modified 14 nm, 98 nm	Dermal fibroblasts HDF and A549 cells	H	ZnO NP surface property affect their cytotoxicity	[43]
ZnO NPs 60 nm Al-doped ZnO NPs 50 nm	A549	H	Contribution of Zn <sup>2+</sup> ions released from NPs is 10% toward total cytotoxicity	[42]

carboxylated < 20 nm	Neutrophils from venous blood	H	ZnO NPs activate neutrophils, delay apoptosis by de novo protein synthesis-dependent and ROS-independent mechanism	[62]
< 50 nm	Macrophages	M	Inflammation dependent on TLR6-mediated MAPK signalling	[61]
< 50 nm	Macrophages	M	ZNPs are internalized through caveolae pathway and the inflammatory responses involve PI3K mediated MAPKs signalling cascade.	[86]
< 50 nm and < 100 nm	THP-1 monocytes	H	Size dependent cytotoxicity and inflammation	[25]
Rods W 15.38 nm L 82.34 nm	JB6 Cl 41-5a epidermal cells	M	ZnO NP induce autophagy and ROS	[74]
Bulk rods 100,30 nm rods. 10-30 nm spheres	alveolar macrophage cell line	M	Cytotoxicity dependent on undissolved ZnO NPs	[51]
Aminopropylsiloxane capped 60 nm	RGC-5 retinal ganglion cells	R	ROS overproduction, ER stress, apoptosis/necrosis, caspase12 overproduction	[87]
45 nm	Primary astrocytes	M	ROS, apoptosis induced via JNK pathway	[72]
30 nm	Hep G2	H	ROS, apoptosis independent of JNK pathway	[69]
70 nm Bulk, cationic, anionic, non-ionic	THP-1 monocytes	H	Sub-toxic concentrations of ZnO NPs did not induce HLA DR and CD14 expression, or TNF $\alpha$ release but modest levels of adhesion molecule CD11b observed	[54]
5.6 to 560 nm	Airway Triple cell co-culture model	H	Differences in aerosol and suspension-exposure of ZnO NPs explored	[30]
50–70 nm, < 1 $\mu$ m	A549 cells	H	Effects of serum on cytotoxicity explored	[18]
ZnO 1-10 ZnO 2 - 18.3 ZnO 3- 28.7 ZnO 4 -8	Jurkat cells	H	Cytotoxicity due to extracellular dissolution of ZnO NP, apoptosis via caspase-independent alternative pathway	[35]
Z-COTE (44 nm X 73 nm) Nanosun 25 nm HP1 (28 nm X 96 nm) Max (36 nm X 95 nm)	Neurosphere-derived cells from olfactory mucosa	H	ZnO –NP cytotoxicity mediated via inflammation, apoptosis but not DNA damage repair mechanisms also surface modification reduces ZnO NP toxicity.	[22]
28 nm	Calu-3 cells	H	NPs translocate in small amounts transcellularly without disrupting cellular junctions	[6]
71 nm	MLE12 cells RAW 264.7 cells	M	ZnO NP mediated inflammation involved MyD88 an adaptor protein involved in signal transduction.	[60]

## 5.9 ZnO NP mediated cytotoxicity and inflammatory responses in animal models

Biologically complex systems consisting of several protein rich environments and cellular diversity together may impact the bio-reactive nature of nanomaterials. *In vivo* animal models thus provide an important platform to assess nanotoxicity. In this section literature on different routes of exposure to ZnO NPs in animal models and their subsequent effects is reviewed (also see Table 5.2).

Zinc is an essential trace element and ZnO NPs are often used as supplements, food additives and also in packaging, therefore it is imperative to assess their toxicological potential *in vivo* for risk assessment purposes [88]. Systemic deposition of NPs *in vivo* may lead to their interaction with immune cells resulting in immunomodulatory consequences. For example, ZnO NPs were reported to behave like adjuvants and induced Th2 responses in mice exposed to the allergen ovalbumin [89].

Orally administered ZnO NPs seem to be mainly retained in the liver, kidney and pancreas as zinc ions [90]. A single oral dose of ZnO NPs (500 mg/kg) delivered daily demonstrated that the toxicity induced by ZnO NPs in mouse liver and brain is mediated via oxidative stress [91]. Sharma et al. also reported an increase in oxidative stress along with induction of DNA damage and apoptosis in liver and kidney cells of mice exposed to a sub-acute oral ZnO NP dose (300 mg/kg) for 14 consecutive days [92]. Similarly, rats exposed to 333.33 mg/kg of ZnO NPs (20–30 nm) through oral gavage for five days showed significant hepatic injury and severe renal toxicological impact [93]. Oral administration of ZnO NPs can also result in significant nephrotoxicity [5] as well as accumulation in mammary tissues of animals and transfer to their offspring [94].

As previously discussed, physicochemical properties of NPs impact their bio-reactivity. When compared to micro sized ZnO, 20 nm NPs were shown to induce high levels of toxicity at lower doses upon oral administration in rats [95]. Also, ZnO NPs were shown to have wider bio-distribution and tissue adsorption

as compared to their bulk counterparts [80]. On the contrary, others have suggested that accumulation of ZnO NPs in lung, liver or kidney is independent of NP size and moreover, animal gender, when administered orally [96]. Yet another study reported that nanoparticles (20 nm) have higher toxic potential as compared to larger particles (120 nm) at lower doses [90].

Li and co-workers reported that absorption and accumulation of ZnO NPs or bulk counterparts in liver, spleen and kidney is similarly irrespective of intraperitoneal or oral routes of administration in mice [80], however, the resulting toxic outcomes may vary [64]. Besides accumulation studies, it is also important to investigate the clearance profile of ZnO NPs. This can provide useful information not only for toxicological assessment but can also help in strategic manipulation of NP surfaces for *in vivo* targeted delivery of bioactive compounds. Cho et al. showed that orally administered ZnO NPs were excreted mainly through urine, while another study reported that excretion of ZnO NPs via faeces was the most prominent way of clearance [96, 97]. ZnO NPs have a high dissolution rate in acidic conditions. Therefore there is a possibility of increased absorption of  $Zn^{2+}$  in circulation following oral exposure to ZnO NPs. A dose dependent increase in  $Zn^{2+}$  levels was recorded in the liver and kidney tissue of rats exposed to ZnO NPs [97]. Similarly, plasma zinc levels were shown to rapidly increase within 24 hr of oral administration of ZnO NPs [96].

Occupational exposure to NPs is an important concern. *In vivo* models addressing airway exposure to NPs, their deposition and clearance from the lung can therefore help to predict potential risks. A recent study demonstrated that inhalation or intratracheal instillation of ZnO NPs not only causes classic pulmonary oxidative-inflammatory responses but also cardiopulmonary impairments [98]. Physicochemical characteristics of NPs may influence the induction of pulmonary inflammation after inhalation [99]. NP mediated lung inflammation may be related to different metrics including NP mass, number, or surface area used for deciding NP dosage. A recent study showed in case of ZnO NPs no difference when mass and surface area were used as metrics for determining the ZnO NP inhalation dose [100]. Inhalation of zinc laden particles has been previously reported to cause metal fume fever and so numerous

studies focus on understanding cytotoxic implication of ZnO NPs with cell systems of pulmonary origin.

It appears that NPs, particularly metal oxide, may leave a unique inflammatory footprint when exposed to the lung environment *in vivo* [101]. Rats exposed to 90 nm ZnO NPs or 111 nm ZnO particulates via intratracheal instillation or inhalation in whole-body chambers were reported to show short-term lung inflammation and cytotoxic responses, which were resolved in a few days post exposure. Interestingly, when used in an *in vitro* system the same NPs were not effective in producing a robust pro-inflammatory response (up regulation of TNF $\alpha$  and MIP-2) [57]. This highlights that comparison of immunotoxic responses of ZnO NPs *in vivo* and *in vitro* remains a challenging task.

Juang et al. used an iTRAQ proteomics based approach to identify differential expression of proteins involved in pulmonary inflammation and also lung cancer in the bronchioalveolar lavage fluid (BALF) of rats that had been exposed to high dose of 35 nm ZnO NPs [102]. ZnO NPs were also shown to enter the central nervous system via an olfactory bulb–brain translocation pathway in rats exposed to these NPs via inhalation [103].

Intratracheal instillation of ZnO nanoparticles was shown to induce an increase in antioxidants such as lipid peroxide, HO-1 and alpha-tocopherol in the lungs of exposed rats [104]. Rapid dissolution of ZnO NPs in the lysosomal compartments of the cells has been previously proposed to be the main mechanism responsible for ZnO NP induced lung injury [105]. Elevated levels of cytosolic and mitochondrial zinc were reported in BALF cells and white blood cells of rats exposed to ZnO NPs via inhalation suggesting ZnO NP interference of zinc homeostasis leading to pulmonary toxicity [3]. Minimal pulmonary inflammation, cytotoxicity or changes in lung histopathology were observed in a 2 or 13 week exposure study where mice inhaled 15 nm ZnO NP aerosols [91].

Inhalation of ZnO NP leads to an increase in Zn<sup>2+</sup> ions in the BALF, although this increase is not permanent and the Zn levels return to basal levels within few weeks. Comparison of the inflammatory potential of Zn and ZnO NPs reveals that ZnO NPs may induce stronger pulmonary inflammation compared to their aqueous extracts [106] however, the mechanisms involved seem to

differ. ZnO NPs and not zinc nitrate (source of Zn<sup>2+</sup> ions) were shown to cause increased LDH levels in the BALF [59]. Doping of ZnO NPs with iron, successfully mitigated release of Zn<sup>2+</sup> ions and subsequent pulmonary toxicity in rodents and also had protective effects in other animal models investigated [107].

Neuro-effects of ZnO NP exposure in mice were recently explored where mice showed behavioural and electrophysiological improvements after ZnO NP intraperitoneal treatment [108]. A review of the literature pertaining to *in vivo* effects of ZnO NP exposure reconfirms that dissolution and subsequent ROS generation seem to be the most important drivers of the observed toxicity. The complex nature of the *in vivo* system obviously compounds the extrapolation of the *in vitro* toxicity mechanisms of these NPs. However, future studies employing well characterised NPs, novel routes of exposure and using realistic exposure doses may help in fully exploring potential applications of ZnO NPs in nano-medicine and can also ascertain their toxic potential so ensure work place and consumer safety.

**Table 5.2 Overview of recent (2012-2014) in vivo studies discussing effect of exposure to ZnO NPs via various routes in animals**

Route	Animals	Treatment and Duration	Observations	Ref
Intratracheal instillation	Rat	ZnO NP 0.2 mg/0.4 ml or ZnCl <sub>2</sub> 28 µg/0.4 ml single dose Assessment: 1, 24, 72 hr and 1 week after exposure	ZnO nanoparticles induce oxidative stress in the lung in the acute phase	[104]
Intraperitoneal injection	Mouse	500 µl (0.25, 0.5, 1 and 3 mg) ZnO NP with or without Ovalbumin Assessment: 30 days	Adjuvant effect to allergen ovalbumin induced Th2 immune response	[89]
Intratracheal instillation Inhalation exposure	Rat	10 mg/ml up to 72 hr 5 mg/ml up to 24 hr (1.1 & 4.9 mg/m <sup>3</sup> ) (5 h/day, 5 days/week for 30 days)	ZnO NPs may cause cardiopulmonary impairments	[98]
Inhalation exposure	Rat	6 hr for 1 day: 2.1 X 10 <sup>6</sup> particles/cm <sup>3</sup> , 38 nm ZnO NPs	An olfactory bulb–brain translocation pathway for airborne ZnO-NPs verified also interneuron translocation NPs occurs via endocytosis	[109]
Inhalation exposure	Rat	Rats exposed to 35.6 nm ZnO NPs at 1 X 10 <sup>5</sup> mm <sup>2</sup> /m <sup>3</sup> for 6 hr Assessment after 24 hr	ZnO NP exposure caused increased expression of proteins involved in cancer and pulmonary toxicity in BAL fluid of mice	[102]
Intratracheal instillation	Rat	Single dose of 6000 cm <sup>2</sup> /mL of NPs or aqueous extract obtained post centrifugation. Assessment: 24 hr or 4 weeks	Differential pro-inflammatory responses of ZnO NPs and their aqueous extracts observed	[106]
Intratracheal instillation Inhalation exposure	Mouse	80 µg of ZnO NP in 30 µL of distilled water Assessment 48 hr 0.86 mg/m <sup>3</sup> aerosolized ZnO NP, 5 h/day Assessment: 5 days	Pulmonary inflammation induced by ZnO NPs different than that caused by Zn <sup>2+</sup> ions	[59]
Inhalation exposure	Mouse	3.5 mg/m <sup>3</sup> , 4 hr/day Assessment: 2 or 13 weeks	ZnO NPs have low sub-chronic toxicity	[110]
Intraperitoneal Oral	Rat	ZnO NP dosed at 1, 10 and 100 mg/kg (body weight) daily Assessment: end of 14 days	i.p. route more toxic than the g.i route. Liver dysfunction observed.	[64]
Oral	Rat	ZnO NP dosed at 100, 300 and 1000 mg/kg (body weight) daily Assessment: end of 14 days	ZnO NP induce nephrotoxicity by disturbing metabolism and cause mitochondria and cell membrane disruption in rat kidney	[111]
Oral	Rats	ZnO NPs (500, 1000, and 2000 mg/kg) three times by gavage at 0, 24, and 45 hr.	Surface modified ZnO NPs do not induce genotoxicity in vivo	[112]
Oral	Rat	ZnO NPs 10 mL/kg. twice with a 24 hr interval	Surface modified ZnO NPs do not induce genotoxicity in vivo	
Oral	Rat	ZnO NPs administered 333.33 mg/kg/day Assessment: end of 5 days	ZnO NPs cause hepatic injury, nephrotoxicity and lung inflammation	[93]
Oral	Rat	300 mg/kg or 50 mg/kg	Liver is the target organ for sub-	[92]

		ZnO NPs dosed for 14 days Assessment: end of 14 days	acute oral exposure to ZnO NPs. ROS mediated DNA damage and apoptosis also observed.	
Oral	Rat	Single dose acute study: ZnO NPs administered at 536.8, 1073.5, and 2147 mg/kg/day Repeated dose study 10 ml/kg body weight for 13 weeks daily Assessment: final day	Absorption, distribution and excretion of ZnO NPs investigated	[113]
Oral	Rat	Single dose of ZnO NPs 50, 300, or 2000 mg/kg administered Assessment: Blood samples collected at (time zero and hours 0.5, 1, 2, 4, 6, 10, 24, 48, 72, and 96) Tissue samples collected at (hours 1 and 6, and days 1, 2, 3, and 7) Urine and faeces collected using at 4 and 10 hr, and on days 1, 2, 3, 4, 5, 6, 7, 8, 9, 10, and 14	ZnO absorbed in ionic form. The liver, lung, and kidney possible target organs for accumulation. Toxicity of ZnO nanoparticles was independent of particle size or gender. ZnO NP excreted via the faeces.	[114]
Oral	Rat	Single dose of ZnO NPs 500 mg/kg for 21 consecutive days. Assessment: final day	ZnO NPs enhanced levels of (ROS) and altered antioxidant enzymes activities in erythrocytes liver and brain. Also neurotoxic potential assessed.	[91]
Intratracheal instillation	Mouse	Single dose of 80 µg/µl Assessment: 2, 7, 14, and 28 post instillation	Single-dose exposure to ZnO NPs produced the short-term lung inflammation via a MyD88-dependent TLR pathway. Also ZnO NP induced inflammation distinct from that caused by ions.	[60]

## 5.10 Conclusion

Research on the nanotoxicity of ZnO NPs highlights the reactive nature of these NPs. Cytotoxic responses of ZnO NPs may largely depend on the cell type under investigation, exposure conditions or routes, and method of ZnO NPs preparation. Physico-chemical characteristics of ZnO NPs, including presence of surface coatings or ionic impurities along with presence of specific molecules such as proteins phosphates etc. can also influence their overall cytotoxic potential. Dissolution of ZnO NPs either extracellular or within the lysosomal compartment of the cells leads to perturbation of the cellular Zn<sup>2+</sup> homeostasis which can subsequently result in ROS formation. Recent studies have also demonstrated the propensity of ZnO NPs to interact with specific receptor molecules on cell surfaces, subsequently affecting transcription of pro-inflammatory cytokines via definite signalling pathways. ZnO NPs have not only been shown to cause immunomodulation, but also autophagy, apoptosis and genotoxicity in a number of cell types in vitro. In vivo exposure via oral, intratracheal or inhalation routes causes accumulation of these NPs in vital organs such as liver, kidney, heart, lungs, etc. along with toxic and inflammatory outcomes. Toxicokinetic investigation of ZnO NP interaction with a wider range of cell types in vitro and ex-vivo are required to correlate the impact of NP physicochemical properties with the observed cytotoxicity and inflammation. Moreover elegant in vivo studies specifically targeted to understand if ZnO NP mediated nanotoxicity is indeed caused by intact NPs or dissolved zinc ions. Elaborate studies investigating not only realistic exposure doses but also a wider range (very low to very high) of ZnO NP doses can help enhance our existing nanotoxicology knowledge of these NPs. This will also assist in risk assessment and setting safety paradigms pertaining to exposure and release of these materials into the environment.

In terms of toxicity, ZnO-NPs are categorised into the group of high toxicity nanomaterials. However information on the pro-inflammatory potential of these NPs at sub-toxic concentrations is limited. Understanding how the cellular defence mechanisms function in the presence of sub-cytotoxic concentrations of these NPs is vital and has been investigated in details in chapter VI

## 5.11 References

1. Saptarshi S, Duschl A, Lopata A: **Interaction of nanoparticles with proteins: relation to bio-reactivity of the nanoparticle.** *J Nanobiotechnol* 2013, **11**:26.
2. Filippi C, Pryde A, Cowan P, Lee T, Hayes P, Donaldson K, Plevris J, Stone V: **Toxicology of ZnO and TiO<sub>2</sub> nanoparticles on hepatocytes: Impact on metabolism and bioenergetics.** *Nanotoxicology* 2014, **0**:1-9.
3. Kao Y-Y, Chen Y-C, Cheng T-J, Chiung Y-M, Liu P-S: **Zinc Oxide Nanoparticles Interfere With Zinc Ion Homeostasis to Cause Cytotoxicity.** *Toxicol Sci* 2012, **125**:462-472.
4. Jeong SH, Kim HJ, Ryu HJ, Ryu WI, Park Y-H, Bae HC, Jang YS, Son SW: **ZnO nanoparticles induce TNF- $\alpha$  expression via ROS-ERK-Egr-1 pathway in human keratinocytes.** *J Dermatol Sci* 2013, **72**:263-273.
5. Yan Z, Xu L, Han J, Wu Y-J, Wang W, Yao W, Wu W: **Transcriptional and posttranscriptional regulation and endocytosis were involved in zinc oxide nanoparticle-induced interleukin-8 overexpression in human bronchial epithelial cells.** *Cell Biol Toxicol* 2014:1-10.
6. Cohen JM, Derk R, Wang L, Godleski J, Kobzik L, Brain J, Demokritou P: **Tracking translocation of industrially relevant engineered nanomaterials (ENMs) across alveolar epithelial monolayers in vitro.** *Nanotoxicology* 2014, **8**:216-225.
7. Liu H, Yang D, Yang H, Zhang H, Zhang W, Fang Y, Lin Z, Tian L, Lin B, Yan J, Xi Z: **Comparative study of respiratory tract immune toxicity induced by three sterilisation nanoparticles: Silver, zinc oxide and titanium dioxide.** *J Hazard Mater* 2013, **248–249**:478-486.
8. Sayes CM, Reed KL, Warheit DB: **Assessing Toxicity of Fine and Nanoparticles: Comparing In Vitro Measurements to In Vivo Pulmonary Toxicity Profiles.** *Toxicol Sci* 2007, **97**:163-180.
9. Lanone S, Rogerieux F, Geys J, Dupont A, Maillot-Marechal E, Boczkowski J, Lacroix G, Hoet P: **Comparative toxicity of 24 manufactured nanoparticles in human alveolar epithelial and macrophage cell lines.** *Particle and Fibre Toxicology* 2009, **6**:14.

10. Brown JS, Wilson WE, Grant LD: **Dosimetric Comparisons of Particle Deposition and Retention in Rats and Humans.** *Inhal Toxicol* 2005, **17**:355-385.
11. Hanley C, Thurber A, Hanna C, Punnoose A, Zhang JH, Wingett DG: **The Influences of Cell Type and ZnO Nanoparticle Size on Immune Cell Cytotoxicity and Cytokine Induction.** *Nanoscale Research Letters* 2009, **4**:1409-1420.
12. Nair S, Sasidharan A, Divya Rani VV, Menon D, Nair S, Manzoor K, Raina S: **Role of size scale of ZnO nanoparticles and microparticles on toxicity toward bacteria and osteoblast cancer cells.** *J Mater Sci: Mater Med* 2009, **20**:235-241.
13. Sasidharan A, Chandran P, Menon D, Raman S, Nair S, Koyakutty M: **Rapid dissolution of ZnO nanocrystals in acidic cancer microenvironment leading to preferential apoptosis.** *Nanoscale* 2011, **3**:3657-3669.
14. Akhtar MJ, Ahamed M, Kumar S, Khan MAM, Ahmad J, Alrokayan SA: **Zinc oxide nanoparticles selectively induce apoptosis in human cancer cells through reactive oxygen species.** *Int J Nanomedicine* 2012, **7**:845-857.
15. Andersson-Willman B, Gehrmann U, Cansu Z, Buerki-Thurnherr T, Krug HF, Gabrielsson S, Scheynius A: **Effects of subtoxic concentrations of TiO<sub>2</sub> and ZnO nanoparticles on human lymphocytes, dendritic cells and exosome production.** *Toxicol Appl Pharmacol* 2012, **264**:94-103.
16. Taccola L, Raffa V, Riggio C, Vittorio O, Iorio MC, Vanacore R, Pietrabissa A, Cuschieri A: **Zinc oxide nanoparticles as selective killers of proliferating cells.** *Int J Nanomedicine* 2011, **6**:1129-1140.
17. Everett WN, Chern C, Sun D, McMahon RE, Zhang X, Chen W-JA, Hahn MS, Sue HJ: **Phosphate-enhanced cytotoxicity of zinc oxide nanoparticles and agglomerates.** *Toxicol Lett* 2014, **225**:177-184.
18. Hsiao IL, Huang Y-J: **Effects of serum on cytotoxicity of nano- and micro-sized ZnO particles.** *Journal of Nanoparticle Research* 2013, **15**:1-16.

19. Kathiravan A, Paramaguru G, Renganathan R: **Study on the binding of colloidal zinc oxide nanoparticles with bovine serum albumin.** *J Mol Struct* 2009, **934**:129-137.
20. Chatterjee T, Chakraborti S, Joshi P, Singh SP, Gupta V, Chakrabarti P: **The effect of zinc oxide nanoparticles on the structure of the periplasmic domain of the *Vibrio cholerae* ToxR protein.** *FEBS J* 2010, **277**:4184-4194.
21. Yin H, Casey PS, McCall MJ, Fenech M: **Effects of Surface Chemistry on Cytotoxicity, Genotoxicity, and the Generation of Reactive Oxygen Species Induced by ZnO Nanoparticles.** *Langmuir* 2010, **26**:15399-15408.
22. Osmond-McLeod M, Osmond R, Oytam Y, McCall M, Feltis B, Mackay-Sim A, Wood S, Cook A: **Surface coatings of ZnO nanoparticles mitigate differentially a host of transcriptional, protein and signalling responses in primary human olfactory cells.** *Particle and Fibre Toxicology* 2013, **10**:54.
23. Song W, Zhang J, Guo J, Zhang J, Ding F, Li L, Sun Z: **Role of the dissolved zinc ion and reactive oxygen species in cytotoxicity of ZnO nanoparticles.** *Toxicol Lett* 2010, **199**:389-397.
24. Lin W, Xu Y, Huang C-C, Ma Y, Shannon K, Chen D-R, Huang Y-W: **Toxicity of nano- and micro-sized ZnO particles in human lung epithelial cells.** *Journal of Nanoparticle Research* 2009, **11**:25-39.
25. Sahu D, Kannan GM, Vijayaraghavan R: **Size-Dependent Effect of Zinc Oxide on Toxicity and Inflammatory Potential of Human Monocytes.** *J Toxicol Environ Health, Part A* 2014, **77**:177-191.
26. De Berardis B, Civitelli G, Condello M, Lista P, Pozzi R, Arancia G, Meschini S: **Exposure to ZnO nanoparticles induces oxidative stress and cytotoxicity in human colon carcinoma cells.** *Toxicol Appl Pharmacol* 2010, **246**:116-127.
27. Hsiao IL, Huang Y-J: **Effects of various physicochemical characteristics on the toxicities of ZnO and TiO<sub>2</sub> nanoparticles toward human lung epithelial cells.** *Sci Total Environ* 2011, **409**:1219-1228.

28. Heng BC, Zhao XX, Tan EC, Khamis N, Assodani A, Xiong SJ, Ruedl C, Ng KW, Loo JSC: **Evaluation of the cytotoxic and inflammatory potential of differentially shaped zinc oxide nanoparticles.** *Arch Toxicol* 2011, **85**:1517-1528.
29. Cho EC, Zhang Q, Xia Y: **The effect of sedimentation and diffusion on cellular uptake of gold nanoparticles.** *Nat Nano* 2011, **6**:385-391.
30. Raemy D, Grass R, Stark W, Schumacher C, Clift M, Gehr P, Rothen-Rutishauser B: **Effects of flame made zinc oxide particles in human lung cells - a comparison of aerosol and suspension exposures.** *Particle and Fibre Toxicology* 2012, **9**:33.
31. Lenz A, Karg E, Lentner B, Dittrich V, Brandenberger C, Rothen-Rutishauser B, Schulz H, Ferron G, Schmid O: **A dose-controlled system for air-liquid interface cell exposure and application to zinc oxide nanoparticles.** *Particle and Fibre Toxicology* 2009, **6**:32.
32. Mihai C, Chrisler WB, Xie Y, Hu D, Szymanski CJ, Tolic A, Klein JA, Smith JN, Tarasevich BJ, Orr G: **Intracellular accumulation dynamics and fate of zinc ions in alveolar epithelial cells exposed to airborne ZnO nanoparticles at the air-liquid interface.** *Nanotoxicology* 2013, **0**:1-14.
33. Xie Y, Williams NG, Tolic A, Chrisler WB, Teeguarden JG, Maddux BLS, Pounds JG, Laskin A, Orr G: **Aerosolized ZnO nanoparticles induce toxicity in alveolar type II epithelial cells at the air-liquid interface.** *Toxicol Sci* 2011, **125**:450-461.
34. James SA, Feltis BN, de Jonge MD, Sridhar M, Kimpton JA, Altissimo M, Mayo S, Zheng C, Hastings A, Howard DL, et al: **Quantification of ZnO Nanoparticle Uptake, Distribution, and Dissolution within Individual Human Macrophages.** *ACS Nano* 2013, **7**:10621-10635.
35. Buerki-Thurnherr T, Xiao L, Diener L, Arslan O, Hirsch C, Maeder-Althaus X, Grieder K, Wampfler B, Mathur S, Wick P, Krug HF: **In vitro mechanistic study towards a better understanding of ZnO nanoparticle toxicity.** *Nanotoxicology* 2013, **7**:402-416.
36. Kim YH, Fazlollahi F, Kennedy IM, Yacobi NR, Hamm-Alvarez SF, Borok Z, Kim K-J, Crandall ED: **Alveolar Epithelial Cell Injury Due to Zinc**

- Oxide Nanoparticle Exposure.** *Am J Respir Crit Care Med* 2010, **182**:1398-1409.
37. Pujalte I, Passagne I, Brouillaud B, Treguer M, Durand E, Ohayon-Courtes C, L'Azou B: **Cytotoxicity and oxidative stress induced by different metallic nanoparticles on human kidney cells.** *Part Fibre Toxicol* 2011, **8**:10.
38. Tuomela S, Autio R, Buerki-Thurnherr T, Arslan O, Kunzmann A, Andersson-Willman B, Wick P, Mathur S, Scheynius A, Krug HF, et al: **Gene expression profiling of immune-competent human cells exposed to engineered zinc oxide or titanium dioxide nanoparticles.** *PLoS ONE* 2013, **8**.
39. Sahu D, Kannan GM, Vijayaraghavan R, Anand T, Khanum F: **Nanosized Zinc Oxide Induces Toxicity in Human Lung Cells.** *ISRN Toxicology* 2013, **2013**:8.
40. Shen C, James SA, de Jonge MD, Turney TW, Wright PFA, Feltis BN: **Relating Cytotoxicity, Zinc Ions, and Reactive Oxygen in ZnO Nanoparticle-Exposed Human Immune Cells.** *Toxicol Sci* 2013, **136**:120-130.
41. Moos PJ, Chung K, Woessner D, Honeggar M, Cutler NS, Veranth JM: **ZnO Particulate Matter Requires Cell Contact for Toxicity in Human Colon Cancer Cells.** *Chem Res Toxicol* 2010, **23**:733-739.
42. Xu M, Li J, Hanagata N, Su H, Chen H, Fujita D: **Challenge to assess the toxic contribution of metal cation released from nanomaterials for nanotoxicology - the case of ZnO nanoparticles.** *Nanoscale* 2013, **5**:4763-4769.
43. Altunbek M, Baysal A, Çulha M: **Influence of surface properties of zinc oxide nanoparticles on their cytotoxicity.** *Colloids and Surfaces B: Biointerfaces* 2014, **121**:106-113.
44. George S, Pokhrel S, Xia T, Gilbert B, Ji Z, Schowalter M, Rosenauer A, Damoiseaux R, Bradley KA, Mädler L, Nel AE: **Use of a Rapid Cytotoxicity Screening Approach To Engineer a Safer Zinc Oxide Nanoparticle through Iron Doping.** *ACS Nano* 2009, **4**:15-29.

45. Hsiao IL, Huang Y-J: **Titanium Oxide Shell Coatings Decrease the Cytotoxicity of ZnO Nanoparticles.** *Chem Res Toxicol* 2011, **24**:303-313.
46. Luo M, Shen C, Feltis BN, Martin LL, Hughes AE, Wright PFA, Turney TW: **Reducing ZnO nanoparticle cytotoxicity by surface modification.** *Nanoscale* 2014, **6**:5791-5798.
47. Xia T, Kovochich M, Liong M, Madler L, Gilbert B, Shi H, Yeh JI, Zink JI, Nel AE: **Comparison of the Mechanism of Toxicity of Zinc Oxide and Cerium Oxide Nanoparticles Based on Dissolution and Oxidative Stress Properties.** *ACS Nano* 2008, **2**:2121-2134.
48. Heng BC, Zhao X, Xiong S, Woei Ng K, Yin-Chiang Boey F, Say-Chye Loo J: **Toxicity of zinc oxide (ZnO) nanoparticles on human bronchial epithelial cells (BEAS-2B) is accentuated by oxidative stress.** *Food Chem Toxicol* 2010, **48**:1762-1766.
49. Yang H, Liu C, Yang D, Zhang H, Xi Z: **Comparative study of cytotoxicity, oxidative stress and genotoxicity induced by four typical nanomaterials: the role of particle size, shape and composition.** *J Appl Toxicol* 2009, **29**:69-78.
50. Huang C-C, Aronstam RS, Chen D-R, Huang Y-W: **Oxidative stress, calcium homeostasis, and altered gene expression in human lung epithelial cells exposed to ZnO nanoparticles.** *Toxicol In Vitro* 2010, **24**:45-55.
51. Zhang J, Song W, Guo J, Zhang J, Sun Z, Ding F, Gao M: **Toxic effect of different ZnO particles on mouse alveolar macrophages.** *J Hazard Mater* 2012, **219–220**:148-155.
52. Shi J, Karlsson HL, Johansson K, Gogvadze V, Xiao L, Li J, Burks T, Garcia-Bennett A, Uheida A, Muhammed M, et al: **Microsomal Glutathione Transferase 1 Protects Against Toxicity Induced by Silica Nanoparticles but Not by Zinc Oxide Nanoparticles.** *ACS Nano* 2012, **6**:1925-1938.
53. Gojova A, Guo B, Kota RS, Rutledge JC, Kennedy IM, Barakat AI: **Induction of inflammation in vascular endothelial cells by metal oxide nanoparticles: Effect of particle composition.** *Environ Health Perspect* 2007, **115**:403-409.

54. Prach M, Stone V, Proudfoot L: **Zinc oxide nanoparticles and monocytes: Impact of size, charge and solubility on activation status.** *Toxicol Appl Pharmacol* 2013, **266**:19-26.
55. Feltis BN, O'Keefe SJ, Harford AJ, Piva TJ, Turney TW, Wright PFA: **Independent cytotoxic and inflammatory responses to zinc oxide nanoparticles in human monocytes and macrophages.** *Nanotoxicology* 2012, **6**:757-765.
56. Tsou T-C, Yeh S-C, Tsai F-Y, Lin H-J, Cheng T-J, Chao H-R, Tai L-A: **Zinc oxide particles induce inflammatory responses in vascular endothelial cells via NF- $\kappa$ B signaling.** *J Hazard Mater* 2010, **183**:182-188.
57. Warheit DB, Sayes CM, Reed KL: **Nanoscale and Fine Zinc Oxide Particles: Can in Vitro Assays Accurately Forecast Lung Hazards following Inhalation Exposures?** *Environ Sci Technol* 2009, **43**:7939-7945.
58. Wu W, Samet JM, Peden DB, Bromberg PA: **Phosphorylation of p65 Is Required for Zinc Oxide Nanoparticle-Induced Interleukin 8 Expression in Human Bronchial Epithelial Cells.** *Environ Health Perspect* 2010, **118**:982-987.
59. Chen J-K, Ho C-C, Chang H, Lin J-F, Yang CS, Tsai M-H, Tsai H-T, Lin P: **Particulate nature of inhaled zinc oxide nanoparticles determines systemic effects and mechanisms of pulmonary inflammation in mice.** *Nanotoxicology* 2014, **0**:1-11.
60. Chang H, Ho C-C, Yang CS, Chang W-H, Tsai M-H, Tsai H-T, Lin P: **Involvement of MyD88 in zinc oxide nanoparticle-induced lung inflammation.** *Exp Toxicol Pathol* 2013, **65**:887-896.
61. Roy R, Singh SK, Das M, Tripathi A, Dwivedi PD: **Toll-like receptor 6 mediated inflammatory and functional responses of zinc oxide nanoparticles primed macrophages.** *Immunology* 2014, **142**:453-464.
62. Goncalves DM, Girard D: **Zinc oxide nanoparticles delay human neutrophil apoptosis by a de novo protein synthesis-dependent and reactive oxygen species-independent mechanism.** *Toxicol In Vitro* 2014, **28**:926-931.

63. Yamaki K, Yoshino S: **Comparison of inhibitory activities of zinc oxide ultrafine and fine particulates on IgE-induced mast cell activation.** *Biometals* 2009, **22**:1031-1040.
64. Hong T-K, Tripathy N, Son H-J, Ha K-T, Jeong H-S, Hahn Y-B: **A comprehensive in vitro and in vivo study of ZnO nanoparticles toxicity.** *Journal of Materials Chemistry B* 2013, **1**:2985-2992.
65. Moos PJ, Olszewski K, Honegger M, Cassidy P, Leachman S, Woessner D, Cutler NS, Veranth JM: **Responses of human cells to ZnO nanoparticles: a gene transcription study.** *Metallomics* 2011, **3**:1199-1211.
66. Lozano-Fernández T, Ballester-Antxordoki L, Pérez-Temprano N, Rojas E, Sanz D, Iglesias-Gaspar M, Moya S, González-Fernández Á, Rey M: **Potential impact of metal oxide nanoparticles on the immune system: The role of integrins, L-selectin and the chemokine receptor CXCR4.** *Nanomedicine: Nanotechnology, Biology and Medicine* 2014, **10**:1301-1310.
67. Ahamed M, Akhtar MJ, Raja M, Ahmad I, Siddiqui MKJ, AlSalhi MS, Alrokayan SA: **ZnO nanorod-induced apoptosis in human alveolar adenocarcinoma cells via p53, survivin and bax/bcl-2 pathways: role of oxidative stress.** *Nanomedicine: Nanotechnology, Biology and Medicine* 2011, **7**:904-913.
68. Meyer K, Rajanahalli P, Ahamed M, Rowe JJ, Hong Y: **ZnO nanoparticles induce apoptosis in human dermal fibroblasts via p53 and p38 pathways.** *Toxicol In Vitro* 2011, **25**:1721-1726.
69. Sharma V, Anderson D, Dhawan A: **Zinc oxide nanoparticles induce oxidative DNA damage and ROS-triggered mitochondria mediated apoptosis in human liver cells (HepG2).** *Apoptosis* 2012, **17**:852-870.
70. Guo D, Bi H, Liu B, Wu Q, Wang D, Cui Y: **Reactive oxygen species-induced cytotoxic effects of zinc oxide nanoparticles in rat retinal ganglion cells.** *Toxicol In Vitro* 2013, **27**:731-738.
71. Wilhelmi V, Fischer U, Weighardt H, Schulze-Osthoff K, Nickel C, Stahlmecke B, Kuhlbusch TAJ, Scherbart AM, Esser C, Schins RPF, Albrecht C: **Zinc Oxide Nanoparticles Induce Necrosis and**

- Apoptosis in Macrophages in a p47phox- and Nrf2-Independent Manner.** *PLoS ONE* 2013, **8**:e65704.
72. Wang J, Deng X, Zhang F, Chen D, Ding W: **ZnO nanoparticle-induced oxidative stress triggers apoptosis by activating JNK signaling pathway in cultured primary astrocytes.** *Nanoscale Research Letters* 2014, **9**:117.
73. Stern ST, Adisheshaiah PP, Crist RM: **Autophagy and lysosomal dysfunction as emerging mechanisms of nanomaterial toxicity.** *Particle and Fibre Toxicology* 2012, **9**.
74. Yu K-N, Yoon T-J, Minai-Tehrani A, Kim J-E, Park SJ, Jeong MS, Ha S-W, Lee J-K, Kim JS, Cho M-H: **Zinc oxide nanoparticle induced autophagic cell death and mitochondrial damage via reactive oxygen species generation.** *Toxicol In Vitro* 2013, **27**:1187-1195.
75. Sharma V, Shukla RK, Saxena N, Parmar D, Das M, Dhawan A: **DNA damaging potential of zinc oxide nanoparticles in human epidermal cells.** *Toxicol Lett* 2009, **185**:211-218.
76. Kermanizadeh A, Vranic S, Boland S, Moreau K, Baeza-Squiban A, Gaiser B, Andrzejczuk L, Stone V: **An in vitro assessment of panel of engineered nanomaterials using a human renal cell line: cytotoxicity, pro-inflammatory response, oxidative stress and genotoxicity.** *BMC Nephrol* 2013, **14**:1-12.
77. Hackenberg S, Scherzed A, Technau A, Kessler M, Froelich K, Ginzkey C, Koehler C, Burghartz M, Hagen R, Kleinsasser N: **Cytotoxic, genotoxic and pro-inflammatory effects of zinc oxide nanoparticles in human nasal mucosa cells in vitro.** *Toxicology in Vitro* 2011, **25**:657-663.
78. Hackenberg S, Scherzed A, Kessler M, Froelich K, Ginzkey C, Koehler C, Burghartz M, Hagen R, Kleinsasser N: **Zinc oxide nanoparticles induce photocatalytic cell death in human head and neck squamous cell carcinoma cell lines in vitro.** *Int J Oncol* 2010, **37**:1583-1590.
79. Kwon JY, Lee SY, Koedrith P, Lee JY, Kim K-M, Oh J-M, Yang SI, Kim M-K, Lee JK, Jeong J, et al: **Lack of genotoxic potential of ZnO**

- nanoparticles in in vitro and in vivo tests.** *Mutation Research/Genetic Toxicology and Environmental Mutagenesis* 2014, **761**:1-9.
80. Li C-H, Shen C-C, Cheng Y-W, Huang S-H, Wu C-C, Kao C-C, Liao J-W, Kang J-J: **Organ biodistribution, clearance, and genotoxicity of orally administered zinc oxide nanoparticles in mice.** *Nanotoxicology* 2012, **6**:746-756.
81. Demir E, Akça H, Kaya B, Burgucu D, Tokgün O, Turna F, Aksakal S, Vales G, Creus A, Marcos R: **Zinc oxide nanoparticles: Genotoxicity, interactions with UV-light and cell-transforming potential.** *J Hazard Mater* 2014, **264**:420-429.
82. Gamer AO, Leibold E, van Ravenzwaay B: **The in vitro absorption of microfine zinc oxide and titanium dioxide through porcine skin.** *Toxicol In Vitro* 2006, **20**:301-307.
83. Cross SE, Innes B, Roberts MS, Tsuzuki T, Robertson TA, McCormick P: **Human Skin Penetration of Sunscreen Nanoparticles: In-vitro Assessment of a Novel Micronized Zinc Oxide Formulation.** *Skin Pharmacol Physiol* 2007, **20**:148-154.
84. Monteiro-Riviere NA, Wiench K, Landsiedel R, Schulte S, Inman AO, Riviere JE: **Safety Evaluation of Sunscreen Formulations Containing Titanium Dioxide and Zinc Oxide Nanoparticles in UVB Sunburned Skin: An In Vitro and In Vivo Study.** *Toxicol Sci* 2011, **123**:264-280.
85. Shen C, Turney TW, Piva TJ, Feltis BN, Wright PFA: **Comparison of UVA-induced ROS and sunscreen nanoparticle-generated ROS in human immune cells.** *Photochem Photobiol Sci* 2014, **13**:781-788.
86. Roy R, Parashar V, Chauhan LKS, Shanker R, Das M, Tripathi A, Dwivedi PD: **Mechanism of uptake of ZnO nanoparticles and inflammatory responses in macrophages require PI3K mediated MAPKs signaling.** *Toxicol In Vitro* 2014, **28**:457-467.
87. Guo D, Bi H, Liu B, Wu Q, Wang D, Cui Y: **Reactive oxygen species-induced cytotoxic effects of zinc oxide nanoparticles in rat retinal ganglion cells.** *Toxicol In Vitro* 2012.
88. Rincker MJ, Hill GM, Link JE, Meyer AM, Rowntree JE: **Effects of dietary zinc and iron supplementation on mineral excretion, body**

- composition, and mineral status of nursery pigs.** *Journal of Animal Science* 2005, **83**:2762-2774.
89. Roy R, Kumar S, Verma AK, Sharma A, Chaudhari BP, Tripathi A, Das M, Dwivedi PD: **Zinc oxide nanoparticles provide an adjuvant effect to ovalbumin via a Th2 response in Balb/c mice.** *Int Immunol* 2014, **26**:159-172.
90. Wang B, Feng W, Wang M, Wang T, Gu Y, Zhu M, Ouyang H, Shi J, Zhang F, Zhao Y, et al: **Acute toxicological impact of nano- and submicro-scaled zinc oxide powder on healthy adult mice.** *Journal of Nanoparticle Research* 2008, **10**:263-276.
91. Shrivastava R, Raza S, Yadav A, Kushwaha P, Flora SJS: **Effects of sub-acute exposure to TiO<sub>2</sub>, ZnO and Al<sub>2</sub>O<sub>3</sub> nanoparticles on oxidative stress and histological changes in mouse liver and brain.** *Drug Chem Toxicol* 2014, **37**:336-347.
92. Sharma V, Singh P, Pandey AK, Dhawan A: **Induction of oxidative stress, DNA damage and apoptosis in mouse liver after sub-acute oral exposure to zinc oxide nanoparticles.** *Mutation Research/Genetic Toxicology and Environmental Mutagenesis* 2012, **745**:84-91.
93. Esmaeillou M, Moharamnejad M, Hsankhani R, Tehrani AA, Maadi H: **Toxicity of ZnO nanoparticles in healthy adult mice.** *Environ Toxicol Pharmacol* 2013, **35**:67-71.
94. Jo E, Seo G, Kwon J-T, Lee M, Lee Bc, Eom I, Kim P, Choi K: **Exposure to zinc oxide nanoparticles affects reproductive development and biodistribution in offspring rats.** *The Journal of Toxicological Sciences* 2013, **38**:525-530.
95. Pasupuleti S, Alapati S, Ganapathy S, Anumolu G, Pully NR, Prakhya BM: **Toxicity of zinc oxide nanoparticles through oral route.** *Toxicology and Industrial Health* 2012, **28**:675-686.
96. Baek M, Chung HE, Yu J, Lee JA, Kim TH, Oh JM, Lee WJ, Paek SM, Lee JK, Jeong J, et al: **Pharmacokinetics, tissue distribution, and excretion of zinc oxide nanoparticles.** *International Journal of Nanomedicine* 2012, **7**:3081-3097.

97. Cho WS, Kang BC, Lee JK, Jeong J, Che JH, Seok SH: **Comparative absorption, distribution, and excretion of titanium dioxide and zinc oxide nanoparticles after repeated oral administration.** *Particle and Fibre Toxicology* 2013, **10**.
98. Chuang H-C, Juan H-T, Chang C-N, Yan Y-H, Yuan T-H, Wang J-S, Chen H-C, Hwang Y-H, Lee C-H, Cheng T-J: **Cardiopulmonary toxicity of pulmonary exposure to occupationally relevant zinc oxide nanoparticles.** *Nanotoxicology* 2014, **8**:593-604.
99. Prasad A: **Zinc and immunity.** *Mol Cell Biochem* 1998, **188**:63-69.
100. Fraker PJ, King LE, Laakko T, Vollmer TL: **The Dynamic Link between the Integrity of the Immune System and Zinc Status.** *The Journal of Nutrition* 2000, **130**:1399S-1406S.
101. Cho WS, Duffin R, Poland CA, Howie SEM, MacNee W, Bradley M, Megson IL, Donaldson K: **Metal Oxide Nanoparticles Induce Unique Inflammatory Footprints in the Lung: Important Implications for Nanoparticle Testing.** *Environ Health Perspect* 2010, **118**:1699-1706.
102. Juang Y-M, Lai B-H, Chien H-J, Ho M, Cheng T-J, Lai C-C: **Changes in protein expression in rat bronchoalveolar lavage fluid after exposure to zinc oxide nanoparticles: an iTRAQ proteomic approach.** *Rapid Commun Mass Spectrom* 2014, **28**:974-980.
103. Kao Y-Y, Cheng T-J, Yang D-M, Wang C-T, Chiung Y-M, Liu P-S: **Demonstration of an Olfactory Bulb-Brain Translocation Pathway for ZnO Nanoparticles in Rodent Cells In Vitro and In Vivo.** *Journal of Molecular Neuroscience* 2012, **48**:464-471.
104. Fukui H, Horie M, Endoh S, Kato H, Fujita K, Nishio K, Komaba LK, Maru J, Miyauhi A, Nakamura A, et al: **Association of zinc ion release and oxidative stress induced by intratracheal instillation of ZnO nanoparticles to rat lung.** *Chem Biol Interact* 2012, **198**:29-37.
105. Cho WS, Duffin R, Howie SEM, Scotton CJ, Wallace WAH, MacNee W, Bradley M, Megson IL, Donaldson K: **Progressive severe lung injury by zinc oxide nanoparticles; the role of Zn<sup>2+</sup> dissolution inside lysosomes.** *Particle and Fibre Toxicology* 2011, **8**.
106. Cho W-S, Duffin R, Poland CA, Duschl A, Oostingh GJ, MacNee W, Bradley M, Megson IL, Donaldson K: **Differential pro-inflammatory**

- effects of metal oxide nanoparticles and their soluble ions in vitro and in vivo; zinc and copper nanoparticles, but not their ions, recruit eosinophils to the lungs.** *Nanotoxicology* 2012, **6**:22-35.
107. Xia T, Zhao Y, Sager T, George S, Pokhrel S, Li N, Schoenfeld D, Meng H, Lin S, Wang X, et al: **Decreased Dissolution of ZnO by Iron Doping Yields Nanoparticles with Reduced Toxicity in the Rodent Lung and Zebrafish Embryos.** *ACS Nano* 2011, **5**:1223-1235.
108. Xie Y, Wang Y, Zhang T, Ren G, Yang Z: **Effects of nanoparticle zinc oxide on spatial cognition and synaptic plasticity in mice with depressive-like behaviors.** *J Biomed Sci* 2012, **19**:14.
109. Kao Y-Y, Cheng T-J, Yang D-M, Wang C-T, Chiung Y-M, Liu P-S: **Demonstration of an Olfactory Bulb-Brain Translocation Pathway for ZnO Nanoparticles in Rodent Cells In Vitro and In Vivo.** *J Mol Neurosci* 2012, **48**:464-471.
110. Adamcakova-Dodd A, Stebounova L, Kim J, Vorrink S, Ault A, O'Shaughnessy P, Grassian V, Thorne P: **Toxicity assessment of zinc oxide nanoparticles using sub-acute and sub-chronic murine inhalation models.** *Particle and Fibre Toxicology* 2014, **11**:15.
111. Yan G, Huang Y, Bu Q, Lv L, Deng P, Zhou J, Wang Y, Yang Y, Liu Q, Cen X, Zhao Y: **Zinc oxide nanoparticles cause nephrotoxicity and kidney metabolism alterations in rats.** *Journal of Environmental Science and Health, Part A* 2012, **47**:577-588.
112. Kwon JY, Lee SY, Koedrith P, Lee JY, Kim K-M, Oh J-M, Yang SI, Kim M-K, Lee JK, Jeong J, et al: **Lack of genotoxic potential of ZnO nanoparticles in in vitro and in vivo tests.** *Mutation Research-Genetic Toxicology and Environmental Mutagenesis* 2014, **761**:1-9.
113. Cho W-S, Kang B-C, Lee JK, Jeong J, Che J-H, Seok SH: **Comparative absorption, distribution, and excretion of titanium dioxide and zinc oxide nanoparticles after repeated oral administration.** *Particle and Fibre Toxicology* 2013, **10**:9.
114. Baek M, Chung H-E, Yu J, Lee J-A, Kim T-H, Oh J-M, Lee W-J, Paek S-M, Lee JK, Jeong J, et al: **Pharmacokinetics, tissue distribution, and excretion of zinc oxide nanoparticles.** *Int J Nanomedicine* 2012, **7**:3081-3097.



---

## Chapter VI

### **Time dependent pro-inflammatory response of zinc oxide nanoparticles on human lung epithelial cells at sub-cytotoxic levels**

**Publication:**

**Saptarshi SR**, Feltis BN, Wright PF, Lopata AL. Investigating the immunomodulatory nature of zinc oxide nanoparticles at sub-cytotoxic levels in vitro and after intranasal instillation in vivo J Nanobiotechnol 2015, 13:6



## 6.1 Introduction

Engineered nanomaterials offer versatility and unique physicochemical properties that are utilised in a broad range of applications, ranging from household goods to medical devices. However, an unintentional side-effect of the small size of these materials is increased reactivity at the biological level [1]. It is therefore vital to further understand the fate, immunotoxic potential and clearance of nanoparticles (NPs) in biological systems in an attempt to address safety concerns associated with their use. ZnO NPs are widely used in cosmetics and personal care products, such as sunscreens and ointments, because of their excellent UV absorption properties and aesthetic appeal [2].

Inadvertent exposure to NPs can occur via inhalation. This is of particular significance in the occupational setting, where nanomaterials are manufactured or added to products [3]. Inhaled NPs, first encountered by lung epithelial cells can cause cellular damage, subsequent injury and inflammation [4, 5]. In general, ZnO NPs are often reported to elicit a high level of *in vitro* cytotoxicity when compared to other commonly-used metal oxide NPs [6, 7]. Furthermore, genotoxic effects have also been reported in human liver (Hep G2) and epidermal (A431) carcinoma cell lines exposed *in vitro* to ZnO NPs [8, 9]. Likewise, several *in vivo* rat studies have also shown lung toxicity following ZnO NP exposure [7, 10, 11]. Immunotoxicity of NPs can be attributed to their material properties, such as size or dissolution characteristics [12]. In the case of ZnO NPs, size-dependent cytotoxicity has been previously shown upon exposure of monocytes and macrophages, lung epithelial cells, and colorectal epithelial adenocarcinoma (CaCo-2) cells [13-16]. Similarly, extracellular dissolution of ZnO NPs and release of Zn<sup>2+</sup> ions have been reported to induce cell death in human T-cell leukaemia (Jurkat) cells [17], mouse macrophage (Ana-1) cells [18] or apically-exposed rat alveolar epithelial cell monolayers [19]. Other studies have specifically demonstrated that ZnO cytotoxicity is not dependent on extracellular NP dissolution [20], but requires direct particle-cell contact and uptake, resulting in the release of high intracellular concentrations of Zn<sup>2+</sup> ions from ZnO dissolution in the acidic environment within lysosomes and late endosomes [21, 22]

Zinc is an essential trace element and plays an important role in regulating cellular metabolism. However, inhalation of ZnO fumes has been well documented to cause the transient pulmonary inflammatory condition known as metal fume fever [11, 23, 24]. It is therefore possible that increased exposure to ZnO NPs may cause immunomodulation by either stimulating or suppressing specific immune functions. ZnO NPs were shown to induce a pro-inflammatory response in human aortic endothelial cells by increasing the gene expression of pro-inflammatory cytokines in a dose-dependent manner, including interleukin 8 IL-8 and monocyte chemoattractant protein 1 (MCP-1), as well as the intercellular adhesion molecule 1 (ICAM-1) membrane protein also an important marker of endothelial inflammation [25]. Hanley and co-workers observed the release of cytokines interferon gamma (IFN $\gamma$ ), TNF $\alpha$  and IL-12 when human peripheral blood monocytes were exposed to ZnO NPs [26]. On the contrary, their interaction with THP-1 cells was shown to be unsuccessful in stimulating HLA-DA and CD14 expression, which are known to activate these cells via the type I pathway [16]. This highlights the ambiguity in the available information concerning the inflammatory responses resulting from ZnO NP *in vitro* exposure of different cell types.

Formation of reactive oxygen species (ROS) is yet another important consequence of ZnO NP interaction with cells. It has been hypothesised that following cellular uptake, the dissolution of ZnO NPs leads to elevated intracellular Zn<sup>2+</sup> ions that displace redox-active transition metal ions bound to metallothioneins and other oxidative stress defence proteins, which in turn cause an imbalance in the redox state of the cell [21]. Some studies have discussed the relationship between ROS formation and cytotoxicity in depth [18, 27, 28]. ZnO NPs were reported to adversely affect mitochondrial membrane potential to cause overproduction of ROS, leading to apoptosis in rat retinal ganglion cells [29]. Zinc ion dissolution from fluorescently-labelled ZnO NPs was shown to induce toxicity in the mouse leukaemia (RAW 264.7) and human bronchial epithelial (BEAS-2B) cell lines via production of oxidative stress [30]. In contrast, Song and co-workers reported that in the case of ZnO NP-exposed mouse macrophages (Ana-1 cells), the intracellular ROS induction was not the major factor causing cytotoxicity [18].

In general, physicochemical attributes of ZnO NPs appear to be influential in determining their immunomodulatory potential. However, there is a need to link all of these factors together to understand the kinetics of ZnO NP interactions with cellular systems. In this chapter the immunomodulatory potential of industrially manufactured ZnO NPs, of three different particle sizes (30, 80 and 200 nm).has been addressed. Furthermore, human lung epithelial (A549) cells have been used for the *in vitro* exposure system as they are representative of the alveolar type II cells in lungs, which are among the first live cells encountered by inhaled particulate matter. The overall aim of the current chapter was to systematically investigate the time-course responses of human alveolar epithelial cells exposed to sub-cytotoxic levels of ZnO NPs, over 24 hr. The data generated can help further understand the kinetics involved, and elucidate the mechanisms underlying the observed immune modulatory and cytotoxic effects of ZnO NPs.

## **6.2 Materials and Methods**

### **6.2.1 Nanoparticles**

Industrially manufactured ZnO NPs and particulates of three different particle sizes (30, 80 and 200 nm) with and without surfactant dispersant were used as test NPs in this chapter. Methods for preparation of NP working solutions and information on their size, agglomeration status in cell culture medium and their dissolution properties have been described in chapter III.

### **6.2.2 *In vitro* nanoparticle exposure**

Human alveolar lung epithelial A549 cells were used as the *in vitro* test system in this chapter. Detailed information about culturing and maintenance of these cells has been described in chapter IV.

For the study of cytotoxic effects, 10,000 cells in 100  $\mu$ L were seeded into wells of 96-well tissue culture plates (Sarstedt, Germany). After allowing for overnight attachment, the cells were exposed to a range of ZnO NP concentrations (0.2-200  $\mu$ g/mL) for 24 hr. For the study of mRNA up-regulation, release of cytokines and the immunoblotting experiments,  $10^6$  cells per well were seeded in 6-well

tissue culture plates and allowed to attach overnight. Subsequently cells were exposed to the ZnO NP dose, 20 µg/mL, for 1, 2, 4, 6 or 24 hr.

Additionally, to confirm intracellular effects of ZnO NPs for inducing immunomodulatory effects, A549 cells were stimulated with the 20 µg/mL dose for 1 hr after which the NP-containing media was discarded and replaced with fresh medium and further incubated for 4 hr. q-PCR analysis and ELISA measurements were then carried out as described in sections (6.2.6 and 6.2.7).

### 6.2.3 Cytotoxicity assays

Following the *in vitro* exposure procedure described above, the viability of A549 cells was assessed via two methods: MTS assay (Promega MTS Cell Titer 96<sup>®</sup> aqueous kit, Promega, USA), and lactate dehydrogenase (LDH) release from leaky cell membranes into the surrounding medium, assessed using the CytoTox 96<sup>®</sup> Non-Radioactive Cytotoxicity Assay (Promega, USA). The soluble formazan dye generated at the end of the two assays absorbs light strongly at 490 nm. The amount of light absorbed is directly proportional to the number of viable cells in the well .

At the end of the 4 or 24 hr exposure periods, MTS assay was conducted as per method detailed in chapter IV section (4.2.7.3).

For LDH assay, 50 µL supernatant obtained at the end of the NP exposure period, was mixed with an equal amount of LDH substrate mix. Following incubation at room temperature for 30 min, the absorbance was recorded at 490 nm (VersaMax, Molecular Devices, USA). Supernatant from wells exposed to 5 µL of lysis solution were used as the 100% LDH release positive control. Wells containing cells exposed to medium-only provided the spontaneous LDH release control values. Background absorbance from wells containing medium and substrate mix but no cells, was subtracted from all LDH absorbance readings. Data were obtained from five independent experiments, each performed in triplicate.

#### **6.2.4 Visualisation of intracellular zinc levels of A549 cells exposed to ZnO NPs**

Intracellular levels of zinc ions, after treatment with 20 µg/mL ZnO NPs for 1 hr were visualised using a lipophilic, zinc-sensitive fluorophore, zinquin ethyl ester (Sigma- Aldrich, USA). Briefly, A549 cells were allowed to attach overnight in cover glass bottom culture dishes (Proscitech, Australia) at a density of  $10^5$  cells/mL following which they were incubated with ZnO NPs (20 µg/mL) for 1hr. At the end of the exposure period, cells were gently washed with Dulbecco's Ca<sup>2+</sup> and Mg<sup>2+</sup> free phosphate-buffered saline (DPBS) (Invitrogen, USA) to remove traces of ZnO NPs following which the cells were incubated with 25 µM zinquin ethyl ester. The cells were further incubated for 30 min in a humidified incubator (at 37°C and 5% CO<sub>2</sub>). After subsequent washings with DPBS, plasma membrane staining was carried out using the CellMask™ Deep red stain (Molecular Probes, Life Technologies, USA) as per manufacturer's instructions. Finally the stained cells were fixed using 4% paraformaldehyde fixing solution in DPBS for 15 min. Cells were then washed with DPBS to remove traces of the fixative and placed on a coverslip; excess liquid removed and mounted using ProLong® Gold Antifade Reagent (Molecular Probes, Life Technologies, USA). The slides were subsequently incubated at room temperature for 24 hr in the dark before visualization using a Zeiss LSM 710 confocal laser scanning microscope (Carl Zeiss, Germany).

#### **6.2.5 4', 6-Diamidino-2-phenylindole (DAPI) staining and confocal microscopy**

DAPI staining was carried out to study the changes in nuclear morphology of A549 cells after treatment with a cytotoxic dose of ZnO NPs, as per the method described in chapter IV. In addition, Camptothecin (Sigma- Aldrich, USA) 5 µM was used as a positive control to induce apoptosis in control A549 cells. The 200 nm particulates were also dosed at the same concentration of 100 µg/mL, although this was still sub-cytotoxic for these larger particles.

### 6.2.6 RNA isolation and quantitative-PCR (q-PCR)

Total RNA isolation from treated A549 cells was carried out using the ISOLATE RNA Mini Kit (Bioline, USA) as per manufacturer's instructions. Concentrations of extracted RNA samples were determined using a Nanodrop 8000 spectrophotometer (Thermo Scientific, Germany) and reverse transcribed into cDNA using the Tetro cDNA Synthesis kit (Bioline, USA). Changes in expression levels of the pro-inflammatory cytokine IL-8 and the oxidative stress response enzyme heme oxygenase-1 (HO-1) were determined using q-PCR. The reaction mixture was setup using the SsoAdvanced™ SYBR® Green Supermix (BioRad, USA) containing specific primers. Primers used were: HO-1 primers, sense 5'-CGCCTTCCTGCTCAACATT-3' and antisense 5'-TGTGTTC-CTCTGTCAGCATCAC-3'. IL-8: sense 5'-GGCACAAACTTTCAGAGACAG-3' and antisense 5'-ACACAGAGCTGCAGAAATCAGG-3'. The housekeeping gene used was ubiquitin, sense 5'-GCAAGCTACAATAATGGGGC-3' and antisense 5'-TGTAATGCAACCTTAGGTGGT-3'. q-PCR was performed using the Piko Real real-time PCR System (Thermo Scientific, Germany). Thermal cycle parameters used were 7 min at 95°C, followed by 45 cycles (95°C, 15 sec; 55°C, 15 sec; 72°C, 30 sec). Data were analysed using relative quantitation.

### 6.2.7 IL-8 ELISA

The ability of ZnO NPs to induce release of the pro-inflammatory cytokine IL-8 was assessed using enzyme-linked immunosorbent assay (ELISA). Cell supernatants were collected after treating A549 cells for up to 24 hr with 20 µg/mL of ZnO NPs and were used to quantify IL-8 protein levels using the BD OptEIA human IL-8 ELISA kit (BD Systems, USA) as per manufacturer's instructions. Three independent experiments were performed, each with triplicate samples.

### 6.2.8 Effect of sulfhydryl antioxidant

The role of oxidative stress in eliciting the pro-inflammatory response was assessed by pre-treatment of A549 cells with 5 mM of the sulfhydryl antioxidant N-acetylcysteine (NAC) (Sigma-Aldrich, USA) for 1 hr before exposure to ZnO

NPs. The NAC dose was confirmed to be non-cytotoxic to A549 cells using the MTS assay.

### **6.2.9 Cell signalling: Immunoblotting for NFκB, p-38 MAPK pathway activation**

At the end of the *in vitro* NP exposures for 1, 4, 6 or 24 hr, A549 cells were washed with DPBS and lysed using NP40 cell lysis buffer (Life Technologies, USA) supplemented with 1 mM phenylmethylsulfonyl fluoride (PMSF) and protease inhibitor cocktail (Sigma-Aldrich, USA). The cell lysates obtained were subjected to SDS-PAGE followed by transfer onto a nitrocellulose membrane using the semi-dry transfer system (BioRad, USA). After blocking with 1% Superblock (Sigma-Aldrich, USA) blocking solution for 1 hr, the membranes were probed overnight with specific primary antibodies: Phospho p38 (Thr180/Tyr182), p38 MAPK antibody, along with phospho-NFκB p65 Ser536 or NFκB p65 antibodies (Cell Signalling, USA), followed by washing with tris buffered saline and 0.05% Tween-20 (TBS-T) (Sigma-Aldrich, USA). Proteins were detected using horseradish peroxidase-tagged secondary antibodies (Cell Signalling, USA) and enhanced chemiluminescence substrate (Pierce, USA), followed by exposure to photographic film (GE Healthcare, Australia).

### **6.2.10 Statistics**

Data are presented as mean  $\pm$  standard error of mean (SEM) and was analysed using two way ANOVA for cytotoxicity assays or one-way ANOVA for all other analyses, followed by Bonferroni post-hoc test (Prism 6.0, GraphPad Software, USA), with a p value  $<0.05$  considered as significant.

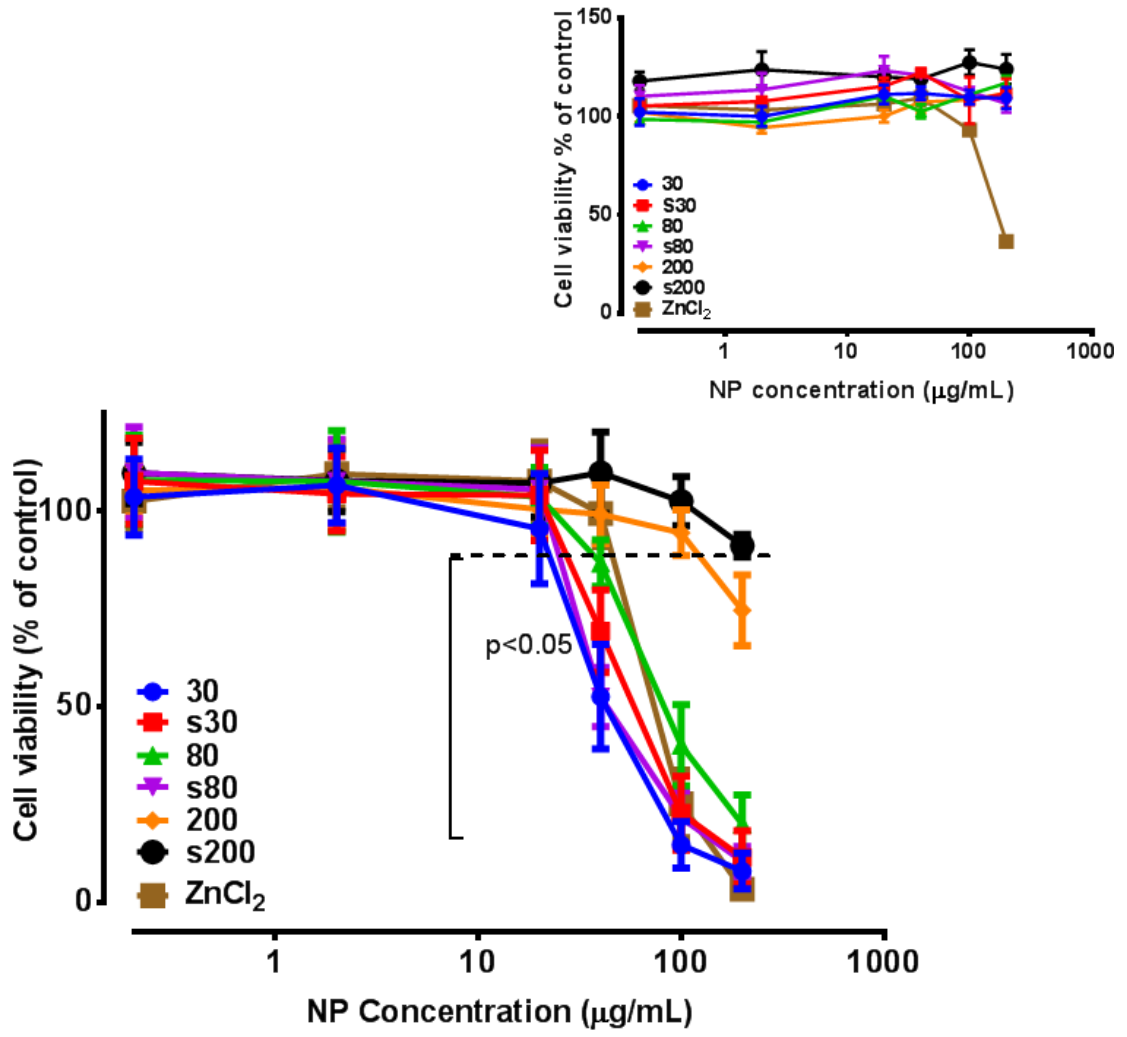
## 6.3 Results

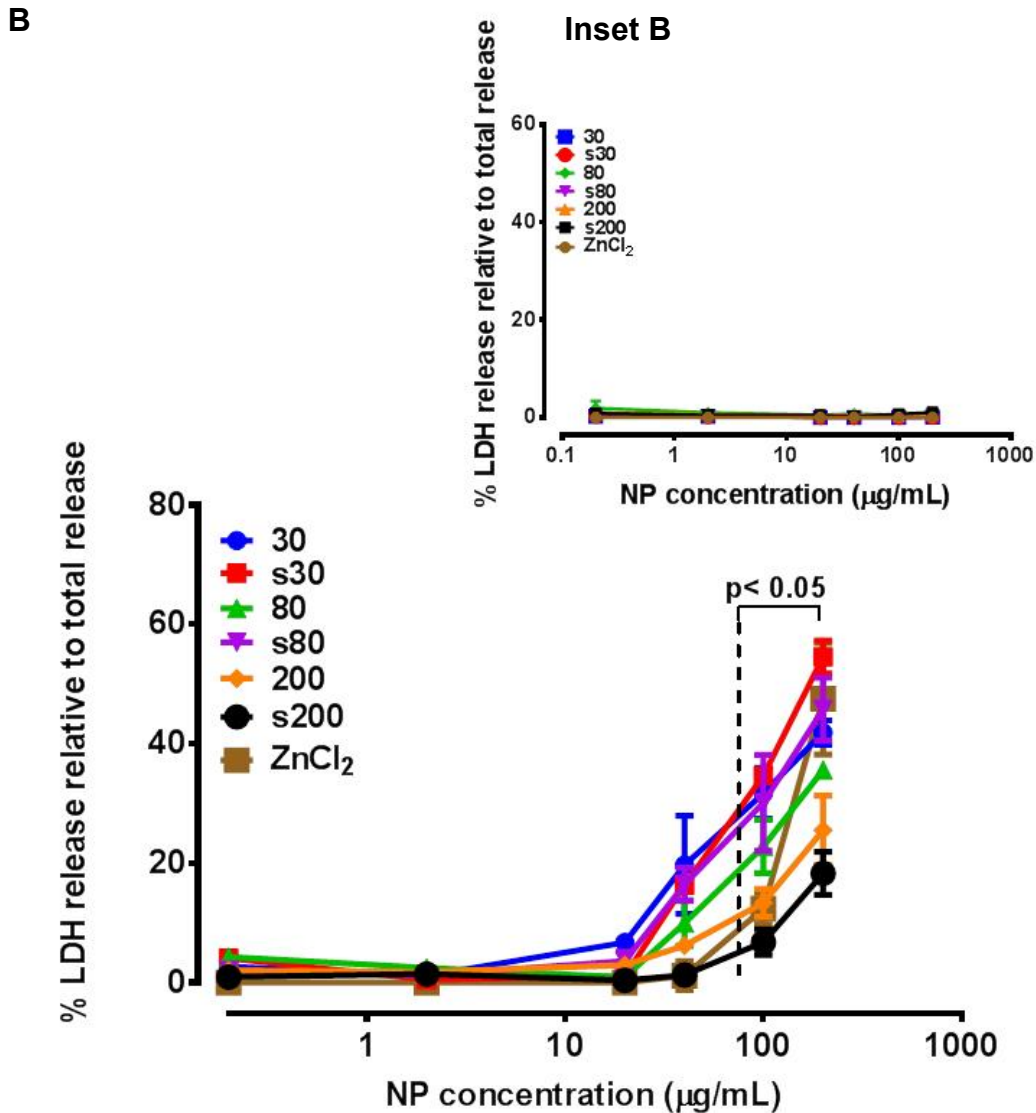
### 6.3.1 Cytotoxicity profile

Cytotoxicity observed for all ZnO NPs was concentration dependent and similar to ZnCl<sub>2</sub>. ZnO NP treatment did not affect cell viability or cell membrane integrity 4 hr after exposure although, ZnCl<sub>2</sub> did show reduction in cell viability at the highest tested concentration (Figure 6.1 inset A & B). After the 24 hr exposure, surfactant-dispersed 80 nm ZnO NPs demonstrated greater cytotoxicity than their pristine counterparts when comparing the effective concentrations that produced 50% cell death (EC<sub>50</sub>) (Figure 6.1A). Whereas, the cytotoxicity observed for the pristine particulates was marginally greater ( $p < 0.05$ ) than the surfactant-dispersed 200 nm ZnO at the highest tested concentration. Overall, the surfactant-dispersed 200 nm ZnO particulates were found to be the least cytotoxic material, achieving less than an EC<sub>25</sub> response at the highest dose of 200 µg/mL. This surfactant by itself has previously been shown to be non-cytotoxic over this same dose-range [14]. The LDH enzyme normally present in the cell cytoplasm is rapidly released into the surrounding medium upon damage to the cell membrane. LDH release was measured after the 24 hr exposure and was concentration dependent (Figure 6.1B), but less sensitive than MTS, as all NPs up to the highest dose of 200 µg/mL showed a higher degree of similarity in LDH release. LDH values were significantly different to untreated control cells at 100 µg/mL, compared to the MTS assay achieving statistical significance at 30 µg/mL

A

Inset A

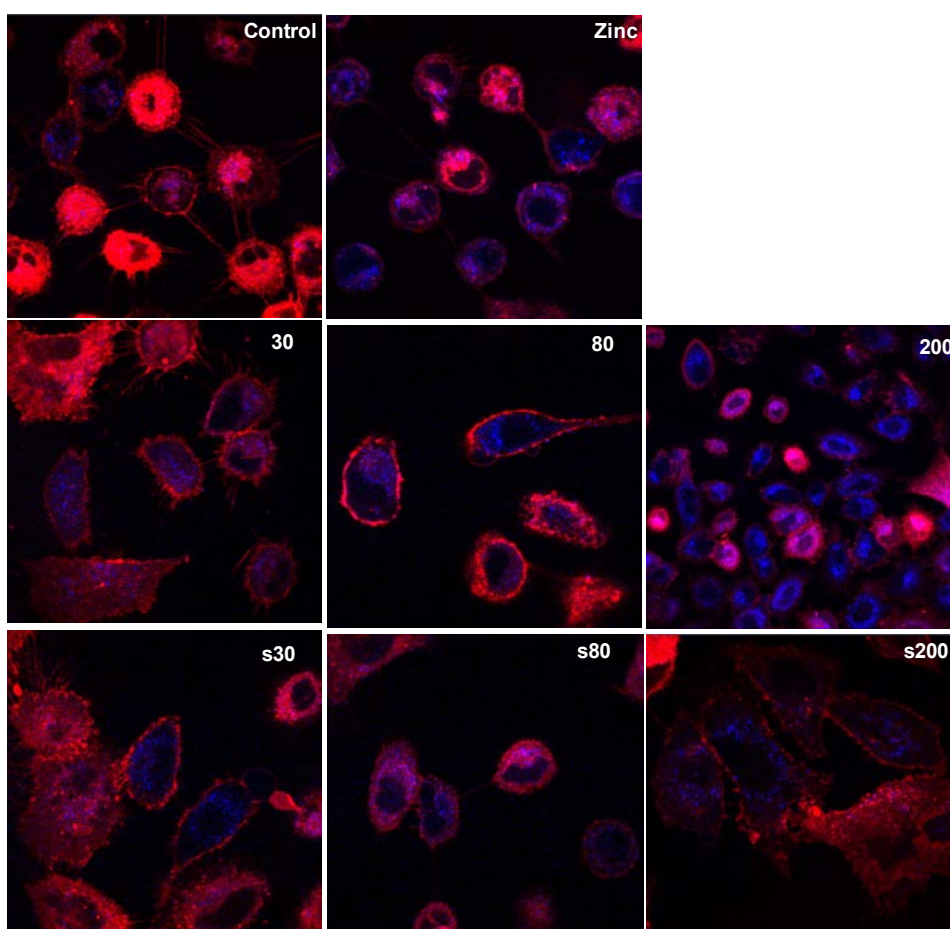




**Figure 6.1** Cytotoxicity profiles of pristine and surfactant-dispersed ZnO NPs after 24 hr exposure of human lung epithelial A549 cells, using the (A) MTS assay and (B) lactate dehydrogenase release assays. Cytotoxicity was dependent on NP size and dispersal state. Concentrations at or below the dotted line (MTS assay) and beyond the dotted line (LDH release assay) were significantly different from untreated control cells. Inset figures describe MTS cell viability and LDH release after 4 hr ZnO NP exposure. Values are expressed as mean  $\pm$  SEM ( $n = 5$  separate experiments).

### 6.3.2 Visualisation of intracellular zinc levels of A549 cells exposed to ZnO NPs

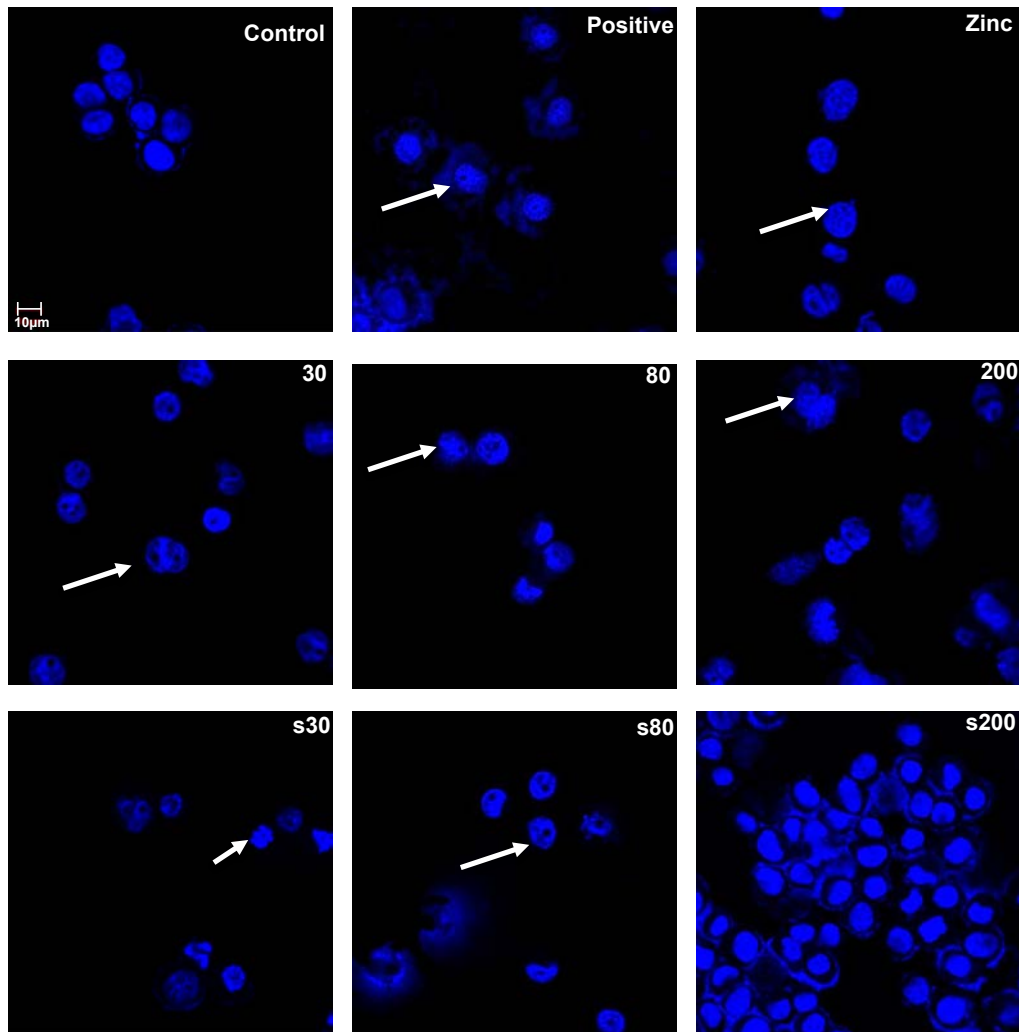
A549 cells treated with  $\text{ZnCl}_2$  or ZnO NPs showed characteristic blue fluorescence indicative of increase in zinc in the cytoplasmic compartments of the cells. This was demonstrated by intracellular staining of labile zinc using zinquin dye (Figure 6.2). The nuclear region of the cell did not display blue fluorescence. Deep red fluorescence corresponds to staining of the cellular plasma membrane with the lipophilic Cell Mask dye.



**Figure 6.2 Visualizing labile zinc using zinquin a zinc specific dye in A549 cells exposed to sub-cytotoxic concentration of ZnO NPs or  $\text{ZnCl}_2$  for 1 hr. blue fluorescence corresponds to zinc bound zinquin diethyl ester and red fluorescence corresponds to plasma membrane staining**

### 6.3.3 DAPI staining

Exposure to the 100  $\mu\text{g}/\text{mL}$  dose of ZnO NPs or  $\text{ZnCl}_2$  caused severe cytotoxicity in A549 cells after 24 hr (Figure 6.3). DAPI staining of the nuclei demonstrated characteristic condensation of the nuclear material and formation of apoptotic bodies in ZnO NP or  $\text{ZnCl}_2$  treated A549 cells (indicated by white arrows).

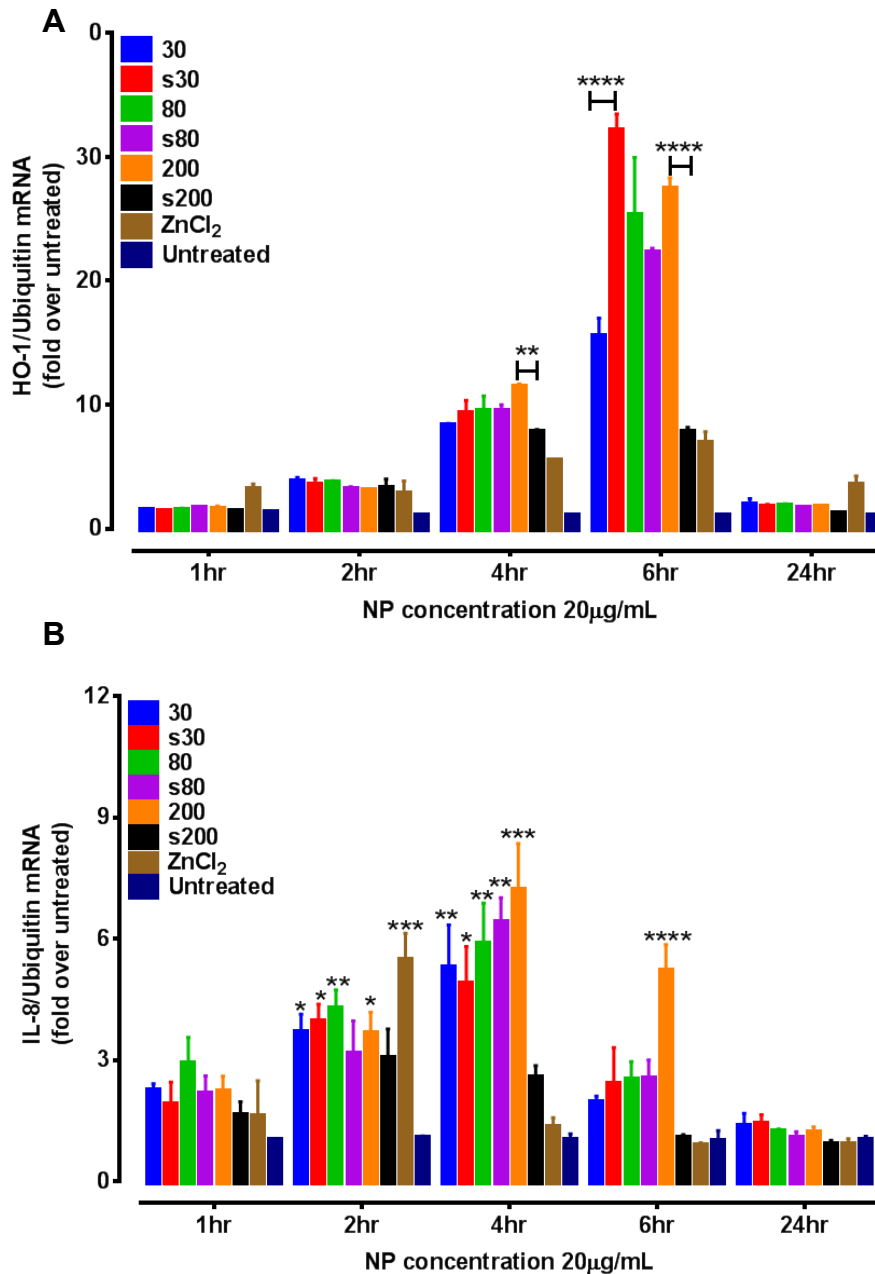


**Figure 6.3** Confocal images of A549 cells treated with 100  $\mu\text{g}/\text{mL}$  (cytotoxic dose) ZnO NPs for 24 hr, followed by staining with DAPI nuclear stain to visualise changes in nuclear morphology characteristic of apoptotic cell death. Camptothecin 5  $\mu\text{M}$  was used as a positive control to induce apoptosis in control cells. White arrows indicate condensed nuclear material in exposed cells when compared to untreated cells. Scale bar applies to all figures

#### **6.3.4 Up-regulation of pro-inflammatory IL-8 and stress-responsive HO-1 genes**

Systematic investigation of HO-1 up-regulation as a function of time revealed that the activation started at 4 hr after exposure, peaked at 6 hr and had subsided by 24 hr, when compared to basal levels of HO-1 gene activation in untreated cells (Figure 6.4A). At 4 hr, HO-1 gene up-regulation was similar for all zinc exposures and ranged from 6 to 12-fold. Overall, the highest up-regulation at the 6hr time point was induced by s30 ZnO NPs, showing a 30-fold increase compared to untreated cells. In decreasing order, HO-1 gene up-regulation at 6hr was caused by: s30 > 80 ~ s80 ~ 200 > 30 > s200 ~ ZnCl<sub>2</sub>.

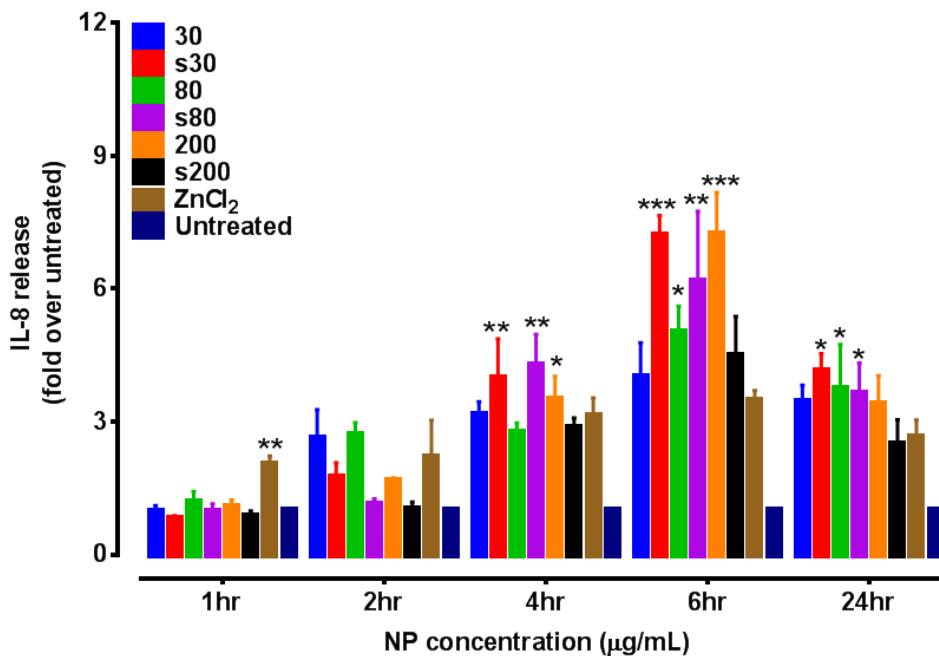
In the case of IL-8 gene expression, maximum stimulation occurred at 4 hr exposure when compared to the untreated control cells. IL-8 induction from all particulates, except surfactant-treated 200 nm ZnO, ranged from 5 to 7-fold that of the untreated control (Figure 6.4B). However, after 24 hr exposure IL-8 gene expression had returned to basal levels. Interestingly, ZnCl<sub>2</sub> treated cells, after 2 hr exposure, showed IL-8 gene up-regulation that was significantly higher ( $p < 0.05$ ) than all treatments except s80 and s200 ZnO NPs. At all other time points ZnCl<sub>2</sub> induced IL-8 gene mRNA levels were similar to those of untreated control cells. Pristine ZnO 200 nm particles were the most potent at both 4 and 6 hr. Surfactant-dispersed 200 nm particulates did not cause significant IL-8 gene up-regulation.



**Figure 6.4 (A)** ZnO NP induced up-regulation of HO-1 mRNA indicative of a strong antioxidant response in A549 cells. Highest HO-1 expression was seen at 6 hr which was a 30-fold increase in gene expression compared to untreated cells at 6 hr ( $p < 0.001$ ). Block bars compare the statistical significance between pristine or surfactant-dispersed solutions for each ZnO NP size. **(B)** mRNA over expression of the pro-inflammatory cytokine IL-8 in A549 cells stimulated with 20  $\mu\text{g/mL}$  of ZnO NPs at 1, 2, 4, 6 or 24 hr. Maximum expression of IL-8 gene was recorded at 4 hr. Statistical significance is shown in **(B)** compared to untreated cells at each time point. \* $p < 0.05$ , \*\* $p < 0.01$ , \*\*\* $p < 0.001$ , \*\*\*\* $p < 0.0001$ . Data are expressed as mean  $\pm$  SEM of the fold levels compared to untreated controls at each time point ( $n = 3$ ) separate experiments, each performed with triplicates.

### 6.3.5 IL-8 release upon ZnO NP exposure

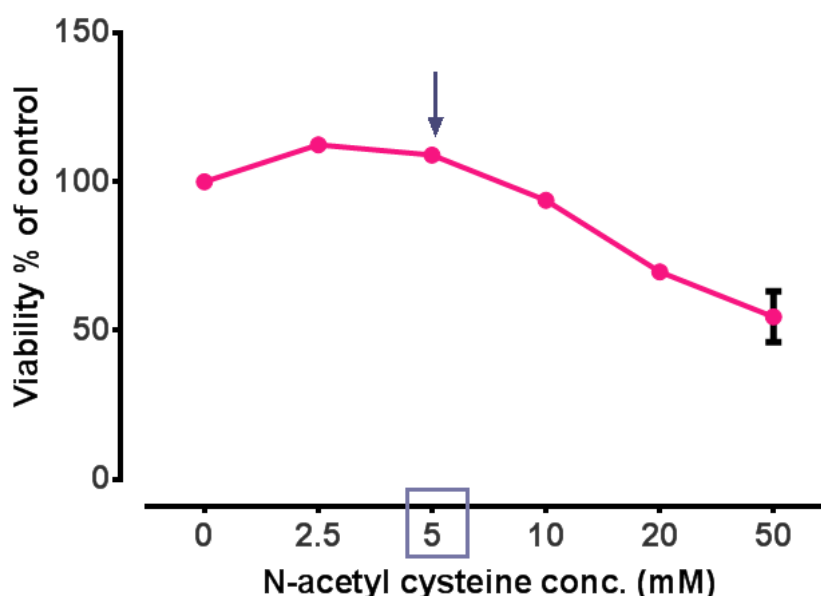
An ELISA-based assay was used to measure the time dependent release of IL-8 into the cell culture supernatants of ZnO-exposed A549 cells. A gradual increase in IL-8 levels in the culture medium was already apparent after 4 hr of ZnO NP exposure time for all NPs except pristine ZnO 80 and surfactant-dispersed 200. Largest IL-8 release was seen at the 6 hr sampling point where all particulates showed at least 4 fold increase in IL-8 release as compared to the untreated control cells. IL-8 levels at 24 hr sampling point were lower than the ones measured at 6 hr (Figure 4B). IL-8 levels were not significantly altered at the earlier time points of 1 and 2 hr.



**Figure 6.5** Release of pro-inflammatory cytokine IL-8 by ZnO NP-exposed A549 cells at 1, 2, 4, 6 or 24 hr. Statistical significance is shown is compared to untreated cells at each time point. \* $p < 0.05$ , \*\* $p < 0.01$ , \*\*\* $p < 0.001$ , \*\*\*\* $p < 0.0001$ . Data are expressed as mean  $\pm$  SEM of the fold levels compared to untreated controls at each time point ( $n = 3$ ) separate experiments, each performed with triplicates.

### 6.3.6 Effect of sulfhydryl antioxidant

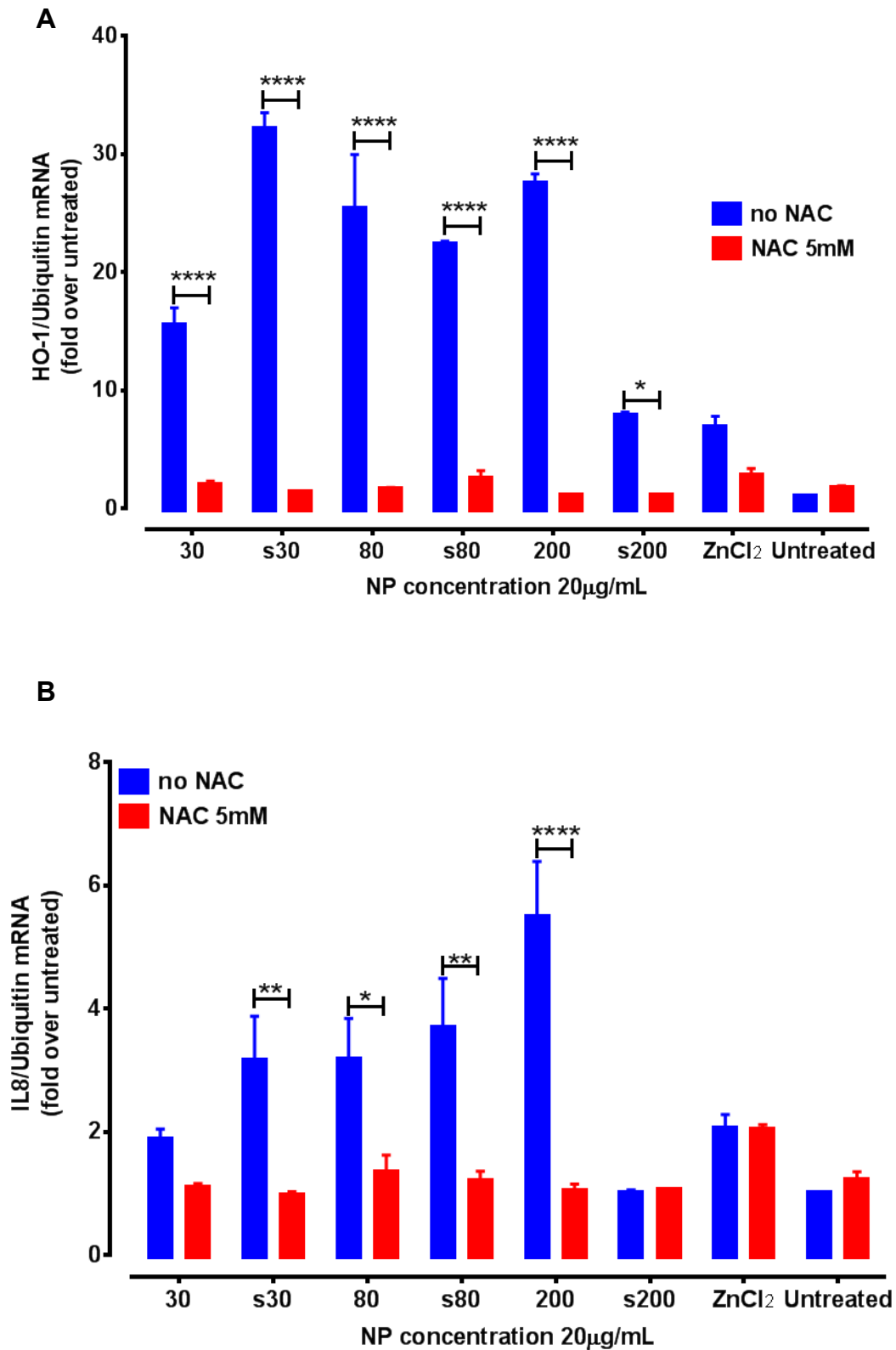
The concentration of NAC used for this experiment did not induce cytotoxicity over the total 7hr exposure period ( $108 \pm 1.5\%$  of control) (Figure 6.6). Pre-treatment with NAC dramatically reduced the ZnO-induced up-regulation of mRNA expression levels for both HO-1 and IL-8 genes (Figure 6.7A & 6.7B). This was not observed in the case of s200 ZnO or ZnCl<sub>2</sub>-treated cells for IL-8 gene expression, as both of these treatments no longer up-regulated IL-8 mRNA levels at 6 hr (Figure 6.4A & 6.4B). Levels of IL-8 release by NAC pre-treated A549 cells following exposure to ZnO and ZnCl<sub>2</sub> were also found to be lower than exposed cells without NAC pre-treatment (Figure 6.5).



**Figure 6.6: Viability of A549 cells exposed to increasing concentrations of antioxidant NAC for 24 hr. 5 mM dose of NAC was finalised for treatment of A549 cells in order to contain reactive oxygen species formed due to ZnO NP exposure. Data are expressed as mean  $\pm$  SEM where  $n = 3$**

Overall, the highest mRNA expression for the ROS-responsive HO-1 gene and the pro-inflammatory IL-8 gene was seen at the 6 hr and 4 hr exposure periods, respectively. To confirm the role of ROS in the observed immunomodulatory responses, A549 cells were pre-treated for 1hr with 5 mM of the sulfhydryl antioxidant NAC followed by exposure to ZnO NPs for 6 hr (at a

time when IL-8 gene expression was also still marginally up-regulated and IL-8 release was progressively increasing).



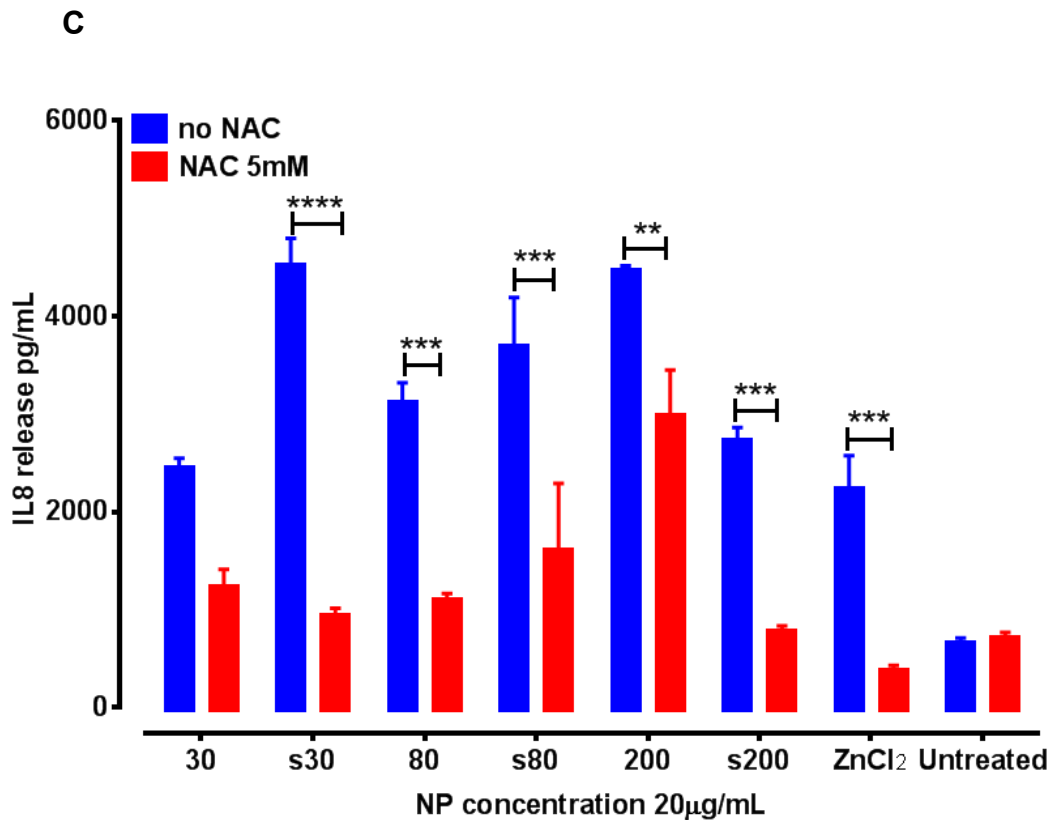


Figure 6.7: Mitigation of the up-regulation of (A) HO-1 mRNA expression and (B) IL-8 mRNA expression (C) IL-8 cytokine release in antioxidant treated A549 cells after exposure to ZnO NPs (20 µg/mL) for 6 hr. Statistical significance after comparing no NAC or 5mM NAC cells where \* $p < 0.05$ , \*\* $p < 0.01$ , \*\*\* $p < 0.001$ , \*\*\*\* $p < 0.0001$ . Data are expressed as mean  $\pm$  SEM of the fold levels compared to untreated controls at each time point ( $n = 3$ ) separate experiments, each performed with triplicates).

### **6.3.7 Confirming role of intact ZnO NPs in eliciting pro-inflammation**

A549 cells pre-treated with ZnO NPs for 1 hr were further grown in fresh complete medium for 4 hr. At the end of the incubation period IL8 mRNA up regulation and release in cell supernatants was determined as per methods described above. Replacement of the ZnO NP containing cell culture medium with fresh medium 1 hr after exposure to ZnO NPs did not stimulate expression of IL-8 gene or release of this cytokine. This is because, 1 hr is insufficient time for significant cellular uptake of ZnO NPs, and the ZnO NPs demonstrated low solubility in cell culture medium, the effects on gene expression clearly requires cellular uptake and intracellular dissolution.

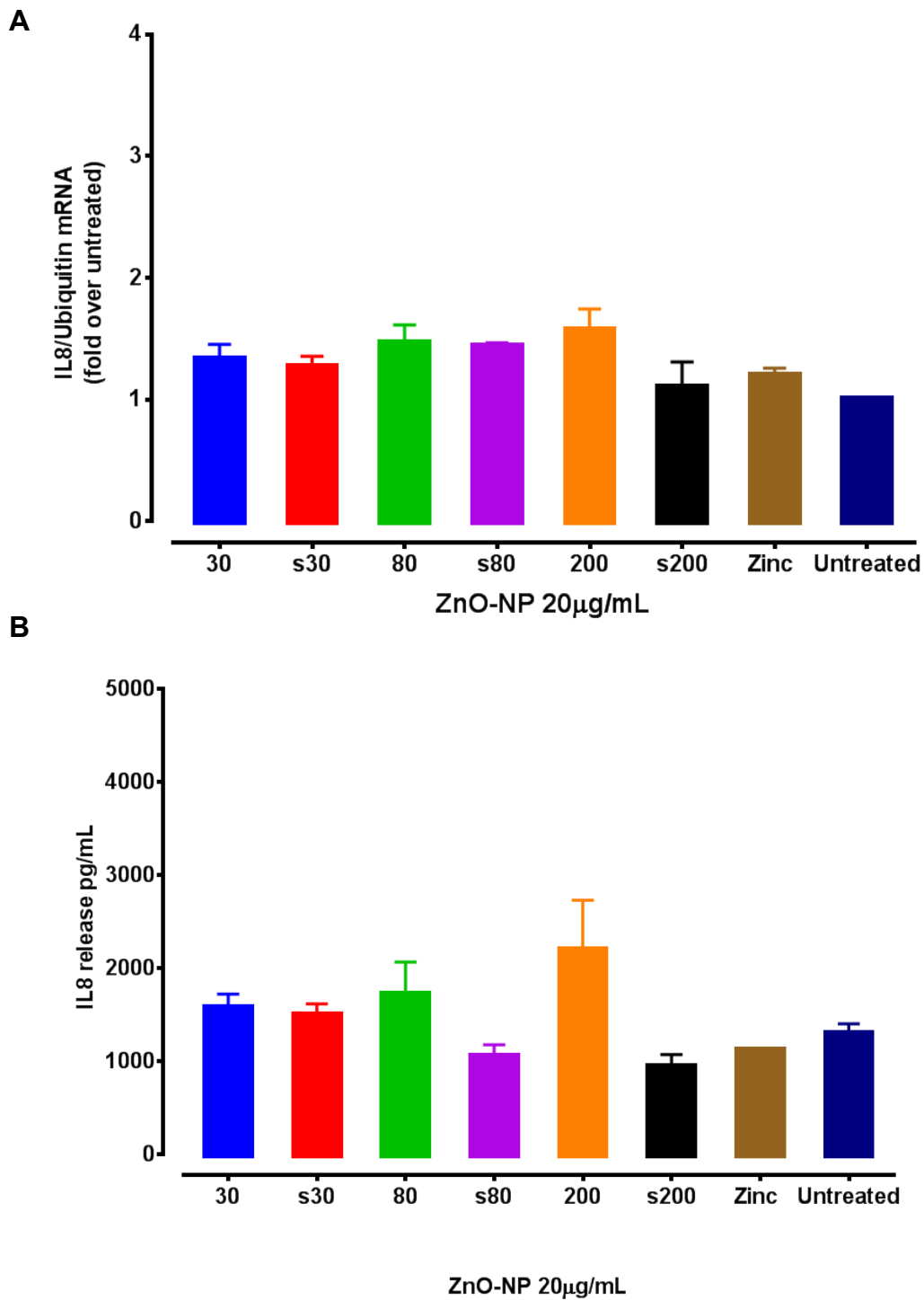
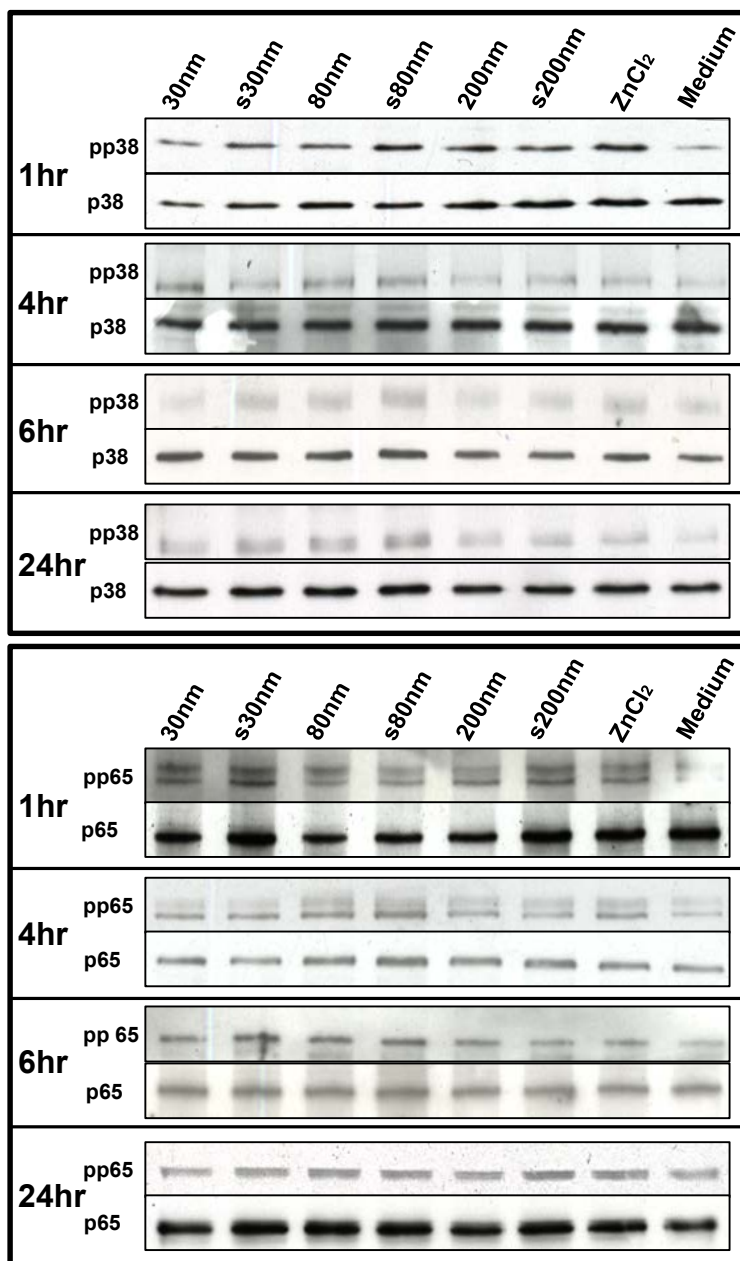


Figure 6.8: (A) IL-8 mRNA expression and (B) IL-8 release for A549 cells exposed to ZnO NPs for 1 hr, after which the NP-containing media was replaced by fresh culture media and cells incubated for a further 4 hr. Data are expressed as mean  $\pm$  SEM (n = 3 separate experiments).

### 6.3.8 Cell signalling

ZnO NPs were able to induce a rapid phosphorylation of the p38 protein, a representative of the MAPK signalling pathway cascade (Figure 6.9A). Exposure of A549 cells to 20 µg/mL of ZnO particulates or ZnCl<sub>2</sub> also induced phosphorylation of the p65 protein, which is pivotal to NFκB signalling (Figure 6.9B). Characteristic bands of phosphorylated p65 protein were observed after 1 hr exposure to ZnO NPs or ZnCl<sub>2</sub> and were significantly stronger than those observed at 6 or 24 hr. Cells exposed to medium-only served as a negative control.



**Figure 6.9:** Immunoblotting showing (A) phosphorylation of p38 protein (pp38), belonging to the redox-sensitive p38 Mitogen activated protein kinase (MAPK) pathway and (B) p65 protein (pp65), involved in NF $\kappa$ B activation, after exposing A549 cells to 20  $\mu$ g/mL dose of ZnO NPs

## 6.4 Discussion

Detailed knowledge of the ability of cells to deal with both cytotoxic and sub-cytotoxic doses of ZnO NPs can help in understanding mechanisms of cellular responses to a range of concentrations of these NPs to which workers may be exposed. The present study highlighted the effect of physical parameters, such as dispersal state and agglomerate size of ZnO NPs, along with duration of contact with cells, on the NP immunomodulatory and cytotoxic potential.

The cytotoxicity of ZnO NPs was quantified using two different assays, the MTS assay which measures the mitochondrial metabolism of metabolically-viable cells, and the LDH release assay which quantifies the release of this cytosolic enzyme from non-viable cells after cell lysis. ZnO NPs induced cytotoxicity in a concentration and time dependent manner. In general, smaller-sized NPs showed greater cytotoxicity as compared to the larger-sized ZnO particulates. These results are in agreement with cytotoxic responses of human monocytes and macrophages (THP-1 cells), to identical ZnO NPs as demonstrated in previous studies [14]. Surfactant-dispersed and undispersed 200 nm particulates used in this study displayed lower cytotoxicity at the highest tested concentrations. In the 80 nm size range, the surfactant-dispersed NPs were more cytotoxic than their undispersed counterparts. Interestingly, for 30 nm NPs, the MTS assay indicated that the pristine 30 nm particles were most cytotoxic, whereas the LDH assay indicated the surfactant-dispersed material was more cytotoxic. It should be noted that the surfactant may alter the membrane permeability of the cells to some extent which could be responsible for the observed inconsistencies in the cytotoxicity profiles of these two assays. Additionally, the LDH assay was also less sensitive than the MTS assay, as the maximum LDH release for the highest concentration of ZnO NPs used at 24 hr was found to be only 50% of LDH release from total cell lysis. Relating this to other measures of cell death, DAPI staining of A549 cells exposed to a cytotoxic dose of ZnO NPs for 24 hr revealed characteristic condensation of the nuclear material, as is typically observed during apoptosis, which has also been previously observed in THP-1 monocytes [14].

Effect of sub-cytotoxic doses of different sizes and dispersal states of ZnO NPs affected A549 cells over 1, 2, 4, 6 and 24 hr was analysed next. The premise being that, at low ZnO NP concentrations, the data should not be confounded by factors expressed during cell death and these should not contribute to the expression of biomarkers used to assess the pro-inflammatory potential of ZnO NPs in the present study.

ROS generation has been extensively implicated as an important driver of nanotoxicity [31]. However, whether cytotoxicity and ROS formation are interdependent or causally linked needs further investigation. A three tiered oxidative stress response has been previously described for NP-mediated toxicity [12, 30]. The lowest level of oxidative stress is characterised by the induction of antioxidant defence genes. This is followed by the second tier where a pro-inflammatory response is initiated. HO-1 and IL-8 genes are representatives of this oxidative stress/pro-inflammatory paradigm. The oxidative stress-responsive HO-1 is primarily involved in the conversion of heme to biliverdin and has been also reported to have anti-inflammatory properties [32]. In this study, a gradual increase in expression levels of HO-1 gene from 2 hr, reaching maximum activation at 6 hr and returning to basal levels at 24 hr was noted. These results are in accordance with studies showing similar results, with human endothelial cells exposed to SiO<sub>2</sub> NPs [33], and A549 cells exposed to Fe<sub>3</sub>O<sub>4</sub> magnetic NPs [34]. In the present study, surfactant-treated 30 nm ZnO NPs maximally induced HO-1 expression, compared to the other NPs studied. This may be because of the enhanced accessibility of these NPs to the cell surface due to their small size and improved dispersal, which may have resulted in greater uptake and subsequent intracellular release of zinc ions. The rapid uptake and release would likely create an imbalance in the cellular antioxidant capacity [35]. It is also worth reiterating that the surfactant may alter membrane permeability to NPs to some extent, which would also potentially increase uptake. The HO-1 and IL-8 results indicate a strong antioxidant response of exposed cells against the ROS generated due to their interaction with ZnO NPs.

Airway epithelial cells not only offer an important physiological barrier against inhaled matter, but are also responsible for releasing a number of crucial

---

cytokines and chemokines. The  $\alpha$  chemokine IL-8 is a potent chemo attractant for neutrophils and eosinophils, and a possible protagonist in the progression of airway inflammation [36]. Sub-cytotoxic doses (2–8  $\mu\text{g/mL}$ ) of ZnO NPs have previously been shown to increase IL-8 mRNA expression and IL-8 release in exposed BEAS-2B cells [3]. Pro-inflammatory effects resulting from exposure to a sub-cytotoxic dose of ZnO NPs have included the release of IL-8 by nasal mucosal cells into the culture medium [37]. In the present study, all tested ZnO NPs were capable of inducing significant up-regulation of IL-8 mRNA in A549 cells, which was maximal after 4 hr exposure compared to untreated cells. Interestingly, the 200 nm ZnO particulates demonstrated a similar response to the s30 ZnO NPs. This may be partially because of the greater heterogeneity in the 200 nm ZnO NPs, which may also contain a proportion of both smaller and larger sized particles. Moreover, while surfactant dispersal allows the NPs to remain in solution for longer intervals, pristine NPs tend to agglomerate and sediment rapidly, resulting in enhanced cellular dosing, which may cause increased activation of cellular mRNA, as has been previously reported [38]. Similar observations have been reported for 100 or 20 nm ZnO NP treated HaCaT cells [39]. In conjunction with IL-8 mRNA up-regulation, we also quantified the relative levels of IL-8 protein release into cell culture medium. At low NP doses, A549 cells in this study demonstrated increased expression of IL-8 involving transcriptional activation of NF $\kappa$ B, followed by further stabilisation of IL-8 mRNA by p38 mitogen activated protein kinase pathway [36]. Transcriptional and post-transcriptional regulation of ZnO NP-mediated over expression of the IL-8 gene has previously been reported for BEAS-2B cells, which required phosphorylation of protein p65 [3]. Similarly, the p38 MAPK pathway is known to be activated by a number of stimuli including oxidative stress, which can lead to phosphorylation of the p38 protein. In this study, ZnO NPs and ZnCl<sub>2</sub> treatment induced rapid phosphorylation of p65 (Ser536) and p38 in treated A549 cells after 1 hr exposure, compared to untreated cells, and this returned to basal levels at 6 or 24 hr. Uptake of ZnO NPs may occur via endocytosis [40]. Once internalised into the acidic lysosomes, ZnO NPs dissolution occurs, which can disrupt intracellular zinc homeostasis (Shen et al., 2013; Luo et al., 2014). Low rates of dissolution in cell culture medium, both with and without protein supplementation have been demonstrated previously

for the ZnO NPs used in this study [14, 41] (Supplementary Table 1). It is therefore unlikely that extracellular dissolution is the driving cause of the pro-inflammatory signals observed for these NPs. Exposure of A549 cells to ZnO NPs for 1 hr followed by washing and supplementing cells with fresh medium and then a further incubation for 4 hr did not stimulate mRNA over expression of the pro-inflammatory cytokines, although increase in zinc levels (as determined by blue fluorescence of zinc binding dye) were already visible after 1 hr exposure of the A549 cells to the ZnO NPs (Figure 6.2). Taken together with the dissolution data, this result demonstrated that a direct and a continued contact of the ZnO NPs with the cell surface is essential. Furthermore, pre-treatment of A549 cells with NAC not only was able to significantly reduce up-regulation of both the HO-1 and IL-8 genes, but also controlled the release of IL-8 protein. This confirmed participation of ROS in the development of the observed tier 1 and 2 redox responses in A549 cells exposed to a sub-cytotoxic concentration of ZnO NPs (Figure 6.10). Recent studies have shown that contamination of NP solutions with lipopolysaccharide (LPS) can occur and it is therefore important to distinguish nanoparticle toxicity from endotoxin related effects. Feltis et al. compared the cytotoxic and inflammatory responses of the same ZnO NPs with that of LPS and demonstrated that, the immunotoxic responses of LPS were significantly different than those of ZnO NPs alone in an *in vitro* system consisting of THP-1 monocytes. Furthermore, A549 cells used in the present study are known to be relatively insensitive to LPS. This further confirmed the immunotoxic potential of the tested ZnO NP solutions at the sub-cytotoxic level.

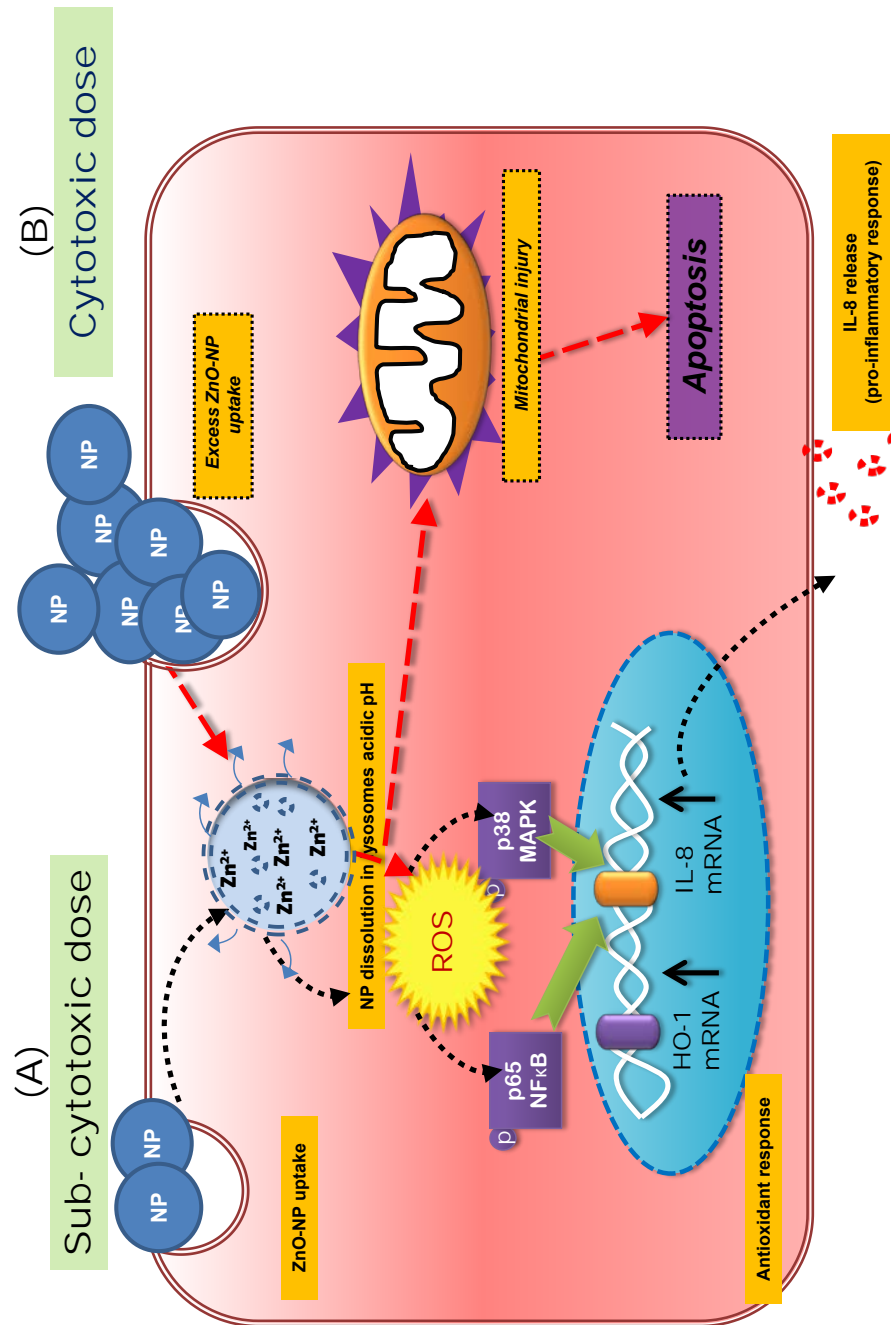


Figure 6.10: A schematic showing the onset of antioxidant and pro-inflammatory responses of A549 cells when exposed to (A) sub-cytotoxic doses of ZnO NPs or cytotoxic response when exposed to (B) cytotoxic doses of ZnO NPs as confirmed in this chapter.

## 6.5 Conclusions

In summary, the data demonstrated that the presence of poorly soluble ZnO NPs in the cellular micro-environment may aid in initiating a strong antioxidant response by A549 cells which is evident by the gradual up-regulation of the HO-1 gene. This is complemented by increased IL-8 gene expression and subsequent release of this pro-inflammatory cytokine. These immunological changes highlight the reactive nature of ZnO NPs even when no immediate cytotoxicity is observed. Dispersal state and particle size influence the overall cytotoxicity and cellular responses of these NPs. NAC pre-treatment of A549 cells confirmed a role for ROS generation as a result of the elevated intracellular Zn<sup>2+</sup> and subsequent phosphorylation of p65 and p38 transcription factors. Consequently, ZnO NP mediated cytotoxicity may be the outcome of the failure of the cellular redox machinery to contain excessive ROS formation. This outcomes of this chapter provide a better understanding of the pro-inflammatory effects of the interaction of ZnO NPs with the *in vitro* cellular systems of the airways.

## 6.6 References

1. Saptarshi S, Duschl A, Lopata A: **Interaction of nanoparticles with proteins: relation to bio-reactivity of the nanoparticle.** *J Nanobiotechnol* 2013, **11**:26.
2. Wang ZL: **Zinc oxide nanostructures: growth, properties and applications.** *Journal of Physics-Condensed Matter* 2004, **16**:R829-R858.
3. Wu W, Samet JM, Peden DB, Bromberg PA: **Phosphorylation of p65 Is Required for Zinc Oxide Nanoparticle-Induced Interleukin 8 Expression in Human Bronchial Epithelial Cells.** *Environ Health Perspect* 2010, **118**:982-987.
4. Yang W, Peters JI, Williams lii RO: **Inhaled nanoparticles—A current review.** *Int J Pharm* 2008, **356**:239-247.
5. Bakand S, Hayes A, Dechsakulthorn F: **Nanoparticles: a review of particle toxicology following inhalation exposure.** *Inhal Toxicol* 2012, **24**:125-135.
6. Lanone S, Rogerieux F, Geys J, Dupont A, Maillot-Marechal E, Boczkowski J, Lacroix G, Hoet P: **Comparative toxicity of 24 manufactured nanoparticles in human alveolar epithelial and macrophage cell lines.** *Particle and Fibre Toxicology* 2009, **6**:14.
7. Liu H, Yang D, Yang H, Zhang H, Zhang W, Fang Y, Lin Z, Tian L, Lin B, Yan J, Xi Z: **Comparative study of respiratory tract immune toxicity induced by three sterilisation nanoparticles: Silver, zinc oxide and titanium dioxide.** *J Hazard Mater* 2013, **248–249**:478-486.
8. Sharma V, Shukla RK, Saxena N, Parmar D, Das M, Dhawan A: **DNA damaging potential of zinc oxide nanoparticles in human epidermal cells.** *Toxicol Lett* 2009, **185**:211-218.
9. Sharma V, Anderson D, Dhawan A: **Zinc oxide nanoparticles induce oxidative DNA damage and ROS-triggered mitochondria mediated apoptosis in human liver cells (HepG2).** *Apoptosis* 2012, **17**:852-870.
10. Cho W-S, Duffin R, Howie S, Scotton C, Wallace W, MacNee W, Bradley M, Megson I, Donaldson K: **Progressive severe lung injury by zinc**

- oxide nanoparticles; the role of Zn<sup>2+</sup> dissolution inside lysosomes.** *Particle and Fibre Toxicology* 2011, **8**:1-16.
11. Kao Y-Y, Chen Y-C, Cheng T-J, Chiung Y-M, Liu P-S: **Zinc Oxide Nanoparticles Interfere With Zinc Ion Homeostasis to Cause Cytotoxicity.** *Toxicol Sci* 2012, **125**:462-472.
  12. Nel A, Xia T, Madler L, Li N: **Toxic potential of materials at the nanolevel.** *Science* 2006, **311**:622 - 627.
  13. Lin W, Xu Y, Huang C-C, Ma Y, Shannon K, Chen D-R, Huang Y-W: **Toxicity of nano- and micro-sized ZnO particles in human lung epithelial cells.** *Journal of Nanoparticle Research* 2009, **11**:25-39.
  14. Feltis BN, O'Keefe SJ, Harford AJ, Piva TJ, Turney TW, Wright PFA: **Independent cytotoxic and inflammatory responses to zinc oxide nanoparticles in human monocytes and macrophages.** *Nanotoxicology* 2012, **6**:757-765.
  15. Kang T, Guan R, Chen X, Song Y, Jiang H, Zhao J: **In vitro toxicity of different-sized ZnO nanoparticles in Caco-2 cells.** *Nanoscale Research Letters* 2013, **8**:496-496.
  16. Prach M, Stone V, Proudfoot L: **Zinc oxide nanoparticles and monocytes: Impact of size, charge and solubility on activation status.** *Toxicol Appl Pharmacol* 2013, **266**:19-26.
  17. Buerki-Thurnherr T, Xiao L, Diener L, Arslan O, Hirsch C, Maeder-Althaus X, Grieder K, Wampfler B, Mathur S, Wick P, Krug HF: **In vitro mechanistic study towards a better understanding of ZnO nanoparticle toxicity.** *Nanotoxicology* 2013, **7**:402-416.
  18. Song W, Zhang J, Guo J, Zhang J, Ding F, Li L, Sun Z: **Role of the dissolved zinc ion and reactive oxygen species in cytotoxicity of ZnO nanoparticles.** *Toxicol Lett* 2010, **199**:389-397.
  19. Kim YH, Fazlollahi F, Kennedy IM, Yacobi NR, Hamm-Alvarez SF, Borok Z, Kim K-J, Crandall ED: **Alveolar Epithelial Cell Injury Due to Zinc Oxide Nanoparticle Exposure.** *Am J Respir Crit Care Med* 2010, **182**:1398-1409.
  20. Turney TW, Duriska MB, Jayaratne V, Elbaz A, O'Keefe SJ, Hastings AS, Piva TJ, Wright PFA, Feltis BN: **Formation of Zinc-Containing**

- Nanoparticles from Zn<sup>2+</sup> Ions in Cell Culture Media: Implications for the Nanotoxicology of ZnO.** *Chem Res Toxicol* 2012, **25**:2057-2066.
21. Shen C, James SA, de Jonge MD, Turney TW, Wright PFA, Feltis BN: **Relating Cytotoxicity, Zinc Ions, and Reactive Oxygen in ZnO Nanoparticle–Exposed Human Immune Cells.** *Toxicol Sci* 2013, **136**:120-130.
  22. Luo M, Shen C, Feltis BN, Martin LL, Hughes AE, Wright PFA, Turney TW: **Reducing ZnO nanoparticle cytotoxicity by surface modification.** *Nanoscale* 2014, **6**:5791-5798.
  23. Fine JM, Gordon T, Chen LC, Kinney P, Falcone G, Beckett WS: **Metal Fume Fever: Characterization of Clinical and Plasma IL-6 Responses in Controlled Human Exposures to Zinc Oxide Fume at and Below the Threshold Limit Value.** *J Occup Environ Med* 1997, **39**:722-726.
  24. Sahu D, Kannan GM, Vijayaraghavan R, Anand T, Khanum F: **Nanosized Zinc Oxide Induces Toxicity in Human Lung Cells.** *ISRN Toxicology* 2013, **2013**:8.
  25. Gojova A, Lee J-T, Jung HS, Guo B, Barakat AI, Kennedy IM: **Effect of cerium oxide nanoparticles on inflammation in vascular endothelial cells.** *Inhal Toxicol* 2009, **21**:123-130.
  26. Hanley C, Thurber A, Hanna C, Punnoose A, Zhang JH, Wingett DG: **The Influences of Cell Type and ZnO Nanoparticle Size on Immune Cell Cytotoxicity and Cytokine Induction.** *Nanoscale Research Letters* 2009, **4**:1409-1420.
  27. Huang C-C, Aronstam RS, Chen D-R, Huang Y-W: **Oxidative stress, calcium homeostasis, and altered gene expression in human lung epithelial cells exposed to ZnO nanoparticles.** *Toxicol In Vitro* 2010, **24**:45-55.
  28. Yu K-N, Yoon T-J, Minai-Tehrani A, Kim J-E, Park SJ, Jeong MS, Ha S-W, Lee J-K, Kim JS, Cho M-H: **Zinc oxide nanoparticle induced autophagic cell death and mitochondrial damage via reactive oxygen species generation.** *Toxicol In Vitro* 2013, **27**:1187-1195.

29. Walkey CD, Olsen JB, Guo H, Emili A, Chan WCW: **Nanoparticle Size and Surface Chemistry Determine Serum Protein Adsorption and Macrophage Uptake.** *J Am Chem Soc* 2011, **134**:2139-2147.
30. Xia T, Kovochich M, Liong M, Madler L, Gilbert B, Shi H, Yeh JI, Zink JI, Nel AE: **Comparison of the Mechanism of Toxicity of Zinc Oxide and Cerium Oxide Nanoparticles Based on Dissolution and Oxidative Stress Properties.** *ACS Nano* 2008, **2**:2121-2134.
31. Avalos A, Haza AI, Mateo D, Morales P: **Cytotoxicity and ROS production of manufactured silver nanoparticles of different sizes in hepatoma and leukemia cells.** *J Appl Toxicol* 2014, **34**:413-423.
32. Gozzelino R, Jeney V, Soares MP: **Mechanisms of Cell Protection by Heme Oxygenase-1.** *Annu Rev Pharmacol Toxicol* 2010, **50**:323-354.
33. Napierska D, Thomassen LCJ, Rabolli V, Lison D, Gonzalez L, Kirsch-Volders M, Martens JA, Hoet PH: **Size-Dependent Cytotoxicity of Monodisperse Silica Nanoparticles in Human Endothelial Cells.** *Small* 2009, **5**:846-853.
34. Watanabe M, Yoneda M, Morohashi A, Hori Y, Okamoto D, Sato A, Kurioka D, Nittami T, Hirokawa Y, Shiraishi T, et al: **Effects of Fe<sub>3</sub>O<sub>4</sub> Magnetic Nanoparticles on A549 Cells.** *Int J Mol Sci* 2013, **14**:15546-15560.
35. Herzog E, Byrne HJ, Davoren M, Casey A, Duschl A, Oostingh GJ: **Dispersion medium modulates oxidative stress response of human lung epithelial cells upon exposure to carbon nanomaterial samples.** *Toxicol Appl Pharmacol* 2009, **236**:276-281.
36. Hoffmann E, Dittrich-Breiholz O, Holtmann H, Kracht M: **Multiple control of interleukin-8 gene expression.** *J Leukoc Biol* 2002, **72**:847-855.
37. Hackenberg S, Zimmermann F-Z, Scherzed A, Friehs G, Froelich K, Ginzkey C, Koehler C, Burghartz M, Hagen R, Kleinsasser N: **Repetitive exposure to zinc oxide nanoparticles induces dna damage in human nasal mucosa mini organ cultures.** *Environ Mol Mutagen* 2011, **52**:582-589.
38. Moos PJ, Olszewski K, Honegger M, Cassidy P, Leachman S, Woessner D, Cutler NS, Veranth JM: **Responses of human cells to ZnO**

- nanoparticles: a gene transcription study.** *Metallomics* 2011, **3**:1199-1211.
39. Bae H, Ryu H, Jeong S, Lee E, Park Y-H, Lee K, Choi B, Maeng E, Kim M-K, Son S: **Oxidative stress and apoptosis induced by ZnO nanoparticles in HaCaT cells.** *Molecular & Cellular Toxicology* 2011, **7**:333-337.
40. Yan Z, Xu L, Han J, Wu Y-J, Wang W, Yao W, Wu W: **Transcriptional and posttranscriptional regulation and endocytosis were involved in zinc oxide nanoparticle-induced interleukin-8 overexpression in human bronchial epithelial cells.** *Cell Biol Toxicol* 2014, **30**:79-88.
41. James SA, Feltis BN, de Jonge MD, Sridhar M, Kimpton JA, Altissimo M, Mayo S, Zheng C, Hastings A, Howard DL, et al: **Quantification of ZnO Nanoparticle Uptake, Distribution, and Dissolution within Individual Human Macrophages.** *ACS Nano* 2013, **7**:10621-10635.



---

## Chapter VII

### Investigating pro-inflammatory effects of acute ZnO NP exposure in a murine model via the intranasal route

**Publication:**

**Saptarshi SR**, Feltis BN, Wright PF, Lopata AL. Investigating the immunomodulatory nature of zinc oxide nanoparticles at sub-cytotoxic levels *in vitro* and after intranasal instillation *in vivo* J Nanobiotechnol 2015, 13:6

---



## 7.1 Introduction

ZnO NPs are increasingly used in a number of industrial applications and there is an urgent need to specifically evaluate their toxic potential. Although, ZnO NP mediated cytotoxicity has been investigated in a number of *in vitro* cell systems (also see chapter IV and VI), animal models are better representatives of the complexity of the *in vivo* environment and provide an ideal platform to assess nanotoxicity [1]. Recent studies have also attempted to address possible correlation between ZnO NP mediated immunotoxicity *in vivo* as well as *in vitro* however, the biological complexity and presence of several protein rich environments and cellular diversity *in vivo* makes this assessment complicated [2-4].

Intratracheal instillation (IT) has been previously used to study effects of ZnO NP exposure to the lung environment. Through this route of exposure, ZnO NPs have the potential to induce eosinophilia, proliferation of airway epithelial cells, goblet cell hyperplasia, and pulmonary fibrosis [5]. Also, inhalation of ZnO NPs may lead to their translocation to the central nervous system and may also interfere with zinc homeostasis leading to pulmonary toxicity [6, 7]. In the acute phase, ZnO NPs may also induce an increase in antioxidants such as lipid peroxide, HO-1 and alpha-tocopherol commonly attributed to NP mediated increase in oxidative stress in the lungs of exposed rats [8]. Yet another route of airway exposure to ZnO NPs is inhalation of aerosolized NPs in whole-body exposure chambers [9-12]. Similar to IT route, inhalation exposure of ZnO NPs can result in acute inflammation in the cells at the bronchoalvolar (BAL) junctions of the lung [12]. Analysis of the BALF of mice exposed to aerosolised ZnO NPs also show an up regulation in differential expression of proteins involved in pulmonary inflammation and also lung cancer [13] Rats exposed to 90 nm ZnO NPs or 111 nm ZnO particulates via intratracheal instillation or exposure to inhalation chambers were reported to show similar short-term lung inflammation and cytotoxic responses which were resolved in a few days post exposure [4].

Interestingly, intranasal instillation of ZnO NPs and their ability to cause systemic inflammatory response in an acute high-dosage exposure animal

model has not been investigated before. Currently, there is an urgent need for additional studies which address airway exposure to NPs, their deposition and clearance from the lung to predict potential risks and determine no-observed-adverse-effect levels upon exposure to these highly commercial ZnO NPs.

In addition, the physicochemical characteristics of NPs may also influence the induction of pulmonary inflammation after inhalation [14]. Based on the findings from the *in vitro* studies as discussed in chapter VI, two ZnO NPs (pristine 30 nm and surfactant-dispersed 30 nm) were chosen for an acute high dosage intranasal exposure study in a murine model. The overall aim of this chapter was to evaluate the effects of an acute exposure of a single high dose of ZnO NPs via the intranasal route of airway exposure *in vivo*.

## 7.2 Materials and methods

### 7.2.1 Nanoparticles

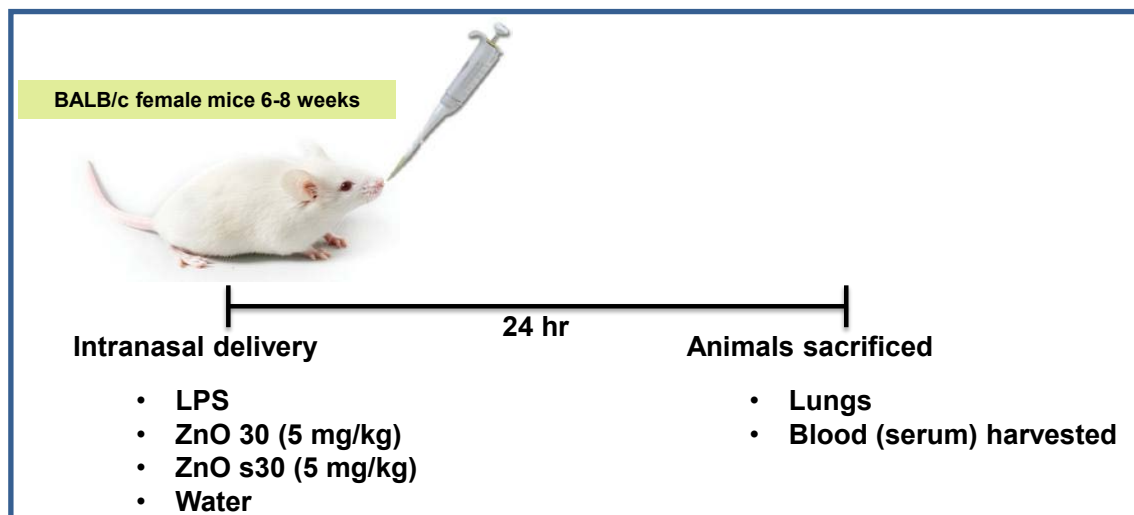
Industrially manufactured 30 nm ZnO NPs with and without surfactant dispersant were analysed in this chapter. Methods for preparation of NP solutions and information on their physico-chemical characterisation are described in chapter III.

### 7.2.2 Animals

Female Balb/c mice (6-8 weeks old) were purchased from the Animal Resource Centre (WA, Australia). All animals were housed in stainless steel cages and provided food and water *ad libitum* in the animal housing facility. All protocols were compliant with the animal ethics committee at James Cook University (*animal ethics approval number A1795*).

### 7.2.3 Experimental strategy

Two separate experiments were performed where animals were randomly assigned to four groups (n = 12) based on body weight (14-19 g). Pristine and surfactant-dispersed 30 nm ZnO NP solutions were prepared in sterile water as detailed in chapter III. The dose used for the study was 5 mg/kg (body weight). Mice without anaesthesia were held in supine position, and then 50 µL total volume of the NP suspension was delivered into each nostril of the mice gently using a 200 µL pipette tip. Two out of the four experimental groups served as controls including groups treated with a non-lethal dose of 0.5 mg/kg lipopolysaccharide (LPS) or water (vehicle control). At the end of the 24 hr exposure period mice were sacrificed and peripheral blood and lungs harvested from each animal (Figure 7.1).



**Figure 7.1 Schematic of the experimental strategy used for the *in vivo* experiment**

#### 7.2.4 Serum Collection

Blood samples collected from killed animals were allowed to clot at room temperature for 30 min following which the tubes were subjected to centrifugation at 1500 *g* for 20 min. Serum prepared was pooled for animals from each group ( $n = 12$ ) and stored at  $-80^{\circ}\text{C}$  for later use.

#### 7.2.5 Lung histology

After exposure for 24 hr, the lung tissues were collected and immediately fixed in 4% phosphate- buffered formalin for at least 24 hr and then embedded in to wax. Paraffin sections 5  $\mu\text{m}$  thick, were cut and fixed on to slides. Haematoxylin and eosin (H&E) staining was performed on the lung sections for histopathological examination.

#### 7.2.6 Lung tissue RNA isolation and quantitative-PCR (q-PCR)

Small sections of the tissue obtained were also used for RNA extraction and subsequent cDNA reverse transcription. Detailed methodology for the same has been described in chapter VI. Changes in expression levels of the pro-inflammatory cytokines were determined using q-PCR using the SsoAdvanced™ SYBR® Green Supermix (BioRad, USA) reaction mixture containing specific primers. Specific primers used were eotaxin, sense 5'-

AGAGGCTGAGATCCAAGCAG-3' and antisense 5'-CAGATCT-CTTTGCCCAACCT-3', TNF $\alpha$ , sense 5'- TACTGAACTTCGG-GGTGATTGGTCC-3' and antisense 5'-CAGCCTTGTCCCTTGAAGAGAACC-3', MCP-1, sense 5'-ACCACAGTCCATGCCATCAC-3' and antisense 5'-TTGAGGTGGTTGTGGAAAAG-3' and the housekeeping gene used was  $\beta$  actin, sense 5'-CGAGCGTGGCTACAGCTTCA-3' and antisense 5'-AGGAAGAGGATGCGGCAGTG-3'. q-PCR was performed using the Piko Real real-time PCR System (Thermo Scientific, Germany). Thermal cycle parameters used were 7 min at 95°C, followed by 45 cycles (95°C, 15 sec; 55°C, 15 sec; 72°C, 30 sec). Data were analysed using the relative quantitation method.

### 7.2.7 Proteome profile assay

A mouse cytokine protein array (R&D systems, USA) was used to assess the levels of pro-inflammatory cytokines in the pooled sera of mice from each experimental group as per manufacturer's instructions. Briefly, pooled serum samples were incubated onto array membranes at 4°C overnight and the membranes were washed three times for 10 min. The array membranes were then incubated with the reconstituted detection antibody cocktail for 1 hr and further washed three times for 10 min. After incubating with horseradish peroxidase (HRP)-linked secondary antibody at a dilution of 1:2000, the signals were visualized by chemiluminescent HRP reagent (Millipore, Australia). Densitometry of protein spot signals was detected and quantified using the Total lab Quant software (Totallab, UK).

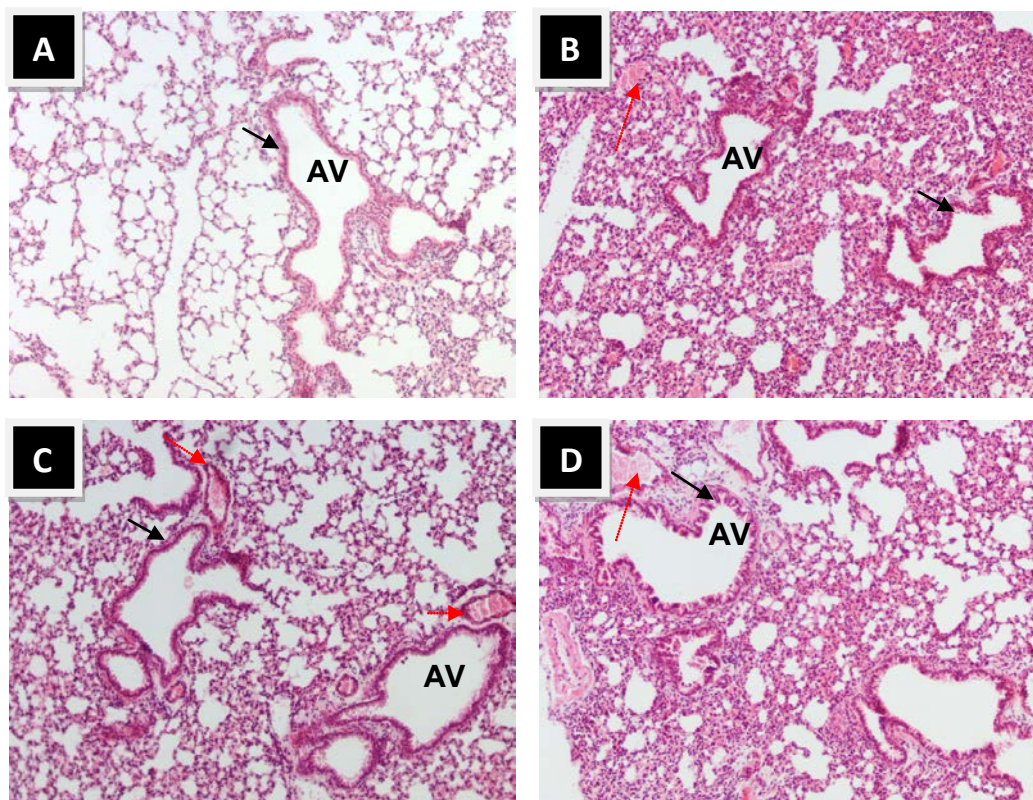
### 7.2.8 Statistical analysis

Data are presented as mean  $\pm$  standard error of mean (SEM) and was analysed using two way ANOVA for cytotoxicity assays or one-way ANOVA for all other analyses, followed by Bonferroni post-hoc test (Prism 6.0, GraphPad Software, USA), with a p value < 0.05 considered as significant.

## 7.3 Results

### 7.3.1 Lung histology

As shown in figure 7.2 haematoxylin and eosin staining of the lung sections of the control group (panel A) treated with water shows normal morphology. In contrast, lung sections of ZnO NP exposed mice show severe inflammatory infiltration in the alveoli and peri bronchial regions. The bronchial and vascular walls also appear to be thickened (black arrows). A moderate level of internal haemorrhage was also observed 24 hr after NP challenge when comparing lung tissue section of control mice (red arrows).



**Figure 7.2 H&E staining of lung sections of mice treated with (A) vehicle control, (B) LPS, (C) pristine 30 nm ZnO NPs and (D) surfactant-dispersed 30 nm ZnO NPs via intratracheal instillation. AV indicates the alveolar region of the lung. Red arrows indicate haemorrhage and black arrows demonstrate thickened bronchial walls.**

### 7.3.2 Lung tissue RNA isolation and quantitative-PCR (q-PCR)

RNA extracted from the lung tissue of ZnO NP treated mice was used for qPCR analysis of key pro-inflammatory markers. A significant up-regulation of the eotaxin gene was observed in mice treated with pristine 30 nm ZnO NPs compared to mice exposed to vehicle control (Figure 7.3A). In contrast, at the end of 24 hr ZnO NPs did not cause significant up-regulation of pro-inflammatory TNF $\alpha$  and MCP-1 genes in the lung tissue of treated mice (Figure 7.3B & 7.3C).

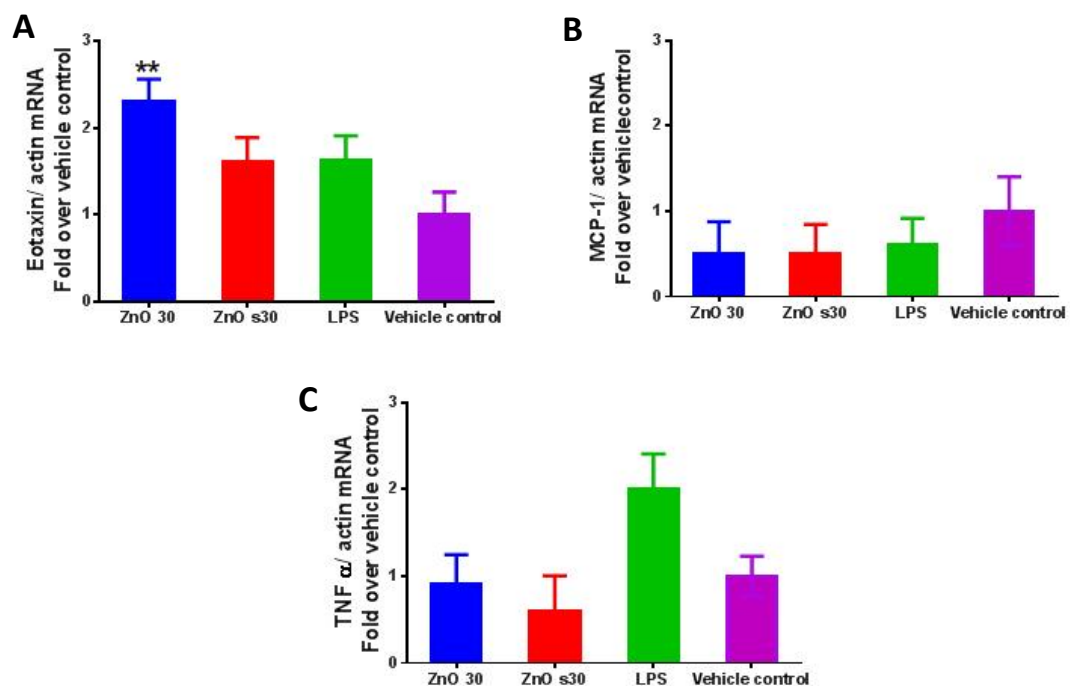


Figure 7.3 q PCR analyses of mRNA levels for inflammatory markers (A) eotaxin, (B) MCP-1 and (C) TNF $\alpha$  in the lung tissues of treated mice. Data are expressed as mean  $\pm$  SEM (n = 12) two separate experiments \*\*p<0.01

### 7.3.3 Proteome profile assay

Cytokine profiling of pooled mouse serum from each experimental group revealed the presence of pro-inflammatory chemokines (Figure 7.4). Significant levels of MCP-1 protein were detected in the pooled sera of mice treated with either ZnO NP solutions. Pristine 30 nm ZnO NP treated mice showed significantly elevated levels of the chemokine IP-10, while 30 nm sZnO NPs caused an increase of CCL5 (RANTES), known to recruit leukocytes to inflammatory sites. Interestingly, eotaxin was not detected in the sera of ZnO NP exposed animals.

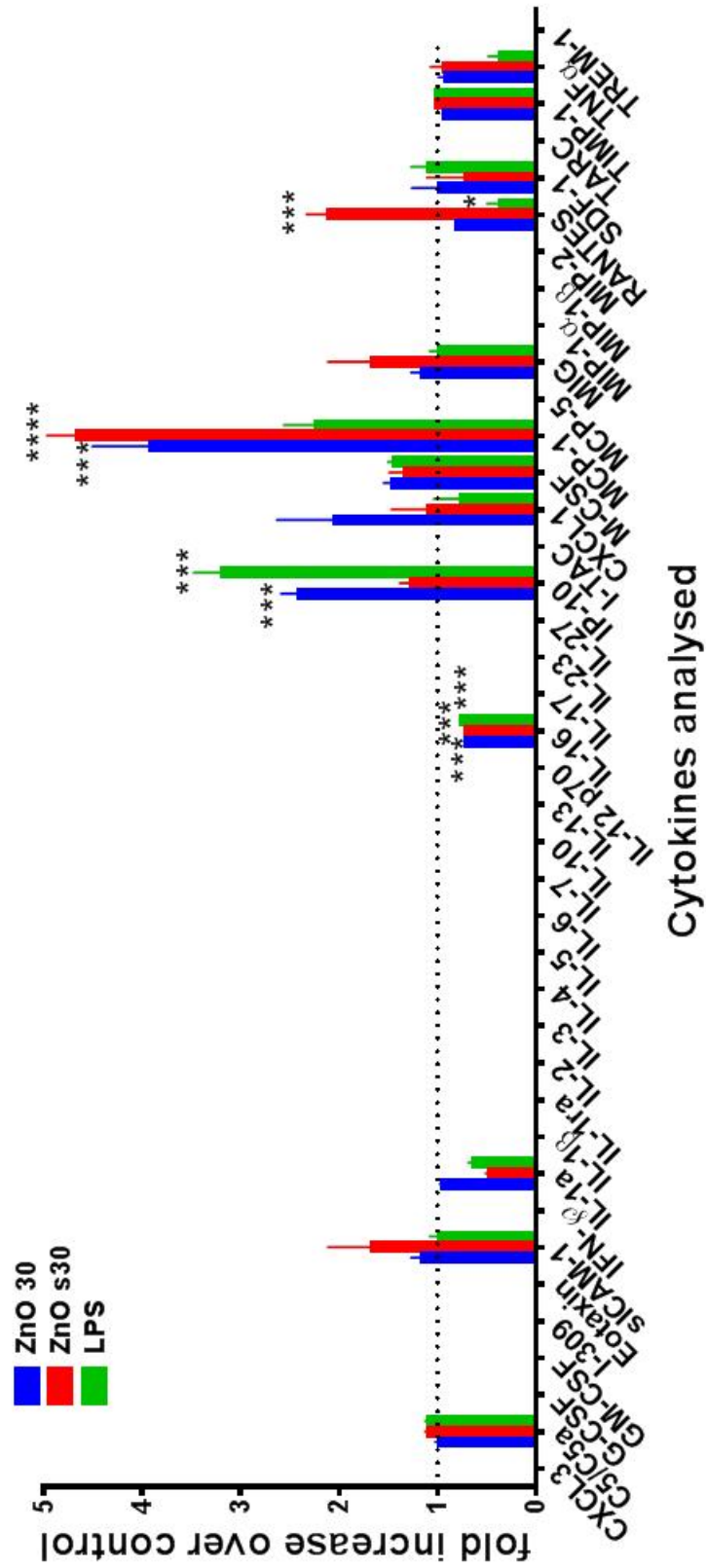


Figure 7.4 Proteome profile array of pro-inflammatory cytokines quantified in pooled sera from each experimental group. Statistical significance is compared to vehicle control. Dotted line represents the vehicle control. Data are expressed as mean  $\pm$  SEM (n = 12) two separate experiments \*\*\*p<0.001, \*\*\*\*p<0.0001

## 7.4 Discussion

Large scale production, processing and handling of nanomaterials has led to concerns regarding incidences of accidental exposure to these materials and may be a potential health risk to workers exposed to these biologically reactive materials in the manufacturing areas [15, 16]. *In vivo* animal studies, addressing airway exposure to NPs, their deposition and clearance from the lung can therefore help to predict potential risks and establish safety paradigms. Inhalation of zinc-laden particles has been previously reported to cause metal fume fever, a pulmonary condition associated with flu-like symptoms and increase in pro-inflammatory cytokines in the bronchioalveolar lavage fluid (BALF) of the lung. This condition is commonly observed in workers exposed to metal fumes during zinc processing [17]. Therefore, systemic deposition of ZnO NPs *in vivo* may lead to their interaction with immune cells resulting in immunomodulatory or toxic consequences.

Cytotoxicity mediated by ZnO NPs *in vitro*, has been reported for numerous cell types of the pulmonary origin [18-21]. In chapter VI of this thesis, cytotoxicity of ZnO NPs in lung epithelial cells was shown to be dependent on NP concentration and size, with smaller sized NPs being more potent. Also at sub-cytotoxic concentrations the 30 nm ZnO NPs were shown to induce higher levels of oxidative stress and inflammation via specific signalling pathways. Interestingly only a small number of studies have been conducted so far addressing the influence of ZnO NPs on *in vivo* airway exposure (Review Chapter V). The main aim of this chapter was to confirm if a single, relatively large dose of 30 nm ZnO NPs can induce inflammation of the lung and systemic up regulation of pro-inflammatory cytokines within 24 hr of administration using intranasal instillation process.

Intranasal instillation of ZnO NPs in this study showed results that were similar to the cytotoxic patterns observed for A549 cells. Intranasal instillation of ZnO NPs was preferred over whole-body chamber inhalation or IT. IT of NPs is not a route of exposure in the occupational setting and can result in less homogenous and focally distributed deposition of the nanomaterial in the lungs, resulting in exaggerated outcomes particularly for the high dose used in this

study. The nasal mucosa aids in rapid absorption of deposited substances and development of systemic effects [22].

Intranasal instillation of 30 nm ZnO NPs have been previously shown to cause inflammation of the olfactory epithelium of exposed rats however possible lower respiratory tract toxicity of these NP via the same route has not been yet investigated. ZnO NP treatment resulted in substantial inflammatory infiltration into the alveoli and peri-bronchial regions in this study. Moderate amounts of haemorrhage were also observed (Figure 7.2 C&D). These findings confirm that intranasal instillation conducted in supine positioning of mice using 50  $\mu$ L volume was delivered in to the lungs of treated mice. Based on the histopathological data, mRNA up regulation in the lung tissue and systemic release of inflammatory mediators were analysed 24 hr after exposure to either ZnO NP solutions. Although no increase was recorded in the serum levels of eotaxin of ZnO NP treated mice, a significant up-regulation of eotaxin mRNA in the lung tissue of mice exposed to pristine 30 nm ZnO NPs was observed. The increased mRNA levels of the eotaxin gene in the lung tissue may be attributed to a localised inflammatory effect arising due to the infiltration of eosinophils into the peri-bronchial regions of the lung. ZnO NPs also caused a significant systemic release of pro-inflammatory serum chemokines including MCP-1, RANTES and IP-10, all associated with the recruitment of inflammatory cells to sites of inflammation [23, 24].

In a recent study, cumulative inhaled ZnO NP doses of 10.9 mg/kg (306  $\mu$ g/mouse) over 13 week exposure period was shown to elicit minimal pulmonary inflammation without causing significant release of pro-inflammatory markers [11]. The preliminary results of the present *in vivo* study highlight the inflammatory potential of inhaled ZnO NPs via intranasal installation, although the overall ZnO NP burden delivered is instantaneous at relatively low with 5 mg/kg (84  $\mu$ g/mouse). This highlights that the route and rate at which ZnO NPs are delivered *in vivo* may influence their toxic potential rather than the dose delivered. Baisch et al. made similar observation in their study with titanium dioxide NPs [25]. They demonstrated that at a constant dose, IT method which essentially causes high dose rate delivery, can elicit greater inflammation as compared to a low dose rate delivery method such as inhalation.

Although the ZnO NPs used in this study demonstrated very low extracellular solubility (Chapter III Table 3.2), it is possible that the lung environment may promote dissolution of ZnO NPs. Zn<sup>2+</sup> ions have been previously shown to result in pulmonary inflammation [6]. It is possible that the observed lung inflammation in the present study is a result of dissolution of ZnO NPs in the lung environment, which consists of surfactant proteins, mucus and phagocytic cellular entities.

The preliminary results of this *in vivo* study highlight the inflammatory potential of inhaled ZnO NPs. In contrast to the *in vitro* studies, no clear differences could be observed in the inflammatory profile of the two differentially dispersed 30 nm ZnO NP solutions. This may be explained by the complexity of the lung environment in terms of its cellular and protein diversity, which may compound the bio-reactivity of NPs. It is also worth noting that surfactant proteins normally present in the lung environment may cover the surface of the pristine ZnO NPs which may explain the insignificant differences in the immunotoxic reactivity of the two ZnO NP solutions. Future detailed studies analysing the long term exposure of instilled NPs via the intranasal route are required.

## 7.5 Conclusion

The data presented in this chapter demonstrate for the first time the pro-inflammatory potential of ZnO NPs *in vivo* when administered using the intranasal instillation method. Instillation of a high burden of ZnO NPs (5 mg/kg) can result in pulmonary inflammation, characterised by infiltration of lung with inflammatory cells and systemic release of pro-inflammatory cytokines into the serum within 24 hr exposure. Furthermore, the agglomeration state of ZnO NPs does not affect their reactivity *in vivo*.

## 7.6 References

1. Rincker MJ, Hill GM, Link JE, Meyer AM, Rowntree JE: **Effects of dietary zinc and iron supplementation on mineral excretion, body composition, and mineral status of nursery pigs.** *Journal of Animal Science* 2005, **83**:2762-2774.
2. Sayes CM, Reed KL, Warheit DB: **Assessing Toxicity of Fine and Nanoparticles: Comparing In Vitro Measurements to In Vivo Pulmonary Toxicity Profiles.** *Toxicol Sci* 2007, **97**:163-180.
3. Warheit D B SCMRKL, Swain KA: **Health effects related to nanoparticle exposures: environmental, health and safety considerations for assessing hazards and risks.** *Pharmacol Ther* 2008, **120**:35.
4. Warheit DB, Sayes CM, Reed KL: **Nanoscale and Fine Zinc Oxide Particles: Can in Vitro Assays Accurately Forecast Lung Hazards following Inhalation Exposures?** *Environ Sci Technol* 2009, **43**:7939-7945.
5. Cho WS, Duffin R, Howie SEM, Scotton CJ, Wallace WAH, MacNee W, Bradley M, Megson IL, Donaldson K: **Progressive severe lung injury by zinc oxide nanoparticles; the role of Zn<sup>2+</sup> dissolution inside lysosomes.** *Particle and Fibre Toxicology* 2011, **8**.
6. Kao Y-Y, Chen Y-C, Cheng T-J, Chiung Y-M, Liu P-S: **Zinc Oxide Nanoparticles Interfere With Zinc Ion Homeostasis to Cause Cytotoxicity.** *Toxicol Sci* 2012, **125**:462-472.
7. Kao Y-Y, Cheng T-J, Yang D-M, Wang C-T, Chiung Y-M, Liu P-S: **Demonstration of an Olfactory Bulb–Brain Translocation Pathway for ZnO Nanoparticles in Rodent Cells In Vitro and In Vivo.** *J Mol Neurosci* 2012, **48**:464-471.
8. Fukui H, Horie M, Endoh S, Kato H, Fujita K, Nishio K, Komaba LK, Maru J, Miyauhi A, Nakamura A, et al: **Association of zinc ion release and oxidative stress induced by intratracheal instillation of ZnO nanoparticles to rat lung.** *Chem Biol Interact* 2012, **198**:29-37.

9. Fraker PJ, King LE, Laakko T, Vollmer TL: **The Dynamic Link between the Integrity of the Immune System and Zinc Status.** *The Journal of Nutrition* 2000, **130**:1399S-1406S.
10. Thannickal VJ, Fanburg BL: *Reactive oxygen species in cell signaling.* 2000.
11. Adamcakova-Dodd A, Stebounova L, Kim J, Vorrink S, Ault A, O'Shaughnessy P, Grassian V, Thorne P: **Toxicity assessment of zinc oxide nanoparticles using sub-acute and sub-chronic murine inhalation models.** *Particle and Fibre Toxicology* 2014, **11**:15.
12. Chen J-K, Ho C-C, Chang H, Lin J-F, Yang CS, Tsai M-H, Tsai H-T, Lin P: **Particulate nature of inhaled zinc oxide nanoparticles determines systemic effects and mechanisms of pulmonary inflammation in mice.** *Nanotoxicology* 2014, **0**:1-11.
13. Juang Y-M, Lai B-H, Chien H-J, Ho M, Cheng T-J, Lai C-C: **Changes in protein expression in rat bronchoalveolar lavage fluid after exposure to zinc oxide nanoparticles: an iTRAQ proteomic approach.** *Rapid Commun Mass Spectrom* 2014, **28**:974-980.
14. Prasad A: **Zinc and immunity.** *Mol Cell Biochem* 1998, **188**:63-69.
15. Plitzko S: **Workplace exposure to engineered nanoparticles.** *Inhal Toxicol* 2009, **21**:25-29.
16. Kuhlbusch T, Asbach C, Fissan H, Gohler D, Stintz M: **Nanoparticle exposure at nanotechnology workplaces: A review.** *Particle and Fibre Toxicology* 2011, **8**:22.
17. Cooper R: *Zinc toxicology following particulate inhalation.* 2008.
18. George S, Pokhrel S, Xia T, Gilbert B, Ji Z, Schowalter M, Rosenauer A, Damoiseaux R, Bradley KA, Mädler L, Nel AE: **Use of a Rapid Cytotoxicity Screening Approach To Engineer a Safer Zinc Oxide Nanoparticle through Iron Doping.** *ACS Nano* 2009, **4**:15-29.
19. Huang C-C, Aronstam RS, Chen D-R, Huang Y-W: **Oxidative stress, calcium homeostasis, and altered gene expression in human lung epithelial cells exposed to ZnO nanoparticles.** *Toxicol In Vitro* 2010, **24**:45-55.
20. Ahamed M, Akhtar MJ, Raja M, Ahmad I, Siddiqui MKJ, AlSalhi MS, Alrokayan SA: **ZnO nanorod-induced apoptosis in human alveolar**

- adenocarcinoma cells via p53, survivin and bax/bcl-2 pathways: role of oxidative stress.** *Nanomedicine: Nanotechnology, Biology and Medicine* 2011, **7**:904-913.
21. Hsiao IL, Huang Y-J: **Titanium Oxide Shell Coatings Decrease the Cytotoxicity of ZnO Nanoparticles.** *Chem Res Toxicol* 2011, **24**:303-313.
22. Turner PV, Brabb T, Pekow C, Vasbinder MA: **Administration of Substances to Laboratory Animals: Routes of Administration and Factors to Consider.** *J Am Assoc Lab Anim Sci* 2011, **50**:600-613.
23. Kabashima H, Yoneda M, Nagata K, Hirofuji T, Maeda K: **The presence of chemokine (MCP-1, MIP-1 $\alpha$ , MIP-1 $\beta$ , IP-10, RANTES)-positive cells and chemokine receptor (CCR5, CXCR3)- positive cells in inflamed human gingival tissues.** *Cytokine* 2002, **20**:70-77.
24. Roy R, Singh SK, Das M, Tripathi A, Dwivedi PD: **Toll-like receptor 6 mediated inflammatory and functional responses of zinc oxide nanoparticles primed macrophages.** *Immunology* 2014, **142**:453-464.
25. Baisch B, Corson N, Wade-Mercer P, Gelein R, Kennell A, Oberdorster G, Elder A: **Equivalent titanium dioxide nanoparticle deposition by intratracheal instillation and whole body inhalation: the effect of dose rate on acute respiratory tract inflammation.** *Particle and Fibre Toxicology* 2014, **11**:5.



---

## **Chapter VIII**

### **General discussion, Conclusions and Future direction**

---



## 8.1 General discussion

Nanotoxicology is an important research field that assesses the potential adverse effects of nanomaterials [1]. In order to fully explore the prospective benefits of nanotechnology, it is urgently required to understand how NPs interact with complex biological systems [2]. Currently, ZnO NPs are being widely used in several consumer and industrial end-products. Therefore, focus has been to ascertain their cytotoxic potential [3-14]. Interestingly, the nano/bio interface is extremely complex in nature and there can be a vast number of factors such as NP surface properties, aggregation characteristics, dissolution potential and surrounding protein environment that can influence the NP behaviour (Chapter II, III & IV) within a biological system [15, 16]. Moreover, to allow efficient dispersal of NPs, surfactants are commonly used. Therefore three different ZnO particulates (30, 80 and 200 nm) dispersed with or without a commercial surfactant dispersant were used in the present study. This PhD thesis aimed at enhancing our existing knowledge on the bioreactive nature of industrial ZnO NPs by addressing their interactions with proteins (Chapter IV) and correlating this knowledge to their cytotoxic and immunomodulatory potential *in vitro* (Chapter VI) and *in vivo* (Chapter VII).

Physico-chemical characterisation data for the ZnO NPs used in this thesis demonstrated their propensity to form agglomerates in protein enriched cell culture medium without significant dissolution (less than 1%). This was central to the research objective of this thesis because it was essential to establish that the cytotoxic endpoints of ZnO NPs interaction resulted due to ZnO NP-cell contact or uptake and not because of extracellular dissolution of ZnO NPs. Interestingly, as outlined in chapter II, the interaction of NPs with the cellular interface predominantly occur via the protein layer adsorbed on the NP surface [17, 18]. Therefore chapter IV set out to further understand the protein conditioning of the ZnO NP surface in a typical cell culture medium environment. The “hard” FBS-ZnO NP protein corona consisting of proteins firmly bound on to the ZnO NP surface was carefully isolated and subsequently identified using mass spectrometry. Consistent with the findings reported for other metal oxide NPs (Chapter II), it was observed that the ZnO NP-FBS

protein corona formation occurs instantly in the cell culture medium environment and is made up of important blood proteins including albumin, haemoglobin subunits, complement protein, glycoproteins and lipoproteins. The amount of protein binding on the surface of ZnO NPs was found to be directly related to their size. Certain proteins such as albumin, alpha1 anti-proteinase, fibrinogen alpha chain apo AII and CIII were clearly more pronounced on the surface of the surfactant-dispersed NPs whereas haemoglobin subunits demonstrated preferential binding to pristine ZnO NPs. This can be attributed to an increase in the dispersal of NPs due to the presence of surfactant which could have allowed for more protein molecules to interact with the ZnO NP surface. Also the non-specific interaction of some proteins with the surfactant molecules cannot be disregarded.

Serum is a complex mixture of proteins, and this further complicates the study of NP-PC formation because of the varied physico-chemical properties of the individual proteins [19]. While serum proteins typically show competitive binding with introduced surfaces including nano-surfaces [16], at a fixed time and NP concentration, no change in the composition of the ZnO NP-FBS corona was observed. This was clearly demonstrated by the consistent protein banding pattern observed for PCs retrieved from the ZnO NP surface either at different times or in presence of different amounts of FBS proteins. It can thus be confirmed that the ZnO NP protein corona in tissue culture medium is albumin rich but not dynamic in nature. This information is of importance for understanding the bio-distribution of these NPs.

BSA pre-coated ZnO-NP surface showed binding of cell lysate proteins after 1 or 24 hr exposure to A549 cell lysate solution in the present study. Immunoblotting with BSA-specific mAb further confirmed that BSA was still present after 24 hr of exposure. *In vivo*, it is possible, for example that the NP can be exposed to several different proteomes derived from the lung environment (surfactant proteins), blood, and cytoplasmic proteins. Because of the NP-PC formation, the NP can not only aid in unintentional translocation of proteins across different protein environments, but also the presence of specific proteins on the NP surface can facilitate direct cellular contact. Noticeably, the ZnO NP surface allows the binding of new proteins onto its surface as it

moves from one protein rich environment to another. It should be noted that the technique used to isolate the adsorbed proteins from the ZnO NP surface takes into account only the “hard” corona, consisting of proteins firmly adsorbed on the NP surface. Adsorption of cell lysate proteins on the pre-coated ZnO NP surface demonstrated that between different proteomes, the ZnO NP surface does change in terms of its protein composition. This change however, may be specific to individual proteins.

This prompted further investigation of the interaction of ZnO NPs with single protein solutions. Protein binding capacity and possible impact on protein secondary structure, after the ZnO NP-protein interaction were examined for important blood proteins. The surfactant-dispersal led to the binding of larger amounts of protein on the ZnO NP surface as compared to the pristine NPs. Interestingly, ZnO NPs (30 nm) were capable of inducing minor conformational changes in the secondary structure of proteins such as BSA and fibrinogen but not transferrin. This indicates that not all proteins undergo conformational changes on the ZnO-NP surface. Protein structural changes mediated by the NP largely depend on the shape of the bound protein molecule and its contact area with the NP surface.

The proteins in the cell culture medium, to some extent, help in controlled interaction of the NP with the cellular interface. This was clear when the ZnO NPs, dispersed in serum-free medium, demonstrated lower uptake or association with A549 cells as compared to the ones dispersed in protein enriched medium. Importantly, suppression of the cytotoxic potential of ZnO NPs was observed when the protein concentration of the NP dispersal media was increased from 10 to 40% FBS concentration. Indeed, the NP-PC can have a profound influence on the bio-reactivity of ZnO NPs *in vitro*.

Next, this thesis investigated the inflammatory potential of ZnO NPs in A549 cells, primarily because these cells are representative of the squamous epithelium of the lung and are first to come in contact with inhaled foreign particles. Because of large scale manufacturing of ZnO NPs accidental exposure of workers in areas where these NPs are manufactured is very likely. Therefore a thorough investigation of not only cytotoxicity but also inflammatory

potential of ZnO NPs is urgently required. Although in chapter IV it was shown that the cytotoxic potential of ZnO NPs can be altered with varying protein concentration of the cell culture medium, all the *in vitro* endpoints were assessed in the presence of 10% FBS to compare the data with the current literature. Interference of NPs with commonly used test assays is possible, particularly in case of ZnO NPs which can undergo dissolution at a low pH. The cytotoxic evaluation of ZnO NPs was therefore carried out using two independent assays mainly to validate the findings (Chapter VI). The cytotoxic profile of ZnO NPs was assessed using a cell viability MTT assay and LDH release assay in addition to DNA staining to confirm that apoptosis was the pathway by which ZnO NPs induce cytotoxicity in A549 cells. It was demonstrated that the MTT assay was more sensitive as compared to the LDH release assay.

Presence of sub cytotoxic amounts of ZnO NPs in the micro-environment of the lung epithelial cells is sufficient to stimulate a strong antioxidant as well as a pro-inflammatory response. Importantly, these stress responses are mediated via up regulation of HO-1 (oxidative stress responsive) and IL-8 (pro-inflammatory) genes, accompanied by the release of IL-8 protein in the cell culture supernatant by stressed cells. At sub-cytotoxic concentrations, ZnO NPs were capable of inducing phosphorylation of p65 and p38 proteins, actively involved in the NF $\kappa$ B and MAPK signalling pathways. Up-regulation of IL-8 gene is known to be associated with the activation of these pathways [20]. Pre-treatment of A549 cells with the sulphhydryl antioxidant NAC was successful in alleviating these responses, which confirmed the participation of ROS generated due to intercellular dissolution of ZnO NPs. The nanotoxicity data presented in this chapter gives a systematic overview of the inflammatory and stress mechanisms that are turned on in A549 cells when exposed to very low amounts of ZnO NPs.

ZnO NPs have been reported to induce pulmonary toxicity in animal models [21-24]. While intratracheal instillation and inhalation of ZnO NPs are the two most commonly used techniques in the literature (Table 5.2, Chapter V), ZnO NP exposure via intranasal instillation was investigated for the first time in this thesis. Intranasal instillation of a single dose (5 mg/kg) of pristine or surfactant-

dispersed ZnO NPs resulted in pulmonary inflammation after 24 hr in exposed mice. This was confirmed by up-regulation of eotaxin mRNA in the lung tissue and release of pro-inflammatory cytokines including MCP-1, RANTES and IP-10, all associated with the recruitment of inflammatory cells to sites of inflammation [25]. The preliminary results of the *in vivo* study highlight the inflammatory potential of ZnO NPs, although the overall ZnO NP burden delivered was instantaneous but relatively low with 5 mg/kg (84 µg/mouse), as compared to recent studies where higher cumulative ZnO NP doses were shown to cause low levels of pulmonary toxicity [24]. This highlights that the route and rate at which ZnO NPs are delivered *in vivo* may influence their toxic potential rather than the dose delivered. It can only be speculated that *in vivo* the ZnO NP surface, pristine or surfactant-dispersed, can undergo several modifications including constant adsorption and desorption of proteins and selective uptake by immune cells such as phagocytes, potentially influencing ZnO NP bio-reactivity.

This thesis provided valuable information on the biological characterisation of industrially important ZnO NP reactivity with important biomolecules such as proteins and a better understanding of their pro-inflammatory and immunomodulatory potential when interacting with cellular systems of the airways.

## 8.2 Conclusion

The most important outcomes of this thesis are:

- ✓ ZnO NP-PC formation in a complex biological system is a multifactorial process depending on NP characteristics and the biochemical properties of interacting proteins.
- ✓ Protein adsorption, NP dispersal state and size influence the cytotoxic and immunomodulatory potential of ZnO-NPs, evident when human lung cells induce a potent antioxidant and pro-inflammatory response in a sequential manner to combat ZnO-NP mediated nanotoxicity.

- ✓ Short-term exposure to a single, but relatively high dose of ZnO NPs via intranasal instillation causes acute pulmonary inflammatory reactions *in vivo*.

### 8.3 Future directions

ZnO NP surface conditioning with fetal bovine serum proteins has been studied in this thesis. This information can be further used to study ZnO NP interaction with other important biological proteomes such as the bronchioalveolar fluid. Identification and characterisation of BAL proteins adsorbed on the ZnO NP surface and subsequent analysis of their secondary structures along with detailed *in vitro* studies using primary airway cells in co-culture *in vitro* system, can be used to extrapolate potential hazards of inhalation of ZnO NPs.

In this project, important preliminary information on the pro-inflammatory nature of ZnO NPs when administered in the form of a single high dose via intranasal route in mice was generated. To extend and validate these findings further, it would be desirable to apply the same experimental strategy over a longer duration and additionally, track the course of these NPs *in vivo*. Moreover a mouse model exploring the effects of allergen-ZnO NP co-exposure can also help in determining if ZnO NPs can elicit or suppress Th2 immune response (allergy) when exposed via inhalation, which can have implications in better understanding NP induced hypersensitivity in humans.

The present thesis provided an important foundation for development of platform technologies to assess bio-distribution and nanotoxicological potential of NPs. This knowledge can be extended to other important tissues where NPs have been shown to accumulate after exposure, for example in neural cells as well as cells of the gastro intestinal tract.

## 8.4 References

1. Donaldson K, Stone V, Tran C, Kreyling W, Borm P: **Nanotoxicology.** *Occup Environ Med* 2004, **61**:727-728.
2. Lynch I, Dawson KA: **Protein-nanoparticle interactions.** *Nano Today* 2008, **3**:40.
3. Hu X, Cook S, Wang P, Hwang H-m: **In vitro evaluation of cytotoxicity of engineered metal oxide nanoparticles.** *Sci Total Environ* 2009, **407**:3070-3072.
4. Lin WS, Xu Y, Huang CC, Ma YF, Shannon KB, Chen DR, Huang YW: **Toxicity of nano- and micro-sized ZnO particles in human lung epithelial cells.** *Journal of Nanoparticle Research* 2009, **11**:25-39.
5. Napierska D, Thomassen LCJ, Rabolli V, Lison D, Gonzalez L, Kirsch-Volders M, Martens JA, Hoet PH: **Size-Dependent Cytotoxicity of Monodisperse Silica Nanoparticles in Human Endothelial Cells.** *Small* 2009, **5**:846-853.
6. Landsiedel R, Ma-Hock L, Kroll A, Hahn D, Schnekenburger J, Wiench K, Wohlleben W: **Testing Metal-Oxide Nanomaterials for Human Safety.** *Adv Mater* 2010, **22**:2601-2627.
7. Bae H, Ryu H, Jeong S, Lee E, Park Y-H, Lee K, Choi B, Maeng E, Kim M-K, Son S: **Oxidative stress and apoptosis induced by ZnO nanoparticles in HaCaT cells.** *Molecular & Cellular Toxicology* 2011, **7**:333-337.
8. Heng B, Zhao X, Xiong S, Ng K, Boey F, Loo J: **Cytotoxicity of zinc oxide (ZnO) nanoparticles is influenced by cell density and culture format.** *Arch Toxicol* 2011, **85**:695 - 704.
9. Heng BC, Zhao XX, Tan EC, Khamis N, Assodani A, Xiong SJ, Ruedl C, Ng KW, Loo JSC: **Evaluation of the cytotoxic and inflammatory potential of differentially shaped zinc oxide nanoparticles.** *Arch Toxicol* 2011, **85**:1517-1528.
10. Akhtar MJ, Ahamed M, Kumar S, Khan MAM, Ahmad J, Alrokayan SA: **Zinc oxide nanoparticles selectively induce apoptosis in human cancer cells through reactive oxygen species.** *Int J Nanomedicine* 2012, **7**:845-857.

11. Kermanizadeh A, Vranic S, Boland S, Moreau K, Baeza-Squiban A, Gaiser BK, Andrzejczuk LA, Stone V: **An in vitro assessment of panel of engineered nanomaterials using a human renal cell line: cytotoxicity, pro-inflammatory response, oxidative stress and genotoxicity.** *BMC Nephrol* 2013, **14**.
12. Everett WN, Chern C, Sun D, McMahon RE, Zhang X, Chen W-JA, Hahn MS, Sue HJ: **Phosphate-enhanced cytotoxicity of zinc oxide nanoparticles and agglomerates.** *Toxicol Lett* 2014, **225**:177-184.
13. Luo M, Shen C, Feltis BN, Martin LL, Hughes AE, Wright PFA, Turney TW: **Reducing ZnO nanoparticle cytotoxicity by surface modification.** *Nanoscale* 2014, **6**:5791-5798.
14. Avalos A, Haza AI, Mateo D, Morales P: **Cytotoxicity and ROS production of manufactured silver nanoparticles of different sizes in hepatoma and leukemia cells.** *J Appl Toxicol* 2014, **34**:413-423.
15. Nel A, Madler L, Velegol D, Xia T, Hoek E, Somasundaran P, Klaessig F, Castranova V, Thompson M: **Understanding biophysicochemical interactions at the nano-bio interface.** *Nat Mater* 2009, **8**:543 - 557.
16. Saptarshi S, Duschl A, Lopata A: **Interaction of nanoparticles with proteins: relation to bio-reactivity of the nanoparticle.** *J Nanobiotechnol* 2013, **11**:26.
17. Lynch I, Dawson K: **Protein-nanoparticle interactions.** *Nano Today* 2008, **3**:40 - 47.
18. Lundqvist M, Stigler J, Cedervall T, Berggård T, Flanagan MB, Lynch I, Elia G, Dawson K: **The Evolution of the Protein Corona around Nanoparticles: A Test Study.** *ACS Nano* 2011, **5**:7503-7509.
19. Casals E, Pfaller T, Duschl A, Oostingh GJ, Puentes V: **Time Evolution of the Nanoparticle Protein Corona.** *ACS Nano* 2010, **4**:3623-3632.
20. Yan Z, Xu L, Han J, Wu Y-J, Wang W, Yao W, Wu W: **Transcriptional and posttranscriptional regulation and endocytosis were involved in zinc oxide nanoparticle-induced interleukin-8 overexpression in human bronchial epithelial cells.** *Cell Biol Toxicol* 2014:1-10.
21. Cho WS, Duffin R, Poland CA, Howie SEM, MacNee W, Bradley M, Megson IL, Donaldson K: **Metal Oxide Nanoparticles Induce Unique**

- Inflammatory Footprints in the Lung: Important Implications for Nanoparticle Testing.** *Environ Health Perspect* 2010, **118**:1699-1706.
22. Cho WS, Duffin R, Howie SEM, Scotton CJ, Wallace WAH, MacNee W, Bradley M, Megson IL, Donaldson K: **Progressive severe lung injury by zinc oxide nanoparticles; the role of Zn<sup>2+</sup> dissolution inside lysosomes.** *Particle and Fibre Toxicology* 2011, **8**.
23. Fukui H, Horie M, Endoh S, Kato H, Fujita K, Nishio K, Komaba LK, Maru J, Miyauhi A, Nakamura A, et al: **Association of zinc ion release and oxidative stress induced by intratracheal instillation of ZnO nanoparticles to rat lung.** *Chem Biol Interact* 2012, **198**:29-37.
24. Adamcakova-Dodd A, Stebounova L, Kim J, Vorrink S, Ault A, O'Shaughnessy P, Grassian V, Thorne P: **Toxicity assessment of zinc oxide nanoparticles using sub-acute and sub-chronic murine inhalation models.** *Particle and Fibre Toxicology* 2014, **11**:15.
25. Kabashima H, Yoneda M, Nagata K, Hirofuji T, Maeda K: **The presence of chemokine (MCP-1, MIP-1 $\alpha$ , MIP-1 $\beta$ , IP-10, RANTES)-positive cells and chemokine receptor (CCR5, CXCR3)- positive cells in inflamed human gingival tissues.** *Cytokine* 2002, **20**:70-77.

## **General buffers**

### **Phosphate buffered Saline**

NaCl – 16 g

KCl – 0.4 g

Na<sub>2</sub>HPO<sub>4</sub> – 2.88 g

KH<sub>2</sub>PO<sub>4</sub> – 0.48 g

ddH<sub>2</sub>O – up to 1L

pH adjusted to pH 7.4 using 6M HCL and autoclaved

### **Tris buffered Saline with Tween20 (10X)**

NaCl – 80 g

KCl – 2 g

Tris base (C<sub>4</sub>H<sub>11</sub>NO<sub>3</sub>) – 30 g

ddH<sub>2</sub>O – up to 1L

pH adjusted to pH 7.4 using 6M HCL and autoclaved

Tween20 – 0.05%

## **SDS-PAGE buffers**

### **5 X Protein sample loading buffer(Laemmli buffer)**

0.6 mL 1M Tris-HCl, pH 6.8 – 60 mM

5 mL 50% Glycerol – 25%

2 mL 10% SDS – 2%

Dithiothreitol – 100 mM

1 mL 1% Bromophenol blue – 0.1%

ddH<sub>2</sub>O – up to 10 mL

### **1X Gel Electrophoresis running buffer**

Tris – 3 g/L

Glycine – 14.4 g/L

SDS – 1 g/L

ddH<sub>2</sub>O – up to 1000 mL

**SDS-PAGE gel de-staining solution**

Methanol (AR grade) – 500mL

Glacial acetic acid – 100mL

ddH<sub>2</sub>O – 400 mL

**Immunoblotting buffers**

Transfer buffer

Tris – 1.164 g

Glycine – 0.58 g

10% SDS – 750 µL

Methanol – 40 mL

ddH<sub>2</sub>O – upto 200mL

**ELISA buffers**

**Coating buffer, pH 9.6 for sample preparation**

50 mM Sodium bicarbonate – 4.25 mL

50 mM Sodium carbonate – 2 mL

ddH<sub>2</sub>O – upto 25 mL

**Washing buffer for ELISA**

PBS with 0.05% Tween20

## Publications

**Saptarshi SR**, Duschl A, Lopata AL: Interaction of nanoparticles with proteins: relation to bio-reactivity of the nanoparticle. *Journal of Nanobiotechnology* 2013, 11:26.

**Saptarshi SR**, Feltis BN, Wright PF: Time dependent pro-inflammatory response of zinc oxide nanoparticles on human lung epithelial cells at sub-toxic levels. *Journal of Nanobiotechnology* 2015, (Editorially Accepted)

**Saptarshi SR**, Lopata AL: A review on immunotoxicity of zinc oxide nanoparticles. *Nanomedicine* (Under review)

**Saptarshi SR**, Feltis BN, Wright PF: Exploring the interactions between zinc oxide nanoparticles and tissue culture medium proteins. *Nanoscale* (In preparation)

## Poster Presentations

**Saptarshi SR**, Wright PA, Lopata AL Understanding immunomodulatory and cytotoxic effects of zinc oxide nanoparticles on human lung epithelial cells. Presented at *NANOTOX 7th International Nanotoxicology Congress Antalya, Turkey 2014*

**Saptarshi SR**, Wright PA, Lopata AL Understanding immunomodulatory and cytotoxic effects of zinc oxide nanoparticles on human lung epithelial cells. Presented at *ACMM23&ICONN International conference Adelaide, Australia 2014*

**Saptarshi SR**, Wright PA, Lopata AL. Proteomic characterisation of zinc oxide nanoparticles and their immunotoxic effects on human lung epithelial cells-implications for occupational exposure. Presented at *Australian Society of Immunology Annual Conference, Melbourne, 2012 and European Academy of Allergology and Clinical Immunology Conference, Geneva, Switzerland 2012*

**Saptarshi SR**, Feltis BN, Wright PA, Turney TW, Lopata AL. Interaction of ZnO nanoparticles, used in sunscreens, with serum proteins and implications on cellular uptake. *Presented at Queensland Tropical Health Alliance, ACTM/QTHA Conference, Cairns, 2011 and 5th Australian Health and Medical Research Conference, Melbourne, Australia 2010.*

## Oral Presentations

Bio-interactions of nanomaterials. North Queensland Festival of Life Sciences, Townsville, 2013

Interaction of ZnO nanoparticles with fetal bovine serum proteins and effect on human lung epithelial cells. MEPSA annual conference, Brisbane, 2011

Impact of Protein adsorption on Nanoparticles used in sunscreen formulations. North Queensland Festival of Life Sciences, Townsville, 2011

## Awards and Grants

### **Robert Logan Memorial Award in Biochemistry 2014**

*Discipline of Biochemistry, James Cook University, Townsville*

### **International Travel Fellowship 2014**

NANOTOX 7th International Nanotoxicology Congress Antalya, Turkey 2014

### **Graduate Research Scheme Student Grant 2013**

Grant awarded to conduct the project titled: "Understanding Immunotoxic effects of commercially used nanoparticles" towards the PhD degree.  
James Cook University, Townsville

### **Best Talk Award 2013**

"Bio-interactions of nanoparticles"

"So You Think You can research?" James Cook University, Townsville

### **International Travel Award 2012**

European Academy of Allergology and Clinical Immunology Conference, Geneva

### **Best Talk Award 2011**

"Interaction of ZnO nanoparticles with fetal bovine serum proteins and effect on human lung epithelial cells"

Molecular and Experimental Pathology Society of Australasia Annual Conference, Brisbane

### **Best Talk Award 2011**

"Impact of Protein adsorption on Nanoparticles used in sunscreen formulations"

"So You Think You can research?" James Cook University, Townsville

**Best Poster Award 2011**

“Interaction of ZnO nanoparticles, used in sunscreens, with serumproteins and implications on cellular uptake”  
North Queensland Festival of Life Sciences” James Cook University, Townsville

**QTHA Travel Award 2011**

“Interaction of ZnO nanoparticles, used in sunscreens, with serumproteins and implications on cellular uptake” Queensland Tropical Health Alliance Conference, Cairns